Neural Plasticity

Neural Plasticity-Based Rehabilitation for Functional Recovery of Paretic Limbs

Lead Guest Editor: Mou-Xiong Zheng
Guest Editors: Ji-Geng Yan, Chun-Lei Shan, Xu-Yun Hua, Jia-Jia Wu, and Rong-Rong Lu

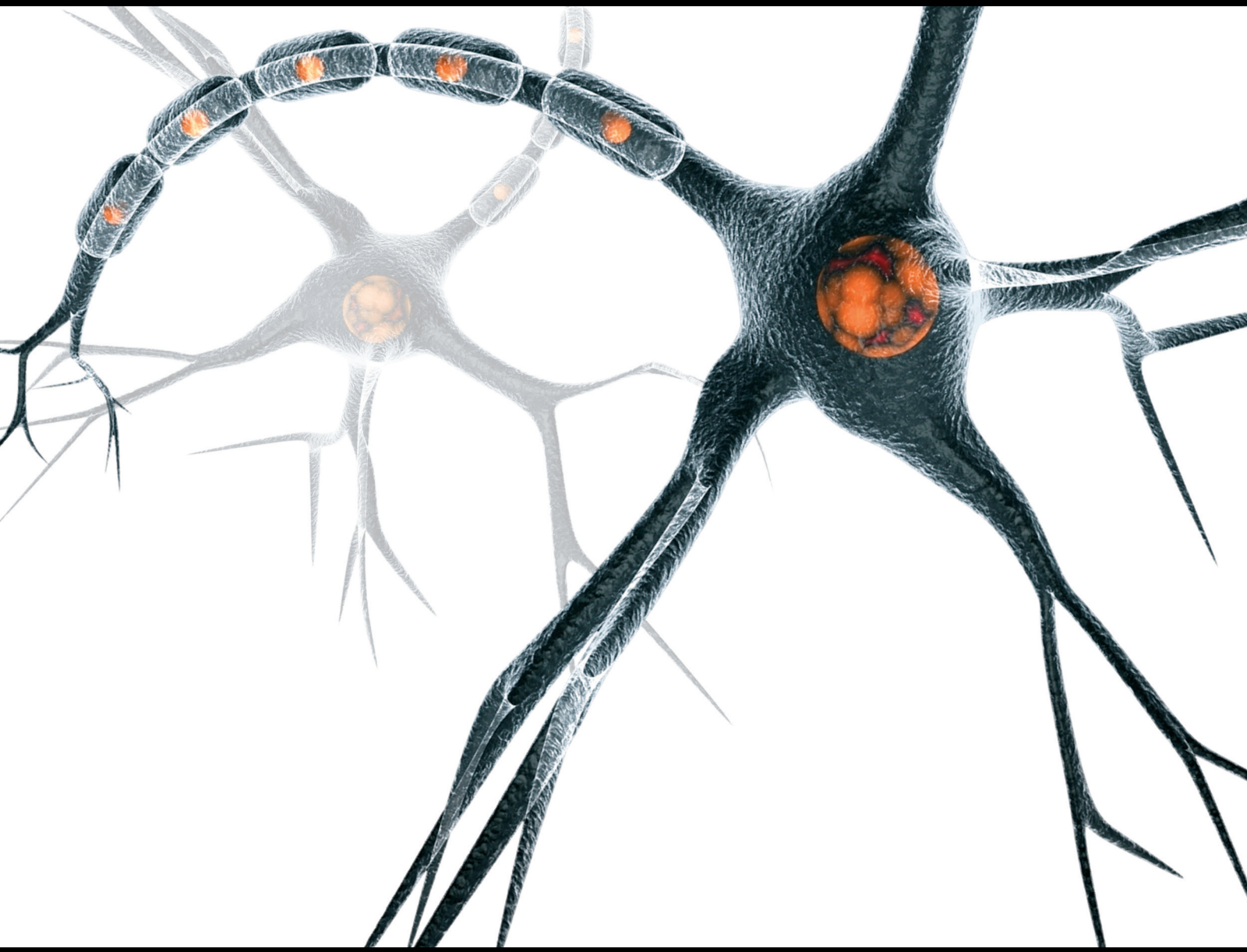

Neural Plasticity-Based Rehabilitation for Functional Recovery of Paretic Limbs

Neural Plasticity-Based Rehabilitation for Functional Recovery of Paretic Limbs

Lead Guest Editor: Mou-Xiong Zheng
Guest Editors: Ji-Geng Yan, Chun-Lei Shan, Xu-Yun Hua, Jia-Jia Wu, and Rong-Rong Lu

Contents

Hindawi
Neural Plasticity
Volume 2022, Article ID 5284044, 12 pages
https://doi.org/10.1155/2022/5284044

Research Article

Effects of Meaningful Action Observation Therapy on Occupational Performance, Upper Limb Function, and Corticospinal Excitability Poststroke: A Double-Blind Randomized Control Trial

Aryan Shamili,[1,2] **Afsoon Hassani Mehraban**,[1] **Akram Azad**,[1] **Gholam Reza Raissi**,[3] **and Mohsen Shati**[4]

[1]*Rehabilitation Research Center, Department of Occupational Therapy, School of Rehabilitation Sciences, Iran University of Medical Sciences (IUMS), Tehran, Iran*
[2]*Research Center for War-Affected People, Tehran University of Medical Sciences, Tehran, Iran*
[3]*Neuromusculoskeletal Research Center, Iran University of Medical Sciences (IUMS), Tehran, Iran*
[4]*Mental Health Research Center, School of Behavioral Sciences and Mental Health, Tehran Institute of Psychiatry, Iran University of Medical Sciences (IUMS), Tehran, Iran*

Correspondence should be addressed to Afsoon Hassani Mehraban; mehraban.a@iums.ac.ir

Received 6 October 2021; Revised 5 January 2022; Accepted 22 July 2022; Published 16 September 2022

Academic Editor: Chun Lei Shan

Introduction. Action observation therapy (AOT) is a mirror neuron-based approach that has been recently used in poststroke rehabilitation. The main goal of this study was to investigate the effectiveness of AOT of occupations and tasks that are meaningful for chronic stroke patients on occupational performance, upper-extremity function, and corticospinal changes. *Method*. A randomized control trial was designed to compare between experimental ($n = 13$) and control groups ($n = 14$). In both groups, the execution of meaningful tasks was practiced, but the videos of those tasks were just shown to the experiment group. Instead, patients in the control group watched nature videos as a placebo. Clinical outcomes were evaluated using the Canadian Occupational Performance Measure (COPM), Fugl-Meyer Assessment (FMA), Action Research Arm Test (ARAT), and Box-Block Test (BBT) on 3 occasions: baseline, post (at 4 weeks), and follow-up (at 8 weeks). The assessments of central motor conduction time (CMCT) for abductor policis brevis (APB) and extensor indicis (EI) were only recorded at baseline and posttreatment. Both assessors of clinical and neurophysiological outcomes were blinded to the allocation of subjects. *Result*. Finally, the results of outcomes in 24 patients who completed the study were analyzed. In both groups, significant improvements after treatment were seen for most outcomes ($p \leq 0.05$). These changes were persistent until follow-up. There were significant differences in COPM performance ($p = 0.03$) and satisfaction ($p = 0.001$) between the experimental and control groups. In contrast, other clinical assessments such as FMA, ARAT, and BBT did not show significant differences between the two treatments ($p \geq 0.05$). The results of CMCT related to APB showed a more significant change in the experiment group compared to the control group ($p = 0.022$). There was no difference in change detected between the two groups for CMCT related to EI after treatments. *Conclusion*. Observation and execution of meaningful activities can enhance the effects of simply practicing those activities on occupational performance/satisfaction and corticospinal excitability poststroke.

1. Introduction

Stroke is still a main cause of death and disability globally, with many healthy lives lost each year [1]. It has been reported that at 12 months after stroke, approximately 61% of patients die or become disabled [2]. After a year post-stroke, many of those who live with disability face physical and/or occupational dependency (66%–75%) [3]. Participation in daily life and social activities is closely related to upper limb function [4]. About two-thirds of patients with

stroke will have continued upper extremity problems for months and years [5], which reduce their participation in meaningful occupations [6]. Therefore, improving the motor and functional recovery of the upper extremities might be a key for appropriate occupational function and consequently for enhancing the quality of life poststroke [4].

Due to the fact that the results of many rehabilitation methods available after stroke are not satisfactory, conducting research with basic and clinical rationale is very important to achieve better results, especially in the field of upper limb problems [7, 8].

Action observation therapy (AOT) is a new method used in upper limb rehabilitation of various neurological disorders, especially in cerebral palsy [9] and stroke [10]. In the process of AOT, patients watch some movements and actions of healthy subjects on a video or a live show; afterwards, the patients should try to imitate and perform those actions [10]. Researches have argued that the theory behind AOT is explained by the evidence that observation of a purposeful action [11, 12] stimulates the mirror neuron system (MNS) which is the neural active mechanism, while the same action is being executed [13]. It is reported that mirror neuron areas of the brain have functional connections with the motor cortex [14, 15]. So it might be possible to change cortical motor representations as well as motor recovery of impaired limbs after stroke by the activation of MNS during the AOT process [16].

Mirror neurons form a system in the brain that has characteristics such as being (1) purposeful, (2) context-dependent, (3) experience-based, and (4) multisensory [17]. It seems that the more these features are amplified, the more likely the MNS and other brain circuits will be excited and prepared for the potential neuroplasticity. The mentioned characteristics of the MNS are inherent in many activities of patients' daily life. It is believed that the mirror neuron system is more active when observing a complex and purposeful activity compared to a simple action, so one way for more MNS excitation might be using activities that are in line with everyday activities and based on one's experiences [18, 19].

As explained above, AOT is on the basis of MNS theories, and it might be possible that by augmenting MNS function, progress will be achieved within this technique. This advantage might lead to a better motor recovery and upper limb function in relative occupations of stroke patients. On the one hand, there are studies that have investigated the effectiveness of AOT on upper limb motor function poststroke [20–23]. However, there are no considerable studies and evidence on the effects of AOT on occupation and participation areas [23] as well as effects on central nervous system neural changes [24].

On the other hand, there are many studies that have used simple movements or less purposeful tasks for observation and execution, such as finger movements and manipulating objects such as ball or blocks [22–28]. Even those studies that provided more complicated and purposeful activities during AOT, such as drinking a cup of tea and playing with coins and cards [29], did not consider the occupational priorities and meaningfulness of the activities from the patient's view. According to theories, purposefulness can promote motor learning but not all purposeful activities are meaningful and there are some differences between these two concepts [30]. Therefore, a shortage of research still remains on the use of activities/occupations which are selected by the patients and are meaningful to them. Meaningfulness is believed to make the therapy more collaborative and motivational because it originates from issues such as the client's needs, experiences, and context [31]. These issues seem to be the same as the characteristics of the MNS that was mentioned earlier. Taking into account the common characteristics of the MNS and meaningful occupations, in this study, observing and performing meaningful daily occupations close to real world was investigated whether it might be a beneficial intervention.

The main hypothesis of this study was: "observation and execution of meaningful tasks/occupations selected by the patients can enhance occupational performance/satisfaction compared to only execution of the same tasks/occupations." We also compared the changes in motor recovery and performance of upper limb and also cortical excitability between these two interventions.

2. Methods

2.1. Participants. With regard to the aim of this study to examine meaningful AOT, determining and selecting a popular and highly important occupation among the priorities of chronic stroke patients were a necessity. According to evidence [32], the opinion of the experts, and interview with 104 available chronic stroke patients, the occupation of *eating* was recognized as an important and meaningful occupation for many of these clients; therefore, it was considered as a main inclusion criteria. The criteria for entering the study were choosing the *eating* occupation in the priority list of Canadian Occupational Performance Measure (COPM) with an importance score ≥6 out of 10, age between 40 and 70, at least 6 months poststroke, a score above 23 on the Persian version of cognitive test of Mini Mental Status Exam (MMSE) [33], no other neurological diseases, history of only 1 stroke, motor recovery stage between 3 and 5 according to Brunnstrom's classification, and no history of cranial implants or seizures. Chronic stroke patients attending rehabilitation centers or local hospitals were recruited with a convenience sampling method. If any of the patients had the following situations, he/she would have been excluded from the research: occurrence of orthopedic lesions in the upper extremity; occurrence of any neurological disease; having visual, hearing, and/or cognitive impairments; inability to sit at least 1 hour independently on a chair; and absence in posttest evaluation.

2.2. Experimental Design. This study was a double-blind randomized clinical trial with two arms. The research was done at rehabilitation clinics in Tehran. There were 49 patients with chronic stroke screened and interviewed from October 2019 to December 2020; 17 of them were excluded because of not meeting the inclusion criteria, and 5 patients declined to participate (Figure 1). The eligible participants were

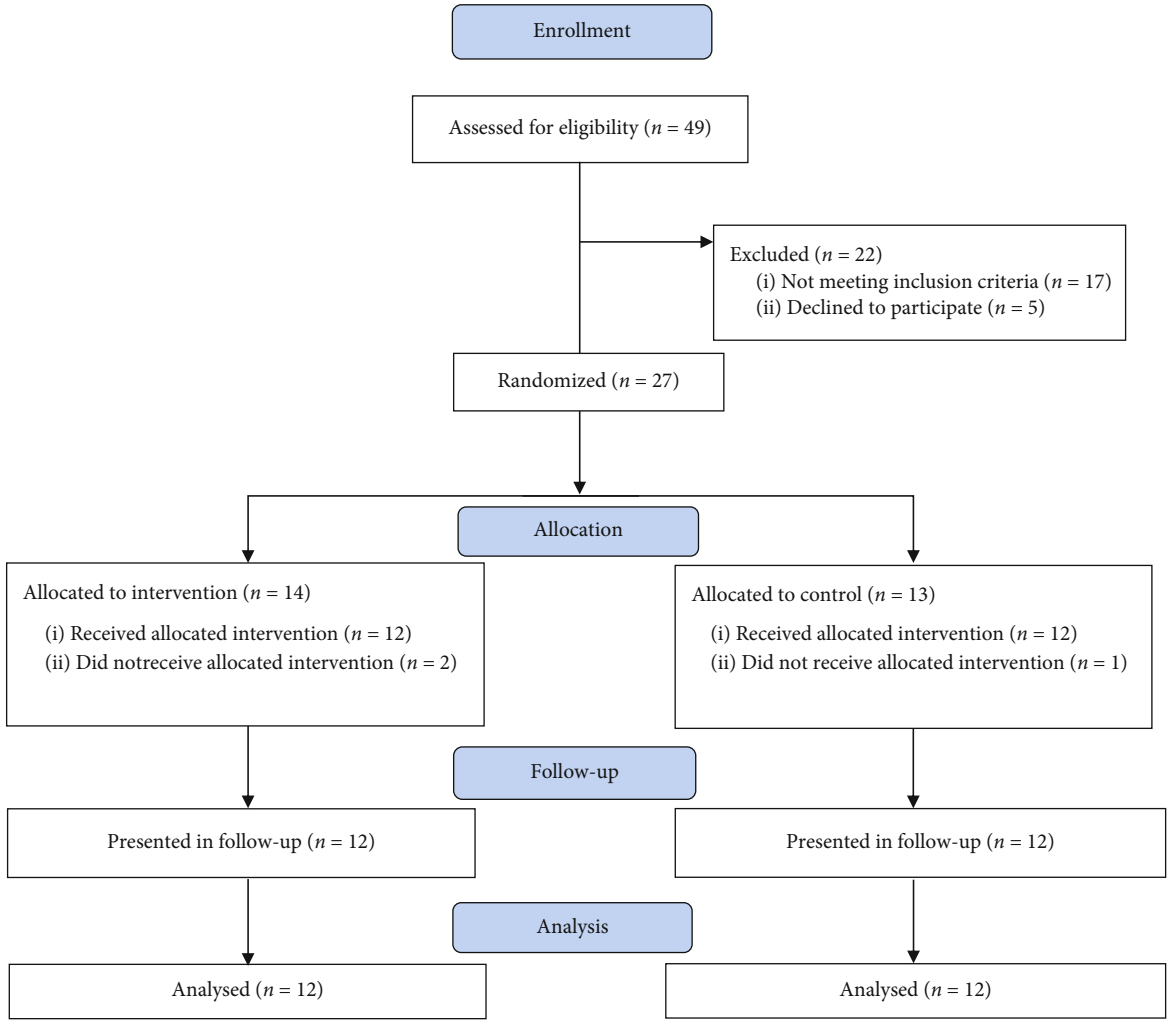

Figure 1: Flowchart of the participants included in the study.

allocated into two groups: AOT ($n = 13$) and control group ($n = 14$) by stratified block randomization regarding positive/negative motor evoked potential (MEP) in abductor policis brevis (APB) and also the side of stroke. The randomization was administered by an epidemiologist unaware of the study with the use of Excel software. It has to be mentioned that in this study, patients and the assessors were blind to the group allocations.

2.3. Outcome Measures. In this study, the COPM was considered as the primary outcome measure and ARAT, BBT, MEP, and Actual Task Performance Assessment were selected as secondary outcome measures. All clinical assessments were administered in a constant order by a trained occupational therapist with a 10-year experience. An expert in physical medicine and rehabilitation specialized in the use of transcranial magnetic stimulation (TMS) assessed the MEP in a separate session from other evaluations.

2.3.1. Canadian Occupational Performance Measure (COPM). This measurement has been used in a semi-structured interview to identify patients' main concerns in the occupational areas including self-care, productivity, and leisure/play on a 0–10-point self-rating scale. The COPM enabled team research to identify occupational problems and measure patients' perception of their performance and satisfaction with the selected tasks before and after each intervention. The validity, reliability, and responsiveness of the COPM are reported as acceptable in many diseases such as stroke [34]. A change of two points or more on the COPM is considered clinically significant [35].

2.3.2. Fugl-Meyer Assessment of Upper Extremity (FMA-UE). FMA-UE is a stroke-specific measure of sensorimotor impairment and includes 33 items on a 3-point ordinal scale (0 = cannot perform, 1 = can partially perform, 2 = can perform fully). The summation of scores will be a maximum of 66 [36, 37]. The construct validity, inter-rater reliability, and intra-rater reliability of this scale have been reported as very good [37].

2.3.3. Action Research Arm Test (ARAT). ARAT is a 19-item scale divided into four basic movements [38] of grasp, grip, pinch, and gross movements that measures UE (arm and

hand) function. It is scored with 0, 1, 2, or 3, with a total summation of 57 in which higher scores indicating better arm motor performance. The test has been reported as valid [38, 39] and sensitive to therapy-related [40, 41] and spontaneous [38, 39, 42] changes post stroke. It is a reliable and valid measure to assess upper limb functions in stroke subjects [39].

2.3.4. Box and Block Test (BBT). The BBT is frequently used as a measure of dexterity. The BBT apparatus consists of a box of specified dimensions divided into two sections. The test contains picking up a block out of a box and transferring it over a wall into the other side of the box. The total scoring is by counting the number of blocks carried over the partition from one side to the other during 60 seconds [37]. The test has been shown to be valid and reliable [43].

2.3.5. Motor Evoked Potential (MEP). One of the variables related to brain physiology and motor pathways that can be recorded by the TMS device is MEP [44, 45]. By sending pulses and currents through a magnetic coil, local neurons and consequently pyramidal cells, spinal cells, or the corticospinal tract can be stimulated. Depending on the brain stimulation area, there would be a recordable MEP at the end of the path, where the target muscles contract. The tendon muscles or finger extensors are usually used for this recording [46]. In this study, central motor conduction time (CMCT) was the analyzed finding related to the MEP.

To record the MEP using a Magstim 200 stimulator (Magstim Co. Ltd., Whiteland, Dyfed, UK), the patient had to sit in a quiet room in a special chair [45]. Cerebral cortex area M1 and appendix of the seventh cervical vertebra (C7) were selected as stimulation points for extensor indicis (EI) and abductor policis brevis (APB) as target muscles. The thumbs and index fingers play an important role in many daily activities, such as the eating tasks [47, 48].

In the case of the thumb, the abducted positions contribute to about two-thirds of the grips, and for this reason, we recorded the APB muscle, which is the main active muscle of the thumb during these positions. Also, to record MEP of the index finger, EI was selected due to its independence from other finger extensors during the excitation and palpation. There are other studies that have considered APB [49, 50] and EI [51, 52] for their MEP recording as well.

To record the MEP, about 3 to 5 waves with good reproducibility and high intensity were selected, and then, by subtracting cervical latency from the M1 latency, the CMCT was calculated [49].

2.3.6. Actual Task Performance Assessment. To improve the validity of the data and the results of the interventions, a scale derived from the Chedoke Arm and Hand Activity Inventory was used as an objective assessment [32]. Scoring of the eating subtasks, which were used as training components in the study, was according to the assessor's opinion.

2.4. Intervention Protocol. Because the occupations and tasks for the intervention were related to eating, thereby some basic eating-related tasks were selected such as using fork, pouring water from bottle to glass, and drinking from a hard glass with the affected limb. In an expert panel consisting of one neuroscientist and four proficient occupational therapists working in neurologic rehabilitation settings, based on the evidence and expert opinions, the selected tasks were analyzed and divided to short part sequences of the whole task execution (Table 1).

It has to be mentioned that to consider the upper limb ability and progress of the participants during the sessions, some meaningful tasks with more difficulties such as pouring water from pitcher to glass, eating soup with spoon from bowl, and drinking from a soft glass with the affected limb were also provided. If a patient had adequate performance and satisfaction in performing any of the activities (I–IV) earlier than the time expected, he/she could perform the more difficult activities in the next sessions.

Afterwards, to prepare videos for AOT intervention, a Fujifilm X-H1 camera filmed those actions and tasks while acted by a young healthy model. The performance of subtasks A–H by the model was recorded from 3 angles: lateral view, point of view, and front view (Figures 2(a)–2(c)). Also, for the control group, nature and landscape videos were provided as sham observation videos (Figure 3). The quality for all videos was chosen with a 1080p resolution. After providing a final version of the edited video footages, to identify the time required for assessments and to ensure patient safety and technical considerations of the interventions mainly the AOT, a 4-week pilot study was conducted with three stroke patients.

2.4.1. AOT Group. Due to motor learning theories and recent approaches [53, 54], we dedicated 3 sessions to observe and practice each task, so a total of 12 sessions were considered for the 4 tasks (3 times a week). To maintain the effects of the previous practiced task, at the end of each task practice period (after 3 sessions), at the beginning of the next sessions, the previous tasks had been viewed as a complete task for 6 minutes and then performed as a whole. For example, activity I was selected for the first 3 sessions and activity II for the next 3 sessions. Therefore, in the fourth session of the study, before observing and performing the components of activity II, the whole task observation/execution of the activity I should have been performed for 6 minutes (3 minutes observation + 3 minutes execution).

Each of the I–IV activities included functional components that were briefly explained to the patients at the beginning of each of the three intervention sessions. Each session lasted 45–60 minutes, and the steps followed in each session were as described below:

(1) The video of how to perform each component (part-task) was played from 3 angles for a total of about 2 minutes; each angle was being shown approximately 3 times

(2) After watching the video (action observation) of each activity component, the participant should have performed the same movements and tasks for 3 minutes. If necessary, in addition to monitoring the intervention session, the therapist provided

Table 1: Eating-related meaningful tasks (I–IV), their subtasks, and the procedure time.

Subtask	Task Task I Pour water from bottle to glass	Task II Eating food bimanually	Task III Drink water from a hard glass	Task IV Eat a piece of carrot with fork	*Time for watching films (AOT * or sham **)*	*Time for performance*
A	Reach to the bottle	Reach to the spoon and fork	Reach to the glass	Reach to the fork	2 m	3 m
B	Grasp the bottle	Grasp the spoon and fork	Grasp the glass	Grasp the fork	2 m	3 m
C	Bring the bottle near to the glass	Take some meal	Bring the glass near to the mouth	Bring the fork near to the carrot	2 m	3 m
D	Pour water into glass	Bring spoon to mouth and eat	Drink from the glass	Bring the carrot to the mouth	2 m	3 m
E	Reach out to desktop	Reach out and place spoon and fork beside the plate	Reach out to the desktop	Reach out to the dish	2 m	3 m
F	Release the bottle	Release the spoon and fork	Release the glass	Release the fork	2 m	3 m
G	Rest arm	Rest arm	Rest arm	Rest arm	2 m	3 m
H	Whole task	Whole task	Whole task	Whole task	2 m	3 m

*Films in AOT includes videos of a model performing the A-H subtasks for intervention group. ** Films in sham include videos of nature and landscapes for control group. *m: minute; whole task: the combination of subtasks A–G.*

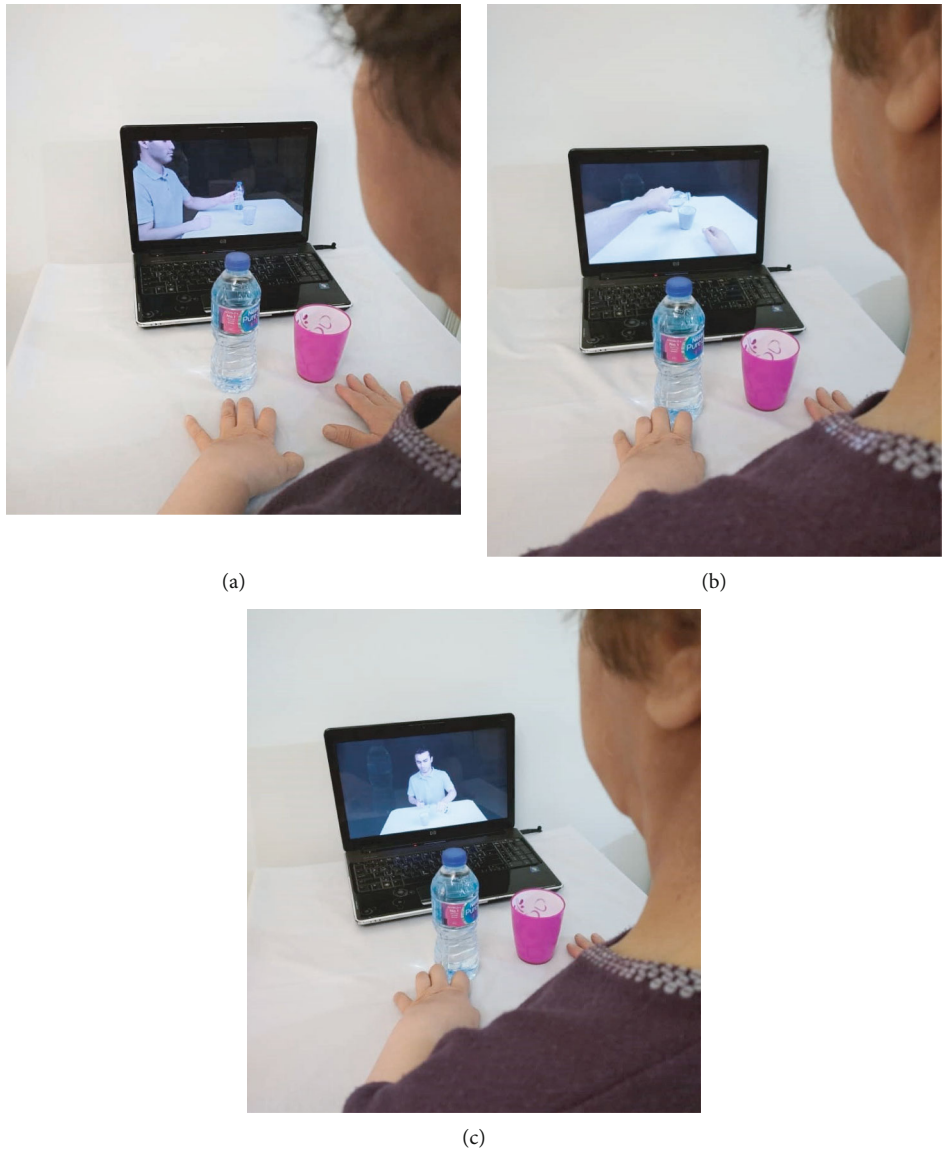

(a) (b) (c)

Figure 2: A left hemiplegic patient in AOT group watching AOT videos of (a) lateral view, (b) point of view, and (c) front view.

appropriate physical assistance for the patient to complete the activity

(3) Before the end of each session and after observing and performing all the components, the whole task was shown for about 3 minutes in 3 angles (i.e., each angle for 1 minute)

(4) After watching the whole task video, the participants should have practiced the same movements and tasks for 3 minutes

2.4.2. Control Group. Similarly, in the control group, the protocol was designed with 12 sessions, 3 days a week, and in each session about 45–60 minutes. In contrast to the AOT group, before performing eating-related tasks, the patients in this group should have observed landscape and nature videos (sham) despite the observation of the eating-related videos. All other items such as the eating-related tasks, sequences, time, and order of subtask executions in the control group were the same as the AOT group (Table 1). Activities I–IV including functional components were briefly explained to the patients at the beginning of each of the three intervention sessions. Furthermore, like the AOT group, if practicing these tasks were too easy for any patient, the more difficult tasks mentioned earlier were possible to be practiced in the following sessions.

2.5. Sample Size. The sample size was calculated regarding the occupational performance (COPM) as the primary outcome measure of this study. A moderate effect size was considered ($f = 0.25$ or eta − squared = 0.06) [55] due to the reported effectiveness of AOT on occupational performance [56].

With regard to the study design, using the G∗Power 3.1 statistic software, the following values were applied: $\alpha = 0.05$, power = 80%, number of groups = 2, number of

Figure 3: A right hemiplegic patient in control group watching landscape (sham) videos.

measurements = 3, correlation among repeated measures = 0.5, and nonsphericity correction = 1. Although a total sample size of 27 patients was estimated, because of many limitations during the COVID-19 pandemic and 3 dropouts, an interim analysis was done. The results showed a significant difference between two study groups for the primary outcome (COPM), and the main hypothesis was confirmed. Thereby, the patient recruitment was stopped with 24 participants who completed the follow-up (Figure 1).

2.6. Statistical Analysis. We calculated the descriptive and analytic statistics using the software SPSS, version 16 (SPSS Inc., Chicago, IL, USA). To compare the effects of two interventions on most outcomes during the study, analyses of variance (ANOVAs) with repeated measures with a between-subject factor at 2 levels (2 groups) and a within-subject factor at 3 levels (time: before, after, and follow-up) were conducted. Also, the time × group interaction effect was analyzed. Analysis of post hoc with a Bonferroni correction was used when a significant interaction effect was detected. To investigate the repeated measure effect size, values based on partial eta squared (η^2) were considered as small (=0.01), medium (=0.06), and large (=0.14) [55]. In the present study, MEP was just recorded at baseline and posttest; therefore, to analyze CMCT data before and after the interventions, we calculated change scores for each group and compared them by using the Mann-Whitney U test. Significance was set at 0.05.

3. Results

Of 27 participants who enrolled in the study, 12 subjects in the control (9 males, 3 females; mean ± SD age, 56.58 ± 11.21) and 12 subjects in the AOT (7 males, 5 females; mean ± SD age, 53.50 ± 10.55) groups completed the study and were finally considered for statistical analyses. In the intervention group, 1 participant was excluded from the study because of an arm fracture incidence. In the control group, 2 participants were excluded; the first one was because of traveling and the second one was because of not willing to go outdoor during the COVID-19 pandemic. All characteristics of the analyzed participants and the study flowchart are presented in Table 2 and Figure 1, respectively.

Both groups showed improvements in the mean score of the primary outcome measure (COPM) and most of the secondary outcome measures (FMA, ARAT, BBT, CMCT, and the actual task performance test) during the study. After 1 month of study, the changes in the mean scores were maintained and did not decrease until follow-up assessments.

The time × group effect was significant for COPM performance ($F(1.15, 25.40) = 7.2$, $p = 0.03$) and satisfaction ($F(1.16, 25.67) = 19.3$, $p = 0.001$) with large effect sizes (performance $\eta^2 = 0.26$, satisfaction $\eta^2 = 0.46$) (Table 3). Similarly, the actual task performance of eating significantly changed ($F(1.25, 27.66) = 6.43$, $p = 0.04$) with a large effect size ($\eta^2 = 0.26$) (Table 3). In contrast, other clinical assessments such as FMA, ARAT, and BBT did not show significant differences among two treatments during the study ($p \geq 0.05$). In contrast, other clinical assessments such as FMA, ARAT, and BBT did not show significant differences among two treatments during the study ($p \geq 0.05$).

Comparisons of all pairs were analyzed using the Bonferroni correction test, and a significant difference between premeans and postmeans was observed ($p < 0.05$) for all the outcomes, while there was not a significant difference between post and follow-up results ($p \geq 0.05$).

It has to be mentioned that because MEP could not be detected in some patients, the obtained CMCT was analyzed with 13 and 17 samples for APB and EI, respectively. The results of CMCT were different in APB and EI muscles (Table 4). While there was not a significant change in the CMCT of APB in the control group, this outcome measure in the AOT group showed significant improvement. In the EI muscles, CMCT has been changed in both groups, but there was not a significant difference between treatments (Table 4).

4. Discussion

This novel study focuses on employing the important and meaningful occupations of the clients into the AOT process, while heretofore, this method was being practiced with simple movements and activities that were not asked if they were meaningful or meaningless to the participants. As mentioned earlier, the meaningfulness can become a source of motivation and volition during the treatment process and could lead to more therapy engagement. Thereby, watching and imitating the videos of performing a contextual, individualized and real occupation could help the patients feel the sense of accomplishment and mastery over that occupation/task. Other new information that may be extracted from this research is the impact of meaningful AOT as a top-down intervention on occupational, functional, and neurophysiological outcomes. This randomized clinical trial

Table 2: Distribution of demographic variables in the intervention and control groups.

Qualitative variables	Intervention ($n = 12$)	Control ($n = 12$)
Sex	n (%)	n (%)
Female	5 (41.7%)	3 (25%)
Male	7 (58.3%)	9 (75%)
Type of stroke		
Hemorrhagic	4 (33.3%)	2 (16.7%)
Ischemic	8 (66.7%)	10 (83.3)
Affected side		
Right	5 (41.7%)	6 (50%)
Left	7 (58.3%)	6 (50%)
Handedness		
Right	11 (91.7%)	10 (83.3%)
Left	1 (8.3%)	2 (16.7%)
Upper arm Brunnstrom stage		
III	3 (25%)	4 (33.3%)
IV	6 (50%)	2(16.7%)
V	3 (25%)	6 (50%)
Hand Brunnstrom stage		
III	4 (33.3%)	4 (33.3%)
IV	6 (50%)	3 (25%)
V	2 (16.7%)	5 (41.7%)
Motor evoked potential (APB)		
+	6 (50%)	7 (58.3%)
−	6 (50%)	5 (41.7%)
Quantitative variables	Intervention ($n = 12$) Mean ± SD	Control ($n = 12$) Mean ± SD
Age (year)	53.5 ± 10.55	56.58 ± 11.21
Time since stroke (month)	39.75 ± 28.35	42.58 ± 29.25

Table 3: Pre, post, and follow-up outcome measures of the intervention and control groups (time × group interaction).

	Baseline Mean ± SD		Post (at 4 weeks) Mean ± SD		Follow-up (at 8 weeks) Mean ± SD					
	Intervention ($n = 12$)	Control ($n = 12$)	Intervention ($n = 12$)	Control ($n = 12$)	Intervention ($n = 12$)	Control ($n = 12$)	Wilks lambda	F	$P - v$	Effect size (Eta^2)
COPM (performance)	3.00 ± 1.34	3.41 ± 2.35	6.58 ± 2.02	5.29 ± 2.43	6.50 ± 1.97	5.37 ± 2.44	0.73	3.83	0.03*	0.26
COPM (satisfaction)	2.75 ± 1.76	3.66 ± 2.60	6.58 ± 2.46	4.83 ± 2.48	6.66 ± 2.38	4.91 ± 2.39	0.50	10.36	0.001*	0.49
Actual task performance	19.41 ± 13.96	23.08 ± 11.07	29.00 ± 15.67	28.75 ± 11.81	29.00 ± 15.40	28.08 ± 11.95	0.73	3.71	0.042*	0.26
FMA-UE	38.66 ± 12.57	41.33 ± 14.53	46.16 ± 7.1	46.41 ± 12.0	46.33 ± 14.72	46.66 ± 12.68	0.91	0.96	0.39	0.08
ARAT	23.08 ± 24.18	25.83 ± 19.78	27.00 ± 23.41	30.16 ± 20.70	26.83 ± 23.53	29.58 ± 20.76	0.96	0.41	0.66	0.03
BBT	9.82 ± 12.22	12.38 ± 10.45	13.16 ± 15.48	13.46 ± 10.95	13.08 ± 15.52	13.25 ± 11.19	0.88	1.37	0.275	0.11

Note: * = statistically significant; COPM: Canadian Occupational Performance Measure; F: test for repeated measures 2-way ANOVA; FMA-UE: Fugl-Meyer Assessment (upper extremity); ARAT: Action Research Arm Test; BBT: Box and Block Test.

indicated that either with or without watching meaningful and self-selected activities, practicing these activities would help chronic stroke patients to make improvements in their desired occupational performance/satisfaction and also in motor recovery and function of the affected upper limb. Although determining the superiority between meaningful

Table 4: MEP comparison between the intervention and control groups, before and after the therapy.

	Baseline Mean ± SD		Post (at 4 weeks) Mean ± SD		Mean change ± SD		Mann-Whitney test	P -value
CMCT (APB)	Intervention ($n = 6$)	Control ($n = 7$)	Intervention ($n = 6$)	Control ($n = 7$)	Intervention ($n = 6$)	Control ($n = 7$)		
	12.41 ± 3.15	13.24 ± 2.05	10.20 ± 2.20	13.24 ± 1.68	−2.21 ± 2.32	0.00 ± 1.01	−2.29	0.022*
CMCT (EI)	Intervention ($n = 7$)	Control ($n = 10$)	Intervention ($n = 7$)	Control ($n = 10$)	Intervention ($n = 7$)	Control ($n = 10$)	−0.48	0.625
	12.38 ± 4.10	14.60 ± 4.59	11.42 ± 2.00	13.75 ± 3.40	−0.96 ± 2.04	−0.84 ± 2.88		

* = statistically significant; MEP: motor evoked potential; CMCT: central motor conduction time; APB: abductor policis brevis; EI: extensor indicis.

and less meaningful AOT remains questionable, at first and in this stage, it was necessary to confirm the novelty and effectiveness of the meaningful AOT protocol on clinical and neurophysiological changes in the brain.

As a result of this study, both experimental and control groups showed changes in COPM, FMA, ARAT, and BBT significantly. Although CMCT of the EI was improved in both groups, the APB just showed significant changes in the AOT group. The main findings of this research were the significant differences between groups which were only seen in COPM, actual task performance assessment, and CMCT of the APB.

In this study, COPM besides the actual performance assessment was used to evaluate occupational participation and also to set the treatment protocol. Since this study is the first AOT trial using these assessments, the comparison with other AOT studies would be just feasible regarding other participation outcomes. Similar studies have reported that improvement in Stroke Impact Scale (SIS), Functional Importance Measure (FIM), and Barthel Index (BI) was more significant through watching a model's action execution during AOT in comparison with watching landscape or sham videos as control treatment [11, 50, 57, 58]. In another study, this advantage of AOT was also seen over the mirror therapy method [59]. In contrast to the above results, a study claimed that there was no significant difference between the changes in FIM scores due to AOT and control treatment [20]. The possible reason for this might be the short period of each AOT session. The time for watching videos in that study was reported to be about 15 minutes each session, in contrast to 45–60 minutes devoted to AOT sessions in the present study.

Regarding CMCT, related changes in APB as a result of AOT showed significant advantages over the control group. This probably means that watching a video of meaningful activities can increase the effect of execution of those activities on the excitability of the cortical-spinal pathway and decrease the time of transmitting motor commands from M1 to the tendon muscle (APB). Only two similar studies have investigated the changes in MEP due to AOT poststroke [50, 60]. In a randomized control trial, results of CMCT showed a significant decrease for APB within and between groups [50]. Although it studied acute patients and lasted for 8 weeks, the results were in agreement with the present study. In another study, the results could not show a significant change in CMCT of APB as after AOT [60]. Many of neurophysiological research use APB to record MEP [50, 60], but there are scarce studies that investigated the EI [52]. Because the extensor muscles play an important role in many activities, in this study, it was decided to examine the EI beside the APB to observe the impact of AOT on CMCT. Although both groups had significant improvements, between-group changes were not considerable. This result could be a subject of future research.

In the present study, although motor recovery of upper limb (reflected by FMA) after AOT was more than after control treatment, the difference did not reach a significant statistical level between groups. The results might be more significant if a larger sample was recruited or the therapy sessions would be continued. Some studies have reported that the motor recovery of impaired upper limb was significantly higher due to AOT compared to control [11, 50, 57, 61]. It has to be mentioned that in the present study, the focus of AOT in chronic patients was on meaningful and complex activities rather than basic movements. In contrast, all of the mentioned studies (1) were investigated in acute stroke patients (<6 months poststroke) and (2) used various tasks from simple to complex for the observation and execution process. Therefore, it might be argued that the earlier the treatment and the more basic the movements, the better the motor recovery.

The results of the upper extremity function in this study (reflected by ARAT and BBT) did not show statistically meaningful changes between groups. In contrast to the present study considering ARAT, in an 8-week AOT study, advantage over control treatment was reported [50]. There are also controversial results related to BBT after AOT [20, 59, 61].

Overall, this study indicates that action observation and execution of meaningful activities as a MNS-based technique can enhance the performance/satisfaction of the selected occupation in chronic stroke patients more than just executing those activities. Meaningful AOT can also improve cortical excitation; therefore, it probably provides the brain neural networks for a higher chance of persistent plasticity.

5. Limitations

In this study, to make the situation more meaningful and realistic for the participants, some activities such as eating a daily meal (rice or soup) were tried to be practiced in a lunchtime session. Therefore, fixing the session times and

avoiding overlaps between lunchtime sessions was a challenge during the study. However, this problem was also solved by the cooperation of subjects and setting a dynamic weekly time schedule for the sessions.

The COVID-19 pandemic slowed the process of patient recruitment for the study. Disease recurrent waves, in addition to national lockdowns, made the brain-mapping laboratory located in the hospital isolated and semi-closed. However, these restrictions were managed by planning the time for patients to enter the study in nonpeak periods of the pandemic, as well as holding a few sessions at the patients' homes when it was not possible to attend the clinic, and most importantly, by observing health protocols during the sessions.

6. Recommendations

(i) Implementing a study with more subjects to provide the sample size needed for examining secondary variables of this study, such as corticospinal excitability

(ii) Comparing the effectiveness of AOT of meaningful and selected activities with AOT of nonselected and less meaningful activities, as well as comparing these two with a combination of them

(iii) Using patients themselves and their healthy limbs as models in producing videos of activities through graphic technologies

(iv) Investigating the method of meaningful action observation in the form of novel technologies such as virtual reality (VR) systems that can provide patients with various environments and meaningful activities

(v) Studying the effects of simple observation of the activities without execution in patients with very low motor function as an adjunct therapy in the early stages of stroke

7. Conclusion

Meaningful action observation training could possibly enhance the effects of activity/occupation-based interventions on occupational performance and satisfaction, as well as cortical-spinal excitability. This method of AOT seemed to be innovative, client-centered, and affecting neuroplasticity. However, it might not make much difference in improving the effectiveness of activity/occupation-based interventions on upper limb motor recovery and functions of the impaired upper limb in patients with chronic stroke.

Data Availability

The data gathered in this research could be reached on request from the corresponding author.

Ethical Approval

This study was ethically approved by the Ethics Committee of Iran University of Medical Sciences, Tehran, Iran (Ethical Code: IR.IUMS.REC.1397.840), and the RCT protocol was registered with the IRCT20160808029260N2 code.

Consent

The subjects signed a written informed consent before participating in this study.

Conflicts of Interest

The authors did not declare any conflict of interest.

Authors' Contributions

All authors equally contributed to preparing this article.

Acknowledgments

We would like to thank the stroke patients who had a great cooperation during this study. This research was supported by the Iran University of Medical Sciences (IUMS) as a part of occupational therapy doctoral thesis.

References

[1] M. P. Lindsay, B. Norrving, R. L. Sacco et al., "World stroke organization (WSO): global stroke fact sheet 2019," *International Journal of Stroke*, vol. 14, no. 8, pp. 806–817, 2019.

[2] F. Lanas and P. Seron, "Facing the stroke burden worldwide," *The Lancet Global Health*, vol. 9, no. 3, pp. e235–e236, 2021.

[3] E. M. Steultjens, J. Dekker, L. M. Bouter, J. C. Van de Nes, E. H. Cup, and C. H. Van den Ende, "Occupational therapy for stroke Patients," *Stroke*, vol. 34, no. 3, pp. 676–687, 2003.

[4] D. Kim, "The effects of hand strength on upper extremity function and activities of daily living in stroke patients, with a focus on right hemiplegia," *Journal of Physical Therapy Science*, vol. 28, no. 9, pp. 2565–2567, 2016.

[5] P. Langhorne, J. Bernhardt, and G. Kwakkel, "Stroke rehabilitation," *Lancet*, vol. 377, no. 9778, pp. 1693–1702, 2011.

[6] D. F. Edwards, M. Hahn, C. M. Baum, and A. W. Dromerick, "The impact of mild stroke on meaningful activity and life satisfaction," *Journal of stroke and cerebrovascular diseases*, vol. 15, no. 4, pp. 151–157, 2006.

[7] C. M. Stinear, "Stroke rehabilitation research needs to be different to make a difference," *F1000Research*, vol. 5, p. 1467, 2016.

[8] K. S. Hayward, S. F. Kramer, V. Thijs et al., "A systematic review protocol of timing, efficacy and cost effectiveness of upper limb therapy for motor recovery post-stroke," *Systematic reviews*, vol. 8, no. 1, p. 187, 2019.

[9] G. Buccino, A. Molinaro, C. Ambrosi et al., "Action observation treatment improves upper limb motor functions in children with cerebral palsy: a combined clinical and brain imaging study," *Neural Plasticity*, vol. 2018, Article ID 4843985, 11 pages, 2018.

[10] L. R. Borges, A. B. Fernandes, L. P. Melo, R. O. Guerra, T. F. Campos, and Cochrane Stroke Group, "Action observation

for upper limb rehabilitation after stroke," *Cochrane Database of Systematic Reviews*, vol. 2018, no. 10, 2018.

[11] M.-H. Zhu, J. Wang, X.-D. Gu et al., "Effect of action observation therapy on daily activities and motor recovery in stroke patients," *International Journal of Nursing Sciences*, vol. 2, no. 3, pp. 279–282, 2015.

[12] G. Buccino, F. Binkofski, G. R. Fink et al., "Action observation activates premotor and parietal areas in a somatotopic manner: an fMRI study," *European journal of neuroscience*, vol. 13, no. 2, pp. 400–404, 2001.

[13] B. Buchignani, E. Beani, V. Pomeroy et al., "Action observation training for rehabilitation in brain injuries: a systematic review and meta-analysis," *BMC Neurology*, vol. 19, no. 1, p. 344, 2019.

[14] J. M. Kilner, J. L. Marchant, and C. D. Frith, "Relationship between activity in human primary motor cortex during action observation and the mirror neuron system," *PLoS One*, vol. 4, no. 3, article e4925, 2009.

[15] K. A. Garrison, C. J. Winstein, and L. Aziz-Zadeh, "The mirror neuron system: a neural substrate for methods in stroke rehabilitation," *Neurorehabilitation and neural repair*, vol. 24, no. 5, pp. 404–412, 2010.

[16] D. Carvalho, S. Teixeira, M. Lucas et al., "The mirror neuron system in post-stroke rehabilitation," *International archives of medicine*, vol. 6, no. 1, p. 41, 2013.

[17] S. Liew, K. Garrison, J. Werner, and L. Aziz-Zadeh, "The mirror neuron system: innovations and implications for occupational therapy," *OTJR: Occupation, participation and health*, vol. 32, no. 3, pp. 79–86, 2012.

[18] L. Fogassi, P. F. Ferrari, B. Gesierich, S. Rozzi, F. Chersi, and G. Rizzolatti, "Parietal lobe: from action organization to intention understanding," *Science*, vol. 308, no. 5722, pp. 662–667, 2005.

[19] M. Y. Lee and J. S. Kim, "A comparison of the activation of mirror neurons induced by action observation between simple and complex hand movement," *The Journal of Korean Physical Therapy*, vol. 31, no. 3, pp. 157–160, 2019.

[20] D. Lee, H. Roh, J. Park, S. Lee, and S. Han, "Drinking behavior training for stroke patients using action observation and practice of upper limb function," *Journal of physical therapy science*, vol. 25, no. 5, pp. 611–614, 2013.

[21] M. Franceschini, M. G. Ceravolo, M. Agosti et al., "Clinical relevance of action observation in upper-limb stroke rehabilitation: a possible role in recovery of functional dexterity. A randomized clinical trial," *Neurorehabilitation and neural repair*, vol. 26, no. 5, pp. 456–462, 2012.

[22] D. Ertelt, S. Small, A. Solodkin et al., "Action observation has a positive impact on rehabilitation of motor deficits after stroke," *NeuroImage*, vol. 36, pp. T164–T173, 2007.

[23] T. Cowles, A. Clark, K. Mares, G. Peryer, R. Stuck, and V. Pomeroy, "Observation-to-imitate plus practice could add little to physical therapy benefits within 31 days of stroke: translational randomized controlled trial," *Neurorehabilitation and Neural Repair*, vol. 27, no. 2, pp. 173–182, 2013.

[24] D. Nilsen, G. Gillen, M. Arbesman, and D. Lieberman, "Occupational therapy interventions for adults with stroke," *American Journal of Occupational Therapy*, vol. 69, no. 5, pp. 6905395010p1–6905395010p3, 2015.

[25] J. J. Zhang, K. N. Fong, N. Welage, and K. P. Liu, "The activation of the mirror neuron system during action observation and action execution with mirror visual feedback in stroke: a systematic review," *Neural plasticity*, vol. 2018, Article ID 2321045, 14 pages, 2018.

[26] P. Celnik, B. Webster, D. M. Glasser, and L. G. Cohen, "Effects of action observation on physical training after stroke," *Stroke*, vol. 39, no. 6, pp. 1814–1820, 2008.

[27] A. Bhasin, M. P. Srivastava, S. S. Kumaran, R. Bhatia, and S. Mohanty, "Neural interface of mirror therapy in chronic stroke patients: a functional magnetic resonance imaging study," *Neurology India*, vol. 60, no. 6, pp. 570–576, 2012.

[28] Y. Sun, W. Wei, Z. Luo, H. Gan, and X. Hu, "Improving motor imagery practice with synchronous action observation in stroke patients," *Topics in Stroke Rehabilitation*, vol. 23, no. 4, pp. 245–253, 2016.

[29] E.-J. Kuk, J.-M. Kim, D.-W. Oh, and H.-J. Hwang, "Effects of action observation therapy on hand dexterity and EEG-based cortical activation patterns in patients with post-stroke hemiparesis," *Topics in stroke rehabilitation*, vol. 23, no. 5, pp. 318–325, 2016.

[30] J. M. Ferguson and C. A. Trombly, "The effect of added-purpose and meaningful occupation on motor learning," *American Journal of Occupational Therapy*, vol. 51, no. 7, pp. 508–515, 1997.

[31] C. A. Trombly, "Occupation: purposefulness and meaningfulness as therapeutic mechanisms," *American Journal of Occupational Therapy*, vol. 49, no. 10, pp. 960–972, 1995.

[32] S. Barreca, C. Gowland, P. Stratford et al., "Development of the Chedoke Arm and Hand Activity Inventory: theoretical constructs, item generation, and selection," *Topics in stroke rehabilitation*, vol. 11, no. 4, pp. 31–42, 2004.

[33] N. N. Ansari, S. Naghdi, S. Hasson, L. Valizadeh, and S. Jalaie, "Validation of a Mini-Mental State Examination (MMSE) for the Persian population: a pilot study," *Applied Neuropsychology*, vol. 17, no. 3, pp. 190–195, 2010.

[34] A. Carswell, M. A. McColl, S. Baptiste, M. Law, H. Polatajko, and N. Pollock, "The Canadian Occupational Performance Measure: a research and clinical literature review," *Canadian journal of occupational therapy*, vol. 71, no. 4, pp. 210–222, 2004.

[35] E. Wressle, K. Samuelsson, and C. Henriksson, "Responsiveness of the Swedish version of the Canadian occupational performance measure," *Scandinavian Journal of Occupational Therapy*, vol. 6, no. 2, pp. 84–89, 1999.

[36] D. J. Gladstone, C. J. Danells, and S. E. Black, "The Fugl-Meyer assessment of motor recovery after stroke: a critical review of its measurement properties," *Neurorehabilitation and neural repair*, vol. 16, no. 3, pp. 232–240, 2002.

[37] M. Hejazi-Shirmard, G. Taghizadeh, A. Azad, L. Lajevardi, and M. Rassafiani, "Sensory retraining improves light touch threshold of the paretic hand in chronic stroke survivors: a single-subject A-B design," *Somatosensory & Motor Research*, vol. 37, no. 2, pp. 74–83, 2020.

[38] I.-P. Hsueh and C.-L. Hsieh, "Responsiveness of two upper extremity function instruments for stroke inpatients receiving rehabilitation," *Clinical rehabilitation*, vol. 16, no. 6, pp. 617–624, 2002.

[39] C.-L. Hsieh, I.-P. Hsueh, F.-M. Chiang, and P.-H. Lin, "Inter-rater reliability and validity of the action research arm test in stroke patients," *Age and ageing*, vol. 27, no. 2, pp. 107–113, 1998.

[40] A. W. Dromerick, D. F. Edwards, and M. Hahn, "Does the application of constraint-induced movement therapy during

acute rehabilitation reduce arm impairment after ischemic stroke?," *Stroke*, vol. 31, no. 12, pp. 2984–2988, 2000.

[41] J. Powell, A. D. Pandyan, M. Granat, M. Cameron, and D. J. Stott, "Electrical stimulation of wrist extensors in poststroke hemiplegia," *Stroke*, vol. 30, no. 7, pp. 1384–1389, 1999.

[42] J. H. Van Der Lee, H. Beckerman, G. J. Lankhorst, and L. M. Bouter, "The responsiveness of the action research arm test and the Fugl-Meyer assessment scale in chronic stroke patients," *Journal of rehabilitation medicine*, vol. 33, no. 3, pp. 110–113, 2001.

[43] J. Desrosiers, G. Bravo, R. Hébert, É. Dutil, and L. Mercier, "Validation of the box and block test as a measure of dexterity of elderly people: reliability, validity, and norms studies," *Archives of physical medicine and rehabilitation*, vol. 75, no. 7, pp. 751–755, 1994.

[44] M. Harris-Love, "Transcranial magnetic stimulation for the prediction and enhancement of rehabilitation treatment effects," *Journal of Neurologic Physical Therapy*, vol. 36, no. 2, pp. 87–93, 2012.

[45] Y. Yang, I. Eisner, S. Chen, S. Wang, F. Zhang, and L. Wang, "Neuroplasticity changes on human motor cortex induced by acupuncture therapy: a preliminary study," *Neural plasticity*, vol. 2017, Article ID 4716792, 8 pages, 2017.

[46] W. Klomjai, R. Katz, and A. Lackmy-Vallée, "Basic principles of transcranial magnetic stimulation (TMS) and repetitive TMS (rTMS)," *Annals of physical and rehabilitation medicine*, vol. 58, no. 4, pp. 208–213, 2015.

[47] T. Feix, J. Romero, H. B. Schmiedmayer, A. M. Dollar, and D. Kragic, "The grasp taxonomy of human grasp types," *IEEE Transactions on human-machine systems*, vol. 46, no. 1, pp. 66–77, 2016.

[48] A. M. Dollar, "Classifying human hand use and the activities of daily living," in *The human hand as an inspiration for robot hand development*, pp. 201–216, Springer, Champions, 2014.

[49] K. B. Lim and J. A. Kim, "Activity of daily living and motor evoked potentials in the subacute stroke patients," *Annals of Rehabilitation Medicine*, vol. 37, no. 1, p. 82, 2013.

[50] J. Fu, M. Zeng, F. Shen et al., "Effects of action observation therapy on upper extremity function, daily activities and motion evoked potential in cerebral infarction patients," *Medicine*, vol. 96, no. 42, p. e8080, 2017.

[51] J. N. Leijnse, N. H. Campbell-Kyureghyan, D. Spektor, and P. M. Quesada, "Assessment of individual finger muscle activity in the extensor digitorum communis by surface EMG," *Journal of Neurophysiology*, vol. 100, no. 6, pp. 3225–3235, 2008.

[52] Y. H. Sohn, A. Kaelin-Lang, and M. Hallett, "The effect of transcranial magnetic stimulation on movement selection," *Journal of Neurology, Neurosurgery & Psychiatry*, vol. 74, no. 7, pp. 985–987, 2003.

[53] H. J. Polatajko, "Cognitive orientation to daily occupational performance (CO-OP) approach," in *Perspectives on Human Occupations: Theories Underlying Practice Philadelphia*, pp. 183–206, FA Davis, 2017.

[54] A. Mandich and H. J. Polatajko, *Enabling Occupation in Children: the Cognitive Orientation to Daily Occupational Performance (CO-OP) Approach*, Canadian Association of Occupational Therapists, 2004.

[55] J. M. Maher, J. C. Markey, and D. Ebert-May, "The other half of the story: effect size analysis in quantitative research," *CBE—Life Sciences Education*, vol. 12, no. 3, pp. 345–351, 2013.

[56] T. J. Wolf and D. M. Nilsen, *Occupational therapy practice guidelines for adults with stroke*, American Occupational Therapy Association (AOTA), Bethesda (MD), 2015.

[57] K. M. Philip, P. Jose, S. Sh, and J. J. M. Rajagopal, "Effect of action observation therapy on recovery in upper extremity POST stroke patients," *International Journal of Pharmaceutical Science and Health*, vol. 4, no. 8, 2018.

[58] H. Mao, Y. Li, L. Tang et al., "Effects of mirror neuron system-based training on rehabilitation of stroke patients," *Brain and Behavior*, vol. 10, no. 8, article e01729, 2020.

[59] Y. W. Hsieh, Y. H. Lin, J. D. Zhu, C. Y. Wu, Y. P. Lin, and C. C. Chen, "Treatment effects of upper limb action observation therapy and mirror therapy on rehabilitation outcomes after subacute stroke: a pilot study," *Behavioural Neurology*, vol. 2020, Article ID 6250524, 9 pages, 2020.

[60] J. S. Noh, J. H. Lim, T. W. Choi, S. G. Jang, and S. B. Pyun, "Effects and safety of combined rTMS and action observation for recovery of function in the upper extremities in stroke patients: a randomized controlled trial," *Restorative neurology and neuroscience*, vol. 37, no. 3, pp. 219–230, 2019.

[61] P. Sale, M. G. Ceravolo, and M. Franceschini, "Action observation therapy in the subacute phase promotes dexterity recovery in right-hemisphere stroke patients," *BioMed Research International*, vol. 2014, Article ID 457538, 7 pages, 2014.

Hindawi
Neural Plasticity
Volume 2022, Article ID 7912410, 10 pages
https://doi.org/10.1155/2022/7912410

Research Article

Brain Network Changes in Lumbar Disc Herniation Induced Chronic Nerve Roots Compression Syndromes

Yan-Peng Zhang,[1,2] **Guang-Hui Hong**,[3] **and Chuan-Yin Zhang**[1,2]

[1]*Department of Orthopedics, Renhe Hospital, Baoshan District, Shanghai 200431, China*
[2]*Department of Orthopedics, Affiliated Renhe Hospital of Shanghai University, Shanghai 200431, China*
[3]*Department of Orthopedics, The First Affiliated Hospital of Fujian Medical University, Fujian 350005, China*

Correspondence should be addressed to Chuan-Yin Zhang; zcy333333@sina.com

Received 21 September 2021; Revised 4 January 2022; Accepted 8 April 2022; Published 14 May 2022

Academic Editor: Rongrong Lu

Lumbar disc herniation (LDH) induced nerve compression syndromes have been a prevalent problem with complex neural mechanisms. Changes in distributed brain areas are involved in the occurrence and persistence of syndromes. The present study aimed to investigate the changes of brain functional network in LDH patients with chronic sciatica using graph theory analysis. A total of thirty LDH adults presenting L4 and/or L5 root (s) compression syndromes (LDH group) and thirty age-, sex-, BMI- and education-matched healthy control (HC group) were recruited for functional MRI scan. Whole-brain functional network was constructed for each participant using Pearson's correlation. Global and nodal properties were calculated and compared between two groups, including small-worldness index, clustering coefficient, characteristic path length, degree centrality (*DC*), betweenness centrality (*BC*) and nodal efficiency. Both LDH and HC groups showed small-world architecture in the functional network of brain. However, LDH group showed that nodal centralities (*DC*, *BC* and nodal efficiency) increased in opercular part of inferior frontal gyrus; and decreased in orbital part of inferior frontal gyrus, lingual cortex and inferior occipital gyrus. The DC and efficiency in the right inferior occipital gyrus were negatively related with the Oswestry Disability Index in LDH group. In conclusion, the LDH-related chronic sciatica syndromes may induce regional brain alterations involving self-referential, emotional responses and pain regulation functions. But the whole-brain small-world architecture was not significantly disturbed. It may provide new insights into LDH patients with radicular symptoms from new perspectives.

1. Introduction

Lumbar disc herniation (LDH) is a prevalent disease caused by degenerative pathologies of lumbar intervertebral disc. Low back pain is the most common symptom with a high occurrence rate and great burden of cost [1–3]. Researches have revealed corresponding changes in the brain associated with chronic low back pain using functional magnetic resonance imaging (fMRI). Changes involved specific brain regions, functional connectivity, and properties of whole-brain network [4–9]. These studies have greatly broadened our insight into low back pain related brain alterations. However, low back pain is a highly prevalent symptom with obscure causes in most cases. Only in a minority of cases does it directly links to some defined organic disease exist. It may not be necessarily causally related with LDH neither [10–12]. Even in LDH patients who complain of low back pain, the causes for low back pain may still be unclear. In clinical practice, it is not uncommon that LDH patients merely report nerve compression symptoms without obvious existence of low back pain.

In clinical practice, many LDH patients would develop persistent radicular symptoms, while some even need to receive surgical treatment of decompression and lumbar fusion. However, not all patients reported satisfactory relief of neuropathic pain even following appropriate treatments [13, 14]. It is acknowledged that pathological changes in the peripheral nerve would lead to complex disorders

involving both peripheral and central nervous systems [15–17]. Except for the factors of peripheral nerve, maladaptive changes in the brain may also contribute to the failure of symptom relief. However, brain changes related with sciatica due to herniated nucleus pulposus have not been revealed yet. The present study aimed to explore the changes of brain at whole-brain network level specifically associated with chronic unilateral nerve root (s) compression in LDH patients by functional magnetic resonance image (fMRI). We restricted LDH patients to those who chiefly complained of radicular symptoms that affecting only one leg at the time of recruitment. Graph theoretical analysis was applied to characterize the functional connectivity between each pair of brain regions [18]. Global and nodal properties of the functional brain network were calculated to quantitively describe the network and differences of the properties were compared between LDH-induced sciatica patients and healthy controls.

2. Materials and Methods

2.1. Participants. LDH induced nerve root(s) compression patients (LDH group) were recruited according to the following inclusion criteria: (1) lumbar disc herniation diagnosed by MRI assessment; (2) chiefly complained of unilateral sciatica symptoms for at least 3 months; (3) unilateral L4 and/or L5 nerve root(s) compression confirmed by clinical symptoms [positive in straight leg raising test (SLRT)], physical examination and electrophysiological tests; (4) aged 18 or more, no gender limitation; (5) unilateral nerve compression symptoms persisted for at least 3 months; (6) no other pain except for LDH related pain; (7) no neurological deficiencies, such as visual or hearing loss; (8) no abnormal findings, such as infarction or focal lesion in brain MRI presentation, confirmed by two blinded independent radiologists. Exclusion criteria: (1) with contraindications or inability to tolerate MR scan; (2) with neurological disease or brain lesions, such as traumatic brain injury, stroke, neurodegenerative disease, brain tumor, epilepsy; (2) with psychiatric diseases, such as schizophrenia, depression, anxiety disorder before the onset of current LDH-induced radiculopathy; (3) reported a history of drug abuse or alcohol addiction; (4) for other reasons they were unsuitable to undergo MR scan.

Inclusion criteria for healthy controls (HC group): (1) aged 18 or more, no gender limitation; (2) generally healthy without a record of chronic systemic disease (e.g. diabetes mellitus, hypertension); (3) no record of neurological or psychiatric disorders, such as stroke, depression, or epilepsy; (4) no neurological deficiencies, such as visual or hearing loss; (5) no abnormal findings, such as infarction or focal lesion in brain MRI presentation, confirmed by two blinded independent radiologists. Exclusion criteria: (1) with contraindications or inability to tolerate MR scan; (2) with a history of alcohol/drug addiction; (3) unwilling to participate in the present study or already enrolled in another trial.

This study was approved by the Institutional Review Board of Renhe Hospital (No. KJ2019-06). All the participants provided written consents.

2.2. Clinical Assessments. Oswestry Disability Index (ODI) and Visual Analogue Scale (VAS) were measured in LDH patients. ODI was the standard for evaluating the severity of LDH. The score of ODI ranges from 0 to 100, with higher scores indicating more impaired function [19]. VAS measures the amount of pain that a patient feels, ranges from 0 to 10, indicating from none to extreme amount of pain [19]. It was evaluated both at rest and during SLRT (recorded at 60° of hip flexion on the symptomatic side; recorded as 10 points if the patient was unable to achieve 60°).

2.3. MR Image Acquisition. MR images were acquired with a 3.0 T MRI scanner (Siemens Verio, Erlangen, Germany). During the scan, the participants were instructed to lie still and relax with their eyes open. Foam pad and earplugs were applied to limit head motion and reduce the impact of machine noise. They were asked to keep awake and not to think about anything in particular. Resting-state fMRI were acquired axially with an echo-planar imaging (EPI) sequence according to the following protocol: repetition time (TR) = 3000 ms, echo time (TE) = 30 ms, flip angle = 90°, field of view (FOV) = $240 \times 240\ mm^2$, resolution = 64×64 matrix, slice number = 43, slice thickness = 3 mm, voxel size = $3.75 \times 3.75 \times 3\ mm^3$, gap = 0, number of volume = 240. Three-dimensional T1-weighted images were acquired with magnetization-prepared rapid gradient echo (MPRAGE) sequence with following parameters: repetition time (TR) = 1900 ms, echo time (TE) = 2.93 ms, inversion time = 900 ms, flip angle = 9°, resolution = 256×256 matrix, slice number = 160, slice thickness = 1.0 mm, voxel size = $1 \times 1 \times 1\ mm^3$.

2.4. Data Preprocessing. The brain images were preprocessed with the Data Processing Assistant for Resting-State fMRI (DPARSF) toolbox, which was based on Matlab, SPM12 (https://www.fil.ion.ucl.ac.uk/spm), and DPABI [20]. In patients with right leg affected, brains were left-to-right flipped so that the affected side of brain were localized to one side of the hemisphere [21, 22]. The first 10 volumes of functional images were discarded to allow for adaptation to the signal stabilization. The remaining 190 volumes were corrected for different slice acquisition times with the middle image of each repetition time (TR) as reference. Head motion with the Friston 24-parameter method and nuisance signals of white matter, cerebrospinal fluid and head-motion parameters were regressed out [23]. Structural T1 images were segmented for coregisteration of functional images, which were then normalized to the Montreal Neurological Institute (MNI) space using Diffeomorphic Anatomical Registration Through Exponentiated Lie Algebra (DARTEL). The functional images were resampled to 3 mm isotropic voxels and spatially smoothed with 6 mm full width at half maximum (FWHM) Gaussian kernel. The normalized function images were temporally filtered with 0.01-0.1 Hz bandpass to reduce physiological noises and low frequency drifting. Images with head motion of >3 mm translation or> 3°rotation were excluded from the study.

2.5. Network Construction and Graph Theoretical Analysis. The cortical and subcortical areas of the whole brain were

parcellated into 90 regions of interest (ROIs) based on the prior atlas of Anatomical Automatic Labeling (AAL) [24]. These 90 ROIs were defined as nodes of the network. The mean time series of each ROI was extracted and the correlation between each pair of nodes represented edges. The correlations coefficient (r-value) between each pair of ROIs was calculated with Pearson's correlation measure. The r-values were transformed to z-values with Fisher's z transformation to obtain near-normally-distributed data. An adjacency matrix of z-values was constructed for each subject and binary undirected connectivity network was then obtained with selected thresholds (sparsity). The sparsity was set from 10% to 46% with an interval step of 0.01 [25]. Topological properties of the network were calculated based on the network.

2.6. Network Properties. Global properties included: clustering coefficient (C_p), characteristic path length (L_p), normalized clustering coefficient (γ), normalized characteristic path length (λ) and small-worldness (σ). Nodal properties included: degree centrality (*DC*), betweenness centrality (*BC*), and efficiency (*E*) of a given node (Detailed definition, equations and clinical implications of these properties have been included in the Supplemental Materials (Supplementary Table S1) [26, 27]. The functional networks of whole brain were constructed with GRETNA (v2.0.0) toolbox (https://www.nitrc.org/projects/gretna) [28].

2.7. Statistical Analysis. Two-sample t-test and Chi-squared test were applied in the comparison of demographic characteristics between two groups. The area under the curve (AUC) of properties and nodal properties between two groups were compared with nonparametric permutation tests [29]. The significance level was set at $p < 0.05$ in the analysis of global properties, while in nodal properties set at $p < 0.05$ after false discovery rate (FDR) correction for multiple comparison.

2.8. Correlation Analysis. For properties showing significant between-group differences, partial correlation analysis was performed between these properties and clinical variable (ODI and VAS) in the LDH group. The effects of age and sex were controlled. Software SPSS (V21, SPSS Inc., Chicago, IL, USA) was used.

3. Results

3.1. Characteristics of Participants. Thirty LDH induced nerve compression patients (LDH group) (56.3 ± 9.7 yrs) and thirty HC subjects (HC group) (55.0 ± 12.3 yrs) were enrolled in the analysis (Table 1). Age, sex, body mass index (BMI), and education level (low education: junior middle school or below; high education: senior high school or higher) were comparable between two groups (all $p > 0.05$). In the LDH group, L4 nerve root was involved in six patients, L5 in twenty patients, while both L4 and L5 were involved in the rest four patients. LDH patients received conservative treatments, including oral medicine (neurotrophic drug on a regular basis; NSAIDS or opiates as needed), lying flat, physical therapy, lumbar traction or traditional Chinese treatments (e.g. acupuncture, herbal medicine). But these patients still complained of radicular symptoms at enrollment.

Table 1: Demographic characteristic of the lumbar disc hernia induced unilateral lumbar nerve root compression and healthy control groups.

Characteristics	LDH (n = 30)	HC (n = 30)	*p*-value
Male sex - no. (%)	19 (63.3%)	17 (56.7%)	0.598[a]
Age -yr	56.3 ± 9.7	55.0 ± 12.3	0.635[b]
BMI – Kg/m^2	23.46 ± 3.07	22.27 ± 2.39	0.099[b]
Education			
Low education	10	14	0.292[a]
High education	20	16	
Affected root(s)			
L4	6	—	—
L4 and L5	4	—	—
L5	20	—	—
Affected side			
Left	17	—	—
Right	13	—	—
Duration (month)	5.4 ± 2.4	—	
ODI	65.93 ± 11.46	—	
VAS at rest	3.67 ± 0.99	—	
VAS during SLRT	6.67 ± 0.96	—	

LDH: lumbar disc herniation; HC: healthy control; BMI: body mass index; ODI: Oswestry Disability Index; VAS: Visual Analogous Scale; SLRT: Straight Leg Raising Test. Low education: junior middle school or below; high education: senior high school or higher. [a]Chi-square test; [b]two-sample t-test.

3.2. Clinical Assessments. All patients reported moderate or severe symptoms with unilateral side involved. Left side was affected in seventeen patients, while right side in the rest thirteen patients. The average ODI score was 65.93 ± 11.46. All our patients were able to achieve 60 degree of hip flexion during SLRT. The VAS score was 3.67 ± 0.99 at rest and 6.67 ± 0.96 during SLRT, respectively.

3.3. Global Properties. Over the sparsity range of 0.05-0.46, both LDH and HC groups showed small-world topology of functional network, which was characterized by normalized clustering coefficient (γ)$> > 1$, normalized characteristic path length (λ) ≈ 1, and small-worldness (σ) $= \gamma/\lambda > 1$. No significant difference was found in γ, λ, σ, C_p, and L_p by comparing area under curve (AUC) between groups (all $p > 0.05$) (Figure 1). Results without flipping procedure see Supplemental Materials (Supplementary Figure S1).

3.4. Nodal Properties. Compared with HCs, the LDH group showed increased betweenness centrality (*BC*) in right inferior frontal gyrus (orbital part) (ORBinf.R); and no decreased *BC* (Figure 2(a), Table 2). LDH group showed increased degree centrality (*DC*) in left inferior frontal gyrus, opercular part (IFGoperc.L); and decreased *DC* in left lingual gyrus (LING.L) and right inferior occipital gyrus (IOG.R) (Figure 2(b), Table 3). Nodal efficiency increased

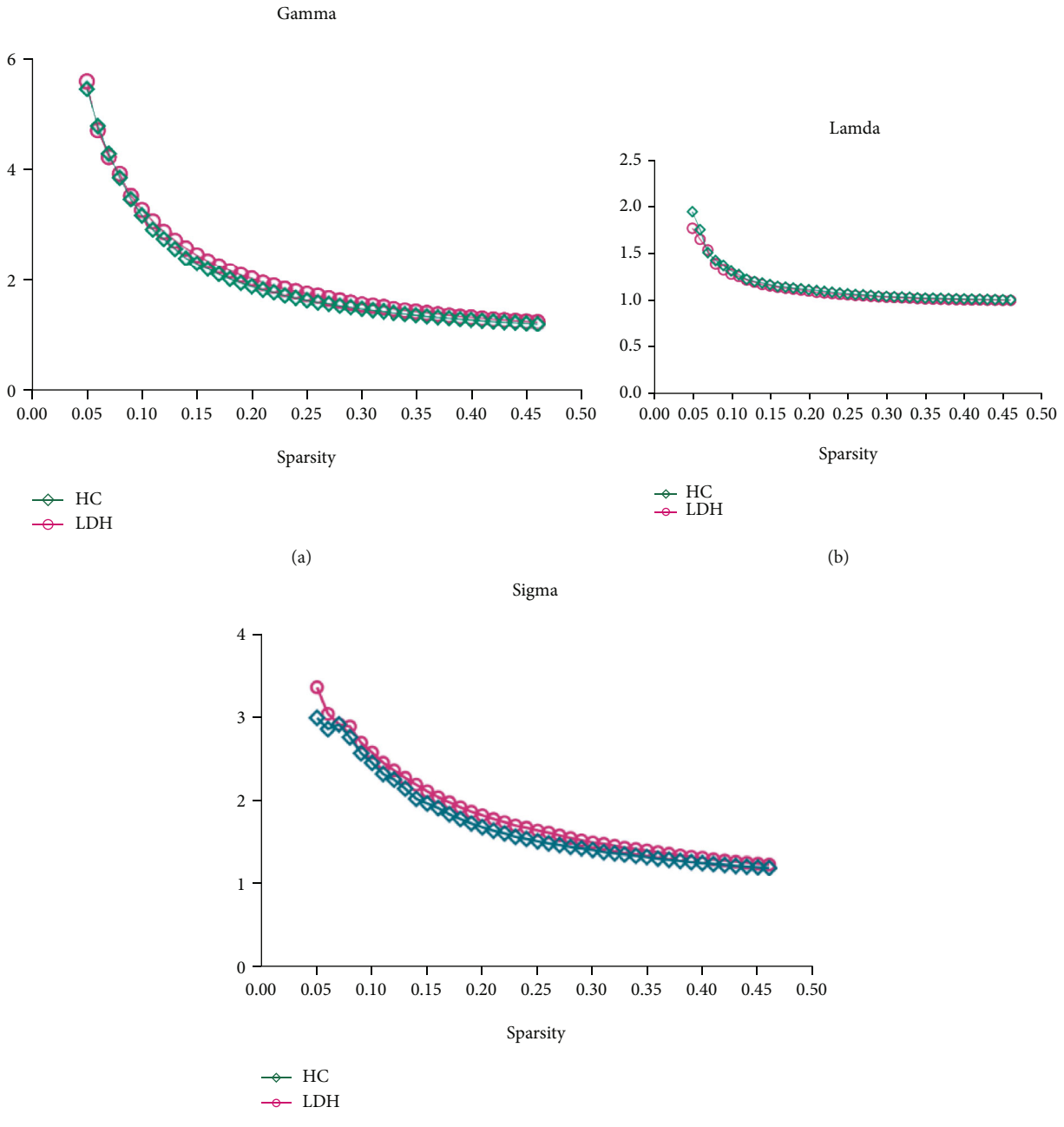

Figure 1: Continued.

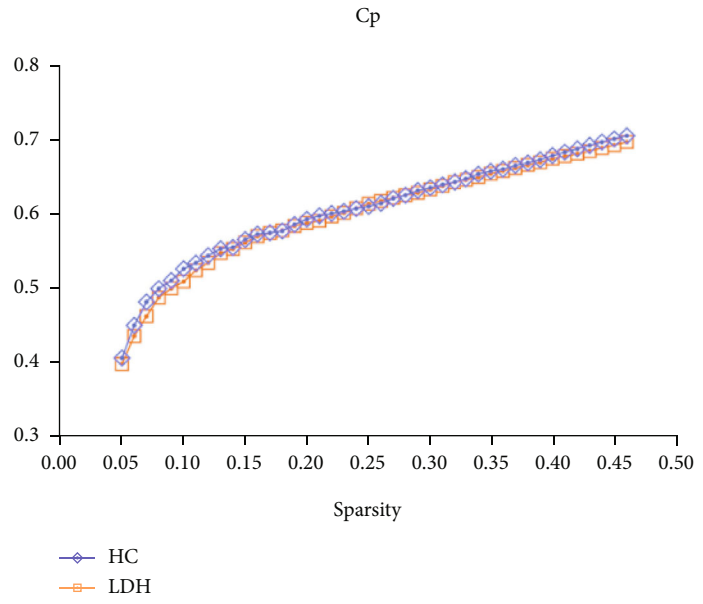

(d)

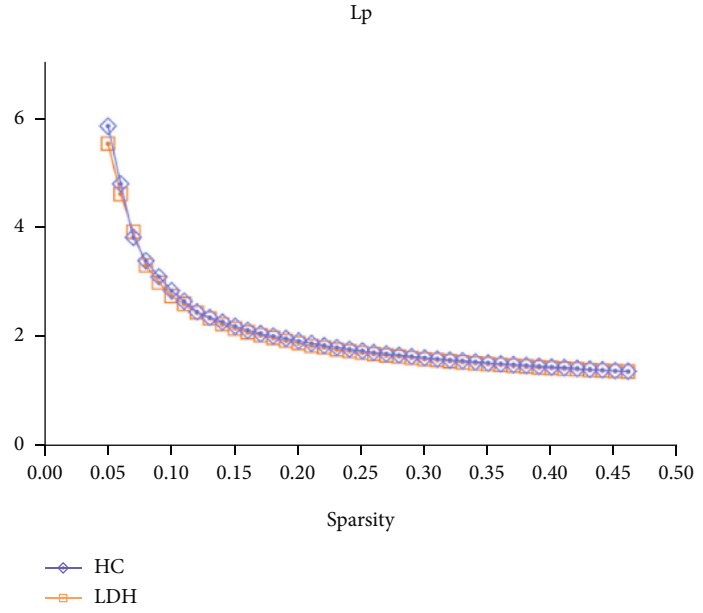

(e)

Figure 1: Changes of small-world parameters, clustering coefficient (C_p) and characteristic path length (L_p) in the lumbar disc herniation induce nerve root compression patients and healthy controls as sparsity ranged from 0.1 to 0.46. No significant difference was found between two groups in the normalized clustering coefficients (γ) (a), normalized characteristic path length (λ) (b). small-worldness (σ) (C), clustering coefficient (D) and characteristic path length (E) over a sparsity range of 0.1-0.46 (all $p > 0.05$).

in left inferior frontal gyrus, opercular part (IFGoperc.L); and decreased in left lingual gyrs (LING.L) and right inferior occipital gyrus (IOG.R) (Figure 2(c), Table 4). Results without flipping procedure see Supplemental Materials (Supplementary Figure S2, Supplementary Tables S2–4).

3.5. Correlation Analysis. Significant partial correlation was found between DC in IOG. R and ODI ($r = -0.412$, $p = 0.029$), E in IOG.R and ODI ($r = -0.464$, $p = 0.013$) (Figure 3). No significant correlation was found in the rest network properties showing significant between-group differences and clinical variables.

4. Discussion

LDH is a common pathology that causes a series of symptoms, including chronic low back pain, radicular leg pain, weakness, and paresthesia in affected area [30, 31]. As the brain is capable of adapting to abnormal physical status, complicated changes would occur in the brain associated

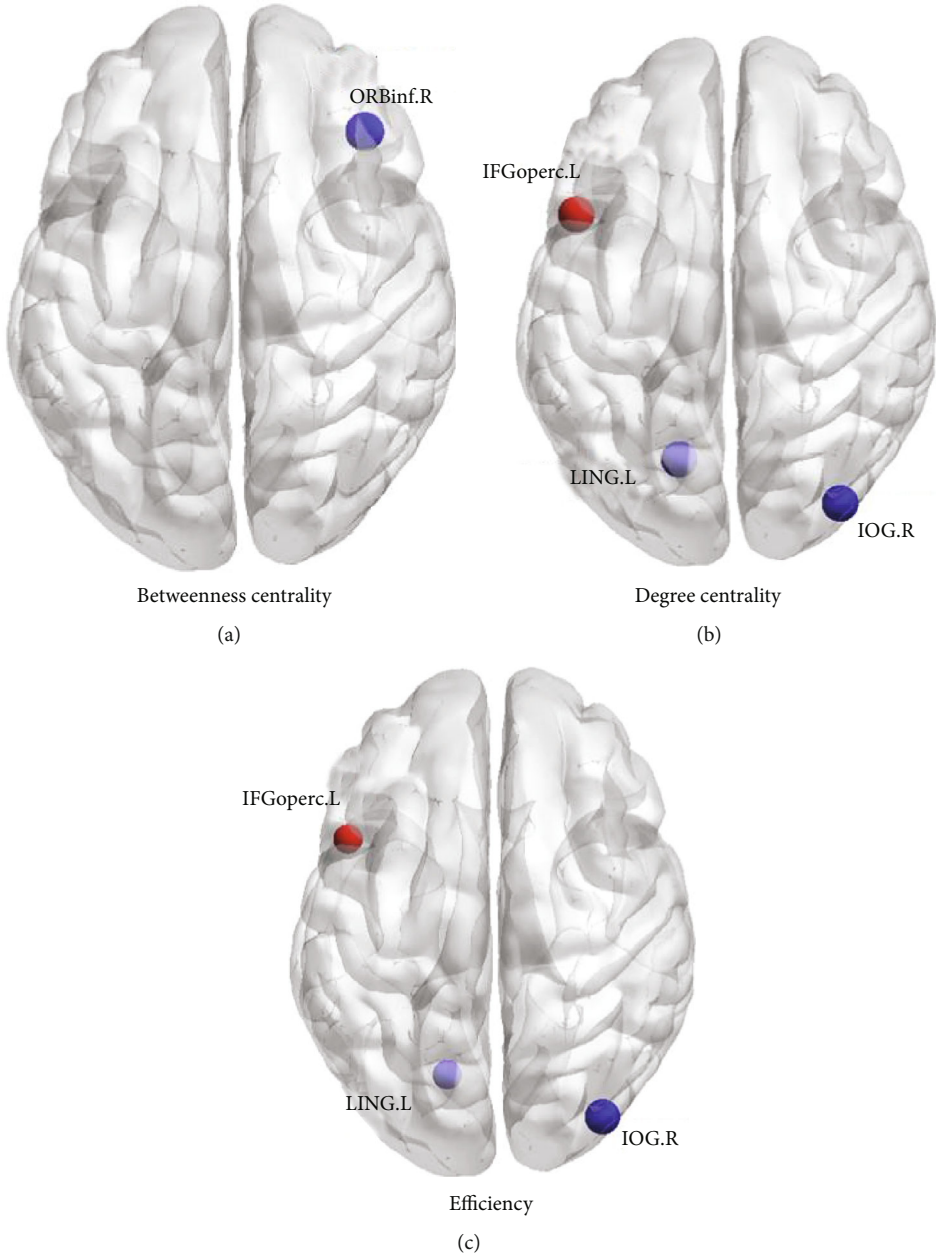

Figure 2: Differences of betweenness centrality (*BC*) (A), degree centrality (*DC*) (B) and efficiency (*E*) (C) of a node between lumbar disc herniation (LDH) induced nerve root(s) compression patients and healthy control subjects. The red balls represent increased values of nodal properties in the LDH group while the blue balls represent decreased, compared with the healthy control (HC) group. The size of ball represents significance, with bigger balls indicating smaller *p*-values. R: right; L: left; ORBinf: inferior frontal gyrus, orbital part; IFGoperc: inferior frontal gyrus, opercular part; LING: lingual gyrus; IOG: inferior occipital gyrus.

Table 2: Brain regions with significant different betweenness centrality (BC) between LDH induced nerve root(s) compression and healthy control groups.

Brain region	*p*-value (uncorrected)
HC > LDH	
ORBinf.R	0.001

LDH: lumbar disc herniation; HC: healthy control; R: right; ORBinf: inferior frontal gyrus, orbital part.

with LDH induced symptoms. Accumulating researches have also provided evidence that pathology-specific brain alterations play a crucial role in the occurrence and maintenance of pain, especially chronic pain [32–36]. Previous studies have confirmed the involvement of brain plasticity in LDH patients. Shishi et al. demonstrated whole-brain network disruption in degree, clustering coefficient, and efficiency in patients with LDH-related chronic pain (including chronic low back pain and/or leg pain), indicating decreased hubness, segregation and integration [5]. According to Jing et al., individuals with low back pain due to LDH showed

Table 3: Brain regions with significant different degree centrality (DC) between LDH induced nerve root(s) compression and healthy control groups.

Brain region	p-value (uncorrected)
HC > LDH	
LING.L	0.001
IOG.R	0.001
LDH > HC	
IFGoperc.L	0.001

LDH: lumbar disc herniation; HC: healthy control; R: right; L: left; LING: lingual gyrus; IOG: inferior occipital gyrus; IFGoperc: inferior frontal gyrus, opercular part.

Table 4: Brain regions with significant different efficiency of a given node between LDH induced nerve root(s) compression and healthy control groups.

Brain region	p-value (uncorrected)
HC > LDH	
LING.L	0.003
IOG.R	0.001
LDH > HC	
IFGoperc.L	0.003

LDH: lumbar disc herniation; HC: healthy control; R: right; L: left; LING: lingual gyrus; IOG: inferior occipital gyrus; IFGoperc: inferior frontal gyrus, opercular part.

significantly longer characteristic path length and lower clustering coefficient, global efficiency and local efficiency. They also showed decreased functional connectivity in several brain regions including anterior cingulate cortex, middle cingulate cortex, et al [6]. However, they did not restrict investigations to LDH patients with unilateral radicular symptoms related with nerve root(s) compression.

The present study focused on patients with chronic radicular symptoms induced by LDH, which has not been investigated yet. Specifically, graph theory was applied in the analysis of resting-state fMRI data. Both LDH-induced sciatica patients and HC showed small-world architecture in the functional brain network at the global level. No significant change of global properties was found in LDH group under a wide range of sparsity thresholds. A small-world network is supposed to be more efficient in information transfer either than the regular or the random network. It was used to characterize a balance between global and local efficiency of information transfer [18, 37]. Therefore, the properties of small-world were not significantly interrupted in these LDH-induced sciatica patients under selected range of sparsities. The results implied that these patients still showed efficient small-world architecture, which was optimal balance of segregation and integration. Human brain is a complex interconnected network. Although 1-2 lumbar nerve roots were in pathological status, the whole brain still organized well in a large scale. It may be due to the capability of the whole brain network to compensate the disturbance of local peripheral nerve roots.

However, abnormal nodal properties were still found in several brain regions in LDH group compared with healthy controls. The nodal properties BC, DC and nodal efficiency represents the importance of a given node in the regional or global network. Specifically, BC characterizes the effect of a given node on information flow between other nodes; DC reflects the information communication ability of a node in the functional network; the nodal efficiency characterizes the efficiency of parallel information transfer of that node in the network.

In the present study, nodal centralities increased in a node located in the frontoparietal network (IFGoperc.L); while decreased in the default mode network (DMN) (ORBinf.R) and visual network (lingual gyrus and inferior occipital gyrus) [38]. The brain DMN composes of a wide range of brain regions, primarily including medial prefrontal cortex (mPFC), posterior cingulate cortex (PCC), and inferior parietal lobule (IPL) [39, 40]. It describes the baseline state of neural activities in the brain which is related with self-related mental activities [41]. Increase in regional neural activity and functional connectivity in DMN were found related with depression [42, 43]. Occipital cortex regions, including calcarine fissure and lingual gyrus were noted showing LDH-related decrease in nodal centralities. According to literature reviewer, lingual gyrus was also involved in the process of pain [44, 45]. Therefore, the present study indicated strengthened coordinating role of several brain regions in these patients, involving functions of self-referential activities and pain modulation. Nodal centralities increase was found in the LDH group in regions within the frontoparietal network (IFGoperc.L) [38]. Frontoparietal network and its functional connectivity with insula were related with emotion regulation [46]. Increased nodal centralities in this region suggested potential compensation in LDH-induced sciatica patients on pain and emotional regulation functions. It may also be a compensation to the abnormal signal afferent of peripheral nerve in pathological status such as nerve compression syndromes. However, the exact relationship between abnormal nodal properties and psychomental status need further explorations. Future studies involving specific scales that representing different aspects of the mind status would be worthwhile.

In the correlation analysis, after controlling the effects of age and sex, we only noted significant negative correlation between ODI and DC in IOG.R, E in IOG.R. No significant correlation was found between clinical variables and other abnormal network properties in the LDH group. It implied correlation of altered nodal properties in IOG.R with clinical performance.

There are still several issues need to be further addressed in future studies. A larger sample size of participants need to be included in future researches to enhance the power of statistics. Altered properties related with intervention and its predictive effects in prognoses also need exploration. The structure network and its relation with functional network would be an important supplement to this field. However, the present study still brought us deeper insights into brain functioning in LDH-induced radiculopathy form the aspect of network. Brain regions with significantly changed local

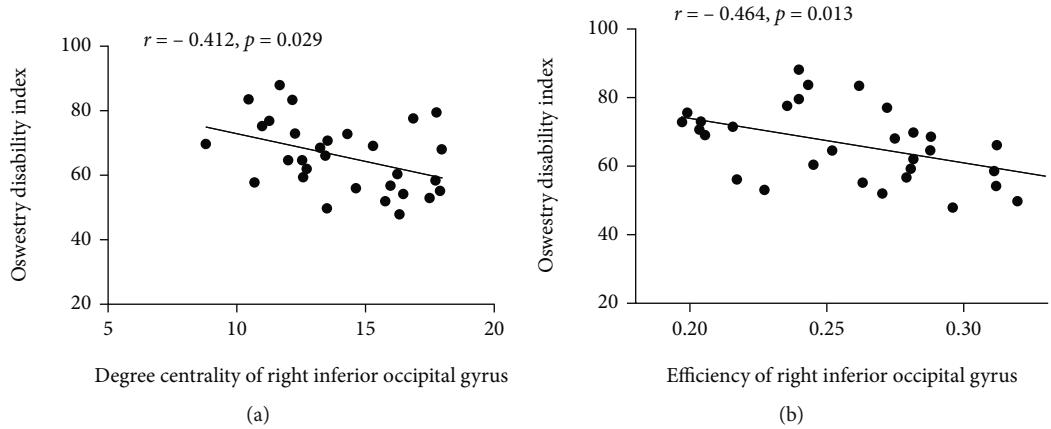

Figure 3: Correlation between Owestry Disability Index and degree centrality and efficiency of right inferior occipital gyrus. Partial correlation analysis indicated positive correlation between Owestry Disability Index and degree centrality of right inferior occipital gyrus (r = -0.412, p = 0.029), as well as between Owestry Disability Index and efficiency of right inferior occipital gyrus (r = -0.464, p = 0.013) while controlling the effects of age and sex.

properties can be potential targets for future intervention, such as neuromodulation.

5. Limitations

As it was an observational study comparing LDH patients with healthy controls, randomization was inapplicable in the assignment of participants. While the confounding factors were controlled, there might be potential bias due to subject selection. As the effects of oral medicine were inevitable in the present clinical study, further researches (eg, experimental studies) with confounding factors controlled are needed to provide supplement evidence.

6. Conclusions

The present study constructed functional network of brain by resting-state fMRI for lumbar disc herniation (LDH) induced chronic nerve root compression patients and healthy controls. Graph theoretical analysis was used to investigate global and local properties of the brain. Both groups showed small-world architecture but no between-group difference was found in small-world measures. The LDH groups exhibited decreased nodal centralities in nodes of limbic, ventral attentional and frontoparietal networks; while increased nodal centralities mainly in nodes of default mode and visual networks. The study provided greater insights into brain network alterations related with LDH-induced chronic sciatica syndromes. A better understanding of brain plasticity may help us in decision making regarding the treatment strategies such as oral medication or surgery. Finally, the sample size was relatively small. In our future work, investigations with a larger sample size are still needed to draw a more convincing conclusion.

Data Availability

The data of the present study would be available from the corresponding author upon request.

Conflicts of Interest

The authors declare that they have no conflict of interest to disclose.

Authors' Contributions

Yan-Peng Zhang and Guang-Hui Hong contributed equally to this work.

Funding

This work was supported by Science and Technology Committee of Shanghai Baoshan District [grant number: 19-E-39].

Supplementary Materials

Figure S1: Changes of small-world parameters, clustering coefficient (Cp) and characteristic path length (Lp) in the lumbar disc herniation induce nerve root compression patients and healthy controls as sparsity ranged from 0.1 to 0.46. Figure S2: Differences of betweenness centrality (BC), degree centrality (DC) and efficiency between lumbar disc herniation (LDH) induced nerve root(s) compression patients and healthy control subjects. Table S1: The definition, equation and clinical implication of network properties. Table S2: Brain regions with significant different betweenness centrality (BC) between LDH induced nerve root(s) compression and healthy control groups. Table S3: Brain regions with significant different degree centrality (DC) between LDH induced nerve root(s) compression and healthy control groups. Table S4: Brain regions with significant different efficiency (E) of a given node between LDH induced nerve root(s) compression and healthy control groups. *(Supplementary Materials)*

References

[1] B. I. Martin, R. A. Deyo, S. K. Mirza et al., "Expenditures and health status among adults with Back and neck problems," *JAMA*, vol. 299, no. 6, pp. 656–664, 2008.

[2] S. P. Cohen, L. Vase, and W. M. Hooten, "Chronic pain: an update on burden, best practices, and new advances," *Lancet*, vol. 397, no. 10289, pp. 2082–2097, 2021.

[3] G. B. Andersson, "Epidemiological features of chronic low-Back pain," *The Lancet*, vol. 354, no. 9178, pp. 581–585, 1999.

[4] W. Li, Y. Gong, J. Liu et al., "Peripheral and Central Pathological Mechanisms of Chronic Low Back Pain: A Narrative Review," *Journal of Pain Research*, vol. 14, pp. 1483–1494, 2021.

[5] S. Huang, K. Wakaizumi, B. Wu et al., "Whole-brain functional network disruption in chronic pain with disk herniation," *Pain*, vol. 160, no. 12, pp. 2829–2840, 2019.

[6] J. Liu, F. Zhang, X. Liu et al., "Altered small-world, functional brain networks in patients with lower Back pain," *Science China Life Sciences*, vol. 61, no. 11, pp. 1420–1424, 2018.

[7] M. Luchtmann, Y. Steinecke, S. Baecke et al., "Structural Brain Alterations in Patients with Lumbar Disc Herniation: A Preliminary Study," *PLoS One*, vol. 9, no. 3, article e90816, 2014.

[8] M. N. Baliki, D. R. Chialvo, P. Y. Geha et al., "Chronic pain and the emotional brain: specific brain activity associated with spontaneous fluctuations of intensity of chronic Back pain," *Journal of Neuroscience*, vol. 26, no. 47, pp. 12165–12173, 2006.

[9] E. Tagliazucchi, P. Balenzuela, D. Fraiman, and D. R. Chialvo, "Brain resting state is disrupted in chronic Back pain patients," *Neuroscience Letters*, vol. 485, no. 1, pp. 26–31, 2010.

[10] N. N. Knezevic, K. D. Candido, J. W. S. Vlaeyen, J. Van Zundert, and S. P. Cohen, "Low Back pain," *The Lancet*, vol. 398, no. 10294, pp. 78–92, 2021.

[11] C. Maher, M. Underwood, and R. Buchbinder, "Non-specific low Back pain," *The Lancet*, vol. 389, no. 10070, pp. 736–747, 2017.

[12] J. Hartvigsen, M. J. Hancock, A. Kongsted et al., "What low Back pain is and why we need to pay attention," *The Lancet*, vol. 391, no. 10137, pp. 2356–2367, 2018.

[13] P. Försth, G. Ólafsson, T. Carlsson et al., "A randomized, controlled trial of fusion surgery for lumbar spinal stenosis," *The New England Journal of Medicine*, vol. 374, no. 15, pp. 1413–1423, 2016.

[14] T. Sinmaz and N. Akansel, "Experience of Pain and Satisfaction with Pain Management in Patients After a Lumbar Disc Herniation Surgery," *Journal of PeriAnesthesia Nursing*, vol. 36, 2021.

[15] K. S. Taylor, D. J. Anastakis, and K. D. Davis, "Cutting your nerve changes your brain," *Brain*, vol. 132, no. 11, pp. 3122–3133, 2009.

[16] Y. Maeda, N. Kettner, J. Kim et al., "Primary somatosensory/motor cortical thickness distinguishes paresthesia-dominant from pain-dominant carpal tunnel syndrome," *Pain*, vol. 157, no. 5, pp. 1085–1093, 2016.

[17] Y. Maeda, N. Kettner, J. Holden et al., "Functional deficits in carpal tunnel syndrome reflect reorganization of primary somatosensory cortex," *Brain*, vol. 137, no. 6, pp. 1741–1752, 2014.

[18] D. J. Watts and S. H. Strogatz, "Collective dynamics of 'Small-World' networks," *Nature*, vol. 393, no. 6684, pp. 440–442, 1998.

[19] B. Strömqvist, P. Fritzell, O. Hägg, and B. Jönsson, "The Swedish Spine Register: Development, Design and Utility," *European Spine Journal*, vol. 18, Supplement 3, pp. 294–304, 2009.

[20] C. G. Yan, X. D. Wang, X. N. Zuo, and Y. F. Zang, "DPABI: Data Processing & Analysis for (resting-state) brain imaging," *Neuroinformatics*, vol. 14, no. 3, pp. 339–351, 2016.

[21] P. G. Mihai, M. Otto, M. Domin, T. Platz, S. Hamdy, and M. Lotze, "Brain Imaging Correlates of Recovered Swallowing After Dysphagic Stroke: A fMRI and DWI Study," *NeuroImage: Clinical*, vol. 12, pp. 1013–1021, 2016.

[22] M. Lotze, W. Beutling, M. Loibl et al., "Contralesional motor cortex activation depends on Ipsilesional corticospinal tract integrity in well-recovered subcortical stroke patients," *Neurorehabilitation and Neural Repair*, vol. 26, no. 6, pp. 594–603, 2012.

[23] K. J. Friston, S. Williams, R. Howard, R. S. Frackowiak, and R. Turner, "Movement-related effects in fMRI time-series," *Magnetic Resonance in Medicine*, vol. 35, no. 3, pp. 346–355, 1996.

[24] N. Tzourio-Mazoyer, B. Landeau, D. Papathanassiou et al., "Automated anatomical labeling of activations in SPM using a macroscopic anatomical Parcellation of the MNI MRI single-subject brain," *NeuroImage*, vol. 15, no. 1, pp. 273–289, 2002.

[25] W. W. Wang, Y. C. Lu, W. J. Tang et al., "Small-Worldness of brain networks after brachial plexus injury: a resting-state functional magnetic resonance imaging study," *Neural Regeneration Research*, vol. 13, no. 6, pp. 1061–1065, 2018.

[26] M. Rubinov and O. Sporns, "Complex network measures of brain connectivity: uses and interpretations," *NeuroImage*, vol. 52, no. 3, pp. 1059–1069, 2010.

[27] O. Sporns, "The Human Connectome: A Complex Network," *Annals of the New York Academy of Sciences*, vol. 1224, pp. 109–125, 2011.

[28] J. Wang, X. Wang, M. Xia, X. Liao, A. Evans, and Y. He, "GRETNA: A Graph Theoretical Network Analysis Toolbox for Imaging Connectomics," *Frontiers in Human Neuroscience*, vol. 9, p. 386, 2015.

[29] E. T. Bullmore, J. Suckling, S. Overmeyer, S. Rabe-Hesketh, E. Taylor, and M. J. Brammer, "Global, voxel, and cluster tests, by theory and permutation, for a difference between two groups of structural MR images of the brain," *IEEE Transactions on Medical Imaging*, vol. 18, no. 1, pp. 32–42, 1999.

[30] N. Vucetic and O. Svensson, "Physical Signs in Lumbar Disc Hernia," *Clinical Orthopaedics and Related Research*, vol. 333, pp. 192–201, 1996.

[31] D. J. Lanska, "Diagnostic value of history and physical examination in patients suspected of lumbosacral nerve root compression," *Journal of Neurology, Neurosurgery, and Psychiatry*, vol. 73, no. 5, pp. 604-605, 2002.

[32] J. J. Lee, H. J. Kim, M. Ceko et al., "A neuroimaging biomarker for sustained experimental and clinical pain," *Nature Medicine*, vol. 27, no. 1, pp. 174–182, 2021.

[33] X. Su, H.-Y. Hu, and C. Xu, "Global Research On Neuropathic Pain Rehabilitation Over the Last 20 Years," *Neural Plasticity*, vol. 2021, Article ID 5594512, 13 pages, 2021.

[34] M. S. Bak, H. Park, and S. K. Kim, "Neural Plasticity in the Brain During Neuropathic Pain," *Biomedicines*, vol. 9, no. 6, p. 624, 2021.

[35] R. D. Treede, W. Rief, A. Barke et al., "Chronic pain as a symptom or a disease: the IASP classification of chronic pain for the international classification of diseases (ICD-11)," *Pain*, vol. 160, no. 1, pp. 19–27, 2019.

[36] S. P. Cohen and J. Mao, "Neuropathic Pain: Mechanisms and their Clinical Implications," *BMJ*, vol. 348, 2014.

[37] D. S. Bassett and E. Bullmore, "Small-world brain networks," *Neuroscientist*, vol. 12, no. 6, pp. 512–523, 2006.

[38] B. T. Thomas Yeo, F. M. Krienen, J. Sepulcre et al., "The Organization of the Human Cerebral Cortex Estimated by intrinsic functional connectivity," *Journal of Neurophysiology*, vol. 106, no. 3, pp. 1125–1165, 2011.

[39] R. L. Buckner, J. R. Andrews-Hanna, and D. L. Schacter, "The Brain's Default Network: Anatomy, Function, and Relevance to Disease," *Annals of the New York Academy of Sciences*, vol. 1124, pp. 1–38, 2008.

[40] M. E. Raichle, A. M. MacLeod, A. Z. Snyder, W. J. Powers, D. A. Gusnard, and G. L. Shulman, "A default mode of brain function," *Proceedings of the National Academy of Sciences of the United States of America*, vol. 98, no. 2, pp. 676–682, 2001.

[41] B. J. Harrison, J. Pujol, M. Lopez-Sola et al., "Consistency and functional specialization in the default mode brain network," *Proceedings of the National Academy of Sciences of the United States of America*, vol. 105, no. 28, pp. 9781–9786, 2008.

[42] Y. I. Sheline, J. L. Price, Z. Yan, and M. A. Mintun, "Resting-state functional MRI in depression unmasks increased connectivity between networks via the dorsal nexus," *Proceedings of the National Academy of Sciences of the United States of America*, vol. 107, no. 24, pp. 11020–11025, 2010.

[43] J. Zhang, J. Wang, Q. Wu et al., "Disrupted brain connectivity networks in drug-naive, First-episode major depressive disorder," *Biological Psychiatry*, vol. 70, no. 4, pp. 334–342, 2011.

[44] T. J. Schwedt, C. C. Chiang, C. D. Chong, and D. W. Dodick, "Functional MRI of migraine," *The Lancet Neurology*, vol. 14, no. 1, pp. 81–91, 2015.

[45] H. L. Wei, X. Zhou, Y. C. Chen et al., "Impaired Intrinsic Functional Connectivity Between the Thalamus and Visual Cortex in Migraine without Aura," *Journal of Headache and Pain*, vol. 20, no. 1, p. 116, 2019.

[46] W. Li, P. Yang, R. K. Ngetich, J. Zhang, Z. Jin, and L. Li, "Differential Involvement of Frontoparietal Network and Insula Cortex in Emotion Regulation," *Neuropsychologia*, vol. 161, article 107991, 2021.

Hindawi
Neural Plasticity
Volume 2022, Article ID 5345269, 10 pages
https://doi.org/10.1155/2022/5345269

Review Article

Plasticity of the Central Nervous System Involving Peripheral Nerve Transfer

Jun Shen

Department of Orthopaedic Oncology, The Second Affiliated Hospital of Naval Medical University, Naval Medical University, No. 415 Fengyang Road, Huangpu District, Shanghai, China

Correspondence should be addressed to Jun Shen; 16111220045@fudan.edu.cn

Received 19 December 2021; Revised 9 February 2022; Accepted 28 February 2022; Published 18 March 2022

Academic Editor: Jia-Jia Wu

Peripheral nerve injury can lead to partial or complete loss of limb function, and nerve transfer is an effective surgical salvage for patients with these injuries. The inability of deprived cortical regions representing damaged nerves to overcome corresponding maladaptive plasticity after the reinnervation of muscle fibers and sensory receptors is thought to be correlated with lasting and unfavorable functional recovery. However, the concept of central nervous system plasticity is rarely elucidated in classical textbooks involving peripheral nerve injury, let alone peripheral nerve transfer. This article is aimed at providing a comprehensive understanding of central nervous system plasticity involving peripheral nerve injury by reviewing studies mainly in human or nonhuman primate and by highlighting the functional and structural modifications in the central nervous system after peripheral nerve transfer. Hopefully, it will help surgeons perform successful nerve transfer under the guidance of modern concepts in neuroplasticity.

1. Introduction

In clinical practice, peripheral nerve transfer (PNT), being an effective addition to medical interventions, has been commonly employed in patients with peripheral nerve injury or cervical spinal cord injury as a surgical salvage for restoration of the crucial function of paralyzed limbs [1–10]. Healthy donor nerves with less vital roles are sacrificed and transferred to the sites of damaged nerves [8]. After PNT, the axons of the donor nerves are expected to functionally reinnervate the formerly paralyzed muscles to regain favorable control of disabled limbs. However, ideal recovery of normal sensation and muscle control cannot be achieved even after complete nerve regeneration [11–13]. Surgeons are becoming increasingly aware of the alterations of the brain and spinal cord circuit triggered by peripheral nerve injury, which can exert a negative impact on the eventual functional restoration. These alterations have been termed neuroplasticity [14].

Plasticity is a unique biological property that refers to the ability of the central nervous system (CNS) to modify itself functionally and structurally in response to changes or demands within the organism itself and the external environment. This allows for the CNS to be constructed out of other body parts, such as the cardiovascular, respiratory, and digestive systems [15]. The most impressive form of neuroplasticity is the capacity for continuous neurogenesis during adulthood [16]. The history of neuroplasticity research involving peripheral nerve injury could date back as far as 1895 [17]. And it began with the phenomenon of "false localization," which refers to the patient's inability to accurately localize a point of stimulation on the skin despite good regeneration of sensory fibers after median nerve transection [17, 18]. During the following century, a large number of animal experiments in nonhuman primates, cats, and raccoons were performed to examine the implicit functional and structural modifications in the CNS triggered by peripheral nerve injury [18–20]. In recent decades, well-developed recording technology has further boosted our knowledge of cortical and subcortical plasticity at the cellular and neuronal circuit levels in rodent models. Meanwhile, bold oxygen level-dependent functional magnetic resonance imaging

(bold fMRI) developed in the 1990s has provided a profound understanding of this issue in humans. However, the concept of neuroplasticity has rarely been elucidated in classical textbooks involving peripheral nerve injury, let alone PNT. This article is aimed at providing a comprehensive understanding of the neuroplasticity involving peripheral nerve injury by reviewing studies mainly in human or nonhuman primates and by highlighting the functional and structural modifications in the CNS after PNT.

2. Plasticity of the CNS Involving Peripheral Nerve Injury

2.1. Time-Dependent Plasticity of the CNS after Sensory Deafferentation and Motor Deefferentation. The earliest experimental studies on peripheral nerve injury-related plasticity of the CNS were performed on animal models of mere sensory deafferentation, which included the transection of the median nerve at the wrist level (restricted deafferentation model) and resection of the dorsal roots of the spinal cord (extensive deafferentation model) [21, 22]. Plasticity of the CNS induced by sensory deafferentation is characterized by time-dependent features [12]. Taking the restricted deafferentation model as an example, the representative regions of the transected nerve (median nerve) in the primary somatosensory cortex immediately turn silent to the stimulation of corresponding skin areas, and the unresponsive state commonly lasts for a few hours [23]. Then, the silent cerebral cortex becomes responsive to inputs from the adjacent skin fields in part within several hours to several days whose representative regions in the primary somatosensory cortex are normally adjacent to the transected nerves' [22]. The immediate reactivation within several hours to several days after nerve injury is attributed to the rapid reduction of gamma-aminobutyric acid receptors modulating the fast inhibitory neurotransmission in layer IV of deprived cortical regions, which permits the exhibition of preexisting subthreshold excitatory inputs from adjacent skin fields [24]. The deprived cortical regions continue to undergo complete territorial reactivation within the following 3 to 4 weeks, which is due to the strengthening of preexisting subthreshold inputs, latent correlations, and the persistent reduction of gamma-aminobutyric acid receptors at the binding level after deafferentation [25]. Normally functioning N-methyl-D-aspartate receptors play a decisive role in the initiation of complete territorial reactivation [24, 25]. When nerve transection is combined with the administration of N-methyl-D-aspartate receptor antagonists, 75% of the deprived cortical regions remain unresponsive to peripheral stimulation 4 weeks after deafferentation [24, 25]. Dramatic internal topographic reorganization, characterized by the sharpening of roughly somatotopic receptive fields to more distinct receptive fields, persists in the reactivated cortical regions four weeks later in conjunction with daily use and rehabilitation [22, 23, 26, 27]. At this phase, the refinement of complete territorial reactivation is due to upregulation of aminomethyl phosphonic acid receptors, expression of latent synapses, and axonal sprouting from neighboring cortical regions into the deprived areas [25, 27–30]. On the other hand, the sprouting of cutaneous nerve fibers in the skin does not occur over all the entire time frame [31].

The spatial extent of the reorganized somatosensory cortex is approximately 1-2 mm in the restricted model, and it can reach approximately 10-20 mm in the extensive model [29]. The resection of the dorsal roots of the spinal cord at the C5 level as a representative of extensive deafferentation results in identical reorganization patterns in the CNS. In monkeys, the chin responsive region can invade a deafferented hand cortex at a wide distance of 7 mm [32]. The growth of chin afferents from their normal target, the trigeminal nucleus, into the deprived cuneate nucleus was responsible for the increased width of reorganization [33]. Responses to chin stimulation in the cortical regions originally representing hand innervation could be completely abolished by the inactivation of the cuneate nucleus in the brainstem [32]. In primates, deprived cortical regions can never respond to facial skin stimulation above the chin after resection of the dorsal roots of the spinal cord at the C5 level. This is due to the organizational boundary limitation of new long-projection afferents [32]. In conclusion, large-scale reorganization in the primary somatosensory cortex following extensive deafferentation is mainly due to the growth of new long-projection afferents which occur at the level of the brainstem nuclei and thalamus rather than the plasticity of cortical regions [33–38]. In addition to the growth of long-projection afferents, increased glial activation in the thalamus reflecting the continuous alteration of peripheral afferents was also revealed by positron emission computed tomography in humans which can persist for many years after deafferentation [39].

The transection of motor fibers directly precludes the information outflow of the motor cortex, and the cortical motor regions corresponding to denervated muscles also immediately turn silent [40, 41]. A few hours later, the silent motor cortex shifts its descending projections to the new muscle groups. Electrical stimulation of the deprived motor regions can yield the activity of muscles initially driven by the adjacent motor representations [41–43]. Taking forearm amputation as an example, the shoulder representation in the primary motor cortex rapidly invades the adjacent regions of forearm muscles within a week, presenting with a dramatic increase in cortical size [40]. In primates with forelimb amputation, stimulation of the motor cortex, originally in charge of the motor function of distal muscles, brings about contractions of proximal muscles in the forelimb stump and shoulder [44, 45]. Transcranial magnetic stimulation and positron emission tomography examinations have revealed the enlargement of hand representation with medial shifting into the original cortical face area in humans suffering from a long-term period of facial palsy [46, 47]. This indicates that mere motor deefferentation is a sufficient stimulus for reorganizational changes in the adult human cortex [40, 43, 47]. The rapid shifting of representation within a few hours is supposedly due to an anatomical framework of preexisting, horizontal projections in the primary motor cortex that traverse representation borders rather than the formation of new synaptic contacts or local sprouting [48, 49].

2.2. Plasticity of the CNS Involving Peripheral Nerve Injury and Regeneration. Plasticity of the CNS involving peripheral nerve injury corresponds with the physiological processes of nerve injury and regeneration. At first, the representative cortical regions of the injured nerve turn silent; they are soon invaded by adjacent cortical regions that respond to other inputs or yield new muscle activation (reoccupation phase). In humans, increased two-point discrimination ability was observed near the lip, and there was a mislocalization of stimulation of the ulnar side of the fourth finger to the third finger after local anesthetic blockade of the radial and median nerves [50]. Transient anesthetic deafferentation of the radial nerve at the elbow was found to lead to a rapid modulation of the cortical processing of median nerve input and output in humans [51]. Then, there is a phase in which the cortical organization displays the combined effects of nerve injury and regeneration (intermediate phase) [31]. The reactivation of silent regions in the somatosensory cortex commonly emerges in a specific manner, reflecting the sequential proximal to distal sensory nerve reinnervation process [31]. After complete regeneration, cortical topography is reestablished, and preinjury periphery-to-cortex correspondences can be reconnected [52]. Finally, internal topographic reorganization can persist in the somatosensory cortex and is reshaped by rehabilitation or daily usage (internal remodeling phase). However, preinjury cortical topography can never be completely recovered [31]. The restoration of cortical topography differs depending on the type of nerve injury, namely, crush or transection [52]. Nerve transection is more likely to lead to misdirected axonal outgrowth than nerve crush, resulting in altered somatotopic representation [52]. In monkeys with transected and regenerated median nerves, recording sites with abnormally located or multiple cutaneous receptive fields and major topographical changes such as reestablishment digit representations in small discontinuous patches of the cortex were revealed [31]. In contrast, almost normal hand representation, which was in a proximal-to-distal (palmar-to-digital skin) cortex arrangement and continuous manner, recovered and could be observed after crushed median nerve injury [31, 52]. Infant monkeys could attain superior restoration of cortical somatosensory maps and sensory function after median nerve transection compared with adults [53]. Hence, the degree of eventual restoration of normal topography in the deprived somatosensory cortex after peripheral nerve injury depends on the correct axonal outgrowth. With regard to motor nerve lesions, the long-lasting changes at a higher motor cortical level include the shrinkage of corresponding area representing the injured peripheral efferents and the reduction of its excitability, which can be observed even after complete nerve regeneration [54].

In clinical practice, nerve repair or transfer is often performed one or several months after peripheral nerve injury. After peripheral nerve injury and regeneration, Ia afferent information regarding muscle length and dynamics is permanently lost from ventral spinal circuits, which degrades motor performance after complete nerve regeneration [55]. Does the delay in nerve repair cause irreversible structural modifications that have a negative impact on the restoration of normal cortical representation, similar to that in the spinal cord? Unfortunately, few experiments have focused on this issue. We can confirm that the deprived cortical regions can be reactivated to original or new charges even after a long period of deprivation. After four years of denervation, hand and arm representations can return to their original cortical areas 6 months after hand graft surgery [56]. Thus, cortical reactivation cannot be the main barrier for functional recovery in patients with peripheral nerve injury.

3. CNS Plasticity after Peripheral Nerve Transfer

Nerve transfer can be considered a special scenario of peripheral nerve injury and regeneration. The physiological processes of nerve regeneration after PNT consist of the following three stages: (1) the transection of healthy donor nerves, (2) the regeneration of donor nerves into the targeted muscles or skin areas (morphological reinnervation), and (3) transformation from morphological reinnervation to functional reinnervation. Functional and structural changes in the CNS after PNT during the first two stages are similar to those involving peripheral nerve injury. The regenerated nerve fibers can be regarded as misdirected axonal outgrowth in consideration of the restoration of normal cortical topography, initially representing the donor nerve. Consequently, the well-organized cortical area of the donor nerve is often transformed into an ill-defined, mosaic-like area in the third stage after PNT [11]. However, the plasticity of the CNS in the third stage plays a paramount role in better functional recovery. This has not yet been fully recognized in clinical practice.

3.1. CNS Plasticity Involving Cross Reinnervation of Motor Nerves

3.1.1. The Inherent Anatomical and Physiological Features Contributing to the Neuroplasticity of the Motor Cortex for Excellent Clinical Outcomes of Nerve Transfer. Oberlin's procedure (in which a fascicle of the ulnar nerve innervating the flexor carpi ulnaris is transferred to the musculocutaneous nerve) is a typical example of nerve transfer; it was initially developed and performed in 1994, and it has, over the years, transformed into a first-line procedure for the restoration of elbow flexion due to its ≥90% success rate [57]. Similar excellent results have been achieved for partial ipsilateral C7 transfer and radial-to-axillary nerve transfer [58–60]. The favorable clinical outcomes have been attributed to both short nerve regeneration distance and plasticity of the CNS [12]. Using Oberlin's procedure as an example, the distance between the anastomosis site and the targeted biceps brachii is no more than a few centimeters, which dramatically diminishes the deleterious effects of prolonged denervation [12]. With regard to neuroplasticity, the cortical regions representing the donor and acceptor nerves in the motor cortex are adjacent to each other which may receive partially identical descending corticospinal projections.

It is well known that the upper, middle, and lower trunks of the brachial plexus send out nerve branches and innervate

the muscles of the upper limbs [61]. The corticospinal projections connecting to the three trunks of the brachial plexus are found to be intermingled in the primary motor cortex, secondary motor cortex, primary somatosensory cortex, and secondary somatosensory cortex, and a third of them connect to two trunks [61]. A considerable number of corticospinal neurons innervate both the cervical and lumbar spinal cord [62]. Hence, we can infer that a portion of corticospinal projections initially connects both the ulnar (donor nerve) and the musculocutaneous nerves (acceptor nerve). Detectable reactivation of the cortical area during flexion of the injured elbow in the patients who had undergone Oberlin's operation was similar to that observed in a healthy volunteer [63]. Meanwhile, corticospinal neurons are found to exhibit heterogeneous correlations, with movement which includes silent, indiscriminately active, movement-active, and quiescence-active states [64]. Individual cells can lead to novel associations between corticospinal activity and movement across days [64]. Hence, the two principles of neuroplasticity (Figure 1) that contribute to excellent clinical outcomes in patients undergoing Oberlin's procedure are as follows: (1) the cortical regions representing donor and acceptor nerves are adjacent to each other which receive partial common corticospinal projections from the motor cortex and (2) the dynamic changes in physiological correlations between corticospinal neurons and movements [12, 64].

3.1.2. The Cortical Shifting Phenomenon Contributing to Moderate PNT Results. Intercostal-to-musculocutaneous nerve transfer performed in patients with complete brachial plexus avulsion, which has an average success rate of 60%-70%, can serve as a typical method for understanding the cortical shifting phenomenon (Figure 2). At the beginning of functional recovery, the contraction of the biceps muscle should be sustained by movements on inspiration or expiration [65]. One to 2 years after intercostal-to-musculocutaneous nerve transfer, elbow flexion can gradually be maintained without the assistance of respiratory movement [65]. Meanwhile, complete independence between the respiratory and elbow flexion movements can never be achieved [65]. The most excitable area of the motor cortex for evoking motor-evoked potential of reinnervated biceps muscle showed a gradual shifting from the cortical map of the intercostal muscles to the arm territory during the same 1-2-year period after intercostal-to-musculocutaneous nerve transfer. This has been termed the cortical shifting phenomenon [65]. Connection of the preexisting cortical network of interneurons in arm representation with intercostal corticospinal neurons is thought to be responsible for this cortical shifting phenomenon [65, 66]. Similarly, patients with complete brachial plexus avulsion, who receive phrenic-to-musculocutaneous nerve transfer for the restoration of elbow flexion, have the same course of clinical recovery and cortical shifting phenomenon of the motor cortex in the third stage as those with intercostal-to-musculocutaneous nerve transfer [67]. The bold fMRI data analyzed using the dynamic causal modeling method indicate that the new neuroplastic connection between the arm and the diaphragm area indeed occurs [66]. A portion of the cortical

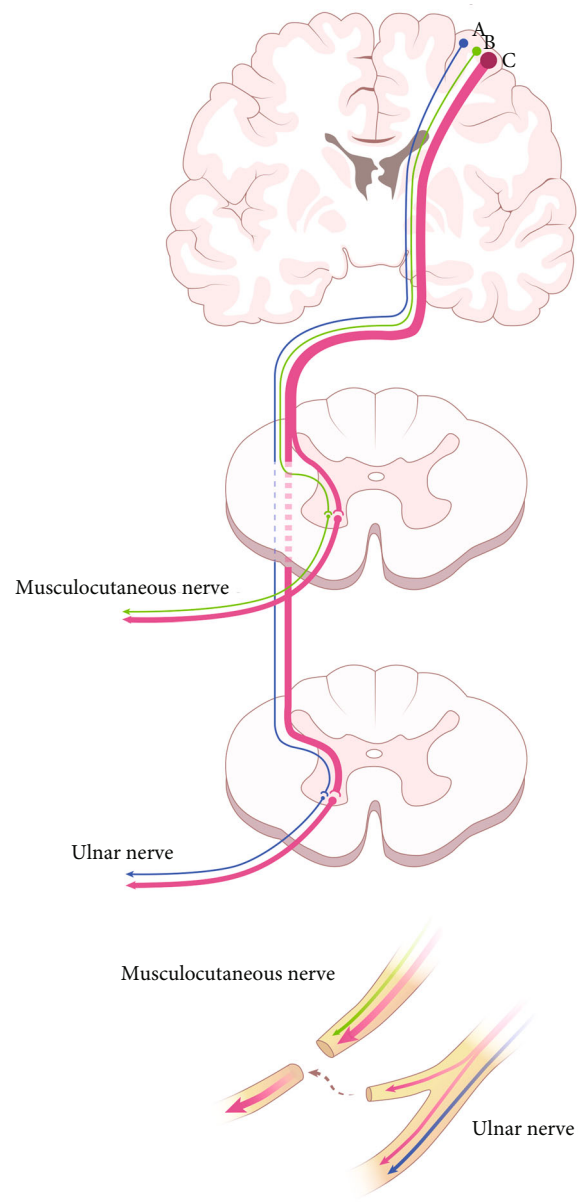

Figure 1: Neuroplasticity of the motor cortex for excellent clinical outcomes of Oberlin's procedure. Corticospinal neurons (corticospinal projection A, B, and C) in the primary motor cortex of layer V projecting into the motor neurons in the spinal cord are the ultimate descending pathways responsible for movement control. A portion of corticospinal projections (corticospinal projection C) can simultaneously connect the ulnar (donor nerve) and the musculocutaneous nerves (acceptor nerve). Hence, the motor command of elbow flexion can quickly be transmitted downward along the common pathway Corticospinal projection C to the ulnar nerve after Oberlin's procedure.

regions representing phrenic nerves could be gradually separated for the charge of the new elbow flexion function [66, 67]. The connection between the separated and original cortical regions weakens, and the separated cortical regions make new connections with the deprived arm area [66, 67]. Finally, the cortical region representing the arm area delivers the motor control command of elbow flexion to the cervical spinal

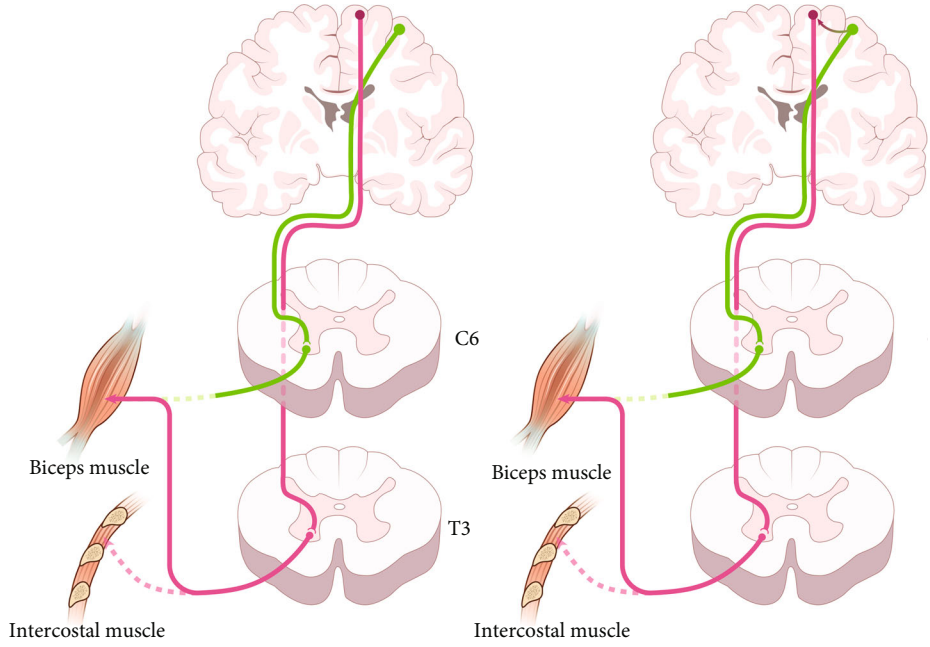

Figure 2: Neuroplasticity after an intercostal-to-musculocutaneous nerve transfer with moderate clinical outcomes. In the early phase of morphological reinnervation (left), biceps contraction is mediated by the original intercostal nerve's primary motor cortex located in the midline. The descending pathway for elbow flexion from the motor cortex to the motor neuron pool of the intercostal nerve T3 is shown in red. Several years later (right), patients begin to contract their biceps independently of respiration. The cortical region representing musculocutaneous nerve delivers the motor control command to biceps brachii via the new relay diaphragm area. The new connection between the 2 cortexes (curved arrow) is reactivated.

cord via the new relay diaphragm area [66, 67]. From this perspective, the donor and acceptor nerves must have some horizontal intrinsic connections between the two motor areas, laying the foundation for the cortical shifting phenomenon [12, 66]. The projection distance of the preexisting cortical network of interneurons (horizontal intrinsic connections) may determine the occurrence of the cortical shifting phenomenon [12, 66]. The technique of anastomosis, end-to-side or end-to-end neurorrhaphy, employed during PNT seems to determine the pattern of motor organization [68]. In rodents with intercostal-to-musculocutaneous nerve transfer, the motor representation of biceps muscle was completely reverted to the original biceps area 10 months later after end-to-end transfer [68]. At the same time point, part of the biceps representation remained in the original diaphragm area in the end-to-side group which was manifested as partial cortical shifting [68]. Similarly, both cortical diaphragm and arm areas in patients with the employment of end-to-side neurorrhaphy during phrenic-to-musculocutaneous nerve transfer were activated during elbow flexion [69].

Both Oberlin's procedure and intercostal-to-musculocutaneous nerve transfer have been employed for the restoration of elbow flexion. With regard to Oberlin's procedure, the donor nerve fascicle innervating the flexor carpi ulnaris is initially responsible for both wrist and elbow flexion, which is synergistic with the movement innervated by the musculocutaneous nerve. However, the intercostal nerve, which is used in intercostal-to-musculocutaneous nerve transfer, is a nerve for inspiration/expiration that is completely unrelated to elbow flexion. The difference in movement between the donor and acceptor nerves also is an important factor for determining clinical outcomes [12].

Contralateral C7 nerve transfer was developed for the treatment of patients with brachial plexus avulsion injury for the restoration of shoulder abduction and elbow flexion [70]. In these patients, bold fMRI also showed that the motor cortex representation of the reinnervated upper limb shifts from the ipsilateral to the contralateral hemisphere after long-term remodeling [71]. The injured limb can be moved by stimulating the contralateral motor cortex [72]. The anatomical pathway and mechanism for the contralateral motor cortex to control the movement of the injured forelimb after contralateral C7 nerve transfer occur via the subcortical connectivity [73]. In patients, high level of cerebral glucose metabolism in the corpus callosum was positively correlated with motor recovery of the injured hand 4 years after contralateral C7 nerve transfer [74].

The presence of cortical shifting after ipsilateral and contralateral PNT demonstrates its paramount importance for good motor recovery and voluntary movement control, which may be due to the modifications of the excitatory projections from layer II/III to layer V in the primary motor cortex [75]. Furthermore, the corticospinal and corticostriatal neurons in layer V also received projections from layer II/III to layer V of contralateral cortical areas through the callosum. Cortical shifting in patients with contralateral C7 nerve transfer may also be due to contralateral projections through the callosum.

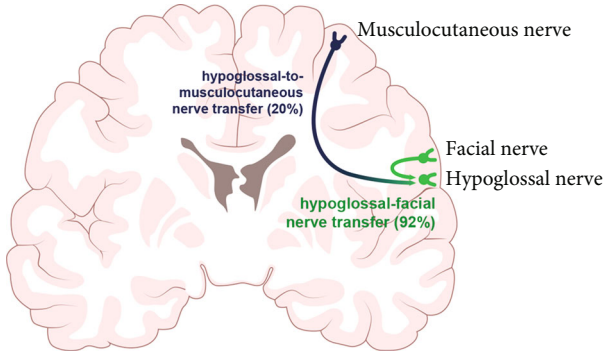

Figure 3: Neuroplasticity responsible for unfavorable clinical results after a hypoglossal-to-musculocutaneous nerve transfer. The distance between the tongue cortical area (hypoglossal nerve) and the arm representation (musculocutaneous nerve) is greater than that between the tongue cortical area (hypoglossal nerve) and the musculus facialis representation (facial nerve). This distance obscures the formation of the new connection to generate the cortical shifting.

3.1.3. The Lack of Cortical Shifting Phenomenon Resulting in Unfavorable PNT Results. Independent voluntary control over reinnervated muscles can never be achieved after hypoglossal-to-musculocutaneous nerve transfer, and involuntary contraction of the biceps muscle can be evoked by talking or chewing [12, 76]. Meanwhile, only 21% of patients achieved M3 or higher elbow flexion strength according to the Medical Research Council's guidelines. In contrast, good results (a 92% success rate) can be expected after unilateral hypoglossal-facial nerve transfer [77–80]. The distance between the tongue cortical area and the arm representation is greater (Figure 3), and this distance may preclude the formation of a new pathway and the germination of cortical shifting in hypoglossal-to-musculocutaneous nerve transfer [76].

3.1.4. The Effects of Antagonistic Movements on Nerve Transfer. Modern concepts of plasticity should also be considered when performing antagonist nerve transfer (the donor and receptor nerves innervating the antagonistic muscles). In patients with proximal median and ulnar nerve injury, transferring the radial nerve branch innervating the extensor carpi radialis brevis to the anterior interosseous nerve can bring about the recovery of full finger and thumb flexion with muscle strength reaching M4 [81, 82]. Pronator quadratus to extensor carpi radialis brevis muscle motor branch nerve transfer can yield a 90% success rate for the reconstruction of wrist extension scored M4 in patients with C5-8 brachial plexus palsy [83–85]. Meanwhile, partial ulnar nerve transfer to the branch of the long head of the triceps has been performed to recover elbow extension, and 90% of patients can achieve M4 or higher elbow extension strength [86–88]. We can come to a conclusion that antagonist nerve transfer in the upper limbs is an effective method. Nevertheless, antagonist nerve transfer does not work in the lower limbs. Tibial branch-to-deep peroneal nerve transfer has been performed for the restoration of ankle dorsiflexion, and only approximately 25% of patients can achieve M3 or greater motor recovery [89]. More studies have to be done before drawing final conclusions on neuroplasticity antagonist nerve transfer [12].

3.2. CNS Plasticity Involving Cross Reinnervation of Sensory Nerves. Peripheral nerve injury causes not only motor dysfunction but also loss of sensation [90]. The loss of protective sensation, especially the loss of temperature and pain sense, can lead to secondary physical injuries and can even ultimately compromise the recovery of motor function [90]. For these reasons, restoration of sensation has been emphasized and has been performed in both upper and lower extremities [90–97]. How is the cerebral cortex reorganized after the cross reinnervation of sensory nerves? The proximal ulnar nerve was sutured to the distal radial nerve at the wrist level in a monkey to interpret this issue [98]. The median nerve skin was consistently located in the cortical region responding to ulnar nerve inputs without cortical shifting to the original area after operation, even 2.9 years later [98]. In other words, topographies in the primary somatosensory cortex are relatively stable and their preservation does not depend on peripheral sensory inputs [99]. We should note that this sensory cortex organizational pattern is distinct from that in the motor cortex.

4. The New Application of PNT and the Modulation of Neuroplasticity for Better Functional Recovery after PNT

PNT has been newly performed for the restoration of limb function in patients with spinal cord injury, which leads to similar functional improvements in those treated with a tendon transfer [3, 4, 6, 90]. The surgical procedure for performing nerve transfer should be based on the functional level of spinal cord injury and the individual's needs [100]. Meanwhile, contralateral C7 nerve transfer from the nonparalyzed side to the paralyzed side has been creatively performed in patients with chronic cerebral injury to ameliorate the spasticity of the affected upper limb, and satisfactory motor functional improvement has been obtained during the one-year follow-up [101]. This fresh application of the contralateral C7 nerve, which was developed in 1992 by Gu et al., is based on much insight into the fundamental rules of neuroscience implicit in the difference between motor and sensory cortex organization [102]. In these patients, extension movement of the paralyzed wrist was preoperatively correlated with weak activation in the contralateral hemisphere (injured side), which became even more dismal within the 1-year follow-up after contralateral C7 nerve transfer [101]. The newly emerging activation region in the ipsilateral hemisphere generated by extension of the wrist of the paralyzed arm could be revealed by bold fMRI from the 8th month after surgery [101]. In patients with unilateral chronic brain injury, the ipsilateral hemisphere can eventually be responsible for partial control of the motor function of the paralyzed upper limb within one year of follow-up [101].

As maladaptive central plasticity contributes to chronic dysfunction after nerve damage, techniques that reestablish normal central network signaling should improve functional

recovery. Motor cortex stimulation can be employed to enhance functional recovery, nerve regeneration, and muscle reinnervation after PNT [103]. Direct stimulation of the motor cortex modulates CNS plasticity for better functional recovery after PNT [12]. Recently, closed-loop vagus nerve stimulation has been shown to improve sensorimotor recovery by enhancing central plasticity, even in the absence of changes to the damaged nerve itself [13, 104, 105]. Rehabilitation, drugs, and electrical stimulation have been commonly employed to improve the nerve regeneration and promote adaptive circuit changes after peripheral nerve injury [106]. Rehabilitative therapies combined with vagus nerve stimulation have emerged as a new trend in targeted plasticity therapy [105, 106]. Meanwhile, the reconstruction of sensory inputs should be emphasized to enhance motor results in clinical practice.

5. Conclusion

The keys to successful PNT under the guidance of modern concepts in neuroplasticity are as follows: (1) donor nerves should be properly selected for the targeted muscles; (2) cortical regions representing donor and recipient nerves should be as close to each other as possible; (3) preoperative training of the movements required to activate the nerve transfer should be reinforced; (4) plasticity should be reinforced, especially during the early stages of motor relearning; and (5) well-designed rehabilitation programs with strengthening exercises should be initiated after the observation of initial motor movement [12, 107].

Conflicts of Interest

The authors report no conflict of interest concerning the materials or methods used in this study or the findings specified in this paper.

Acknowledgments

This work was supported by the post-doctor funding from Naval Medical University.

References

[1] R. Midha and J. Grochmal, "Surgery for nerve injury: current and future perspectives," *Journal of Neurosurgery*, vol. 130, no. 3, pp. 675–685, 2019.

[2] M. S. Bednar and J. C. Woodside, "Management of upper extremities in tetraplegia: current concepts," *The Journal of the American Academy of Orthopaedic Surgeons*, vol. 26, no. 16, pp. e333–e341, 2018.

[3] K. Sananpanich, J. Kraisarin, W. Siriwittayakorn, S. Tongprasert, and S. Suwansirikul, "Double motor nerve transfer for all finger flexion in cervical spinal cord injury: an anatomical study and a clinical report," *The Journal of Hand Surgery*, vol. 43, no. 10, pp. 920–926, 2018.

[4] J. A. Bertelli and M. F. Ghizoni, "Nerve transfers for restoration of finger flexion in patients with tetraplegia," *Journal of Neurosurgery. Spine*, vol. 26, no. 1, pp. 55–61, 2017.

[5] B. F. Yu, Y. Q. Qiu, M. X. du et al., "Contralateral hemi-fifth-lumbar nerve transfer for unilateral lower limb dysfunction due to incomplete traumatic spinal cord injury: a report of two cases," *Microsurgery*, vol. 40, no. 2, pp. 234–240, 2020.

[6] N. van Zyl and L. H. Opie, "Beta-blockade in the elderly," *The Lancet*, vol. 1, no. 8483, pp. 733-734.

[7] K. D. Bergmeister, M. Aman, S. Muceli et al., "Peripheral nerve transfers change target muscle structure and function," *Science advances*, vol. 5, no. 1, article eaau2956, 2019.

[8] S. Bazarek and J. M. Brown, "The evolution of nerve transfers for spinal cord injury," *Experimental Neurology*, vol. 333, p. 113426, 2020.

[9] E. J. R. Hill and I. K. Fox, "Current best peripheral nerve transfers for spinal cord injury," *Plastic and reconstructive surgery*, vol. 143, no. 1, pp. 184e–198e, 2019.

[10] M. J. Berger, L. Robinson, and E. M. Krauss, "Lower motor neuron abnormality in chronic cervical spinal cord injury: implications for nerve transfer surgery," *Journal of Neurotrauma*, vol. 39, no. 3-4, pp. 259–265, 2022.

[11] C. B. Mohanty, D. Bhat, and B. I. Devi, "Role of central plasticity in the outcome of peripheral nerve regeneration," *Neurosurgery*, vol. 77, no. 3, pp. 418–423, 2015.

[12] M. Socolovsky, M. Malessy, D. Lopez, F. Guedes, and L. Flores, "Current concepts in plasticity and nerve transfers: relationship between surgical techniques and outcomes," *Neurosurgical Focus*, vol. 42, no. 3, article E13, 2017.

[13] E. C. Meyers, N. Kasliwal, B. R. Solorzano et al., "Enhancing plasticity in central networks improves motor and sensory recovery after nerve damage," *Nature Communications*, vol. 10, no. 1, p. 5782, 2019.

[14] M. Socolovsky and M. Malessy, "Brain changes after peripheral nerve repair: limitations of neuroplasticity," *Journal of Neurosurgical Sciences*, vol. 65, no. 4, pp. 421–430, 2021.

[15] R. von Bernhardi, L. E. Bernhardi, and J. Eugenin, "What is neural plasticity?," *Advances in Experimental Medicine and Biology*, vol. 1015, pp. 1–15, 2017.

[16] L. Y. Xiao, X. R. Wang, Y. Ye et al., "Applications of acupuncture therapy in modulating plasticity of central nervous system," *Neuromodulation*, vol. 21, no. 8, pp. 762–776, 2018.

[17] J. K. Mitchell, *Remote consequences of injuries of nerves, and their treatment : an examination of the present condition of wounds received 1863-65, with additional illustrative cases*, Lea Brothers, Philadelphia, 1895.

[18] R. L. Paul, H. Goodman, and M. Merzenich, "Alterations in mechanoreceptor input to Brodmann's areas 1 and 3 of the postcentral hand area of *Macaca mulatta* after nerve section and regeneration," *Brain Research*, vol. 39, no. 1, pp. 1–19, 1972.

[19] A. M. Kelahan, R. H. Ray, L. V. Carson, C. E. Massey, and G. S. Doetsch, "Functional reorganization of adult raccoon somatosensory cerebral cortex following neonatal digit amputation," *Brain Research*, vol. 223, no. 1, pp. 152–159, 1981.

[20] J. Kalaska and B. Pomeranz, "Chronic paw denervation causes an age-dependent appearance of novel responses from forearm in "paw cortex" of kittens and adult cats," *Journal of Neurophysiology*, vol. 42, no. 2, pp. 618–633, 1979.

[21] H. Mohammed and E. R. Hollis 2nd, "Cortical reorganization of sensorimotor systems and the role of intracortical circuits after spinal cord injury," *Neurotherapeutics*, vol. 15, no. 3, pp. 588–603, 2018.

[22] M. M. Merzenich, J. H. Kaas, J. T. Wall, M. Sur, R. J. Nelson, and D. J. Felleman, "Progression of change following median nerve section in the cortical representation of the hand in areas 3b and 1 in adult owl and squirrel monkeys," *Neuroscience*, vol. 10, no. 3, pp. 639–665, 1983.

[23] M. M. Merzenich, J. H. Kaas, J. Wall, R. J. Nelson, M. Sur, and D. Felleman, "Topographic reorganization of somatosensory cortical areas 3b and 1 in adult monkeys following restricted deafferentation," *Neuroscience*, vol. 8, no. 1, pp. 33–55, 1983.

[24] P. E. Garraghty and N. Muja, "NMDA receptors and plasticity in adult primate somatosensory cortex," *The Journal of Comparative Neurology*, vol. 367, no. 2, pp. 319–326, 1996.

[25] W. A. Myers, J. D. Churchill, N. Muja, and P. E. Garraghty, "Role of NMDA receptors in adult primate cortical somatosensory plasticity," *The Journal of Comparative Neurology*, vol. 418, no. 4, pp. 373–382, 2000.

[26] T. P. Pons, P. E. Garraghty, A. K. Ommaya, J. H. Kaas, E. Taub, and M. Mishkin, "Massive cortical reorganization after sensory deafferentation in adult macaques," *Science*, vol. 252, no. 5014, pp. 1857–1860, 1991.

[27] J. D. Churchill, N. Muja, W. A. Myers, J. Besheer, and P. E. Garraghty, "Somatotopic consolidation: a third phase of reorganization after peripheral nerve injury in adult squirrel monkeys," *Experimental Brain Research*, vol. 118, no. 2, pp. 189–196, 1998.

[28] E. G. Jones, "Cortical and subcortical contributions to activity-dependent plasticity in primate somatosensory cortex," *Annual Review of Neuroscience*, vol. 23, no. 1, pp. 1–37, 2000.

[29] S. L. Florence, H. B. Taub, and J. H. Kaas, "Large-scale sprouting of cortical connections after peripheral injury in adult macaque monkeys," *Science*, vol. 282, no. 5391, pp. 1117–1121, 1998.

[30] T. M. Mowery, R. M. Sarin, P. V. Kostylev, and P. E. Garraghty, "Differences in AMPA and $GABA_{A/B}$ receptor subunit expression between the chronically reorganized cortex and brainstem of adult squirrel monkeys," *Brain Research*, vol. 1611, pp. 44–55, 2015.

[31] J. T. Wall, J. H. Kaas, M. Sur, R. J. Nelson, D. J. Felleman, and M. M. Merzenich, "Functional reorganization in somatosensory cortical areas 3b and 1 of adult monkeys after median nerve repair: possible relationships to sensory recovery in humans," *The Journal of Neuroscience*, vol. 6, no. 1, pp. 218–233, 1986.

[32] N. Kambi, P. Halder, R. Rajan et al., "Large-scale reorganization of the somatosensory cortex following spinal cord injuries is due to brainstem plasticity," *Nature Communications*, vol. 5, no. 1, p. 3602, 2014.

[33] N. Jain, S. L. Florence, H. X. Qi, and J. H. Kaas, "Growth of new brainstem connections in adult monkeys with massive sensory loss," *Proceedings of the National Academy of Sciences of the United States of America*, vol. 97, no. 10, pp. 5546–5550, 2000.

[34] M. F. Glasser, T. S. Coalson, E. C. Robinson et al., "A multimodal parcellation of human cerebral cortex," *Nature*, vol. 536, no. 7615, pp. 171–178, 2016.

[35] P. Chand and N. Jain, "Intracortical and thalamocortical connections of the hand and face representations in somatosensory area 3b of macaque monkeys and effects of chronic spinal cord injuries," *The Journal of Neuroscience*, vol. 35, no. 39, pp. 13475–13486, 2015.

[36] S. L. Florence and J. H. Kaas, "Large-scale reorganization at multiple levels of the somatosensory pathway follows therapeutic amputation of the hand in monkeys," *The Journal of Neuroscience*, vol. 15, no. 12, pp. 8083–8095, 1995.

[37] P. E. Garraghty and J. H. Kaas, "Large-scale functional reorganization in adult monkey cortex after peripheral nerve injury," *Proceedings of the National Academy of Sciences of the United States of America*, vol. 88, no. 16, pp. 6976–6980, 1991.

[38] S. L. Florence, T. A. Hackett, and F. Strata, "Thalamic and cortical contributions to neural plasticity after limb amputation," *Journal of Neurophysiology*, vol. 83, no. 5, pp. 3154–3159, 2000.

[39] R. B. Banati, A. Cagnin, D. J. Brooks et al., "Long-term trans-synaptic glial responses in the human thalamus after peripheral nerve injury," *Neuroreport*, vol. 12, no. 16, pp. 3439–3442, 2001.

[40] X. Navarro, M. Vivo, and A. Valero-Cabre, "Neural plasticity after peripheral nerve injury and regeneration," *Progress in Neurobiology*, vol. 82, no. 4, pp. 163–201, 2007.

[41] J. N. Sanes, S. Suner, J. F. Lando, and J. P. Donoghue, "Rapid reorganization of adult rat motor cortex somatic representation patterns after motor nerve injury," *Proceedings of the National Academy of Sciences of the United States of America*, vol. 85, no. 6, pp. 2003–2007, 1988.

[42] J. N. Sanes, S. Suner, and J. P. Donoghue, "Dynamic organization of primary motor cortex output to target muscles in adult rats. I. Long-term patterns of reorganization following motor or mixed peripheral nerve lesions," *Experimental Brain Research*, vol. 79, no. 3, pp. 479–491, 1990.

[43] G. Franchi, "Reorganization of vibrissal motor representation following severing and repair of the facial nerve in adult rats," *Experimental Brain Research*, vol. 131, no. 1, pp. 33–43, 2000.

[44] H. X. Qi, I. Stepniewska, and J. H. Kaas, "Reorganization of primary motor cortex in adult macaque monkeys with long-standing amputations," *Journal of Neurophysiology*, vol. 84, no. 4, pp. 2133–2147, 2000.

[45] C. W. Wu and J. H. Kaas, "Reorganization in primary motor cortex of primates with long-standing therapeutic amputations," *The Journal of Neuroscience*, vol. 19, no. 17, pp. 7679–7697, 1999.

[46] M. Rijntjes, M. Tegenthoff, J. Liepert et al., "Cortical reorganization in patients with facial palsy," *Annals of Neurology*, vol. 41, no. 5, pp. 621–630, 1997.

[47] S. Yildiz, F. Bademkiran, N. Yildiz, I. Aydogdu, B. Uludag, and C. Ertekin, "Facial motor cortex plasticity in patients with unilateral peripheral facial paralysis," *NeuroRehabilitation*, vol. 22, no. 2, pp. 133–140, 2007.

[48] G. W. Huntley, "Correlation between patterns of horizontal connectivity and the extend of short-term representational plasticity in rat motor cortex," *Cerebral Cortex*, vol. 7, no. 2, pp. 143–156, 1997.

[49] D. S. Weiss and A. Keller, "Specific patterns of intrinsic connections between representation zones in the rat motor cortex," *Cerebral Cortex*, vol. 4, no. 2, pp. 205–214, 1994.

[50] T. Weiss, W. H. R. Miltner, J. Liepert, W. Meissner, and E. Taub, "Rapid functional plasticity in the primary somatomotor cortex and perceptual changes after nerve block,"

The European Journal of Neuroscience, vol. 20, no. 12, pp. 3413–3423, 2004.

[51] B. A. Murphy, H. H. Taylor, S. A. Wilson, J. A. Knight, K. M. Mathers, and S. Schug, "Changes in median nerve somatosensory transmission and motor output following transient deafferentation of the radial nerve in humans," *Clinical Neurophysiology*, vol. 114, no. 8, pp. 1477–1488, 2003.

[52] J. T. Wall, D. J. Felleman, and J. H. Kaas, "Recovery of normal topography in the somatosensory cortex of monkeys after nerve crush and regeneration," *Science*, vol. 221, no. 4612, pp. 771–773, 1983.

[53] S. L. Florence, N. Jain, M. W. Pospichal, P. D. Beck, D. L. Sly, and J. H. Kaas, "Central reorganization of sensory pathways following peripheral nerve regeneration in fetal monkeys," *Nature*, vol. 381, no. 6577, pp. 69–71, 1996.

[54] G. Franchi, "Persistence of vibrissal motor representation following vibrissal pad deafferentation in adult rats," *Experimental Brain Research*, vol. 137, no. 2, pp. 180–189, 2001.

[55] T. M. Rotterman, E. T. Akhter, A. R. Lane et al., "Spinal motor circuit synaptic plasticity after peripheral nerve injury depends on microglia activation and a CCR2 mechanism," *The Journal of Neuroscience*, vol. 39, no. 18, pp. 3412–3433, 2019.

[56] P. Giraux, A. Sirigu, F. Schneider, and J. M. Dubernard, "Cortical reorganization in motor cortex after graft of both hands," *Nature Neuroscience*, vol. 4, no. 7, pp. 691-692, 2001.

[57] C. Oberlin, D. Béal, S. Leechavengvongs, A. Salon, M. C. Dauge, and J. J. Sarcy, "Nerve transfer to biceps muscle using a part of ulnar nerve for C5-C6 avulsion of the brachial plexus: anatomical study and report of four cases," *The Journal of Hand Surgery*, vol. 19, no. 2, pp. 232–237, 1994.

[58] H. W. Yin, S. Jiang, W. D. Xu, L. Xu, J. G. Xu, and Y. D. Gu, "Partial ipsilateral C7 transfer to the upper trunk for C5-C6 avulsion of the brachial plexus," *Neurosurgery*, vol. 70, no. 5, pp. 1176–1182, 2012, discussion 1181-2.

[59] V. Vanaclocha, J. M. Herrera, M. Rivera-Paz, D. Martínez-Gómez, and L. Vanaclocha, "Radial to axillary nerve transfer," *Neurosurg Focus*, vol. 44, VideoSuppl1, p. V1, 2018.

[60] X. Yang, B. Xu, J. S. Tong, C. G. Zhang, Z. Dong, and J. B. Liu, "Triceps motor branch transfer for isolated axillary nerve injury: outcomes in 9 patients," *Orthopaedics & Traumatology, Surgery & Research*, vol. 103, no. 8, pp. 1283–1286, 2017.

[61] F. Wang, J. Shen, S. Jiang et al., "The recognition of the distribution features of corticospinal neurons by a retrograde trans-synaptic tracing to elucidate the clinical application of contralateral middle trunk transfer," *Neuroscience*, vol. 424, pp. 86–101, 2020.

[62] T. Kamiyama, H. Kameda, N. Murabe et al., "Corticospinal tract development and spinal cord innervation differ between cervical and lumbar targets," *The Journal of Neuroscience*, vol. 35, no. 3, pp. 1181–1191, 2015.

[63] A. C. de Sousa and J. F. Guedes-Correa, "Post-Oberlin procedure cortical neuroplasticity in traumatic injury of the upper brachial plexus," *Radiologia Brasileira*, vol. 49, no. 3, pp. 201-202, 2016.

[64] A. J. Peters, J. Lee, N. G. Hedrick, K. O'Neil, and T. Komiyama, "Reorganization of corticospinal output during motor learning," *Nature Neuroscience*, vol. 20, no. 8, pp. 1133–1141, 2017.

[65] Y. Mano, T. Nakamuro, R. Tamural et al., "Central motor reorganization after anastomosis of the musculocutaneous and intercostal nerves following cervical root avulsion," *Annals of Neurology*, vol. 38, no. 1, pp. 15–20, 1995.

[66] M. J. Malessy, D. Bakker, A. J. Dekker, J. van Duk, and R. T. Thomeer, "Functional magnetic resonance imaging and control over the biceps muscle after intercostal-musculocutaneous nerve transfer," *Journal of Neurosurgery*, vol. 98, no. 2, pp. 261–268, 2003.

[67] A. Amini, F. P. S. Fischmeister, E. Matt, R. Schmidhammer, F. Rattay, and R. Beisteiner, "Peripheral nervous system reconstruction reroutes cortical motor output-brain reorganization uncovered by effective connectivity," *Frontiers in Neurology*, vol. 9, p. 1116, 2018.

[68] M. X. Zheng, Y. D. Shen, X. Y. Hua, A. L. Hou, Y. Zhu, and W. D. Xu, "Cortical reorganization in dual innervation by single peripheral nerve," *Neurosurgery*, vol. 83, no. 4, pp. 819–826, 2018.

[69] R. Beisteiner, I. Höllinger, J. Rath et al., "New type of cortical neuroplasticity after nerve repair in brachial plexus lesions," *Archives of Neurology*, vol. 68, no. 11, pp. 1467–1470, 2011.

[70] L. Li, W. T. He, B. G. Qin, X. L. Liu, J. T. Yang, and L. Q. Gu, "Comparison between direct repair and human acellular nerve allografting during contralateral C7 transfer to the upper trunk for restoration of shoulder abduction and elbow flexion," *Neural Regeneration Research*, vol. 14, no. 12, pp. 2132–2140, 2019.

[71] X. Y. Hua, B. Liu, Y. Q. Qiu et al., "Long-term ongoing cortical remodeling after contralateral C-7 nerve transfer," *Journal of Neurosurgery*, vol. 118, no. 4, pp. 725–729, 2013.

[72] L. Lou, T. Shou, Z. Li, W. Li, and Y. Gu, "Transhemispheric functional reorganization of the motor cortex induced by the peripheral contralateral nerve transfer to the injured arm," *Neuroscience*, vol. 138, no. 4, pp. 1225–1231, 2006.

[73] X. Y. Hua, Z. Y. Li, W. D. Xu, M. X. Zheng, J. G. Xu, and Y. D. Gu, "Interhemispheric functional reorganization after cross nerve transfer: via cortical or subcortical connectivity?," *Brain Research*, vol. 1471, pp. 93–101, 2012.

[74] H. Ma, M. Zheng, Y. Lu, X. Hua, and W. Xu, "Cerebral plasticity after contralateral cervical nerve transfer in human by longitudinal PET evaluation," *Journal of Clinical Neuroscience*, vol. 48, pp. 95–99, 2018.

[75] C. T. Anderson, P. L. Sheets, T. Kiritani, and G. M. G. Shepherd, "Sublayer-specific microcircuits of corticospinal and corticostriatal neurons in motor cortex," *Nature Neuroscience*, vol. 13, no. 6, pp. 739–744, 2010.

[76] M. J. Malessy, C. F. Hoffmann, and R. T. Thomeer, "Initial report on the limited value of hypoglossal nerve transfer to treat brachial plexus root avulsions," *Journal of Neurosurgery*, vol. 91, no. 4, pp. 601–604, 1999.

[77] W. P. Godefroy, M. J. A. Malessy, A. A. M. Tromp, and A. G. L. van der Mey, "Intratemporal facial nerve transfer with direct coaptation to the hypoglossal nerve," *Otology & Neurotology*, vol. 28, no. 4, pp. 546–550, 2007.

[78] A. Hayashi, M. Nishida, H. Seno et al., "Hemihypoglossal nerve transfer for acute facial paralysis," *Journal of Neurosurgery*, vol. 118, no. 1, pp. 160–166, 2013.

[79] S. Rochkind, M. Shafi, M. Alon, K. Salame, and D. Fliss, "Facial nerve reconstruction using a split hypoglossal nerve with preservation of tongue function," *Journal of Reconstructive Microsurgery*, vol. 24, no. 7, pp. 469–474, 2008.

[80] M. Socolovsky, R. S. Martins, G. di Masi, G. Bonilla, and M. Siqueira, "Treatment of complete facial palsy in adults:

comparative study between direct hemihypoglossal-facial neurorrhaphy, hemihipoglossal-facial neurorrhaphy with grafts, and masseter to facial nerve transfer," *Acta Neurochirurgica*, vol. 158, no. 5, pp. 945–957, 2016, discussion 957.

[81] R. Salomão, de Oliveira JP Jr, C. F. Junger, Soares Ricardo LC Jr, C. R. de Lima, and M. A. Acioly, "Delayed transfer of the extensor carpi radialis brevis branch of the radial nerve to the anterior interosseous nerve for restoration of thumb and index finger flexion: case report," *Journal of Neurological Surgery Part A: Central European Neurosurgery*, vol. 81, no. 6, pp. 571–574, 2020.

[82] J. A. Bertelli, "Transfer of the radial nerve branch to the extensor carpi radialis brevis to the anterior interosseous nerve to reconstruct thumb and finger flexion," *The Journal of Hand Surgery*, vol. 40, no. 2, pp. 323–328.e2, 2015.

[83] J. A. Bertelli, M. F. Ghizoni, and C. P. Tacca, "Results of wrist extension reconstruction in C5-8 brachial plexus palsy by transferring the pronator quadratus motor branch to the extensor carpi radialis brevis muscle," *Journal of Neurosurgery*, vol. 124, no. 5, pp. 1442–1449, 2016.

[84] J. A. Bertelli, C. P. Tacca, E. C. Winkelmann Duarte, M. F. Ghizoni, and H. Duarte, "Transfer of the pronator quadratus motor branch for wrist extension reconstruction in brachial plexus palsy," *Plastic and Reconstructive Surgery*, vol. 130, no. 6, pp. 1269–1278, 2012.

[85] A. Bhatia and M. Salama, "Pronator quadratus to extensor carpi radialis brevis nerve transfer in C5-C7 or C5-C8 brachial plexus injuries for independent wrist extension," *Indian Journal of Plastic Surgery*, vol. 53, no. 1, pp. 36–41, 2020.

[86] J. N. Goubier, C. Maillot, G. Asmar, and F. Teboul, "Partial ulnar nerve transfer to the branch of the long head of the triceps to recover elbow extension in C5, C6 and C7 brachial plexus palsy," *Injury*, vol. 50, Supplement 5, pp. S68–s70, 2019.

[87] L. P. Flores, "Transfer of a motor fascicle from the ulnar nerve to the branch of the radial nerve destined to the long head of the triceps for restoration of elbow extension in brachial plexus surgery: technical case report," *Neurosurgery*, vol. 70, no. 2, pp. E516–E520, 2012.

[88] P. Atthakomol, S. Ozkan, N. Chen, and S. G. Lee, "Combined flexor carpi ulnaris and flexor carpi radialis transfer for restoring elbow function after brachial plexus injury," *BML Case Reports*, vol. 12, no. 7, 2019.

[89] L. P. Flores, R. S. Martins, and M. G. Siqueira, "Clinical results of transferring a motor branch of the tibial nerve to the deep peroneal nerve for treatment of foot drop," *Neurosurgery*, vol. 73, no. 4, pp. 609–616, 2013, discussion 615-6.

[90] T. J. Wilson, "Novel uses of nerve transfers," *Neurotherapeutics*, vol. 16, no. 1, pp. 26–35, 2019.

[91] B. Xu, Z. Dong, C. G. Zhang, and Y. D. Gu, "Transfer of the radial branch of the superficial radial nerve to the sensory branch of the ulnar nerve for sensory restoration after C7-T1 brachial plexus injury," *Journal of Plastic, Reconstructive & Aesthetic Surgery*, vol. 69, no. 3, pp. 318–322, 2016.

[92] J. A. Bertelli, "Distal sensory nerve transfers in lower-type injuries of the brachial plexus," *The Journal of Hand Surgery*, vol. 37, no. 6, pp. 1194–1199, 2012.

[93] T. Gordon, "Electrical stimulation to enhance axon regeneration after peripheral nerve injuries in animal models and humans," *Neurotherapeutics*, vol. 13, no. 2, pp. 295–310, 2016.

[94] L. Foroni, M. G. Siqueira, R. S. Martins, C. O. Heise, H. Sterman Neto, and A. Y. Imamura, "Good sensory recovery of the hand in brachial plexus surgery using the intercostobrachial nerve as the donor," *Arquivos de Neuro-Psiquiatria*, vol. 75, no. 11, pp. 796–800, 2017.

[95] A. M. Moore, E. M. Krauss, R. P. Parikh, M. J. Franco, and T. H. Tung, "Femoral nerve transfers for restoring tibial nerve function: an anatomical study and clinical correlation: a report of 2 cases," *Journal of Neurosurgery*, vol. 129, no. 4, pp. 1024–1033, 2018.

[96] T. H. Tung, D. Z. Martin, C. B. Novak, C. Lauryssen, and S. E. Mackinnon, "Nerve reconstruction in lumbosacral plexopathy. Case report and review of the literature," *Journal of Neurosurgery*, vol. 102, 1 Suppl, pp. 86–91, 2005.

[97] A. Rodríguez-Lorenzo, B. Gago, A. F. Pineda, M. Bhatti, and T. Audolfsson, "Superficial peroneal and sural nerve transfer to tibial nerve for restoration of plantar sensation after complex injuries of the tibial nerve: cadaver feasibility study," *Journal of Plastic, Reconstructive & Aesthetic Surgery*, vol. 64, no. 11, pp. 1512–1516, 2011.

[98] J. T. Wall and J. H. Kaas, "Long-term cortical consequences of reinnervation errors after nerve regeneration in monkeys," *Brain Research*, vol. 372, no. 2, pp. 400–404, 1986.

[99] T. R. Makin and S. J. Bensmaia, "Stability of sensory topographies in adult cortex," *Trends in Cognitive Sciences*, vol. 21, no. 3, pp. 195–204, 2017.

[100] M. Emamhadi, M. Haghani Dogahe, and A. Gohritz, "Nerve transfers in tetraplegia: a review and practical guide," *Journal of Neurosurgical Sciences*, vol. 65, no. 4, pp. 431–441, 2021.

[101] M. X. Zheng, X. Y. Hua, J. T. Feng et al., "Trial of contralateral seventh cervical nerve transfer for spastic arm paralysis," *The New England Journal of Medicine*, vol. 378, no. 1, pp. 22–34, 2018.

[102] Y. D. Gu, G. M. Zhang, D. S. Chen, J. G. Yan, X. M. Cheng, and L. Chen, "Seventh cervical nerve root transfer from the contralateral healthy side for treatment of brachial plexus root avulsion," *Journal of Hand Surgery: British & European Volume*, vol. 17, no. 5, pp. 518–521, 1992.

[103] N. Nicolas, S. Kobaiter-Maarrawi, S. Georges, G. Abadjian, and J. Maarrawi, "Motor cortex stimulation regenerative effects in peripheral nerve injury: an experimental rat model," *World Neurosurgery*, vol. 114, pp. e800–e808, 2018.

[104] S. A. Hays, R. L. Rennaker, and M. P. Kilgard, "Targeting plasticity with vagus nerve stimulation to treat neurological disease," *Progress in Brain Research*, vol. 207, pp. 275–299, 2013.

[105] C. T. Engineer, N. D. Engineer, J. R. Riley, J. D. Seale, and M. P. Kilgard, "Pairing speech sounds with vagus nerve stimulation drives stimulus-specific cortical plasticity," *Brain Stimulation*, vol. 8, no. 3, pp. 637–644, 2015.

[106] S. A. Hays, "Enhancing rehabilitative therapies with vagus nerve stimulation," *Neurotherapeutics*, vol. 13, no. 2, pp. 382–394, 2016.

[107] D. J. Anastakis, M. J. A. Malessy, R. Chen, K. D. Davis, and D. Mikulis, "Cortical plasticity following nerve transfer in the upper extremity," *Hand Clinics*, vol. 24, no. 4, pp. 425–444, 2008, vi-vii.

Hindawi
Neural Plasticity
Volume 2022, Article ID 3895514, 10 pages
https://doi.org/10.1155/2022/3895514

Research Article

Effects of Tai Chi Exercise on Balance Function in Stroke Patients: An Overview of Systematic Review

Caixia Hu,[1] **Xiaohui Qin**,[1,2] **Minqing Jiang**,[1] **Miaoqing Tan**,[1] **Shuying Liu**,[1] **Yuhua Lu**,[1] **Changting Lin**,[1] **and Richun Ye**[1]

[1]*Department of Neurology, The Second Affiliated Hospital of Guangzhou University of Chinese Medicine (Guangdong Provincial Hospital of Chinese Medicine), Guangzhou, China*
[2]*Guangzhou University of Chinese Medicine, Guangzhou, China*

Correspondence should be addressed to Richun Ye; yerichun555@126.com

Received 9 December 2021; Revised 27 January 2022; Accepted 23 February 2022; Published 9 March 2022

Academic Editor: Mou-Xiong Zheng

Background. Tai chi (TC) has received increased attention in stroke rehabilitation, yet services are greatly underutilized. An increasing number of systematic reviews and meta-analyses (SRs/MAs) have begun to investigate the effects of TC on balance function in stroke patients. The aim of this current study was to systematically collate, appraise, and synthesize the results of these SRs/MAs using a systematic overview. *Methods*. Eight databases were searched: PubMed, Cochrane Library, Embase, Web of Science, CNKI, SinoMed, Chongqing VIP, and Wanfang Data. SRs/MAs of TC on balance function in stroke patients were included. Literature selection, data extraction, and assessment of the review quality were performed by two independent reviewers. Methodological quality was assessed by the Assessing the Methodological Quality of Systematic Reviews 2 (AMSTAR-2), reporting quality by Preferred Reporting Items for Systematic Reviews and Meta-Analyses (PRISMA), and evidence quality by Grading of Recommendations, Assessment, Development, and Evaluation (GRADE). *Results*. Nine SRs/MAs were included in this study. For methodological quality, what resulted in unsatisfactory methodological quality was noncompliance with critical item 4 (using a comprehensive literature search strategy) and critical item 7 (providing the list of excluded research literature). For reporting quality, what resulted in unsatisfactory reporting quality was inadequate reporting of Q1 (protocol and registration), Q8 (search), Q15 (risk of bias across studies), Q16 (additional analyses), Q22 (risk of bias across studies), Q23 (additional analysis), and Q27 (funding). For GRADE, the evidence quality was high in 0, moderate in 3, low in 11, and very low in 6. Risk of bias was the most common factor leading to downgrading of evidence, followed by inconsistency, imprecision, publication bias, and indirectness. *Conclusions*. TC may have beneficial effects on balance function in stroke survivors; however, this finding is limited by the generally low methodology, reporting quality, and evidence quality for published SRs/MAs.

1. Introduction

Stroke, a common and frequently occurring disease among elderly people, is considered to be the second most common cause of death and the third most common cause of disability worldwide [1].Stroke is a major global health challenge with a global incidence of 76-119 per 100,000 populations each year [2]. Despite the advances in stroke management in recent decades, up to 50% of stroke patients still have residual effects [3]. Impaired balance is the most common poststroke sequela [4] and an important predictor of functional independence after stroke [5]. Stroke survivors with impaired balance are more likely to fall and are associated with a higher risk of fracture, depression, anxiety, and even death [6]. Therefore, effective interventions to improve balance function in stroke survivors are urgently needed [7].

Various rehabilitation methods have been applied to improve balance functional training in stroke survivors [8], however with limited efficacy [9]. As a traditional martial art widely practiced in China for centuries, tai chi (TC) is well known for its slow and graceful rhythm transformation [10]. Recently, in December 2020, the United Nations Education

Scientific and Cultural Organization (UNESCO) announced that TC has been included in the representative list of the intangible cultural heritage of humanity. TC was instilled by ancient Chinese philosophies and Chinese medicine, such as Confucian and Taoist cultures, and the ancient Chinese dialectical thinking can be reflected in the various movements of TC [11]. TC is characterized by fluidity and gentleness, calmness and consistency, and most importantly movement based on awareness [10]. As a mind-body exercise, TC involves the coordination of posture and breathing patterns, which are distinctly different from other aerobic exercises [12]. Performing TC exercises requires low space and equipment and almost zero cost, making it suitable for people of all ages in different conditions. There is ample evidence that tai chi is beneficial for dementia, depression, and cardiac and stroke rehabilitation [12]. For stroke rehabilitation, previous studies have shown that TC may be effective in improving balance, flexibility, and coordination and enhancing muscle strength, therefore helping to reduce the risk of falls [13]. Thus, TC has received increasing attention in stroke rehabilitation.

SRs/MAs are considered the gold standard for assessing the efficacy of clinical interventions, but the evidence derived from them is currently facing challenges due to the various risks of bias generated during the formation of evidence by SRs/MAs [14]. High-quality SRs/MAs can provide reliable evidence, while low-quality SRs/MAs may instead mislead decision-makers [15]. Thus, the evidence of uneven quality leads to a gap between its use and practical implementation in real-world dynamics. Where multiple SRs/MAs are published for overlapping topics in a relatively short time frame, an overview is needed to systematically collate, evaluate, and synthesize the evidence from these SRs/MAs [16]. The ultimate goal of an overview is to provide a comprehensive evaluation of the current evidence on multiple identical topics, to provide more focused high-quality evidence to evidence users, and to identify key flaws in evidence use [14]. A literature search yielded a growing number of systematic reviews, and the meta-analyses (SRs/MAs) have examined the effects of TC on balance function of stroke patients. To systematically collate, appraise, and synthesize the results of these SRs/MAs, we carried out this study.

2. Methods

This study was conducted according to the Cochrane Handbook [17] and some high-quality methodological articles [10, 11]. The protocol was prospectively registered on the PROSPERO (CRD42021240693).

2.1. Inclusion and Exclusion Criteria

2.1.1. Type of Studies. SRs/MAs only included clinical random control trails (RCTs) investigating the therapeutic effects of TC on balance function in stroke patient. No language constraints were placed on this study.

2.1.2. Types of Subjects. The subjects were diagnosed as stroke, regardless of age, sex, or race.

2.1.3. Types of Interventions. The experimental intervention was the use of TC in stroke survivors with conventional rehabilitation therapy (CRT) as the control intervention.

2.1.4. Types of Outcomes. The outcome indicators focused on balance and gait after stroke, e.g., short physical performance battery (SPPB), functional reach test (FRT), dynamic gait index (DGI), timed up-and-go test (TUG), Holden walking grading scale, Berg balance scale (BBS), Fugl-Meyer assessment scale (FMA), and fall rates.

2.2. Search Strategy. PubMed, Cochrane Library, Embase, Web of science, CNKI, Chongqing VIP, SinoMed, and Wanfang Data were searched from their inception to April 2021. The following keywords were used: Tai Chi, stroke, balance, systematic review, and meta-analysis. Detailed search strategy in PubMed was given in Appendix file 1.

2.3. Eligibility Assessment and Data Extraction. Search results were imported into Endnote. The titles and abstracts were screened by two independent reviewers firstly; the potential full texts were then evaluated to determine the final eligibility. Any discrepancies were solved by introducing a third researcher for judgment.

Data were extracted from each included SRs/MAs using a predefined form by two independent reviewers. Information of authors, published year, country, sample, quality assessment tool, interventions, comparisons, outcome measures, data synthesis methods, and main results were extracted. Any discrepancies were solved by introducing a third researcher for judgment.

2.4. Review Quality Assessment. The methodological quality, reporting quality, and evidence quality were assessed by two independent reviewers using the Assessing the Methodological Quality of Systematic Reviews 2 (AMSTAR-2) tool [18] and the Preferred Reporting Items for Systematic Reviews and Meta-Analyses (PRISMA) [19], respectively. Any discrepancies were solved by introducing a third researcher for judgment. For evidence quality, each meta-analysis for the outcome of interest was assessed by two independent reviewers using the Grading of Recommendations Assessment, Development and Evaluation (GRADE) system [20]. Any discrepancies were solved by introducing a third researcher for judgment. Detailed items for AMSTAR-2 are provided in Additional file 2 and for PRISMA in Additional file 3.

3. Results

3.1. Results on Literature Selection. The electronic searches resulted in 135 articles. After removal of duplicates, 82 were excluded at the title and abstract stage. Fifteen articles were retrieved for examination on full text, with 9 reviews [21–29] finally included. Figure 1 outlines the process of identifying the qualified articles.

3.2. Studies Characteristics. All studies were published between 2016 and 2021, with 5 [21–25] written in English and 4 in Chinese [26–29]. Authors of all included reviews were from China. The number of RCTs within each review

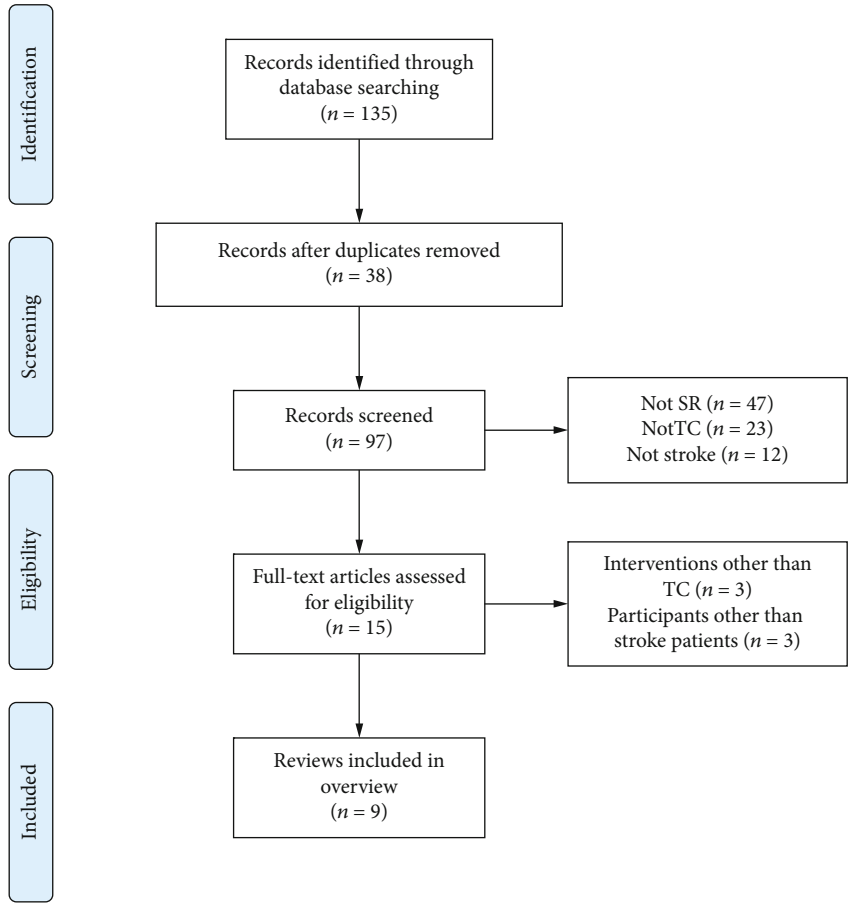

Figure 1: Literature selection procedure.

ranged from 7 to 21, and the participants in these RCTs ranged from 346 to 1297. TC or TC plus CRT was used in the treatment group, and CRT was used lonely in the control group. All reviews evaluated the risk of bias of the RCTs, 3 used the Jadad scale, and the remaining 6 used Cochrane risk of bias criteria. All reviews conducted a meta-analysis, and both of them reached positive results. Details are presented in Table 1.

3.3. Quality Assessment

3.3.1. Methodological Quality. The results of methodological quality are reported in Figure 2. The main weakness affecting the methodological quality was the following: only 2 (22.2%) reviews registered a protocol before conducting the study; no (0%) reviews provided the list of excluded research literature; only 5 (55.6%) reviews provided the use of a specific search strategy; only 6 (66.7%) reviews carried out an investigation of publication bias and discussed its likely impact on the results; and 11.1% did not report the funding source and declare the conflicts of interest. Based on the above assessment, all reviews were judged to provide "low/critically low" methodological quality.

3.3.2. Reporting Quality. The results of reporting quality are reported in Table 2. In summary, only two studies reported all items of PRISMA, and the reaming studies were reported over 75%. The main weakness affecting the reporting quality was the following: only22.2% reviews reported the topic of the protocol and registration, 55.6% reported specific search strategy, 77.8% reported risk of bias across studies, and 66.7% reported additional analyses in the section of the methods; for the result section, 88.9% reported the risk of bias, and 66.7% reported additional analyses; for the funding section, it was reported in only 88.9% reviews.

3.3.3. Evidence Quality. The results of evidence quality are reported in Table 3.Twenty outcomes related to the effectiveness of TC on balance function of stroke patients were included. Among these outcome indicators, the evidence quality was high in 0 (0/20.0%), moderate in 3 (3/20.15%), low in 11 (11/20.55%), and very low in 6 (6/20.30%).

3.4. Efficacy Evaluation. Narrative synthesis was performed for all included outcomes. When the TC group was compared with controls, there were a significant effect for better BBC in 7 reviews; a significant effect for better FMA, balance, and walking in 2 reviews; and a significant effect for TUG, Holden scores, and gait ability in 1 review. However, there were no significant difference in SPBB and FMA between the TC and controls in 2 reviews and no significant difference in balance

Table 1: Study characteristics.

Reviews	Country	Simple	Treatment intervention	Control intervention	Quality assessment	Meta-analysis	Conclusions
Zheng [21]	China	8 (1297)	TC and TC+CRT	CRT	Cochrane criteria	Yes	Balance functions and exercise capacities of stroke patients improved after they did TC exercise regularly.
Wu [22]	China	6 (347)	TC and TC+CRT	CRT	Jadad	Yes	These findings indicated that TC is superior to the CRT in the improvement of balance function, gait speed, and quality of life.
Li [23]	China	5 (346)	TC and TC+CRT	CRT	Cochrane criteria	Yes	TC may be beneficial for balance function in stroke survivors in the short term, but further RCTs with large sample sizes and long-term follow-up are needed to confirm this conclusion.
Lyu [24]	China	21 (1293)	TC and TC+CRT	CRT	Cochrane criteria	Yes	TC was beneficial on ADL, balance, limb motor function, and walking ability among stroke survivors.
Li [25]	China	17 (1209)	TC	CRT	Cochrane criteria	Yes	TC was superior to the CRT in the improvement of balance function and quality of life. However, there were no significant differences in walking function.
Wang [26]	China	8 (408)	TC and TC+CRT	CRT	Jadad	Yes	TC was superior to the CRT in the improvement of balance ability and motor function.
Qin [27]	China	15 (1016)	TC	CRT	Jadad	Yes	These findings indicated that TC was superior to the CRT in the improvement of balance function, gait speed, and quality of life.
Miao [28]	China	9 (698)	TC and TC+CRT	CRT	Cochrane criteria	Yes	The study indicated that TC could improve the balance function for stroke patients. However, further large, long-term RCTs with standard evaluation indicators are needed to confirm this conclusion.
Li [29]	China	7 (629)	TC and TC+CRT	CRT	Cochrane criteria	Yes	These findings indicated that TC was superior to the CRT in the improvement of balance function, gait speed, and quality of life.

and walking in 1 reviews. More details are presented in Table 3.

4. Discussion

Stroke rehabilitation has always been a key health concern worldwide. Complementary and alternative therapies hold promise for improving the quality of life of stroke survivors [30]. TC is widely used in China for functional recovery exercises after stroke, and bibliometric evidence supports that TC may be a frontiers and promising field for stroke rehabilitation [31]. The core of the overview is a comprehensive evaluation of current SR/MA evidence on multiple identical topics, providing a more focused evidence base for users of the evidence [32]. A literature search yielded a growing number of SRs/MAs that examined the effects of TC on balance function of stroke patients. However, the quality of these SRs/MAs has not been evaluated, and their results were not completely consistent. Hence, to systematically collate, appraise, and synthesize the results of these SRs/MAs, a systematic overview was conducted.

4.1. Summary of Main Findings. First, this overview identified 9SRs/MAs which contained evidence relevant to the effects of TC on balance function of stroke patients. However, the methodological quality, reporting quality, and evidence quality of

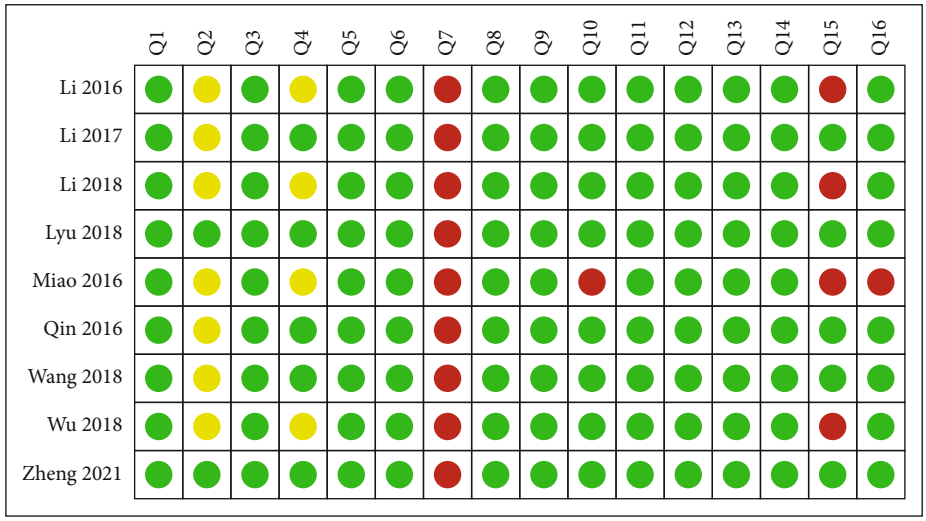

Figure 2: AMSTAR-2 assessments.

the included SRs/MAs were unsatisfactory. For methodological quality, the evaluation results of AMSTAR-2 showed that all included SRs/MAs had one or more critical items that were unmet; thus, these SRs/MAs were all judged to be of low or critically low methodological quality. What resulted in unsatisfactory methodological quality was noncompliance with critical item 4 (using a comprehensive literature search strategy) and critical item 7 (providing the list of excluded research literature). For reporting quality, the evaluation results of PRISMA showed that only 2 reviews had reported all items, and the reaming reviews had various degrees of missing report content. What resulted in unsatisfactory reporting quality was inadequate reporting of Q1 (protocol and registration), Q8 (search), Q15 (risk of bias across studies), Q16 (additional analyses), Q22 (risk of bias across studies), Q23 (additional analysis), and Q 27 (funding). For evidence quality, twenty outcomes were included; however, the evidence quality was high in 0 and moderate in 6, and the reaming were all judged to be of low or critically low evidence quality. Risk of bias was the most common factor leading to downgrading of evidence, followed by inconsistency, imprecision, publication bias, and indirectness.

Second, definitive conclusions of the effects of TC on balance function of stroke patients cannot be drawn based on the published SRs/MAs. In this overview, all included SRs/MAs concluded positive finding of the effects of TC on balance function in stroke patients. However, most authors of these SRs/MAs did not want to draw firm conclusions due to the small size of the included RCTs or their low quality. Furthermore, as we all know, only SRs/MAs with high quality will be helpful to provide scientific evidence. However, the evaluation results of this overview found that the overall methodological quality, reporting quality, and evidence quality of the included SRs/MAs were unsatisfactory, indicating that there were limitations in the reliability of the conclusions of these included SRs/MAs. Hence, caution should be warranted when recommending TC for the rehabilitation of stroke patients.

Third, the authors of these included SRs/MAs used the term "tai chi" to represent all types of this exercise. Actually, TC was performed in a variety of forms, which were named after different Chinese families such as Chen, Yang, Wu, and Sun. Different types obviously can have inconsistent effects; thus, all types of TC will be represented by one term in the included SRs/MAs that could lead to a source of heterogeneity. The evaluation results of the evidence quality in this overview revealed that inconsistency was one of the important factors for evidence degradation, which further verified that it may be unreasonable to represent this exercise in the term of "tai chi" and that subgroup analysis for different types of TC in SRs/MAs is still necessary. In addition, the variety of TC protocols, including differences in training style, form, frequency, and duration, may have contributed to the source of heterogeneity in the included SRs/MAs. Recommendations regarding TC parameters need to be standardized.

4.2. Application, Mechanism, and Frontier of TC in Stroke Rehabilitation. TC has been used in stroke rehabilitation worldwide for more than 10 years [33]. In recent years, researchers have increasingly focused on the role of TC in improving balance function in stroke survivors [21–29]. The improvement of balance function by TC is part of the comprehensive rehabilitation of stroke survivors and has an inherent relationship with functional rehabilitation. Balance function is closely associated with muscle strength, especially in the lower limbs. A recent 3D kinetic study reported that TC leads to similar mechanical behavior of biologically based tissues that can enhance lower limb strength, which in turn can help improve balance function and prevent falls [34]. Another electromyography study found similar results of increased lower limb muscle strength and improved neuromuscular responses after practicing TC for one year [35]. In addition, for stroke survivors with lower extremity paralysis, wheelchair TC can also help improve upper extremity mobility [36]. In terms of mechanistic studies, TC has been reported to act by modulating the neural function and biomechanics of balance; that is, TC improves neuromuscular responses and enhances balance function by controlling the stepping strategy of the swinging leg [37, 38]. In recent years, functional MRI and electroencephalography have been used

Table 2: Result of the PRISMA assessments.

Section/ topic	Items	Zheng 2021	Wu 2018	Li 2018	Lyu 2018	Li 2017	Wang 2018	Qin 2016	Miao 2016	Li 2016	Compliance (%)
Title	Q1	Y	Y	Y	Y	Y	Y	Y	Y	Y	100%
Abstract	Q2	Y	Y	Y	Y	Y	Y	Y	Y	Y	100%
Introduction	Q3	Y	Y	Y	Y	Y	Y	Y	Y	Y	100%
	Q4	Y	Y	Y	Y	Y	Y	Y	Y	Y	100%
	Q5	Y	N	N	Y	N	N	N	N	N	22.2%
	Q6	Y	Y	Y	Y	Y	Y	Y	Y	Y	100%
	Q7	Y	Y	Y	Y	Y	Y	Y	Y	Y	100%
	Q8	Y	PY	PY	Y	Y	Y	Y	PY	PY	55.6%
Methods	Q9	Y	Y	Y	Y	Y	Y	Y	Y	Y	100%
	Q10	Y	Y	Y	Y	Y	Y	Y	Y	Y	100%
	Q11	Y	Y	Y	Y	Y	Y	Y	Y	Y	100%
	Q12	Y	Y	Y	Y	Y	Y	Y	Y	Y	100%
	Q13	Y	Y	Y	Y	Y	Y	Y	Y	Y	100%
	Q14	Y	Y	Y	Y	Y	Y	Y	Y	Y	100%
	Q15	Y	Y	N	Y	Y	Y	Y	Y	N	77.8%
	Q16	Y	N	N	Y	Y	Y	Y	N	Y	66.7%
	Q17	Y	Y	Y	Y	Y	Y	Y	Y	Y	100%
Results	Q18	Y	Y	Y	Y	Y	Y	Y	Y	Y	100%
	Q19	Y	Y	Y	Y	Y	Y	Y	Y	Y	100%
	Q20	Y	Y	Y	Y	Y	Y	Y	Y	Y	100%
	Q21	Y	Y	Y	Y	Y	Y	Y	Y	Y	100%
	Q22	Y	Y	N	Y	Y	Y	Y	Y	Y	88.9%
	Q23	Y	N	N	Y	Y	Y	Y	N	Y	66.7%
	Q24	Y	Y	Y	Y	Y	Y	Y	Y	Y	100%
Discussion	Q25	Y	Y	Y	Y	Y	Y	Y	Y	Y	100%
	Q26	Y	Y	Y	Y	Y	Y	Y	Y	Y	100%
Funding	Q27	Y	Y	Y	Y	Y	Y	Y	N	Y	88.9%

to study central mechanisms. It was found that bilateral dorsolateral prefrontal cortex and hippocampus with enhanced functional connectivity and low frequency fluctuations in amplitude were observed in TC-trained patients [39]. In addition, meaningful functional and structural changes in the default mode network were detected, suggesting that tai chi helps improve patients' attention, which in turn affects balance and walking ability [40]. Greater amplitude of P3b event-related potential switching trials was observed from electroencephalography, suggesting that TC may promote peripheral nervous system recovery through central action [41].

In addition, TC also contributes to the recovery of other functions after stroke, such as cognitive function [42]. The mechanism lies in the positive impact on the patient's immune system by promoting DNA repair and lymphocyte renewal [43].

4.3. Implications for Practice and Research. The evaluation results identified common areas for improvement. First, study protocols should be registered in advance, which is essential to ensure the rigor of the SR/MA and to avoid any possible risk of bias. Second, specific and used search strategies for the exclusion of literature lists should be provided to ensure reproducibility of studies, improve transparency, and avoid publication bias. Third, the scientific nature of the analytical methods should be considered when conducting data analysis. For example, the subgroup analysis may be performed to address study heterogeneity. In addition, because commercially funded research yields results that may be biased in favor of the funder, the source of funding and any conflicts of interest should be fully reported. In summary, the quality of currently published SR/MA is unsatisfactory, and the defects that lead to the low quality have been clearly shown in this overview; future researchers should carry out the SRs/MAs in strict accordance with the standards to ensure the provision of high-quality evidence.

4.4. Limitations. This study uses the method of overview to systematically collate, appraise, and synthesize the results of SRs/MAs regarding to the effects of TC on balance function in stroke patients. However, limitations need to be acknowledged. First, it can be expected that there will be some overlapping trials in the included SRs/MAs. However, these overlaps have not been systematically explored, which may lead to double counting of data in the reported meta-analysis. Second, SRs/MAs included in this overview used the term "tai chi" to

Table 3: Results of evidence quality.

Review	Outcomes	No. of trails	Design	Certainty assessment					No. of patients		Relative effect (95% CI)	*P* value	Quality
				Limitations	Inconsistency	Indirectness	Imprecision	Publication bias	Experimental	Control			
Zheng [21]	BBC	6	Rct	Serious[a]	Serious[b]	No	No	No	231	181	MD 7.67 (3.44, 11.90)	<0.001	⨁⨁⨁◯◯ Low
	FMA	5	Rct	Serious[a]	Serious[b]	No	No	No	335	321	MD 4.15 (1.68, 6.63)	0.001	⨁⨁⨁◯◯ Low
	SPPB	2	Rct	Serious[a]	No	No	Serious[c]	No	69	60	MD -0.22 (-1.00, 0.56)	0.589	⨁⨁⨁◯◯ Low
Wu [22]	BBC	3	Rct	Serious[a]	Serious[b]	No	Serious[c]	Serious[d]			MD 4.823 (2.138, 7.508)	<0.001	⨁◯◯◯◯ Very low
	SPPB	2	Rct	Serious[a]	Serious[b]	No	Serious[c]	Serious[d]			MD 0.293 (-0.099, 0.685)	0.14	⨁◯◯◯◯ Very low
Li [23]	Gait ability (TUG and SPBB)	4	Rct	Serious[a]	No	No	No	Serious[d]	151	133	SMD -0.26 (-0.50, -0.03)	0.027	⨁⨁⨁◯◯ Low
	Balance (SPBB, DGI, and FRT)	3	Rct	Serious[a]	No	No	No	Serious[d]	77	71	SMD 0.15 (-0.27, 0.58)	0.475	⨁⨁⨁◯◯ Low
Lyu [24]	FMA	3	Rct	Serious[a]	Serious[b]	No	Serious[c]	No	85	81	MD 2.75 (0.95, 4.56)	0.003	⨁⨁◯◯◯ Very low
	BBS	2	Rct	Serious[a]	No	No	Serious[c]	No	75	75	MD 5.23 (3.42, 7.05)	<0.001	⨁⨁⨁◯◯ Low
	Holden scale	3	Rct	Serious[a]	No	No	Serious[c]	No	94	92	MD 0.61 (0.38, 0.85)	<0.001	⨁⨁⨁◯◯ Low
	TUG	5	Rct	Serious[a]	No	No	No	No	200	180	MD 2.59 (1.76, 3.43)	<0.001	⨁⨁⨁⨁◯ Moderate
Li [25]	BBS	9	Rct	No	Serious[b]	No	No	No	333	337	MD 9.34 (6.49, 12.19)	<0.001	⨁⨁⨁⨁◯ Moderate
	Walking (TUG and Holden scale)	4	Rct	No	Serious[b]	No	No	No	259	248	MD 0.84 (-0.31, 0.55)	0.05	⨁⨁⨁⨁◯ Moderate
Wang [26]	BBS	6	Rct	Serious[a]	Serious[b]	No	Serious[c]	No	118	118	SMD 2.49 (0.90, 4.07)	<0.001	⨁⨁◯◯◯ Very low
	FMA	3	Rct	Seriousa	Seriousb	No	Serious[c]	No	64	64	SMD 0.84 (-0.91, 2.58)	0.35	⨁⨁◯◯◯ Very low
Qin [27]	Balance (BBS, SPBB, and DGI)	9	Rct	Serious[a]	Serious[b]	No	No	No	283	275	MD 2.49 (0.90, 4.07)	<0.001	⨁⨁⨁◯◯ Low
	Walking (SPBB and TUG)	4	Rct	Seriousa	Seriousb	No	No	No	129	120	MD 0.27 (0.04, 0.50)	0.02	⨁⨁⨁◯◯ Low

Table 3: Continued.

Review	Outcomes	No. of trails	Design	Certainty assessment					No. of patients		Relative effect (95% CI)	*P* value	Quality
				Limitations	Inconsistency	Indirectness	Imprecision	Publication bias	Experimental	Control			
Miao [28]	BBS	7	Rct	No	Serious[b]	No	No	Serious[d]	344	379	MD 11.43 (7.43, 15.42)	<0.001	⨁⨁⨁◯◯ Low
	FMA	2	Rct	No	Serious[b]	No	Serious[c]	Serious[d]	110	114	MD 12.77 (-5.07, 30.60)	0.16	⨁⨁◯◯◯ Very low
Li [29]	BBS	2	Rct	Serious[a]	No	No	No	Serious[d]	283	306	MD 6.36 (5.23, 7.49)	<0.01	⨁⨁⨁◯◯ Low

CI: confidence interval; MD: mean difference; SMD: standardized mean difference; [a]the experimental design had a large bias in random and distributive findings or was blind; [b]the confidence interval overlap less, the heterogeneity test *P* was very small, and the I^2 was larger; [c]the confidence interval was not narrow enough, or the simple size is too small; [d]funnel graph asymmetry, or fewer studies were included, and there may have been greater publication bias.

represent all types of this exercise, and relevant information on the different types of TC was lacking, so this overview cannot draw recommendations for the use of specific types of TC. Additionally, in the context of the coronavirus disease 2019 (COVID-19) pandemic, the isolation may lead to less exercise and more health-related problems; hence, the effects of TC on balance function and stroke patients under COVID were not included in is a pity.

5. Conclusion

TC may have beneficial effects on balance function in stroke survivors; however, this finding is limited by the generally low methodology, reporting quality, and evidence quality for published SRs/MAs.

Abbreviations

TC: Tai chi
SR: Systematic review
MA: Meta-analysis
AMSTAR-2: Assessing the Methodological Quality of Systematic Reviews 2
PRISMA: Preferred Reporting Items for Systematic Reviews and Meta-Analyses
GRADE: Grading of Recommendations, Assessment, Development, and Evaluation
RCT: Random control trails
CRT: Conventional rehabilitation therapy
BBS: Berg balance scale
SPBB: Short physical performance battery
FRT: Functional reach test
FGI: Dynamic gait index
TUG: Timed up-and-go test
FMA: Fugl-Meyer assessment.

Data Availability

All analyses were based on previously published studies; thus, no informed consent is required.

Disclosure

Caixia Hu and Xiaohui Qin are the co-first authors.

Conflicts of Interest

The authors declare that there is no conflict of interest.

Authors' Contributions

Caixia Hu and Xiaohui Qin designed the study and drafted the manuscript; they have contributed equally to this work. Minqing Jiang, Miaoqing Tan, Shuying Liu, Yuhua Lu, and Changting Lin contributed to the literature search, figures, data collection, and data analysis. Richun Ye provided guidance on the methodology. All authors read and approved the final manuscript.

Supplementary Materials

Appendix 1: search strategies of PubMed. Additional file 2: the 16 items of AMSTAR-2. Additional file 3: the 27 checklists of PRISMA. *(Supplementary Materials)*

References

[1] GBD 2016 Stroke Collaborators, "A systematic analysis for the global burden of disease study 2016," *Lancet Neurology*, vol. 18, pp. 439–458, 2019.

[2] A. G. Thrift, T. Thayabaranathan, G. Howard et al., "Global stroke statistics," *International Journal of Stroke*, vol. 12, no. 1, pp. 13–32, 2017.

[3] E. S. Donkor, "Stroke in the century: a snapshot of the burden, epidemiology, and quality of life," *Stroke Research and Treatment*, vol. 2018, Article ID 3238165, 10 pages, 2018.

[4] S. H. Jang, "The recovery of walking in stroke patients: a review," *International Journal of Rehabilitation Research*, vol. 33, no. 4, pp. 285–289, 2010.

[5] Z. Tan, H. Liu, T. Yan et al., "The effectiveness of functional electrical stimulation based on a normal gait pattern on subjects with early stroke: a randomized controlled trial," *BioMed Research International*, vol. 2014, Article ID 545408, 2014.

[6] L. Zou, A. Yeung, C. Li et al., "Effects of mind-body movements on balance function in stroke survivors: a meta-analysis of randomized controlled trials," *International Journal of Environmental Research and Public Health*, vol. 15, no. 6, p. 1292, 2018.

[7] P. Nayak, A. Mahmood, M. Natarajan, A. Hombali, C. G. Prashanth, and J. M. Solomon, "Effect of aquatic therapy on balance and gait in stroke survivors: a systematic review and meta-analysis," *Complementary Therapies in Clinical Practice*, vol. 39, article 101110, 2020.

[8] C. Arienti, S. G. Lazzarini, A. Pollock, and S. Negrini, "Rehabilitation interventions for improving balance following stroke: an overview of systematic reviews," *PLoS One*, vol. 14, no. 7, article e0219781, 2019.

[9] A. Pollock, G. Baer, V. Pomeroy, and P. Langhorne, "Physiotherapy treatment approaches for the recovery of postural control and lower limb function following stroke," *Cochrane Database of Systematic Reviews*, 2007.

[10] J. Huang, X. Qin, M. Shen, Y. Xu, and Y. Huang, "The Effects of Tai Chi Exercise Among Adults With Chronic Heart Failure: An Overview of Systematic Review and Meta-Analysis," *Frontiers in Cardiovascular Medicine*, vol. 8, 2021.

[11] J. Huang, H. Liu, J. Chen, X. Cai, and Y. Huang, "The effectiveness of tai chi in patients with breast cancer: an overview of systematic reviews and meta-analyses," *Journal of Pain and Symptom Management*, vol. 61, no. 5, pp. 1052–1059, 2021.

[12] P. Huston and B. McFarlane, "Health benefits of tai chi: what is the evidence?," *Canadian Family Physician*, vol. 62, no. 11, pp. 881–890, 2016.

[13] S. J. Winser, W. W. N. Tsang, K. Krishnamurthy, and P. Kannan, "Does tai chi improve balance and reduce falls incidence in neurological disorders? A systematic review and meta-analysis," *Clinical Rehabilitation*, vol. 32, no. 9, pp. 1157–1168, 2018.

[14] J. Huang, M. Shen, X. Qin, W. Guo, and H. Li, "Acupuncture for the treatment of tension-type headache: an overview of

systematic reviews," *Evidence-based Complementary and Alternative Medicine*, vol. 2020, Article ID 4262910, 10 pages, 2020.

[15] J. Huang, M. Lu, Y. Zheng et al., "Quality of evidence supporting the role of acupuncture for the treatment of irritable bowel syndrome," *Pain Research and Management*, vol. 2021, Article ID 2752246, 10 pages, 2021.

[16] J. Huang, M. Wu, S. Liang et al., "A critical overview of systematic reviews and meta-analyses on acupuncture for poststroke insomnia," *Evidence-based Complementary and Alternative Medicine*, vol. 2020, Article ID 2032575, 7 pages, 2020.

[17] J. Higgins and S. Green, "Cochrane handbook for systematic reviews for interventions," in *Cochrane Database of Systematic Reviews*, p. S38, The Cochrane Collaboration, 2011.

[18] B. J. Shea, B. C. Reeves, G. Wells et al., "AMSTAR 2: a critical appraisal tool for systematic reviews that include randomised or non-randomised studies of healthcare interventions, or both," *BMJ*, vol. 358, article j4008, 2017.

[19] D. Moher, A. Liberati, J. Tetzlaff, D. G. Altman, and for the PRISMA Group, "Preferred reporting items for systematic reviews and meta-analyses: the PRISMA statement," *BMJ*, vol. 339, article b2535, 2009.

[20] D. Atkins, D. Best, P. A. Briss et al., "Grading quality of evidence and strength of recommendations," *BMJ*, vol. 328, no. 7454, p. 1490, 2004.

[21] X. Zheng, X. Wu, Z. Liu et al., "The influences of tai chi on balance function and exercise capacity among stroke patients: a meta-analysis," *Evidence-based Complementary and Alternative Medicine*, vol. 2021, Article ID 6636847, 12 pages, 2021.

[22] S. Wu, J. Chen, S. Wang, M. Jiang, X. Wang, and Y. Wen, "Effect of tai chi exercise on balance function of stroke patients: a meta-analysis," *Medical Science Monitor Basic Research*, vol. 24, pp. 210–215, 2018.

[23] G. Yan Li, W. Wang, G. L. Liu, and Y. Zhang, "Effects of tai chi on balance and gait in stroke survivors: a systematic meta-analysis of randomized controlled trials," *Journal of Rehabilitation Medicine*, vol. 50, no. 7, pp. 582–588, 2018.

[24] D. Lyu, X. Lyu, Y. Zhang et al., "Tai chi for stroke rehabilitation: a systematic review and meta-analysis of randomized controlled trials," *Frontiers in Physiology*, vol. 9, p. 983, 2018.

[25] Y. Li, Y. Zhang, C. Cui et al., "The effect of tai chi exercise on motor function and sleep quality in patients with stroke: a meta-analysis," *International Journal of Nursing Sciences*, vol. 4, no. 3, pp. 314–321, 2017.

[26] C. Wang, J. Yang, R. W. Wang, and Y. Zhang, "Meta-analysis of short-term tai chi combined with conventional rehabilitation training in the treatment of balance ability and motor function in stroke patients with hemiplegia," *Chinese Journal of Rehabilitation Medicine*, vol. 33, no. 11, pp. 1322–1328, 2018.

[27] L. Qin, X. Wei, L. Liu, and H. Zhu, "Effectiveness of tai chi on movement, emotion and quality of life in patients with stroke: a meta-analysis," *Chinese Journal of Tissue Engineering Research*, vol. 20, no. 2, pp. 297–303, 2016.

[28] Y. Miao, "Meta-analysis of effect of tai chi on balance function of stroke patients," *Tianjin Journal of Nursing*, vol. 24, no. 6, pp. 501–504, 2016.

[29] S. Z. Li, G. H. Zheng, Y. C. Wang, S. Li, and J. He, "Effect of tai chi exercise on balance function of patients with stroke: a systematic review," *Rehabilitation Medicine*, vol. 26, no. 2, pp. 57–62, 2016.

[30] N. Venketasubramanian, "Complementary and alternative interventions for stroke recovery - a narrative overview of the published evidence," *J Complement Integr Med.*, vol. 18, no. 3, pp. 553–559, 2021.

[31] Y. You, L. Min, M. Tang, Y. Chen, and X. Ma, "Bibliometric evaluation of global tai chi research from 1980-2020," *International Journal of Environmental Research and Public Health*, vol. 18, no. 11, p. 6150, 2021.

[32] J. Huang, M. Shen, X. Qin, M. Wu, S. Liang, and Y. Huang, "Acupuncture for the treatment of Alzheimer's disease: an overview of systematic reviews," *Frontiers in Aging Neuroscience*, vol. 12, p. 574023, 2020.

[33] J. Hart, H. Kanner, R. Gilboa-Mayo, O. Haroeh-Peer, N. Rozenthul-Sorokin, and R. Eldar, "Tai chi chuan practice in community-dwelling persons after stroke," *International Journal of Rehabilitation Research*, vol. 27, no. 4, pp. 303-304, 2004.

[34] J. X. Li and N.-Y. Law, "Kinetics of the lower limb during two typical tai chi movements in the elderly," *Research in Sports Medicine*, vol. 26, no. 1, pp. 112–123, 2018.

[35] W. Sun, C. Zhang, Q. Song et al., "Effect of 1-year regular tai chi on neuromuscular reaction in elderly women: a randomized controlled study," *Research in Sports Medicine*, vol. 24, no. 2, pp. 145–156, 2016.

[36] Y. T. Wang, Z. Li, Y. Yang et al., "Effects of wheelchair tai chi on physical and mental health among elderly with disability," *Research in Sports Medicine*, vol. 24, no. 3, pp. 157–170, 2016.

[37] S. K. Gatts and M. H. Woollacott, "Neural mechanisms underlying balance improvement with short term tai chi training," *Aging Clinical and Experimental Research*, vol. 18, no. 1, pp. 7–19, 2006.

[38] D. W. Man, W. W. Tsang, and C. W. Hui-Chan, "Do older t'ai chi practitioners have better attention and memory function?," *Journal of Alternative and Complementary Medicine*, vol. 16, no. 12, pp. 1259–1264, 2010.

[39] J. Tao, X. Chen, J. Liu et al., "Tai chi chuan and baduanjin mind-body training changes resting-state low-frequency fluctuations in the frontal lobe of older adults: a resting-state fMRI study," *Frontiers in Human Neuroscience*, vol. 11, p. 514, 2017.

[40] G. Wei, H. Dong, Z. Yang, J. Luo, and X. Zuo, "Tai chi chuan optimizes the functional organization of the intrinsic human brain architecture in older adults," *Frontiers in Aging Neuroscience*, vol. 6, p. 74, 2014.

[41] T. D. Hawkes, W. Manselle, and M. H. Woollacott, "Tai chi and meditation-plus-exercise benefit neural substrates of executive function: a cross-sectional, controlled study," *J. Complement. Integr. Med.*, vol. 11, no. 4, pp. 279–288, 2014.

[42] L. C. W. Lam, R. C. M. Chau, B. M. L. Wong et al., "Interim follow-up of a randomized controlled trial comparing Chinese style mind body (tai chi) and stretching exercises on cognitive function in subjects at risk of progressive cognitive decline," *International Journal of Geriatric Psychiatry*, vol. 26, no. 7, pp. 733–740, 2011.

[43] J. Goon, A. Aini, M. Musalmah, M. Anum, and W. Wan Ngah, "Long term tai chi exercise reduced DNA damage and increased lymphocyte apoptosis and proliferation in older adults," *The Medical Journal of Malaysia*, vol. 63, no. 4, pp. 319–324, 2008.

Hindawi
Neural Plasticity
Volume 2022, Article ID 4217593, 13 pages
https://doi.org/10.1155/2022/4217593

Review Article

Current Understanding of the Neural Circuitry in the Comorbidity of Chronic Pain and Anxiety

Teng Chen,[1] Jing Wang,[2] Yan-Qing Wang,[1,3,4,5] and Yu-Xia Chu[1,4,5]

[1]*Department of Integrative Medicine and Neurobiology, School of Basic Medical Sciences, Shanghai Medical College, Institute of Acupuncture Research, Institutes of Integrative Medicine, Fudan University, Shanghai, China*
[2]*Department of Nephropathy, The Third Affiliated Hospital of Shenzhen University, Luohu Hospital Group, Shenzhen, China*
[3]*State Key Laboratory of Medical Neurobiology and MOE Frontiers Center for Brain Science, Institutes of Brain Science, Fudan University, Shanghai, China*
[4]*Shanghai Key Laboratory of Acupuncture Mechanism and Acupoint Function, Department of Aeronautics and Astronautics, Fudan University, Shanghai, China*
[5]*Shanghai Research Center for Acupuncture and Meridian, Shanghai, China*

Correspondence should be addressed to Yu-Xia Chu; yuxiachu@fudan.edu.cn

Received 11 November 2021; Revised 13 January 2022; Accepted 27 January 2022; Published 15 February 2022

Academic Editor: Mou-Xiong Zheng

Chronic pain patients often develop mental disorders, and anxiety disorders are common. We hypothesize that the comorbid anxiety results from an imbalance between the reward and antireward system due to persistent pain, which leads to the dysfunction of the pain and anxiety regulatory system. In this review, we will focus on changes in neuroplasticity, especially in neural circuits, during chronic pain and anxiety as observed in animal studies. Several neural circuits within specific regions of the brain, including the nucleus accumbens, lateral habenular, parabrachial nucleus, medial septum, anterior cingulate cortex, amygdala, hippocampus, medial prefrontal cortex, and bed nucleus of the stria terminalis, will be discussed based on novel findings after chemogenetic or optogenetic manipulation. We believe that these animal studies provide novel insights into human conditions and can guide clinical practice.

1. Introduction

Pain is an unpleasant experience that comprises sensory, emotional, and cognitive dimensions [1]. Physiological pain protects people from tissue damage, while pathologic pain such as chronic pain can lead to unnecessary suffering. Many chronic pain patients suffer from comorbid mental disorders, thus making their treatment particularly difficult, and anxiety symptoms are among the most common comorbidities in chronic pain patients [2]. Anxiety is a temporally diffused emotional state caused by a potential threat, but a threat with low likelihood of occurrence and low likelihood of producing serious harm [3]. Like pain, physiological anxiety protects people from potential danger, while pathologic anxiety leads people to overestimate the potential danger, which can impair their mental health. The lack of effective treatments is not only due to the complexity of the comorbidity, but also to a lack of understanding of the underlying mechanisms. Cumulative neuroimaging studies have shown that several different brain areas are involved in both pain and anxiety [4], but imaging studies cannot identify the causal roles of the specific regions. However, improved methods in animal models have provided an ever-greater understanding of the relationship between pain and anxiety at both the molecular, synaptic, and neural network levels. In this review, we will mainly discuss changes in neuroplasticity at the level of neurocircuits in cases of chronic pain and anxiety (Table 1).

2. The Hypothesis of the Comorbidity of Chronic Pain and Anxiety

The traditional hypothesis of the cooccurrence of pain and anxiety is that chronic pain causes anxiety, and that anxiety

Table 1: Neural circuits that serve to promote or inhibit pain and anxiety. Summary of the current understanding of the neural circuits involved in or potentially involved in the comorbidity of chronic pain and anxiety. Pain-like behaviors can be measured in two aspects—sensory pain and affective pain. We measure sensory pain via withdrawal thresholds or latencies, and we measure affective pain via conditioned place avoidance or preference. ?, not confirmed; ×, no effect.

Summary Neural circuits	Chronic pain state	Pain (sensory or affective pain)	Anxiety	Reference
3.1 The nucleus accumbens (NAc)				
VTA-NAc	Suppressed	Analgesic when activated (sensory pain)	?	[17]
VTA-IPN	Suppressed	?	Anxiolytic when activated	[19]
PL-NAc	Suppressed	Analgesic when activated (sensory pain and affective pain)	?	[20]
IL-NAc	Suppressed	?	Anxiolytic when activated	[22]
3.2 The lateral habenula (LHb)				
LHb-DRN	Activated	Analgesic when inhibited (sensory pain)	?	[25]
LHb-VTA	?	?	Anxiogenic when activated	[26]
$DRN^{5\text{-}HT+}$-CeA^{SOM+}-LHb	Suppressed	Analgesic when activated (sensory pain)	?	[33]
4.1 Parabrachial nucleus (PB)				
Lateral PB GABA+-lateral PB Glu+	Suppressed	Analgesic when activated (sensory pain and affective pain)	×	[35]
Lateral PB-BNST	?	Generate aversive learning	?	[36]
Lateral PB-VMH	?	Drives escape behaviors	?	[36]
Lateral PB-lPAG	?	Drives escape behaviors	?	[36]
Lateral PB-CeA	Activated	No effect on sensory pain and generate aversive learning	Anxiogenic when activated	[36, 37]
CeA^{SOM+}-lateral PB	Suppressed	Analgesic when activated (sensory pain)	?	[39]
Lateral PB $Tacr1^{+}$-ILN	Activated	Promote pain when activated	?	[40]
4.2 The medial septum (MS)				
MS^{choli+}-rACC	Activated	Analgesic when inhibited (sensory pain and affective pain)	Anxiolytic when inhibited	[41, 43]
MS^{choli+}-vCA1	Suppressed	Analgesic when activated (sensory pain and affective pain)	×	[41]
4.3 ACC				
ACC-amygdala	Activated	Analgesic when inhibited (sensory pain and affective pain)	?	[4]
ACC-thalamus-amygdala	Activated	Analgesic when inhibited (sensory pain)	?	[48]
ACC-PAG-RVM-SDH	Activated	Analgesic when inhibited (sensory pain and affective pain)	?	[49]
4.4 The amygdala				
CeA^{SOM+}-cSEA	?	?	Anxiogenic when activated	[51]
pPVT-CeA	Activated	Promote pain when activated (sensory pain)	?	[53]
BLA-CeA	Suppressed	Analgesic when activated (sensory pain)	Anxiolytic when activated	[37, 54]
BLA-mPFC-PAG-SDH	Activated	Promote pain when activated (sensory pain)	×	[57]
$aBLA\text{-}vCA1^{Calb1-}$	?	?	Anxiogenic when activated	[59]
$pBLA\text{-}vCA1^{Calb1+}$	?	?	Anxiolytic when activated	[59]
4.5 The hippocampus				
vCA1-IL	Suppressed	Analgesic when activated (sensory pain and affective pain)	Anxiolytic when activated	[64]
vHPC-LS	?	?	Anxiolytic when activated	[68]
LS^{Crfr2+}-AHA	?	?	Anxiogenic when activated	[69]
vCA1-LH	?	?	Anxiogenic when activated	[72]

Table 1: Continued.

Summary Neural circuits	Chronic pain state	Pain (sensory or affective pain)	Anxiety	Reference
vHPC-mPFC	?	?	Anxiolytic when inhibited	[74]
MRN 5-HT+-dHPC	?	?	Anxiogenic when activated	[77]
4.6 The bed nucleus of the stria terminalis (BNST)				
aBLA-adBNST	?	?	Anxiolytic when activated	[79]
dlBNST-CeA	?	?	Anxiogenic when activated	[80]
CeA-dlBNST	Activated	Promote pain when activated (sensory pain)	Anxiogenic when activated	[81, 82]
dlBNST-VTA	Activated	?	?	[83]
$DRN^{5\text{-}HT+}$-$BNST^{CRF+}$	?	?	Anxiogenic when activated	[84]
$vBNST^{Glu+}$-VTA	?	?	Anxiogenic when activated	[85]
$vBNST^{GABA+}$-VTA	?	?	Anxiolytic when activated	[85]
Medullary A1/A2 cell groups-vBNST	Activated	Promote pain when activated (sensory pain)	?	[87, 88]
adBNST GABA+-NAc shell	?	?	Anxiolytic when activated	[89]
vSUB/CA1-amBNST	?	?	Anxiolytic when activated	[90]

NAc: nucleus accumbens; VTA: ventral tegmental area; IPN: interpeduncular nucleus; PL: prefrontal cortex; IL: infralimbic cortex; LHb: lateral habenula; DRN: dorsal raphe nucleus; CeA: central amygdala; PB: parabrachial nucleus; BNST: bed nucleus stria terminalis; VMH: ventromedial hypothalamus; lPAG: lateral PAG; ILN: intralaminar thalamic nuclei; MS: medial septum; ACC: anterior cingulate cortex; rACC: rostral ACC; PAG: periaqueductal gray; RVM: rostromedial ventral medulla; SDH: spinal dorsal horn; pPVT: posterior thalamic paraventricular nucleus; BLA: basolateral amygdala; cSEA: central sublenticular extended amygdala; mPFC: medial prefrontal cortex; vCA1: ventral CA1; vHPC: ventral hippocampus; LS: lateral septum; AHA: anterior hypothalamic area; LH: lateral hypothalamus; MRN: median raphe nucleus; dHPC: dorsal HPC; aBLA: anterior BLA; adBNST: anterodorsal part of the BNST; dlBNST: dorsolateral BNST; amBNST: anteromedial BNST; vBNST: ventral BNST; vSUB/CA1: ventral subiculum/CA1.

in turn exacerbates pain [2]. Zhuo has proposed that the amygdala and its related network play a key role in physiological anxiety, while the anterior cingulate cortex (ACC) and its related network are involved in pathological anxiety triggered by chronic pain. It is further argued that presynaptic long-term potentiation (LTP) in the ACC in turn plays an important role in chronic pain-induced anxiety [4]. Borsook et al. proposed a model for chronic pain called the Combined Reward Deficiency Antireward Model [5]. In this model, acute pain activates the reward system for pain relief, but failure to relieve the pain inhibits the brain's reward and motivational centers and diminishes the motivational/incentive salience of natural reinforcers, and this is referred to as a reward-deficiency state. In response to this state, the antireward system releases massive stress-related chemicals leading to diminished dopaminergic neurotransmission (reduced dopamine receptors, diminished dopamine synthesis, and increased dopamine transporters), and this is referred to as an antireward state. This maladaptive state in chronic pain enhances pain perception and comorbid changes, including addiction, depression, and anxiety.

Based on this model, we hypothesize that the comorbid anxiety originates from an imbalance in the interaction between the reward and antireward systems due to persistent pain that leads to dysfunction of the pain and anxiety regulatory system (Figure 1). Apart from stress-related chemicals—including corticotropin-releasing factor and norepinephrine—pain-induced changes in the endogenous opioid system also play an important role in mediating chronic anxiety. Kappa opioid receptor and its endogenous dynorphin are one of the key molecular elements mediating aversion [6]. Chronic pain induces kappa opioid receptor activation, which in turn inhibits dopamine release and finally results in a state of anxiety. Furthermore, it is found that kappa opioid receptor activation in the central amygdala generates both pain-like behavior [7] and anxiety-like behavior [8]. Secondly, Mu opioid receptor activity after nerve injury enhances mechanical pain sensitivity and increases anxiety-like responses, while delta opioid receptors decrease nociceptive and depressive-like behaviors after nerve injury [9], suggesting that different types of opioid systems mediate different aspects of pain and its comorbid actions. Finally, functional switching of delta opioid receptor 1 (DOR1) to delta opioid receptor 2 (DOR2) is associated with anxious states during pain chronification. DOR1 inhibits both the anxiolytic circuit from the basolateral amygdala (BLA) to the central nucleus amygdala (CeA) and the anxiogenic circuit from the parabrachial nucleus (PB) to the CeA. In contrast, activation of DOR2 mainly inhibits the PB-CeA circuit [10].

In the following sections, we first discuss the precise mechanisms of the reward deficiency and the antireward imbalance by focusing on the centers of the reward and antireward systems—the nucleus accumbens and lateral habenular, respectively. In the second part, we focus on recent studies on the dysfunction of the pain and anxiety regulatory system, including several neural circuits in the medial septum, anterior cingulate cortex, amygdala, medial prefrontal

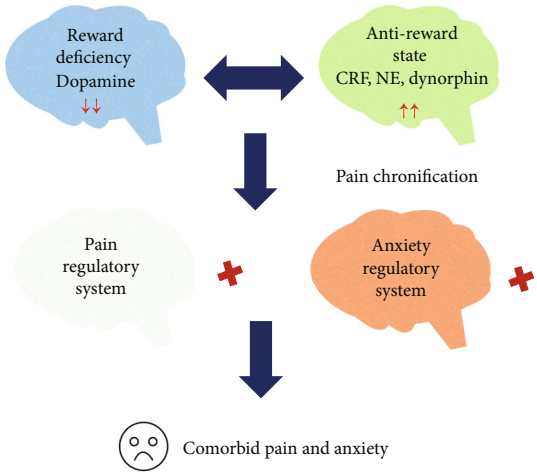

Figure 1: Possible explanation of the comorbidity of chronic pain and anxiety. Persistent pain inhibits the brain's reward and motivational center—the nucleus accumbens (NAc)—and diminishes the motivational/incentive salience of natural reinforcers (reward deficiency). In response to this state, the antireward system center—the lateral habenular (LHb)—is overexcited, releasing stress-related chemicals—including corticotropin-releasing factor (CRF), norepinephrine (NE), and dynorphin—leading to excessive dopaminergic trafficking (reduced dopamine receptors, diminished dopamine synthesis, and increased dopamine transporters) that results in the dysfunction of the pain and anxiety regulatory system (pain chronification). The pain and anxiety syndromes in chronic pain patients are thus the result of the dysfunction of the regulatory system.

cortex, hippocampus, and the bed nucleus of the stria terminalis. Finally, we discuss future directions for studying the comorbidity between chronic pain and anxiety.

3. Reward Deficiency and Antireward Imbalance

3.1. The Nucleus Accumbens (NAc). The NAc is composed of core and shell subregions and is a key regulator of the brain reward system, and thus, the NAc plays an important role in the regulation of chronic pain and anxiety. There are two fundamental pathways of NAc outputs—the direct pathway to striatonigral neurons marked by dopamine D1 receptors in the basal ganglia and the indirect pathway to striatopallidal neurons marked by D2 receptors in the basal ganglia. The direct pathway is considered to be correlated with reward and positive effect, while the indirect pathway is correlated with aversive events [11, 12]. It has been found that spared nerve injury (SNI) increases the excitability of NAc shell neurons that are involved in the indirect pathway, and chemogenetically inhibiting the NAc shell neurons alleviates pain-like behaviors [13]. It should be noted that this phenomenon is observed at early time points (5 days after the SNI surgery), which means that the NAc might be involved in the transition from acute pain to chronic pain but might not be responsible for the persistent state of chronic pain. It has also been reported that chronic pain elicits long-term depression of the D2 receptors expressing medium spiny neurons in the NAc core, and this phenomenon appears to be responsible for the decreased motivation that is associated with chronic pain [14]. Whole-cell recording shows that during chronic pain, the excitatory postsynaptic currents are significantly decreased in neurons expressing the D2 receptor, and the presynaptic expression of vesicular glutamate transporter1 is also reduced in the NAc [15], thus indicating that reduced glutamate release from presynaptic terminals of the NAc might be critical in the maintenance of chronic pain. A recent study found that the gene expression of *Fos*-family transcription factors in the NAc is significantly reduced after SNI of the sciatic nerve model, which is a widely used neuropathic pain model [16]. Interestingly, c-Fos transcript levels decrease only at the 5-day time point in the ipsilateral and contralateral NAc after SNI surgery, while ΔFosB, the stable isoform, decreases only at the 28-day time point in the contralateral NAc after SNI surgery. Moreover, unilateral overexpression of ΔFosB in the NAc improves neuropathic pain, indicating that ΔFosB serves as the long-term regulator of gene expression in persistent pain. Inhibition of the NAc during chronic pain might be explained by the suppressed ventral tegmental area (VTA), a key dopaminergic center in the brain, and it has been shown that optogenetic activation of the dopaminergic neurons in the VTA that project into the NAc core produces an analgesic effect in chronic pain [17]. Recently, it has been found that optogenetic activation of GABAergic VTA neurons induce anxiety-like behaviors [18]. Dopaminergic projections from the VTA innervate the interpeduncular nucleus (IPN), and photoinhibition or photoactivation VTA-IPN results in anxiety-like behavior or anxiolytic behavior, respectively [19].

Another important circuit within the NAc is the prelimbic area of the prefrontal cortex- (PL-) NAc core loop, and it has been reported that activating the PL-NAc circuit relieves both the sensory components and the affective syndromes of chronic pain as well as the comorbid depressive symptoms [20], while inhibition of the PL-NAc circuit amplifies sensory and affective pain [21]. It would be interesting in future work to explore the role of the PL-NAc circuit in comorbid anxiety. The infralimbic cortex- (IL-) NAc core circuitry might be responsible for pain-related anxiety, and using the pain-predicted cue- (PPC-) avoidance paradigm (PPC is the avoidance of pain using contextual cues that predict painful outcomes, and in this study, the mice were trained to associate an auditory cue with noxious stimuli, and the avoidance behavior was reflected by reduced consumption of sucrose), researchers found that chronic pain reinforced PPC avoidance while optostimulating the IL-NAc circuit suppressed PPC avoidance in a chronic pain model [22]. The increased PPC avoidance can be viewed as the result of pain-related anxiety.

3.2. The Lateral Habenula (LHb). The LHb has been proposed to be the center of the antireward system. Most LHb neurons are glutamatergic with few GABAergic neurons [23]. The connectivity of the LHb is extremely complex, and the LHb receives pain signals directly from the spinal dorsal horn (SDH) or indirectly from the lateral hypothalamus

(LH). The main outputs of the LHb are the dorsal raphe and median raphe, the periaqueductal gray (PAG), the VTA, and the lateral dorsal tegmental nucleus [24]. Considering that the dorsal raphe nucleus (DRN) plays a key role in descending pain modulation, a recent study found that lesion of the LHb improves the pain threshold and depression-like behaviors caused by nerve injury and increases the concentration of 5-hydroxytryptamine (5-HT) in the DRN [25]. The LHb-DRN circuit might also be important for pain-related anxiety. Another important circuit for the comorbidity of pain and anxiety might be the LHb-VTA circuit, which acts as a regulatory center for the dopaminergic system, and a study showed that either pharmacological activation or inhibition of D1 receptors in the LHb increased anxiety-like behavior while decreasing depressive-like behaviors [26]. It would be interesting to study the role of the LHb-VTA circuit in controlling pain-related anxiety using highly specific chemogenetic and optogenetic methods.

Our group recently found that bilateral inhibition of overexcited LHb glutamatergic neurons has anxiolytic and analgesic effects in the partial transection of the infraorbital nerve model, which is used to study the mechanisms of trigeminal neuropathic pain [27]. Using microarray analysis and real-time PCR, we found that gene expression in the LHb is different in chronic pain compared with the normal state, and among these, the *Tacr3* gene—which encodes the neurokinin 3 receptor that is important in the modulation of pain and negative emotion [28, 29]—is downregulated. Intriguingly, unilateral inhibition of the LHb or overexpression of the *Tacr3* gene alleviates only anxiety-like behaviors with no effect on pain-related behaviors, while bilateral overexpression of the *Tacr3* gene alleviates both. This interesting phenomenon might be explained by the left-right asymmetry of the LHb [30] because the input/output circuits between the left and right Hb have been shown to be different [31]. Considering that the LHb is divided into several functionally different subnuclei marked with various neurochemical contents [32], the failure to reduce pain unilaterally might also be correlated with different levels of inhibition of the subnuclear regions. Taken together, these results suggest that the connectivity and function of each side of the LHb and the included subnuclei should be considered in future studies.

A recent study found that 5-HT-expressing neurons in the DRN ($DRN^{5\text{-}HT+}$) project to somatostatin- (SOM-) expressing neurons in the central amygdala (CeA^{SOM+}), and the LHb is the output of the $DRN^{5\text{-}HT+}$-CeA^{SOM+} circuit. That study found that the activity of the $DRN^{5\text{-}HT+}$-CeA^{SOM+} circuit is decreased in the comorbid condition of pain, anxiety, and depression, and that activation of the $DRN^{5\text{-}HT+}$-CeA^{SOM+}-LHb circuit could reverse the nerve injury-induced reduction in pain threshold and the depression-like behavior [33]. Because this group focused on the comorbidity of pain and depression, they did not check the role of the $DRN^{5\text{-}HT+}$-CeA^{SOM+}-LHb circuit in anxiety-like behaviors. Considering that the CeA and LHb are crucial for anxiety, the $DRN^{5\text{-}HT+}$-CeA^{SOM+}-LHb circuit might also be important for the comorbidity of pain and anxiety.

4. Dysfunction of the Pain and Anxiety Regulatory System

4.1. The Parabrachial Nucleus (PB). The PB is known to relay pain-related information from the spinal cord in the affective pain pathway. The PB-nociceptive neurons project to multiple emotion and instinct-related centers, including the bed nucleus of the stria terminalis (BNST), the paraventricular thalamic nucleus, the paraventricular nucleus of the hypothalamus, the CeA, the ventral tegmental area, the ventrolateral periaqueductal grey, the nucleus of the solitary tract, and the intermediate reticular nucleus in the hindbrain [34]. A recent study found that short-term optogenetic activation of GABAergic lateral PB neurons or inhibition of glutamatergic lateral PB neurons alleviates pain-like behavior in a common peroneal nerve ligation model, but short-term activation of glutamatergic lateral PB neurons is not sufficient to induce anxiety-like behaviors [35]. Also, activation of the lateral PB to the BNST or CeA generates an aversive learning to noxious stimulation, while activation of the ventromedial hypothalamus or lateral periaqueductal gray drives escape behaviors [36].

The CeA receives direct nociceptive information from the PB via the spino-ponto-amygdaloid pathway that relays the pain signals from the spinal cord to the CeA. Activating the PB-CeA pathway to stimulate pain signals in normal mice produces anxiety-like behaviors with no influence on pain responses [37]. Two subtypes of CeA neurons that are targeted by the PB and that mediate opposing effects after nerve injury have been identified by molecular genetic approaches [38]. CeA neurons expressing protein kinase C-delta ($Ce^{APKC\delta+}$) display hyperexcitability and promote pain-like behaviors after nerve injury, while CeA^{SOM+} display hypoexcitability and drive antinociception. Because both types of cells receive excitatory inputs from the PB, it is believed that changes in the outputs of these cells are the main cause of pain-related plasticity. The antinociceptive effect of CeA^{SOM+} neurons has recently been found to be related to the CeA^{SOM+}-PB pathway, and a study showed that CeA^{SOM+} neurons send inhibitory GABAergic inputs into the PB [39]. The CeA^{SOM+}-PB circuit is weakened under conditions of chronic pain, thus overexciting PB neurons and resulting in pain-like behaviors. A recent group challenged the traditional notion that the PB conveys nociceptive information directly to the CeA. Inconsistently, they found that $Tacr1^{+}$ neurons in the PB represent the major target of spinal projection, which projects directly to the intralaminar thalamic nuclei but not the CeA [40]. This might be related to differential projections of the dorsal lateral PB versus the external lateral PB.

4.2. The Medial Septum (MS). The MS consists of cholinergic neurons and receives noxious stimuli from widespread peripheral regions and then projects to a broad range of pain-modulatory sites in the neocortex such as the ACC and the hippocampus, thus playing a vital role in various cognitive and emotional behaviors. A recent study showed that chemogenetic inhibition of MS cholinergic neurons (MS^{choli+}) and the MS^{choli+}-rostral ACC (rACC) circuit

alleviates chronic inflammatory pain-induced anxiety-like behaviors in the elevated plus maze (EPM) and the open-field test (OFT) [41]. The EPM is conducted in a plus-shaped maze with four arms, two of which are enclosed by high walls, called the closed arms, and two of which are left open, called the open arms. Animals making fewer entries into and spending less time exploring the aversive open arms are considered to be exhibiting anxiety-like behaviors. The OFT consists of a square arena enclosed by high walls, and animals spending less time exploring the center of the arena are considered to be exhibiting anxiety-like behavior [42]. The same group also found that inhibiting the MS^{choli+}-rACC or MS^{choli+}-ventral CA1 (vCA1) circuit has an analgesic effect [43]. Interestingly, the authors found that chemogenetic inhibition of the MS^{choli+}-vCA1 circuit seems to have no effect on pain-related anxiety [41]. One explanation for this is that persistent chronic pain can impair the activity of the hippocampus [44], thus making the MS-vCA1 circuit ineffective.

4.3. The ACC. The ACC is involved in both pain perception and anxiety [4]. Two forms of LTP, a form of synaptic plasticity, have been identified in the ACC—a presynaptic form (pre-LTP) that requires kainate receptors and a postsynaptic form (post-LTP) that requires N-methyl-D-aspartate receptors. Surprisingly, pharmacological inhibition of pre-LTP has anxiolytic and analgesic effects in chronic pain models [45], while pharmacological inhibition of post-LTP has only analgesic effects [46]. Therefore, it has been proposed that pre-LTP is the primary mechanism through which the ACC mediates pain-induced anxiety (for detailed mechanisms of the pre-LTP, see Zhuo's review about long-term cortical synaptic changes [47]) However, considering the diverging output and input of ACC neurons and considering the limitations of pharmacological methods, even though pre-LTP is crucial for pain-induced anxiety, some ACC neurons might not depend on pre-LTP but might still be important for pain-induced anxiety for specific neural connections.

There are several neural circuits that are important for understanding the comorbidity of pain and anxiety. First, the ACC neurons form bidirectional innervations with the amygdala, a central region in anxiety modulation, both directly (the ACC-amygdala circuit) and indirectly (the ACC-thalamus-amygdala circuit) [4]. Optical inhibition of the ACC decreases abnormal ventral posteromedial thalamus activities, which increases the pain response in a chronic constriction injury of the infraorbital nerve model [48]. Second, the ACC-PAG-rostromedial ventral medulla-(RVM-) SDH pathway, known as the descending pain regulation system, and the ACC-SDH pathway complementarily regulate nociceptive sensory transmission [49]. It is possible that the traditional pain-related circuits might convert into anxiety-related circuits under comorbid conditions or might have some as yet undiscovered anxiety-modulating effect due to limitations in experimental methods. More work thus needs to be done to explore the possible role of these circuits in pain-anxiety comorbidity.

4.4. The Amygdala. The amygdala, including the BLA and the CeA, is important for emotional processing and has a role in sensations of pain and feelings of anxiety [50]. The CeA encompasses the centrolateral (CeL) and centromedial (CeM) nuclei, and the CeM is the primary output region of the amygdala. A recent study showed that CeA^{SOM+} neurons in CeL mediate anxiety-like behavior by inhibiting GABAergic neurons in the central sublenticular extended amygdala [51]. Optogenetic activation of a distinct group of GABAergic neurons in the CeA, which can be activated by general anesthesia, inhibits pain-like behaviors in normal and chronic pain states [52]. The CeA received projections from the posterior thalamic paraventricular nucleus (pPVT), and stimulating the pPVT-CeA pathway induces pain-like behavior [53].

About 90% of the BLA consists of glutamatergic neurons, while about 95% of the CeA consists of GABAergic neurons. Optogenetic stimulation of BLA termini in the CeA decreases anxiety-related behaviors in both the EPM and the OFT [54], and it is hypothesized that BLA neurons excite GABAergic CeL neurons that then exert feed-forward inhibition onto CeM output neurons to produce the anxiolytic effect [54]. Because the BLA is a site for converging negative and positive stimuli and because of the functional differences in the anterior and posterior BLA (aBLA and pBLA), it is argued that the BLA neurons that contribute to positive behaviors (positive neurons) and negative behaviors (negative neurons) might be genetically distinguishable. The putative negative neurons are targeted by exposing male mice to foot shocks, and positive neurons are targeted by exposing male mice to a female mouse. Utilizing a c-Fos-based genetic expression system, *Ppp1r1b*-(protein phosphatase 1 regulatory inhibitor subunit 1B-) expressing neurons were identified as positive neurons mainly located in the pBLA, and *Rspo2*- (R-spondin 2-) expressing BLA neurons were identified as negative neurons in the aBLA [55]. Contrary to a previous hypothesis, retrograde and anterograde tracing suggests that $Ppp1r1b^+$ BLA neurons make distinct projections to the CeL, CeM, and infralimbic cortex, while $Rspo2^+$ neurons make distinct projections to the capsular nucleus of the central amygdala and prelimbic cortex [55]. Although *Ppp1r1b* and *Rspo2* can distinguish between positive and negative BLA neurons, it should be noted that there might be other genetic markers and that $Ppp1r1b^+$ and $Rspo2^+$ neurons can be further divided into subgroups based on specific behavior paradigms and by using improved analytic methods. Therefore, this hypothesis should be modified to suggest that $Ppp1r1b^+$ BLA neurons, which are positive neurons, excite the CeL neurons that exert feed-forward inhibition onto CeM output neurons and finally produce the anxiolytic effect. Interestingly, activating the BLA-CeA pathway in a chronic inflammatory pain model alleviates both mechanical and thermal pain responses [37].

Recently, a distinct group of neurons that encode the negative affective valence of pain has been found in the BLA [56]. Normally, silencing this nociceptive ensemble reduces attending and escape behaviors in response to noxious stimuli without changing stimulus detection, withdrawal, anxiety, or reward. Moreover, this nociceptive ensemble that is normally activated by noxious stimuli can

also be activated by innocuous stimuli during conditions of chronic pain. It thus seems reasonable to hypothesize that this ensemble contributes to pain-related anxiety as a result of dysfunctional perceptual changes. The BLA-medial prefrontal cortex- (mPFC-) PAG-SDH circuit is crucial for the development of neuropathic pain, and it has been found that increased inputs from the BLA to the mPFC GABAergic interneurons—which send feed-forward inhibition to pyramidal neurons in the mPFC—induced by nerve injury lead to the net inhibition of mPFC output [57]. Therefore, feed-forward inhibition of the downstream mPFC-PAG-SDH circuit occurs. One thing to be noted is that even though inhibiting the BLA-mPFC circuit alleviates pain responses in SNI mice, the pain-related anxiety is insensitive to the same manipulation, indicating that there might be other pathways within the BLA that mediate pain-related anxiety.

In addition to the BLA-CeL-CeM circuit, the BLA-ventral hippocampus (vHPC) circuit also plays a vital role in modulating anxiety-related behaviors [58]. A recent study showed that the aBLA and pBLA innervate the deep-layer calbindin1- (Calb1-) negative and superficial-layer Calb1-positive neurons in the vCA1, respectively, and thus, the aBLA-vCA1$^{\mathrm{Calb1-}}$ circuit drives avoidance behavior and exerts anxiogenic effects, while the pBLA-vCA1$^{\mathrm{Calb1+}}$ circuit drives approach behavior and exerts anxiolytic effects [59]. The functional diversity along the anterior–posterior axis of the BLA is based on genetic spatiality, and the genetic spatiality of the vCA1 also exerts different effects. Calb1, a Ca^{2+} binding protein, functions as a buffer, transporter, and sensor of Ca^{2+} [60], and the different Ca^{2+} signals, which are important in a wide range of cellular functions, are spatially and temporally modified depending on the Ca^{2+} binding property and the intracellular concentration of the buffer [61]. Calb1 knockdown in the vCA1 abolishes the anxiolytic effect of the pBLA-vCA1 circuit [59], and thus, both the input specificity and the Calb1 levels determine the specific circuit-associated amelioration of anxiety. It would be interesting to identify the differences between the information transmitted by vCA1$^{\mathrm{Calb1+}}$ neurons and vCA1$^{\mathrm{Calb1-}}$ neurons, and thus, what kind of information depends on Calb1, and to identify the downstream effects of the different circuits.

4.5. The Hippocampus. While the hippocampus is known to be a cognitive structure involved in memory, it is also implicated in controlling emotions such as anxiety. Chronic pain causes memory deficits and atrophy of CA1 pyramidal neurons, and an increase in the dendritic tree complexity of the dentate gyrus hippocampal subregions after nerve injury has been observed [62]. Neuroimaging confirms that reduced connectivity in the hippocampus is associated with the transition from acute pain to chronic pain [63], and a recent study showed that peripheral inflammation-induced spontaneous pain disrupts vCA1-IL connectivity, while optogenetic activation of the vCA1-IL relieves pain [64]. Thus, impairment of the hippocampus from chronic pain leads to the failure of the anxiety-related modulatory system within the hippocampus.

There is functional heterogeneity along the dorsoventral axis of the hippocampus, and gene expression within the dorsal hippocampus (dHPC) correlates with cognitive functions such as learning and memory, while the ventral hippocampus (vHPC) is involved in emotional regulation [65]. The septohippocampal pathway plays an important role in controlling anxiety responses, and it has long been postulated that the hippocampus monitors the environment and sends contextual information regarding conflict and novelty to the septum in order to control anxiety [66]. The septum that projects to the hippocampus contains cholinergic, GABAergic, and glutamatergic neurons, while the hippocampus projects to the septum mainly via glutamatergic afferents. An early study found that disconnection of the lateral septum (LS) and the vHPC using asymmetric pharmacological inhibition reduced anxiety-related behaviors in the EPM, indicating that the vHPC and the LS work in tandem to modulate anxiety [67], and a recent study found that chemogenetic activation of the vHPC cells that project to the LS decreased anxiety-related behaviors [68]. Although chemogenetic techniques can selectively manipulate the vHPC-LS circuit by injecting the retrogradely propagating canine adenovirus encoding Cre recombinase into the LS and injecting the Cre-responsive adeno-associated virus into the vHPC, it should be noted that retrograde-targeted vHPC cells also send axon collaterals to other structures. The authors found that the LS-projecting vHPC cells were most abundant in the LS but less so in the dorsal CA1 and the BLA. Therefore, the behavioral change relies on the combined effects of altering multiple axon collaterals. The LS is thought to regulate anxiety through its outputs to the hypothalamus, and a recent study showed that a subset of GABAergic LS neurons expressing type 2 corticotropin-releasing factor receptor (*Crfr2*) project to the anterior hypothalamic area (AHA) of the medial hypothalamus, and that optogenetic stimulation of the LS^{Crfr2+}-AHA circuit promotes anxiety-related behaviors and increases corticosterone levels [69]. Subsequent experiments showed that the LS^{Crfr2+} neurons form inhibitory synapses with the AHA neurons that project to the paraventricular nucleus, which is part of the hypothalamic-pituitary-adrenocortical (HPA) axis and regulates corticosterone release. Therefore, the anxiogenic role of the LS^{Crfr2+}-AHA circuit is due to disinhibiting the HPA axis. Because the LS^{Crfr2+} output is anxiogenic, while the vHPC-LS circuit is anxiolytic, it is possible that the vHPC might innervate a distinct population of LS neurons that in turn inhibit the LS^{Crfr2+} neurons and ultimately downregulate the HPA axis. However, we cannot rule out the possibility that the LS might also contain an anxiolytic subpopulation that might be activated by the vHPC. A study has shown that excitotoxic ablation of LS neurons can enhance HPA axis responses [70], thus confirming the existence of anxiolytic LS neurons, but the existence of the anxiolytic output remains to be determined.

Interestingly, LS^{Crfr2+} neurons also make connections with the midbrain PAG, a region known to regulate defensive behaviors relevant to anxiety, via their projections to the AHA [69]. Retrogradely targeted LS-projecting vHPC cells are distributed in the ventral CA3 (vCA3) subregion and the vCA1 [68], but unlike the vCA1, the vCA3 receives glutamatergic inputs from the ventral dentate gyrus (vDG),

and a recent study has shown that optogenetically stimulating the vDG suppresses anxiety-related behaviors and has no effect on contextual learning [71], while the anxiolytic effect of vDG activation might be caused by the vCA3-LS circuit. Future work should determine the different roles of the vCA1-LS and vCA3-LS circuits. In addition to the indirect vHPC-LS-AHA circuit, the vCA1 also directly projects to the LH, and a study has shown that activation of the vCA1-LH circuit can increase anxiety and avoidance behaviors [72]. The vCA1-LH can be a direct way for the vHPC to rapidly control anxiety-like behaviors, but how the vHPC-LS-AHA and the vCA1-LH coordinate with each other when animals feel anxiety needs to be determined.

In addition to the LS and LH, the vHPC also projects directly to the mPFC, which is implicated in the regulation and expression of defensive behaviors in rodents. Theta frequency (4–12 Hz) activity in the mPFC and vHPC synchronizes and increases during exposure to anxiogenic arenas [73]. Single units in the mPFC that are synchronized with the vHPC are involved in the anxiety-related behavior in the EPM [74], and subsets of vCA1 neurons projecting to the mPFC change their firing patterns under conditions of elevated anxiety [75]. In addition, optogenetic inhibition of the vHPC-mPFC circuit reduces anxiety-like behavior and the spatial representations of aversion and anxiety valence in mPFC neurons [74]. Taken together, these observations suggest that the vHPC conveys valence information to the mPFC and then the mPFC regulates the anxiety-related activities that guide the animal's anxiety-related behavior in the EPM. Classically speaking, the dHPC seems to be less involved in regulating emotional control. A recent study showed that overexpressing extracellular signal-regulated kinase-2, a signaling molecule known to regulate gene expression, in the dHPC downregulates anxiety-related behaviors in the EPM [76]. Contrary to the anxiolytic role of the dHPC, another study found that stimulation of the median raphe nucleus (MRN) 5-HT-positive neurons together with 5-HT-positive neuron innervation to the dHPC promotes anxiety-like behaviors [77]. Somewhat paradoxically, although photostimulation of MRN 5-HT-positive neurons produces anxiety-like behavior in a variety of behavioral tests, photostimulation of 5-HT-positive neuron terminals in the dHPC produces anxiety-like behaviors only in the novelty-suppressed feeding and marble-burying tests and not in the EPM. First, this might be explained by different anxiety-related paradigms and specific contributions of 5-HT-positive neuron terminals in other structures. Second, these experiments indicate that different regulation of vHPC neurons is enough to decrease or increase anxiety in a persistent manner, but they do not address whether the activity of these neurons is normally required for anxiety. Last but not least, the role of the dHPC in anxiety might not be through emotional management, but perhaps it can influence anxiety-related behaviors, and further experiments such as *in vivo* Ca^{2+} imaging should be performed to confirm the role of the dHPC in anxiety. Taken together, the work described here suggests that dysfunction of the anxiety regulatory system within the hippocampus might explain the comorbidity of anxiety with chronic pain.

4.6. The Bed Nucleus of the Stria Terminalis (BNST). The BNST has been implicated in pathological and adaptive anxiety [78], and there is heterogeneity among the BNST neurons that regulate negative emotional states. The anterodorsal part of the BNST (adBNST) receives projections from the aBLA, but contrary to the vCA1, the aBLA-adBNST circuit decreases anxiety-related states when photostimulated [79]. The adBNST projections to the LH, the PB, and the VTA mediate the different features of the anxiolytic effect of the aBLA-adBNST as indicated by reduced risk avoidance, reduced respiratory rate, and increased positive valence, respectively [79]. The dorsolateral BNST (dlBNST) neurons form GABAergic connections with the CeA, and stimulating the dlBNST-CeA produces the opposite effect of stimulating the adBNST-LH circuit [80]. A recent study confirmed that CeA neurons release corticotropin-releasing factor (CRF) that binds to CRF1 receptors on dlBNST neurons resulting in anxiety-like behaviors [81]. Under conditions of emotional pain, CRF excites dlBNST neurons through adenylate cyclase-cyclic AMP-protein kinase A signaling, thus resulting in pain-induced aversion [82], and this might be the same pathway for regulating anxiety. The same group found that enhanced CRF signaling within the dlBNST also suppresses the dlBNST-VTA circuit through increased inhibitory input under conditions of chronic pain [83]. The CRF-positive neurons in the BNST ($BNST^{CRF+}$) also receive projections from $DRN^{5\text{-}HT+}$ neurons via $5\text{-}HT_{2C}$ receptors, and a study showed that stimulating the $DRN^{5\text{-}HT+}$-$BNST^{CRF+}$ circuit results in enhanced anxiety-like behaviors by inhibiting the anxiolytic ventral BNST- (vBNST-) LH and vBNST-VTA circuits [84]. Photostimulation of the vBNST glutamatergic projections ($vBNST^{Glu+}$) to the VTA results in aversive and anxiogenic behaviors, while stimulating the GABAergic vBNST ($vBNST^{GABA+}$) projections to the VTA results in rewarding and anxiolytic behaviors [85]. The vBNST also plays a vital role in the affective component of pain [86]. The vBNST receives noradrenergic projections from the medullary A1/A2 cell groups, and noradrenaline acts on α2-adrenoceptors and β-adrenoceptors located in the vBNST and thereby mediates pain-induced aversion [87, 88]. It would therefore be interesting to explore the role of the $vBNST^{Glu}$-VTA and the $vBNST^{GABA}$-VTA circuits in emotional pain using the conditioned place aversion paradigm. Recently, a novel circuit was found that GABAergic adBNST neurons projected directly to the parvalbumin interneurons in the shell NAc, which has an inhibitory influence on anxiety-like responses when activated [89].

Long-lasting plasticity in the BNST might also promote the comorbidity of chronic pain and anxiety. Researchers found that the IL and ventral subiculum/CA1 (vSUB/CA1) neurons project to the same anteromedial BNST (amBNST) neurons. Interestingly, vSUB/CA1-amBNST synapses promote NMDA-dependent LTP with NMDA-independent long-term depression in IL-amBNST synapses when stimulated by high frequency *in vivo*, while the same protocol in the IL fails to change the plasticity of the IL or the vSUB/CA1. *In vivo* LTP in the amBNST reduces the anxiety induced by anxiogenic situations [90]. An interesting question to address is whether the high-frequency stimulation

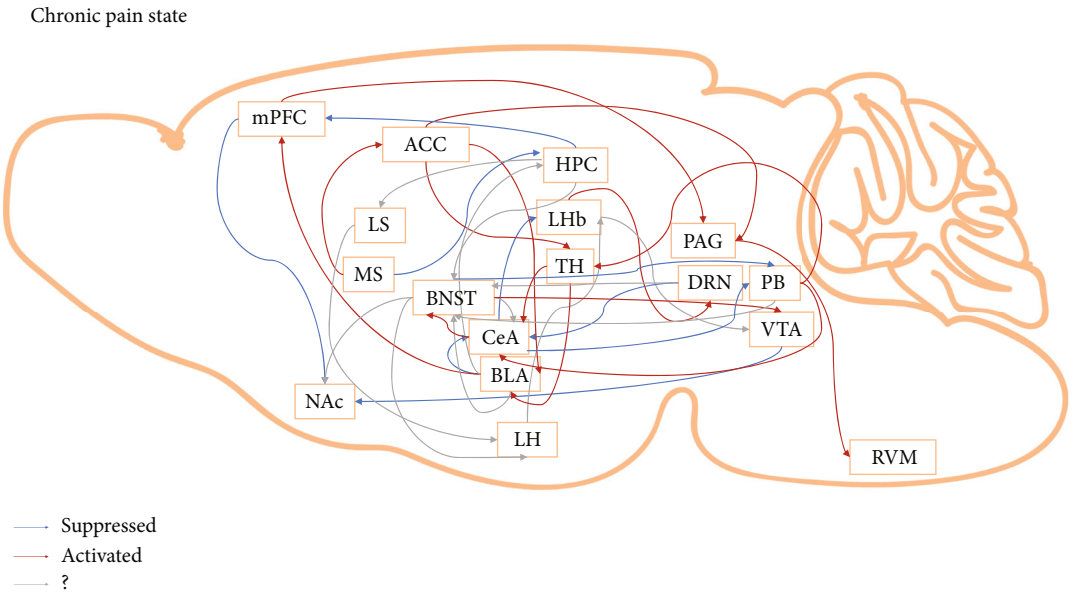

Figure 2: Potential neural circuits underlying the comorbidity of chronic pain and anxiety. ACC: anterior cingulate cortex; BLA: basolateral amygdala; BNST: bed nucleus of the stria terminalis; CeA: central amygdala; DRN: dorsal raphe nucleus; HPC: hippocampus; LH: lateral hypothalamus; LHb: lateral habenula; LS: lateral septum; mPFC: medial prefrontal cortex; MS: medial septum; NAc: nucleus accumbens; PAG: periaqueductal gray; PB: parabrachial nucleus; RVM: rostromedial ventral medulla; TH: thalamus; VTA: ventral tegmental area. ?, not confirmed for chronic pain-related anxiety.

of the vSUB/CA1 is enough to trigger plasticity changes in other anxiety-related areas like the BLA or mPFC because the vSUB/CA1 is one of the major output structures of the hippocampal signals in a high-frequency bursting mode. Taken together, studies of the BNST suggest that anxiety and the affective component of chronic pain might share the same mechanisms, which means that anxiety and emotional pain might be different representations of the same neural network changes.

5. Concluding Remarks and Future Directions

In summary, the research presented here expands our knowledge of the comorbidity of chronic pain and anxiety. From our perspective, the comorbidity of chronic pain and anxiety is the result of dysfunction in the pain and anxiety regulatory systems, which means that specific dysfunctions in the functional and structural connectivity of the neural circuits that govern sensory, emotional, and cognitive functions define the unique biotypes of pain and anxiety (Figure 2). However, there are still some questions that need to be answered. First, under physiological conditions, some circuits that are normally considered to regulate anxiety seem to be involved in pain regulation. For example, studies show that activating the BLA-CeA circuit, which is generally an anxiolytic circuit, under physiological conditions alleviates thermal pain with no effect on mechanical pain [37]. The authors explain that these differential effects might reflect the different features of the two pain tests, where the thermal pain test measures paw withdrawal responses to an infrared heat stimulus (a noxious stimulus), while the mechanical pain test measures paw withdrawal responses to *von Frey* filaments (a nonnoxious stimulus). This indicates that the anxiety regulatory system and pain regulatory system partly share common circuits. In clinical practice, chronic pain patients are found to easily develop anxiety, while some anxiety disorder patients easily develop pain syndromes [2]. Therefore, the original hypothesis that pain induces anxiety and that anxiety in turn exacerbates pain might be inappropriate considering that pain and anxiety might be different representations of the same system. It would therefore be interesting to study the classical pain regulatory system in regulating anxiety behaviors. Second, some studies have focused on the mechanisms of depressive syndromes in chronic pain [20, 33], and some circuits involved in comorbid depression might also regulate comorbid anxiety. In addition, it is important to elucidate the difference between comorbid depression and comorbid anxiety because even though both syndromes can be observed in chronic pain patients, some individuals might develop comorbid anxiety, some might develop comorbid depression, and some might develop both. Thus, in future studies, it would be worthwhile to dissect the different phenotypes of chronic pain models based on behavioral tests and to study the mechanisms behind the different phenotypes. Third, the behavioral paradigm for studying comorbidity needs to be improved. Some research has demonstrated the relief of chronic pain-related anxiety using the EPM and OPT, but they are not able to explain whether or not the anxiolytic effect is based on approach-avoidance decision-making, in other words, whether the improved behavior is the result of enhanced approaching behaviors or to reduced aversive behaviors or to reduced pain perception. A novel behavioral test called the L-type elevated maze that consists of one open

arm and one closed arm has been used in anxiety studies [59], and compared with the EPM, the L-type maze has a definite movement direction such that animals only have two choices, to go in the opposite direction or return to the previous direction, and this will help investigators accurately determine the animals' decision-making behaviors. We recommend this paradigm for future studies of comorbid anxiety. Fourth, more and more studies show that even in the same brain area, there is functional diversity and different connectivity. Genetic marking of these circuits is supposed to be effective in dissecting them, but specifically, marked neurons also exhibit differences. Single cell analysis might be helpful for explaining the variance and for categorizing these neurons into more distinct groups. Last but not the least, the symptoms that characterize mental disease are the result of dysfunctions within and between these circuits. However, language about brain circuits has not been incorporated into clinically meaningful taxonomies for clinical practice, and the development of a neural circuit taxonomy suited to clinical actions is needed [91]. We hope the neural circuits identified in the comorbidity of pain and anxiety from animal studies will provide novel insights into human conditions and will guide clinical practice.

Conflicts of Interest

The authors declare that there is no conflict of interest regarding the publication of this paper.

Acknowledgments

This study was financially supported by the National Natural Science Foundation of China (81971056, 31600852, 81771202, and 81873101), the Innovative Research Team of High-level Local Universities in Shanghai, the Foundation of Science, Technology and Innovation Commission of Shenzhen Municipality (JCYJ20180302153701406), the National Key R&D Program of China (2017YFB0403803), the Shanghai Municipal Science and Technology Major Project (2018SHZDZX01), and the ZJLab, Shanghai Key Laboratory for Acupuncture Mechanism and Acupoint Function (21DZ2271800).

References

[1] M. F. DosSantos, B. S. Moura, and A. F. DaSilva, "Reward circuitry plasticity in pain perception and modulation," *Frontiers in Pharmacology*, vol. 8, p. 790, 2017.

[2] B. Bandelow, "Generalized anxiety disorder and pain," *Mod Trends Pharmacopsychiatry*, vol. 30, pp. 153–165, 2015.

[3] N. Daviu, M. R. Bruchas, B. Moghaddam, C. Sandi, and A. Beyeler, "Neurobiological links between stress and anxiety," *Neurobiol Stress*, vol. 11, article 100191, 2019.

[4] M. Zhuo, "Neural mechanisms underlying anxiety-chronic pain interactions," *Trends in Neurosciences*, vol. 39, no. 3, pp. 136–145, 2016.

[5] D. Borsook, C. Linnman, V. Faria, A. M. Strassman, L. Becerra, and I. Elman, "Reward deficiency and anti-reward in pain chronification," *Neuroscience and Biobehavioral Reviews*, vol. 68, pp. 282–297, 2016.

[6] E. B. Margolisa and A. N. Karkhanisb, "Dopaminergic cellular and circuit contributions to kappa opioid receptor mediated aversion," *Neurochemistry International*, vol. 129, article 104504, 2019.

[7] M. Hein, G. Ji, D. Tidwell et al., "Kappa opioid receptor activation in the amygdala disinhibits CRF neurons to generate pain-like behaviors," *Neuropharmacology*, vol. 185, article 108456, 2021.

[8] M. A. Baird, T. T. Y. Hsu, R. Wang, B. Juarez, and L. S. Zweifel, "κ opioid receptor-dynorphin signaling in the central amygdala regulates conditioned threat discrimination and anxiety," *eNeuro*, vol. 8, no. 1, pp. ENEURO.0370–ENEU20.2020, 2021.

[9] M. Martínez-Navarro, D. Cabañero, A. Wawrzczak-Bargiela et al., "Mu and delta opioid receptors play opposite nociceptive and behavioural roles on nerve-injured mice," *Br J Pharmacol*, vol. 177, no. 5, pp. 1187–1205, 2020.

[10] W. Zhou, Y. Li, X. Meng et al., "Switching of delta opioid receptor subtypes in central amygdala microcircuits is associated with anxiety states in pain," *The Journal of Biological Chemistry*, vol. 296, article ???, 2021.

[11] T. Hikida, K. Kimura, N. Wada, K. Funabiki, and S. Nakanishi, "Distinct roles of synaptic transmission in direct and indirect striatal pathways to reward and aversive behavior," *Neuron*, vol. 66, no. 6, pp. 896–907, 2010.

[12] T. Danjo, K. Yoshimi, K. Funabiki, S. Yawata, and S. Nakanishi, "Aversive behavior induced by optogenetic inactivation of ventral tegmental area dopamine neurons is mediated by dopamine D2 receptors in the nucleus accumbens," *Proceedings of the National Academy of Sciences of the United States of America*, vol. 111, no. 17, pp. 6455–6460, 2014.

[13] W. Ren, M. V. Centeno, S. Berger et al., "The indirect pathway of the nucleus accumbens shell amplifies neuropathic pain," *Nature Neuroscience*, vol. 19, no. 2, pp. 220–222, 2016.

[14] N. Schwartz, P. Temkin, S. Jurado et al., "Decreased motivation during chronic pain requires long-term depression in the nucleus accumbens," *Science*, vol. 345, no. 6196, pp. 535–542, 2014.

[15] C. Qi, B. Guo, K. Ren et al., "Chronic inflammatory pain decreases the glutamate vesicles in presynaptic terminals of the nucleus accumbens," *Molecular Pain*, vol. 14, p. 174480691878125, 2018.

[16] S. L. Pollema-Mays, M. V. Centeno, Z. Chang, A. V. Apkarian, and M. Martina, "Reduced ΔFosB expression in the rat nucleus accumbens has causal role in the neuropathic pain phenotype," *Neuroscience Letters*, vol. 702, pp. 77–83, 2019.

[17] M. Watanabe, M. Narita, Y. Hamada et al., "Activation of ventral tegmental area dopaminergic neurons reverses pathological allodynia resulting from nerve injury or bone cancer," *Molecular Pain*, vol. 14, p. 174480691875640, 2018.

[18] L. Chen, Y. P. Lu, H. Y. Chen et al., "Ventral tegmental area GABAergic neurons induce anxiety-like behaviors and promote palatable food intake," *Neuropharmacology*, vol. 173, article 108114, 2020.

[19] S. R. DeGroot, R. Zhao-Shea, L. Chung et al., "Midbrain dopamine controls anxiety-like behavior by engaging unique interpeduncular nucleus microcircuitry," *Biological Psychiatry*, vol. 88, no. 11, pp. 855–866, 2020.

[20] M. Lee, T. R. Manders, S. E. Eberle et al., "Activation of corticostriatal circuitry relieves chronic neuropathic pain," *The Journal of Neuroscience*, vol. 35, no. 13, pp. 5247–5259, 2015.

[21] H. Zhou, E. Martinez, H. H. Lin et al., "Inhibition of the prefrontal projection to the nucleus accumbens enhances pain sensitivity and affect," *Frontiers in Cellular Neuroscience*, vol. 12, p. 240, 2018.

[22] N. Schwartz, C. Miller, and H. L. Fields, "Cortico-accumbens regulation of approach-avoidance behavior is modified by experience and chronic pain," *Cell Reports*, vol. 19, no. 8, pp. 1522–1531, 2017.

[23] L. Zhang, V. S. Hernández, E. Vázquez-Juárez, F. K. Chay, and R. A. Barrio, "Thirst is associated with suppression of habenula output and active stress coping: is there a role for a non-canonical vasopressin-glutamate pathway?," *Front Neural Circuits*, vol. 10, p. 13, 2016.

[24] L. Shelton, L. Becerra, and D. Borsook, "Unmasking the mysteries of the habenula in pain and analgesia," *Progress in Neurobiology*, vol. 96, no. 2, pp. 208–219, 2012.

[25] Y. Li, Y. Wang, C. Xuan et al., "Role of the lateral habenula in pain-associated depression," *Frontiers in Behavioral Neuroscience*, vol. 11, p. 31, 2017.

[26] J. Chan, Y. Ni, P. Zhang, J. Zhang, and Y. Chen, "D1-like dopamine receptor dysfunction in the lateral habenula nucleus increased anxiety-like behavior in rat," *Neuroscience*, vol. 340, pp. 542–550, 2017.

[27] W. Q. Cui, W. W. Zhang, T. Chen et al., "Tacr3 in the lateral habenula differentially regulates orofacial allodynia and anxiety-like behaviors in a mouse model of trigeminal neuralgia," *Acta Neuropathologica Communications*, vol. 8, no. 1, p. 44, 2020.

[28] I. Panocka, M. Massi, I. Lapo, T. Swiderski, M. Kowalczyk, and B. Sadowski, "Antidepressant-type effect of the NK3 tachykinin receptor agonist aminosenktide in mouse lines differing in endogenous opioid system activity," *Peptides*, vol. 22, no. 7, pp. 1037–1042, 2001.

[29] E. H. Kamp, D. R. Beck, and G. F. Gebhart, "Combinations of neurokinin receptor antagonists reduce visceral hyperalgesia," *The Journal of Pharmacology and Experimental Therapeutics*, vol. 299, no. 1, pp. 105–113, 2001.

[30] I. H. Bianco and S. W. Wilson, "The habenular nuclei: a conserved asymmetric relay station in the vertebrate brain," *Philosophical Transactions of the Royal Society of London. Series B, Biological Sciences*, vol. 364, no. 1519, pp. 1005–1020, 2009.

[31] S. Hetu, Y. Luo, I. Saez, K. D'Ardenne, T. Lohrenz, and P. R. Montague, "Asymmetry in functional connectivity of the human habenula revealed by high-resolution cardiac-gated resting state imaging," *Human Brain Mapping*, vol. 37, no. 7, pp. 2602–2615, 2016.

[32] F. Wagner, T. Stroh, and R. W. Veh, "Correlating habenular subnuclei in rat and mouse by using topographic, morphological, and cytochemical criteria," *The Journal of Comparative Neurology*, vol. 522, no. 11, pp. 2650–2662, 2014.

[33] W. Zhou, Y. Jin, Q. Meng et al., "A neural circuit for comorbid depressive symptoms in chronic pain," *Nature Neuroscience*, vol. 22, no. 10, pp. 1649–1658, 2019.

[34] E. Rodriguez, K. Sakurai, J. Xu et al., "A craniofacial-specific monosynaptic circuit enables heightened affective pain," *Nature Neuroscience*, vol. 20, no. 12, pp. 1734–1743, 2017.

[35] L. Sun, R. Liu, F. Guo et al., "Parabrachial nucleus circuit governs neuropathic pain-like behavior," *Nature Communications*, vol. 11, no. 1, p. 5974, 2020.

[36] M. C. Chiang, E. K. Nguyen, M. Canto-Bustos, A. E. Papale, A. M. Oswald, and S. E. Ross, "Divergent neural pathways emanating from the lateral parabrachial nucleus mediate distinct components of the pain response," *Neuron*, vol. 106, no. 6, pp. 927–939.e5, 2020.

[37] Y. Q. Cai, W. Wang, A. Paulucci-Holthauzen, and Z. Z. Pan, "Brain circuits mediating opposing effects on emotion and pain," *The Journal of Neuroscience*, vol. 38, no. 28, pp. 6340–6349, 2018.

[38] T. D. Wilson, S. Valdivia, A. Khan et al., "Dual and opposing functions of the central amygdala in the modulation of pain," *Cell Reports*, vol. 29, no. 2, pp. 332–346.e5, 2019.

[39] C. Raver, O. Uddin, Y. Ji et al., "An amygdalo-parabrachial pathway regulates pain perception and chronic pain," *The Journal of Neuroscience*, vol. 40, no. 17, pp. 3424–3442, 2020.

[40] J. Deng, H. Zhou, J. K. Lin et al., "The parabrachial nucleus directly channels spinal nociceptive signals to the intralaminar thalamic nuclei, but not the amygdala," *Neuron*, vol. 107, no. 5, pp. 909–923.e6, 2020.

[41] Y. Y. Jiang, Y. Zhang, S. Cui, F. Y. Liu, M. Yi, and Y. Wan, "Cholinergic neurons in medial septum maintain anxiety-like behaviors induced by chronic inflammatory pain," *Neuroscience Letters*, vol. 671, pp. 7–12, 2018.

[42] V. Carola, F. D'Olimpio, E. Brunamonti, F. Mangia, and P. Renzi, "Evaluation of the elevated plus-maze and open-field tests for the assessment of anxiety-related behaviour in inbred mice," *Behavioural Brain Research*, vol. 134, no. 1-2, pp. 49–57, 2002.

[43] Y. Y. Jiang, S. Shao, Y. Zhang et al., "Neural pathways in medial septal cholinergic modulation of chronic pain: distinct contribution of the anterior cingulate cortex and ventral hippocampus," *Pain*, vol. 159, no. 8, pp. 1550–1561, 2018.

[44] A. A. Mutso, D. Radzicki, M. N. Baliki et al., "Abnormalities in hippocampal functioning with persistent pain," *The Journal of Neuroscience*, vol. 32, no. 17, pp. 5747–5756, 2012.

[45] K. Koga, G. Descalzi, T. Chen et al., "Coexistence of two forms of LTP in ACC provides a synaptic mechanism for the interactions between anxiety and chronic pain," *Neuron*, vol. 85, no. 2, pp. 377–389, 2015.

[46] X. Y. Li, H. G. Ko, T. Chen, G. L. Collingridge, B. K. Kaang, and M. Zhuo, "Erasing injury-related cortical synaptic potentiation as a new treatment for chronic pain," *Journal of Molecular Medicine*, vol. 89, no. 9, pp. 847–855, 2011.

[47] M. Zhuo, "Long-term cortical synaptic changes contribute to chronic pain and emotional disorders," *Neuroscience Letters*, vol. 702, pp. 66–70, 2019.

[48] H. C. Moon, W. I. Heo, Y. J. Kim et al., "Optical inactivation of the anterior cingulate cortex modulate descending pain pathway in a rat model of trigeminal neuropathic pain created via chronic constriction injury of the infraorbital nerve," *Journal of Pain Research*, vol. Volume 10, pp. 2355–2364, 2017.

[49] M. Tsuda, K. Koga, T. Chen, and M. Zhuo, "Neuronal and microglial mechanisms for neuropathic pain in the spinal dorsal horn and anterior cingulate cortex," *Journal of Neurochemistry*, vol. 141, no. 4, pp. 486–498, 2017.

[50] J. M. Thompson and V. Neugebauer, "Amygdala plasticity and pain," *Pain Research & Management*, vol. 2017, p. 8296501, 2017.

[51] Y. Sun, L. Qian, L. Xu, S. Hunt, and P. Sah, "Somatostatin neurons in the central amygdala mediate anxiety by disinhibition of the central sublenticular extended amygdala," *Molecular Psychiatry*, vol. 2020, 2020.

[52] T. Hua, B. Chen, D. Lu et al., "General anesthetics activate a potent central pain-suppression circuit in the amygdala," *Nature Neuroscience*, vol. 23, no. 7, pp. 854–868, 2020.

[53] S. H. Liang, W. J. Zhao, J. B. Yin et al., "A neural circuit from thalamic paraventricular nucleus to central amygdala for the facilitation of neuropathic pain," *The Journal of Neuroscience*, vol. 40, no. 41, pp. 7837–7854, 2020.

[54] K. M. Tye, R. Prakash, S. Y. Kim et al., "Amygdala circuitry mediating reversible and bidirectional control of anxiety," *Nature*, vol. 471, no. 7338, pp. 358–362, 2011.

[55] J. Kim, M. Pignatelli, S. Xu, S. Itohara, and S. Tonegawa, "Antagonistic negative and positive neurons of the basolateral amygdala," *Nature Neuroscience*, vol. 19, no. 12, pp. 1636–1646, 2016.

[56] G. Corder, B. Ahanonu, B. F. Grewe, D. Wang, M. J. Schnitzer, and G. Scherrer, "An amygdalar neural ensemble that encodes the unpleasantness of pain," *Science*, vol. 363, no. 6424, pp. 276–281, 2019.

[57] J. Huang, V. M. Gadotti, L. Chen et al., "A neuronal circuit for activating descending modulation of neuropathic pain," *Nature Neuroscience*, vol. 22, no. 10, pp. 1659–1668, 2019.

[58] A. C. Felix-Ortiz, A. Beyeler, C. Seo, C. A. Leppla, C. P. Wildes, and K. M. Tye, "BLA to vHPC inputs modulate anxiety-related behaviors," *Neuron*, vol. 79, no. 4, pp. 658–664, 2013.

[59] G. Pi, D. Gao, D. Wu et al., "Posterior basolateral amygdala to ventral hippocampal CA1 drives approach behaviour to exert an anxiolytic effect," *Nature Communications*, vol. 11, no. 1, p. 183, 2020.

[60] H. Schmidt, "Three functional facets of calbindin D-28k," *Frontiers in Molecular Neuroscience*, vol. 5, p. 25, 2012.

[61] A. Müller, M. Kukley, P. Stausberg, H. Beck, W. Müller, and D. Dietrich, "Endogenous Ca2+ buffer concentration and Ca2+ microdomains in hippocampal neurons," *The Journal of Neuroscience*, vol. 25, no. 3, pp. 558–565, 2005.

[62] A. Tyrtyshnaia and I. Manzhulo, "Neuropathic pain causes memory deficits and dendrite tree morphology changes in mouse hippocampus," *Journal of Pain Research*, vol. Volume 13, pp. 345–354, 2020.

[63] A. Bilbao, C. Falfán-Melgoza, S. Leixner et al., "Longitudinal structural and functional brain network alterations in a mouse model of neuropathic pain," *Neuroscience*, vol. 387, pp. 104–115, 2018.

[64] L. Ma, L. Yue, Y. Zhang et al., "Spontaneous pain disrupts ventral hippocampal CA1-infralimbic cortex connectivity and modulates pain progression in rats with peripheral inflammation," *Cell Reports*, vol. 29, no. 6, pp. 1579–1593.e6, 2019.

[65] M. S. Fanselow and H. W. Dong, "Are the dorsal and ventral hippocampus functionally distinct structures?," *Neuron*, vol. 65, no. 1, pp. 7–19, 2010.

[66] N. McNaughton and J. A. Gray, "Anxiolytic action on the behavioural inhibition system implies multiple types of arousal contribute to anxiety," *Journal of Affective Disorders*, vol. 61, no. 3, pp. 161–176, 2000.

[67] N. L. Trent and J. L. Menard, "The ventral hippocampus and the lateral septum work in tandem to regulate rats' open-arm exploration in the elevated plus-maze," *Physiology & Behavior*, vol. 101, no. 1, pp. 141–152, 2010.

[68] G. M. Parfitt, R. Nguyen, J. Y. Bang et al., "Bidirectional control of anxiety-related behaviors in mice: role of inputs arising from the ventral hippocampus to the lateral septum and medial prefrontal cortex," *Neuropsychopharmacology*, vol. 42, no. 8, pp. 1715–1728, 2017.

[69] T. E. Anthony, N. Dee, A. Bernard, W. Lerchner, N. Heintz, and D. J. Anderson, "Control of stress-induced persistent anxiety by an extra-amygdala septohypothalamic circuit," *Cell*, vol. 156, no. 3, pp. 522–536, 2014.

[70] G. M. Singewald, A. Rjabokon, N. Singewald, and K. Ebner, "The modulatory role of the lateral septum on neuroendocrine and behavioral stress responses," *Neuropsychopharmacology*, vol. 36, no. 4, pp. 793–804, 2011.

[71] M. A. Kheirbek, L. J. Drew, N. S. Burghardt et al., "Differential control of learning and anxiety along the dorsoventral axis of the dentate gyrus," *Neuron*, vol. 77, no. 5, pp. 955–968, 2013.

[72] J. C. Jimenez, K. Su, A. R. Goldberg et al., "Anxiety cells in a hippocampal-hypothalamic circuit," *Neuron*, vol. 97, no. 3, pp. 670–683.e6, 2018.

[73] A. Adhikari, M. A. Topiwala, and J. A. Gordon, "Synchronized activity between the ventral hippocampus and the medial prefrontal cortex during anxiety," *Neuron*, vol. 65, no. 2, pp. 257–269, 2010.

[74] N. Padilla-Coreano, S. S. Bolkan, G. M. Pierce et al., "Direct ventral hippocampal-prefrontal input is required for anxiety-related neural activity and behavior," *Neuron*, vol. 89, no. 4, pp. 857–866, 2016.

[75] S. Ciocchi, J. Passecker, H. Malagon-Vina, N. Mikus, and T. Klausberger, "Selective information routing by ventral hippocampal CA1 projection neurons," *Science*, vol. 348, no. 6234, pp. 560–563, 2015.

[76] J. A. Sierra-Fonseca, L. F. Parise, F. J. Flores-Ramirez, E. H. Robles, I. Garcia-Carachure, and S. D. Iniguez, "Dorsal hippocampus ERK2 signaling mediates anxiolytic-related behavior in male rats," *Chronic Stress (Thousand Oaks)*, vol. 3, p. 247054701989703, 2019.

[77] A. R. Abela, C. J. Browne, D. Sargin et al., "Median raphe serotonin neurons promote anxiety-like behavior via inputs to the dorsal hippocampus," *Neuropharmacology*, vol. 168, article 107985, 2020.

[78] L. K. Knight and B. E. Depue, "New frontiers in anxiety research: the translational potential of the bed nucleus of the stria terminalis," *Frontiers in Psychiatry*, vol. 10, p. 510, 2019.

[79] S. Y. Kim, A. Adhikari, S. Y. Lee et al., "Diverging neural pathways assemble a behavioural state from separable features in anxiety," *Nature*, vol. 496, no. 7444, pp. 219–223, 2013.

[80] N. Yamauchi, D. Takahashi, Y. K. Sugimura, F. Kato, T. Amano, and M. Minami, "Activation of the neural pathway from the dorsolateral bed nucleus of the stria terminalis to the central amygdala induces anxiety-like behaviors," *The European Journal of Neuroscience*, vol. 48, no. 9, pp. 3052–3061, 2018.

[81] M. B. Pomrenze, J. Tovar-Diaz, A. Blasio et al., "A corticotropin releasing factor network in the extended amygdala for anxiety," *The Journal of Neuroscience*, vol. 39, no. 6, pp. 1030–1043, 2019.

[82] T. Kaneko, K. Kaneda, A. Ohno et al., "Activation of adenylate cyclase-cyclic AMP-protein kinase A signaling by corticotropin-releasing factor within the dorsolateral bed

nucleus of the stria terminalis is involved in pain-induced aversion," *The European Journal of Neuroscience*, vol. 44, no. 11, pp. 2914–2924, 2016.

[83] D. Takahashi, Y. Asaoka, K. Kimura et al., "Tonic suppression of the mesolimbic dopaminergic system by enhanced corticotropin-releasing factor signaling within the bed nucleus of the stria terminalis in chronic pain model rats," *The Journal of Neuroscience*, vol. 39, no. 42, pp. 8376–8385, 2019.

[84] C. A. Marcinkiewcz, C. M. Mazzone, G. D'Agostino et al., "Serotonin engages an anxiety and fear-promoting circuit in the extended amygdala," *Nature*, vol. 537, no. 7618, pp. 97–101, 2016.

[85] J. H. Jennings, D. R. Sparta, A. M. Stamatakis et al., "Distinct extended amygdala circuits for divergent motivational states," *Nature*, vol. 496, no. 7444, pp. 224–228, 2013.

[86] S. Deyama, T. Katayama, N. Kondoh et al., "Role of enhanced noradrenergic transmission within the ventral bed nucleus of the stria terminalis in visceral pain-induced aversion in rats," *Behavioural Brain Research*, vol. 197, no. 2, pp. 279–283, 2009.

[87] S. Deyama, T. Katayama, A. Ohno et al., "Activation of the beta-adrenoceptor-protein kinase A signaling pathway within the ventral bed nucleus of the stria terminalis mediates the negative affective component of pain in rats," *The Journal of Neuroscience*, vol. 28, no. 31, pp. 7728–7736, 2008.

[88] S. Deyama, S. Ide, N. Kondoh, T. Yamaguchi, M. Yoshioka, and M. Minami, "Inhibition of noradrenaline release by clonidine in the ventral bed nucleus of the stria terminalis attenuates pain-induced aversion in rats," *Neuropharmacology*, vol. 61, no. 1-2, pp. 156–160, 2011.

[89] Q. Xiao, X. Zhou, P. Wei et al., "A new GABAergic somatostatin projection from the BNST onto accumbal parvalbumin neurons controls anxiety," *Molecular Psychiatry*, vol. 2020, 2020.

[90] C. Glangetas, L. Massi, G. R. Fois et al., "NMDA-receptor-dependent plasticity in the bed nucleus of the stria terminalis triggers long-term anxiolysis," *Nature Communications*, vol. 8, no. 1, p. 14456, 2017.

[91] L. M. Williams, "Precision psychiatry: a neural circuit taxonomy for depression and anxiety," *The Lancet Psychiatry*, vol. 3, no. 5, pp. 472–480, 2016.

Hindawi
Neural Plasticity
Volume 2022, Article ID 2191011, 10 pages
https://doi.org/10.1155/2022/2191011

Research Article

P2Y2 Receptor Mediated Neuronal Regeneration and Angiogenesis to Affect Functional Recovery in Rats with Spinal Cord Injury

Ruidong Cheng,[1,2] **Genying Zhu**,[1,2] **Chengtao Ni**,[3] **Rui Wang**,[3] **Peng Sun**,[2] **Liang Tian**,[2] **Li Zhang**,[2] **Jie Zhang**,[2] **Xiangming Ye**,[2] **and Benyan Luo**[1,4]

[1]*Department of Neurology & Brain Medical Center, The First Affiliated Hospital, Zhejiang University School of Medicine, Hangzhou, Zhejiang, China*
[2]*Rehabilitation Medicine Center, Department of Rehabilitation Medicine, Zhejiang Provincial People's Hospital, Affiliated People's Hospital of Hangzhou Medical College, Hangzhou, Zhejiang, China*
[3]*Graduate School, Bengbu Medical College, Bengbu, Anhui, China*
[4]*Collaborative Innovation Center for Brain Science, Zhejiang University School of Medicine, Hangzhou, Zhejiang, China*

Correspondence should be addressed to Benyan Luo; luobenyan@zju.edu.cn

Received 19 August 2021; Revised 7 December 2021; Accepted 17 December 2021; Published 2 February 2022

Academic Editor: Mou-Xiong Zheng

The aim of this study was to investigate the effect of the P2Y2 receptor (P2Y2R) signaling pathway on neuronal regeneration and angiogenesis during spinal cord injury (SCI). The rats were randomly divided into 3 groups, including the sham+dimethyl sulfoxide (DMSO), SCI+DMSO, and SCI+P2Y2R groups. The SCI animal models were constructed. A locomotor rating scale was used for behavioral assessments. The apoptosis of spinal cord tissues was detected by TUNEL staining. The expression levels of P2Y2R, GFAP, nestin, Tuj1, and CD34 were detected by immunofluorescence staining, and the expression levels of TNF-α, IL-1β, and IL-6 were detected by enzyme-linked immunosorbent assay. The locomotor score in the model group was significantly lower than the sham group. The expression of P2Y2R was increased after SCI. The expression levels of TNF-α, IL-1β, and IL-6 were increased remarkably in the SCI model group compared with the sham group. The P2Y2R inhibitor relieved neuronal inflammation after SCI. Compared with the sham group, the apoptotic rate of spinal cord tissue cells in the model group was significantly increased. The P2Y2R inhibitor reduced the apoptosis of the spinal cord tissue. The expressions of CD34, Tuj1, and nestin in the model group were decreased, while the expressions of GFAP and P2Y2R were increased. The P2Y2R inhibitor reversed their expression levels. The P2Y2R inhibitor could alleviate SCI by relieving the neuronal inflammation, inhibiting the spinal cord tissue apoptosis, and promoting neuronal differentiation and vascular proliferation after SCI. P2Y2R may serve as a target for the treatment of SCI.

1. Introduction

Spinal cord injury (SCI) is a devastating neurological state causing major sensory motor and autonomic dysfunctions [1]. SCI leads to a series of molecular and cellular events, such as demyelination of surviving axons, free radical production, and release of nucleotides and excitatory amino acids, followed by neural tissue loss because of necrosis, apoptosis, macrophage infiltration, and inflammation [2]. Presently, the available treatments for SCI are limited, and only the supportive relief was provided for patients with lifetime disability [3]. Therefore, it is necessary to explore a feasible intervention approach for the clinical treatment of SCI.

A study has reported that after SCI, endogenous neural stem cells (ENSCs) are activated, generating progeny cells. However, these cells fail to effectively differentiate into functional neurons but astrocytes, which may be due to their impaired function after SCI [4]. The astrocytes participate

in neural development in the central nervous system (CNS) [5]. During injury to the CNS, the astrocytes could result in reactive astrogliosis, characterized by the upregulated glial fibrillary acidic protein, and the proliferation of astrocytes at the lesion site, finally leading to the formation of glial scar [6]. The formation of a glial scar was one of important factors affecting the regeneration of neuron and nerve fiber [7, 8]. Recent studies have demonstrated that the astrocytes could be induced to differentiate into functional neurons by the intervention of NeuroD, Ascl1, or other signaling pathways [7, 8]. After SCI, the microcirculation and the microenvironment of the injury site play a crucial role in cell regeneration and repair [9], which determines the activation degree of astrocytes. The differentiation of astrocytes plays a key role in glial scar formation, spinal cord and axon repair, neuronal regeneration, and functional recovery of CNS. Therefore, how to induce ENSCs and astrocytes to differentiate into functional neurons is the key to improve the function of CNS after SCI.

Purines and their receptors, as an important neural signaling molecular, have participated in the transmission of peripheral and central nervous information and regulated the physiological activities of nerve tissue cells [9, 10]. Purinergic receptors included P1 adenosine receptors and P2 adenine nucleotide receptors, and the P2 receptors are divided into P2X (ionotropic) and P2Y (metabotropic) receptors [11]. It has been reported that astrocytes express several P2 receptor subtypes, including P2Y2 receptor (P2Y2R) [12]. Studies in human 1321 N1 astrocytoma cells expressing a recombinant P2Y2R have suggested that this receptor plays an important role in survival and neuroprotective mechanisms under pathological conditions [13]. Rodríguez-Zayas et al. [14] have demonstrated that the P2Y2R expression is increased in rats with SCI. Importantly, the expression and activation of P2Y2R are involved in the process of astrogliosis after CNS trauma [15, 16]. Nevertheless, there is no report on whether P2Y2R mediates angiogenesis, nerve repair, and regeneration after SCI.

In this study, we intended to investigate the effect of P2Y2R on the apoptosis of spinal cord tissue cells, neuron differentiation, angiogenesis, and neuronal proliferation. Thus, the SCI animal models were constructed followed by a series of experiments. Our findings may provide a new strategy for clinical treatment of SCI.

2. Materials and Methods

2.1. Animals and Grouping. Male Sprague-Dawley rats (260-300 g) were used in this study, which were housed at 21-25°C with a 12 h light/dark cycle, and were provided water and food ad libitum. All experiments were approved by the Institutional Animal Care and Use Committee of Zhejiang Provincial People's Hospital. The rats were randomly divided into 3 groups, including the sham+dimethyl sulfoxide (DMSO), SCI+DMSO, and SCI+P2Y2R groups, with 10 rats per group.

2.2. SCI Model Establishment. The SD rats were anesthetized by intraperitoneal injection of pentobarbital (30 mg/kg). The backs of the rats were shaved for routine disinfection. Following that, a midline skin incision of approximately 5 cm was made, and the muscles were separated to expose the vertebra. A miniature bone rongeur was used to resect the T9-T11 spinous processes and corresponding lamina. The spinal canal was opened at the T9-T11 level to fully expose the dorsal and bilateral sides of the spinal cord. The above procedures were performed with caution to ensure the dura mater remained intact. The spinal cord injury in the T9-T11 segment of rats was induced by the modified Mascis percussion device. In order to make the spinal cord of the three segments of T9-T11 bear a balanced impact force, a metal spacer with a width of 3 mm and a length and radian consistent with that of the spinal cord of the segments of T8-T10 was placed on the exposed dura of T9-T11 before the impact, and then, a weight of 10 g was dropped onto the metal spacer from a height. The weight and spacer were removed immediately after the blow, the wound was sutured layer by layer, and the incision was disinfected. The markers of the successful establishment of the model were as follows: visible seizure-like wagging of tails, retraction and fluttering of the hind limbs and body, and flaccid paralyses of the hind limbs.

For the sham group, only the spinous process and lamina were resected intraoperatively, and spinal cord shock injury was not performed. For the P2Y2R intervention group, after the model was established, the P2Y2R inhibitor (ar-c126313; 600 pmol/μL; BOC Science, USA) was intrathecally injected at 10 μL/d daily for 4 weeks.

2.3. Behavioral Assessments. Four observation time points were set, which were before injury, 1 day, 2 weeks, and 4 weeks after SCI. The rats were placed on an open test platform, and the locomotor activity of their hind limbs was observed continuously for 4 min by using the BBB (Basso, Beattie, and Bresnahan) locomotor rating scale at the 4 observation time points above. The scale is graded into 21 points with 0 indicating complete paralysis and 21 representing normal locomotion.

2.4. Hematoxylin and Eosin (HE) Staining. The spinal cord tissues were fixed in formaldehyde for 48 h and then rehydrated with different concentrations of ethanol, followed by embedding in paraffin. Then, the tissues were sectioned into 5 μm slices, immersed in hematoxylin for 1 min, and then stained with eosin for 30 s. After being washed with water, the sections were dehydrated with graded alcohol, cleared in xylene, and then sealed for microscopic observation. After completion of the experiment, the rats were perfused with 4% paraformaldehyde. The spinal cord was retrieved from the rats and postfixed in 4% paraformaldehyde solution for another 4 h; and then, it was immersed in 30% sucrose solution overnight. The fixed spinal cord was sliced into 5 μm slices, which were further stained by HE staining.

2.5. Terminal Deoxynucleotidyl Transferase-Mediated Nick End Labeling (TUNEL) Staining. The apoptosis of cells in spinal cord tissues was detected by TUNEL staining,

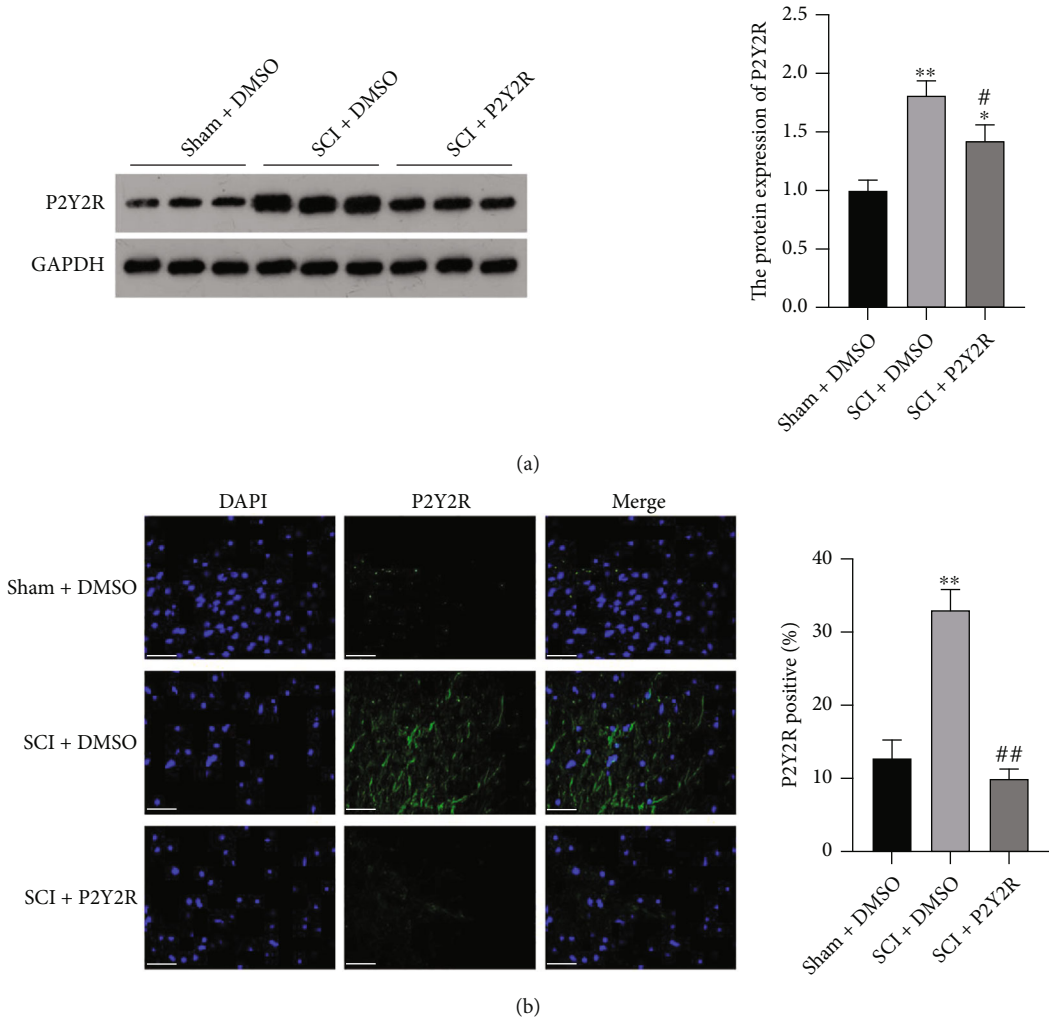

Figure 1: (a) The expression level of P2Y2R in spinal cord tissue detected by western blot. (b) The expression level of P2Y2R in spinal cord tissue detected by immunofluorescence staining. Scale bar = 50 μm. $^{*}p < 0.05$ and $^{**}p < 0.01$ compared with the sham+DMSO group; $^{\#}p < 0.05$ and $^{\#\#}p < 0.01$ compared with the SCI+DMSO group.

according to the manufacturer's recommended instructions of TUNEL Color Labeling Apoptosis Detection Kit (11684817910; Roche Applied Science, USA). Spinal cord tissues were fixed in formaldehyde for 48 h and then rehydrated with different concentrations of ethanol, followed by embedding in paraffin. Then, the paraffin block was cut into 4-7 μm thick sections and then deparaffinized with xylene (2 × 15 minutes) and rehydrated with graded concentrations of ethanol. After that, the sections were performed with antigen retrieval in boiling sodium citrate (0.01 M) in a pressure cooker and then treated with the TUNEL reaction mixture (50 μL TdT + 450 μL fluorescein-labeled dUTP) at 37°C for 1 h in a dark wet box. The sections were stained with DAB, and the numbers of TUNEL-positive cells were assessed using a fluorescence microscope. The apoptotic index was calculated as the percentage of TUNEL-positive cells in a section of 5 randomly selected areas of the specimens.

2.6. Immunofluorescence Staining. For immunofluorescence staining, spinal cord tissues were fixed in formaldehyde for 48 h and then rehydrated with different concentrations of ethanol, followed by embedding in paraffin. Spinal cord sections (4-7 μm thick) from each specimen were deparaffinized with xylene (2 × 15 minutes) and then incubated in graded concentrations of ethanol (100%, 95%, 85%, and 75%). The sections were then subjected to antigen retrieval in boiling sodium citrate (0.01 M) in a pressure cooker, followed by phosphate buffer solution (PBS) washing. After that, the samples were incubated with the primary antibodies overnight at 4°C. The primary antibodies included anti-P2Y2R (1 : 500; P6612; Sigma, USA), glial fibrillary acidic protein (GFAP; 1 : 500; PAA068Ra01; USCN Life Science; Wuhan, China), nestin (1 : 500; PAA500Ra01; USCN Life Science; Wuhan, China), Tuj1 (1 : 1000; ab68193; Abcam, USA), and CD34 (1 : 1000; ab81289; Abcam, USA). The next day, the sections were washed with PBS and then incubated with the fluorescent-labeled secondary antibodies for 30 min at 37°C. After 3 rinses with PBS, DAPI staining was performed, and the nuclei were counterstained with 1 g/mL Hoechst (BioSharp, China) for 5 minutes. The immunofluorescence imaging was conducted using a fluorescence microscope.

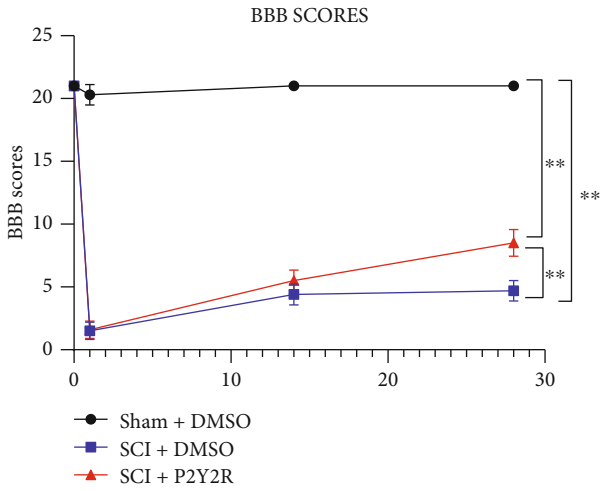

Figure 2: Recovery of motor function assessment. The recovery of the motor function was assessed with the BBB scoring method. After 2 weeks and 4 weeks of modeling, $^{**}p < 0.01$ compared with the sham+DMSO group; $^{\#}p < 0.05$ compared with the SCI +DMSO group.

2.7. Enzyme-Linked Immunosorbent Assay (ELISA). The expression levels of tumor necrosis factor-α (TNF-α), IL-1β, and IL-6 were detected by ELISA. The spinal cord samples were homogenized and centrifuged at 1000*g* for 20 min. The liquid supernatant was collected and tested at a wavelength of 450 nm according to the manufacturer's instructions of ELISA kits (R&D Systems, Minneapolis, Minn., USA).

2.8. Western Blotting. The spinal cord tissues were lysed by homogenization in 300 μL of lysis buffer. Proteins were separated on 12% sodium dodecyl sulfate polyacrylamide gel electrophoresis (SDS-PAGE) gels. Then, the proteins in the gels were transferred to polyvinylidene difluoride (PDVF) membranes. The membranes were blocked for 2 h, followed by incubation with monoclonal antibodies against GAPDH (1 : 3000) and P2Y2R (1 : 200) at 4°C overnight. After 3 washes with TBST, horseradish peroxidase-conjugated goat anti-rabbit IgG was added for an additional 1.5 h. Then, the blots were visualized using an enhanced chemiluminescence (ECL) system.

2.9. Biotinylated Dextran Amine (BDA) Tracing. Two weeks after the model was constructed, the rats were fixed on the stereotaxic apparatus after anesthesia, and the scalp in the parietal area was cut lengthwise. The periosteum was cut and pushed around. Then, the skull was swabbed with hydrogen peroxide. In reference to the location map of the rat brain in *vivo*, the anterior fontanelle was taken as the origin, and 8 locations were selected for drilling. Then, 1 μL of 5% BDA solution was injected into the motor cortex of rats with a microinjector, and the depth of injection was about 3.5 mm from the surface of the skull. The injection time was set for 5 min. After the injection, the scalp was sutured. After 2 weeks, the spinal cord tissue samples below the injured segment were collected for BDA fluorescence staining to observe the nerve fibers of the corticospinal tract.

2.10. Statistical Analysis. Results were analyzed by ANOVA test using GraphPad Prism 6 (Graph Pad Software Inc., San Diego, CA, USA). Data were expressed as means ± standard deviations (SD). Differences were considered to be significant at $p < 0.05$.

3. Results

3.1. The Expression Level of P2Y2R Was Increased after SCI. The expression level of P2Y2R in spinal cord tissues in three groups was detected by western blot and immunofluorescence staining. As shown in Figures 1(a) and 1(b), the expression level of this receptor was increased obviously in the model group in comparison with the sham group. When the P2Y2R inhibitor was added, its expression was significantly decreased compared with the model group.

3.2. BBB Locomotor Score. On the first day of modeling, rats in the model group and the P2Y2R inhibitor group almost lost their hind limb motor ability compared with the sham group. After 2 weeks and 4 weeks of modeling, the hind limb motor ability of rats in the model group and P2Y2R inhibitor group recovered somewhat, and the recovery effect in the P2Y2R inhibitor group was better than that in the model group (Figure 2).

3.3. P2Y2R Inhibitor Reduced Cell Apoptosis in Spinal Cord Tissue. HE staining of the spinal cord showed that the gray matter of the spinal cord in the sham+DMSO group was clearly demarcated, and the nerve cells in the gray matter were large, with abundant Nissl bodies and nucleolus. In the SCI+DMSO group, the damaged area was collapsed, and some nerve cells and fibers disappeared and were replaced by glial cells, resulting in patches of glial scar. The damage degree of the SCI+P2Y2R group was lighter than the SCI+DMSO group (Figure 3(a)).

The results of TUNEL assay in spinal cord tissue of rats in each group are shown in Figure 3(b). Compared with the sham group, the apoptotic rate of spinal cord tissue cells in the model group was significantly increased. Compared with the model group, the degree of spinal cord cell apoptosis was significantly decreased in the P2Y2R inhibitor group. The results indicate that the P2Y2R inhibitor could reduce the apoptosis of the spinal cord tissue, thus effectively alleviating the SCI.

3.4. P2Y2R Inhibitor Relieved Neuronal Inflammation after SCI. The proinflammatory cytokines, including TNF-α, IL-1β, and IL-6, had increased remarkably in the SCI model group compared with the sham group. Interestingly, P2Y2R inhibitor treatment could significantly reduce the release of TNF-α, IL-1β, and IL-6 when compared with the model group (Figure 4). This result indicated that the P2Y2R inhibitor could relieve neuronal inflammation of SCI.

3.5. P2Y2R Inhibitor Inhibited Glial Scar Formation and Promoted Nerve Fiber Growth after SCI. The expression level of GFAP was detected through immunofluorescence staining and western blot, as shown in Figures 5(a) and 5(c). In comparison with the sham group, the expression of GFAP

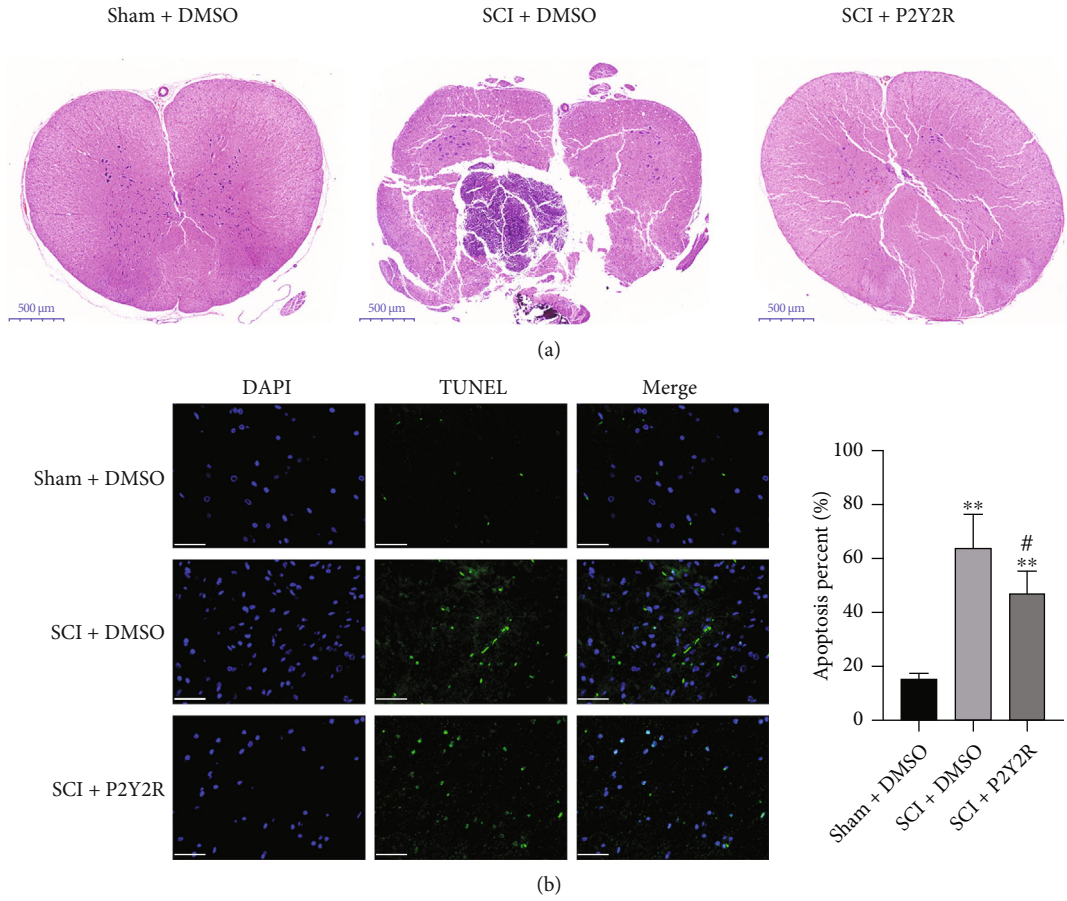

Figure 3: (a) The results of HE staining. (b) The apoptosis of spinal cord tissue detected by TUNEL assay. Scale bar = 50 μm.$^{**}p < 0.01$ compared with the sham+DMSO group; $^{\#}p < 0.05$ compared with the SCI+DMSO group.

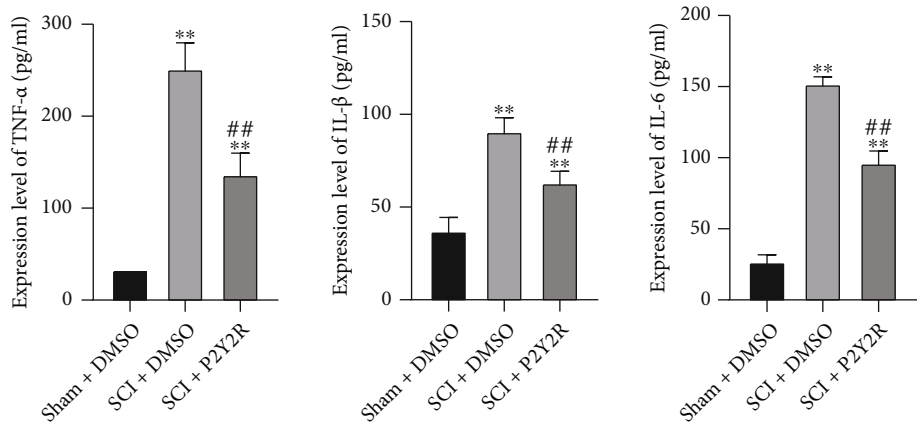

Figure 4: The expression levels of TNF-α, IL-1β, and IL-6 detected by ELISA. $^{*}p < 0.05$ and $^{**}p < 0.01$ compared with the sham+DMSO group; $^{\#\#}p < 0.01$ compared with the SCI+DMSO group.

was significantly increased. Nevertheless, after P2Y2R inhibitor treatment, the expression of GFAP was decreased in the spinal cord of rats when compared with the model group. These results suggested that the P2Y2R inhibitor may inhibit glial scar formation after SCI.

The results of BDA staining of the spinal cord tissue are shown in Figure 5(b). As can be seen from the figure, compared with the sham group, the expression of BDA in the spinal cord of rats in the model group was significantly decreased. When compared with the model group, the expression of BDA was significantly increased in the spinal cord of rats treated with P2Y2R inhibitor. The results indicated that the P2Y2R inhibitor could promote nerve fiber proliferation after SCI to alleviate SCI.

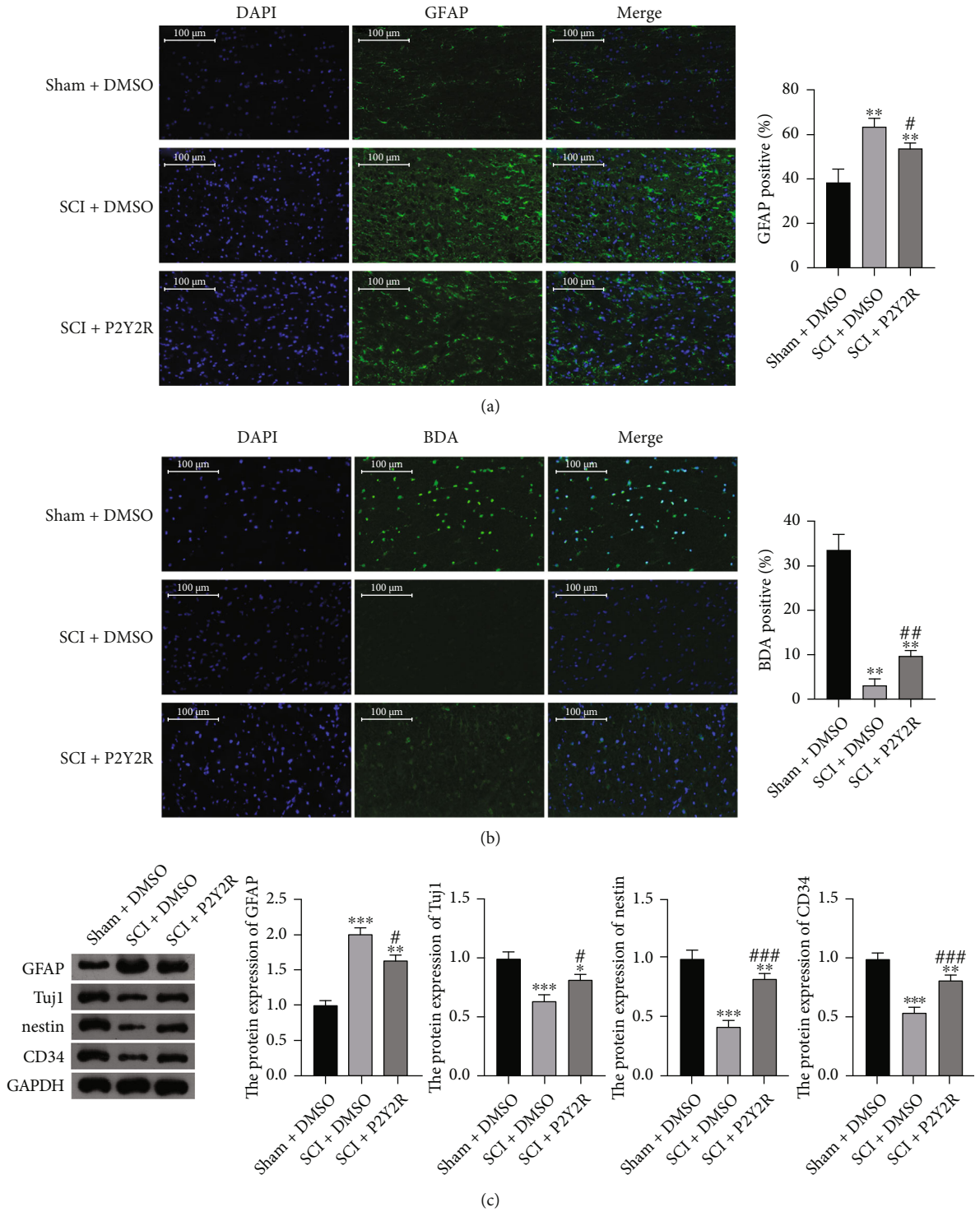

Figure 5: (a) The expression levels of GFAP detected by immunofluorescence staining. (b) Results of BDA staining. Scale bar = 100 μm. (c) The relative protein expression of GFAP, Tuj1, nestin, and CD34 measured by western blotting. $^{**}p < 0.01$ compared with sham+DMSO group; $^{\#}p < 0.05$ and $^{\#\#}p < 0.01$ compared with the SCI+DMSO group.

3.6. P2Y2R Inhibitor Promoted Neuronal Differentiation and Angiogenesis after SCI. The expression levels of Tuj1, nestin, and CD34 were detected through immunofluorescence staining and western blot, as shown in Figures 6 and 5(c). In comparison with the sham group, the expressions of Tuj1, nestin, and CD34 in the spinal cord of rats in the model group were significantly decreased. Nevertheless, after P2Y2R inhibitor treatment, the expressions of Tuj1, nestin, and CD34 were significantly increased in the spinal cord of rats when compared with the model group. These results

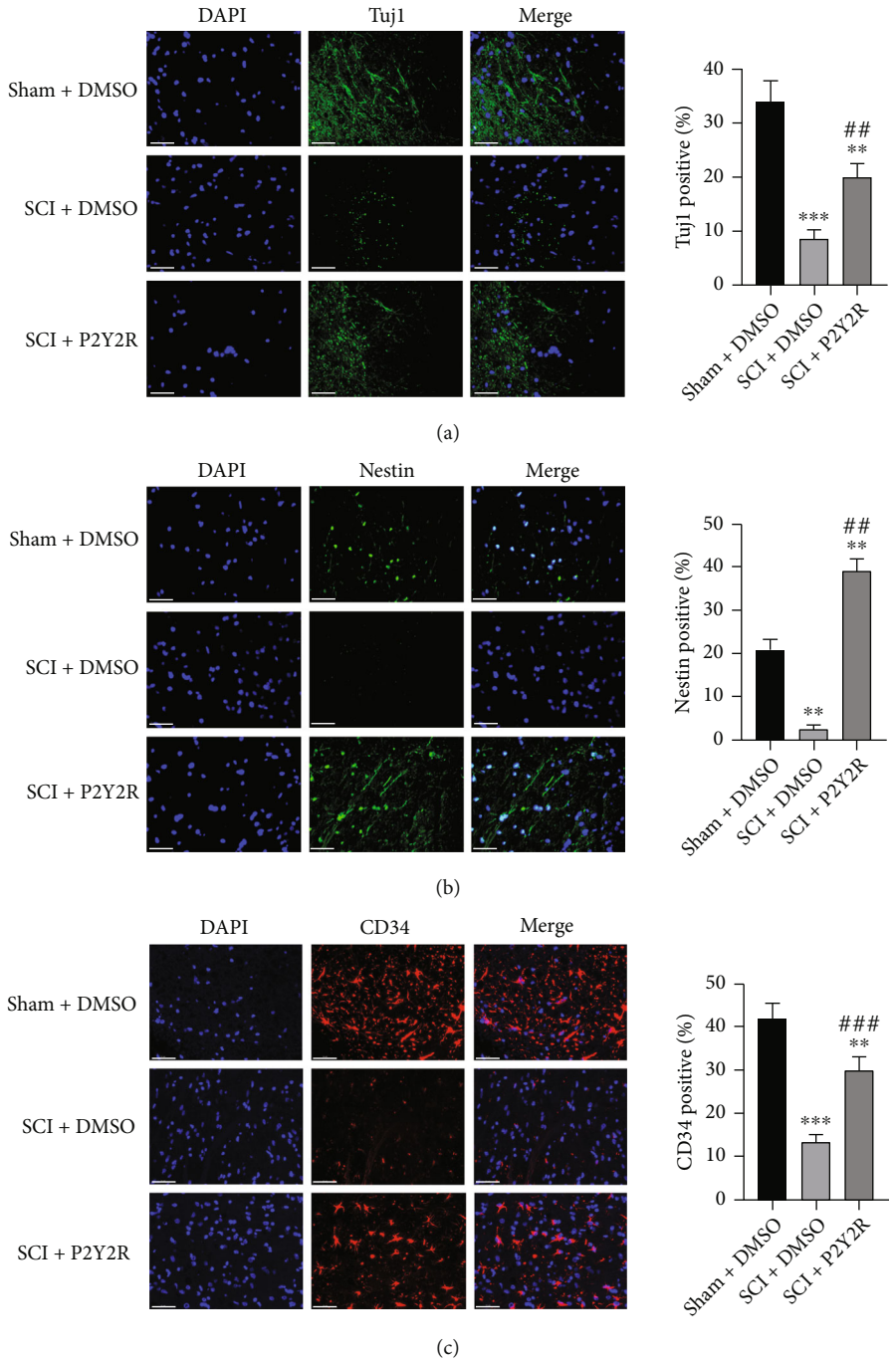

Figure 6: The expression levels of Tuj1, nestin, and CD34 detected by immunofluorescence staining. Scale bar = 50 μm. $^{*}p < 0.05$ and $^{**}p < 0.01$ compared with the sham+DMSO group; $^{\#}p < 0.05$ and $^{\#\#}p < 0.01$ compared with the SCI+DMSO group.

suggested that the P2Y2R inhibitor may promote neuronal differentiation and angiogenesis after SCI, thereby alleviating spinal cord injury effectively.

4. Discussion

SCI can lead to sensory impairment and paraplegia. Recently, the studies on pathological mechanisms have explored many new therapeutic methods for SCI. However, there is still a need to find more precise and specific treatment targets for these adverse outcomes [17]. In this study, our results showed that the expression of P2Y2R was increased after SCI in rats. The P2Y2R inhibitor could relieve the neuronal inflammation of SCI, reduce the apoptosis of the spinal cord tissue, and promote neuronal differentiation and vascular proliferation and neuronal proliferation after SCI.

The presence of P2Y1, P2Y2, P2Y4, P2Y6, P2Y12, and P2X2 receptors in the adult spinal cord was evident. P2Y receptors have been associated with survival responses in

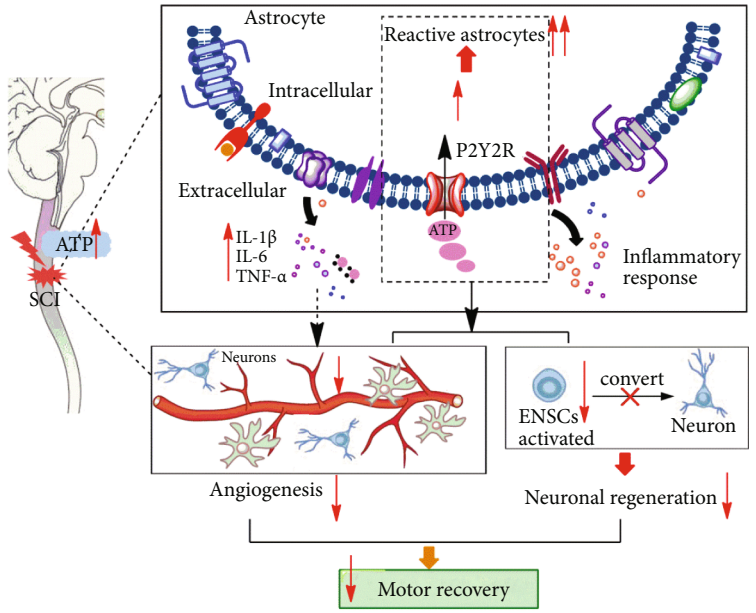

Figure 7: The P2Y2R signaling pathway could play a considerable role in the development of neuronal regeneration and angiogenesis to affect functional recovery in rats following SCI.

nervous tissues [18]. This family of receptors is considered the strong modulator of normal and pathological processes in the CNS [19]. Suramin was originally found to inhibit trypanocidal activity [20]. It has been shown to be a potent inhibitor of various hydrolytic and oxidative enzymes by interfering with the binding of ATP. P2XRs are activated by ATP; thus, suramin was later identified as a P2XR antagonist [21]. Suramin has been reported to inhibit P2YRs except for P2Y4 and P2Y6Rs which are insensitive [22]. In this study, after 2 weeks and 4 weeks of modeling, the hind limb motor ability of rats in the P2Y2R inhibitor (suramin) group recovered somewhat. However, in a previous study, the intrathecal administration of antagonists (suramin and PPDS) and the blockade of the P2 receptor activation do not improve locomotor behavior in the SCI rats. The decrease in reactive gliosis and the increases in the lesion cavity, caused by the infusion of antagonists, may be associated with the lack of locomotor improvement [19].

On the first day of modeling, rats in the model group and the P2Y2R inhibitor group almost lost their hind limb motor ability compared with the sham group. After 2 weeks and 4 weeks of modeling, the hind limb motor ability of rats in the model group and P2Y2R inhibitor group recovered somewhat, and the recovery effect in the P2Y2R inhibitor group was better than that in the model group.

Under various physiological and pathological conditions, extracellular nucleotides are released from cells in the CNS [23]. These nucleotides could activate P2 receptors on the surface of adjacent cells [20]. Previous studies have reported that metabotropic P2Y2R was upregulated in different cellular and animal models of injury [14, 21], suggesting that this receptor plays a critical role in the cellular response to tissue damage [24]. In accordance with the report above, our results also revealed that the expression of P2Y2R was elevated in the SCI model group, further supporting the ideas above.

CD34 is one of the hematopoietic markers, which could regulate migration and trafficking of hematopoietic progenitor cells [25]. CD34 may eventually migrate to the CNS and differentiate into microglia [26]. After CNS injury, CD34-expressing microglia could be found in affected regions, characterized by the damage of microgliosis and blood-brain barrier [27]. In this study, CD34 was found to be downregulated in SCI model rats, while was upregulated in the P2Y2R inhibitor group. This result suggested that the P2Y2R inhibitor may improve angiogenesis after SCI, evidenced by increased CD34 expression.

Tuj1 and nestin are neuron-specific molecular markers, which play important roles during the neural cell maturation. Tuj1 is a beta III microtubule specifically associated with neural differentiation, whose expression is elevated during the early stages of neural differentiation [28]. Nestin is an intermediate filament type VI, and is mainly expressed by neural cells. It affects the radial growth of axons, as well as the survival, proliferation, and self-renewal of neural cells [29]. It has been found to be upregulated in the early stage of neural differentiation [30]. In this study, the downregulation of Tuj1 and nestin in the model group suggested the impaired neuronal differentiation after SCI. After P2Y2R inhibitor treatment, the expression of Tuj1 and nestin was increased, suggesting that suppression of P2Y2R may improve the neuronal differentiation after SCI.

GFAP is an essential component of the astrocyte cytoskeleton. It is one of the best biomarkers for the activation of astrocytes following injury or stress in the CNS [31]. It has been reported that the expression of GFAP negatively correlates with the formation of the inhibitory glial scar. The reduction of the GFAP expression is more desirable

for the repair of SCI [32]. In this study, GFAP expression was reduced in the P2Y2R inhibitor group, suggesting the SCI repair function of the P2Y2R inhibitor.

Future studies should identify other molecular mechanisms that are involved in the P2Y2R signaling pathway in rats with SCI. Neural stem cells are a source of glial scar astrocytes with beneficial functions. Nowadays, SCI is often considered an attractive indication for the development of stem cell transplantation therapies. The discovery of ENSCs in the adult spinal cord offers hope for noninvasive treatment of SCI. Thus, whether the P2Y2R inhibitor has an effect on the ENSC activation needs further investigation [7].

Furthermore, P2Y2R knockout mice could be used to investigate the role of P2Y2R signaling in impair corticospinal tract function, increases calcium load, and the area of spinal injured areas. In light of the relationship between P2Y2R and neuronal regeneration, it will be interesting to explore the potential applications of P2Y2R inhibitors and other molecules that are unique to neuronal repair in spinal cord disease conditions.

5. Conclusion

In summary, our study demonstrated again that P2Y2R was overexpressed after SCI in rats. The P2Y2R inhibitor could alleviate SCI by relieving the neuronal inflammation, inhibiting the spinal cord tissue apoptosis, and promoting neuronal differentiation and angiogenesis after SCI (Figure 7). The P2Y2R may serve as a target for the treatment of SCI.

Data Availability

The data used to support the findings of this study are available from the corresponding authors upon request.

Conflicts of Interest

The authors declare that they have no conflict of interest.

Acknowledgments

This study was supported by the National Natural Science Foundation of China (grant number 81601965) and Natural Science Foundation of Zhejiang Province (grant number LY19H170003). We thank Mr. Xiaoguang Wang for his advice and language correction in this paper.

References

[1] A. Anjum, M. D. Yazid, M. Fauzi Daud et al., "Spinal cord injury: pathophysiology, multimolecular interactions, and underlying recovery mechanisms," *International Journal of Molecular Sciences*, vol. 21, no. 20, p. 7533, 2020.

[2] T. W. Corson and C. M. Crews, "Molecular understanding and modern application of traditional medicines: Triumphs and trials," *Cell*, vol. 130, no. 5, pp. 769–774, 2007.

[3] M. Khorasanizadeh, M. Yousefifard, M. Eskian et al., "Neurological recovery following traumatic spinal cord injury: a systematic review and meta-analysis," *Journal of Neurosurgery. Spine*, vol. 15, pp. 1–17, 2019.

[4] C. A. Grégoire, B. L. Goldenstein, E. M. Floriddia, F. Barnabé-Heider, and K. J. Fernandes, "Endogenous neural stem cell responses to stroke and spinal cord injury," *Glia*, vol. 63, no. 8, pp. 1469–1482, 2015.

[5] M. D. Laird, J. R. Vender, and K. M. Dhandapani, "Opposing roles for reactive astrocytes following traumatic brain injury," *Neuro-Signals*, vol. 16, pp. 154–164, 2008.

[6] E. J. Bradbury and E. R. Burnside, "Moving beyond the glial scar for spinal cord repair," *Nature Communications*, vol. 10, no. 1, pp. 3879–11707, 2019.

[7] M. Stenudd, H. Sabelström, and J. Frisén, "Role of endogenous neural stem cells in spinal cord injury and repair," *JAMA Neurology*, vol. 72, no. 2, pp. 235–237, 2015.

[8] Y. M. Yuan and C. He, "The glial scar in spinal cord injury and repair," *Neuroscience Bulletin*, vol. 29, pp. 421–435, 2013.

[9] I. von Kügelgen and K. Hoffmann, "Pharmacology and structure of p2y receptors," *Neuropharmacology*, vol. 104, pp. 50–61, 2016.

[10] I. von Kügelgen, "Pharmacology of p2y receptors," *Brain Research Bulletin*, vol. 151, pp. 12–24, 2019.

[11] K. A. Jacobson, E. G. Delicado, C. Gachet et al., "Update of p2y receptor pharmacology: Iuphar review 27," *British Journal of Pharmacology*, vol. 177, no. 11, pp. 2413–2433, 2020.

[12] M. Martínez, N. A. Martínez, J. D. Miranda, H. M. Maldonado, and W. I. Silva Ortiz, "Caveolin-1 regulates P2Y2 receptor signaling during mechanical injury in human 1321n1 astrocytoma," *Biomolecules*, vol. 9, no. 10, p. 622, 2019.

[13] N. E. Chorna, L. I. Santiago-Pérez, L. Erb et al., "P2y receptors activate neuroprotective mechanisms in astrocytic cells," *Journal of Neurochemistry*, vol. 91, pp. 119–132, 2004.

[14] A. E. Rodríguez-Zayas, A. I. Torrado, and J. D. Miranda, "P2y2 receptor expression is altered in rats after spinal cord injury," *International Journal of Developmental Neuroscience*, vol. 28, pp. 413–421, 2010.

[15] M. Gabl, M. Winther, A. Welin et al., "P2y2 receptor signaling in neutrophils is regulated from inside by a novel cytoskeleton-dependent mechanism," *Experimental Cell Research*, vol. 336, pp. 242–252, 2015.

[16] Z. Wang, T. Nakayama, N. Sato et al., "Purinergic receptor p2y, g-protein coupled, 2 (p2ry2) gene is associated with cerebral infarction in japanese subjects," *Hypertension Research*, vol. 32, pp. 989–996, 2009.

[17] Z. Zhao, X. Hu, Z. Wu, Q. Chen, and Q. Shao, "A selective p2y purinergic receptor agonist 2-mesadp enhances locomotor recovery after acute spinal cord injury," *European Neurology*, vol. 83, pp. 195–212, 2020.

[18] H. Franke and P. Illes, "Involvement of p2 receptors in the growth and survival of neurons in the cns," *Pharmacology & Therapeutics*, vol. 109, pp. 297–324, 2006.

[19] A. E. Rodríguez-Zayas, A. I. Torrado, O. R. Rosas, J. M. Santiago, J. D. Figueroa, and J. D. Miranda, "Blockade of p2 nucleotide receptors after spinal cord injury reduced the gliotic response and spared tissue," *Journal of Molecular Neuroscience*, vol. 46, pp. 167–176, 2012.

[20] G. Burnstock, "Physiology and pathophysiology of purinergic neurotransmission," *Physiological Reviews*, vol. 87, pp. 659–797, 2007.

[21] A. M. Schrader, J. M. Camden, and G. A. Weisman, "P2y2 nucleotide receptor up-regulation in submandibular gland cells from the nod.B10 mouse model of Sjögren's syndrome," *Archives of Oral Biology*, vol. 50, pp. 533–540, 2005.

[22] S. J. Charlton, C. A. Brown, G. A. Weisman, J. T. Turner, L. Erb, and M. R. Boarder, "Ppads and suramin as antagonists at cloned p2y-and p2u-purinoceptors," *British Journal of Pharmacology*, vol. 118, pp. 704–710, 1996.

[23] P. Bodin and G. Burnstock, "Purinergic signalling: Atp release," *Neurochemical Research*, vol. 26, no. 8/9, pp. 959–969, 2001.

[24] Y. Fukumoto, K. F. Tanaka, B. Parajuli et al., "Neuroprotective effects of microglial P2Y1receptors against ischemic neuronal injury," *Journal of Cerebral Blood Flow and Metabolism*, vol. 39, no. 11, pp. 2144–2156, 2019.

[25] S. Silvestro, P. Bramanti, O. Trubiani, and E. Mazzon, "Stem cells therapy for spinal cord injury: an overview of clinical trials," *International Journal of Molecular Sciences*, vol. 21, no. 2, p. 659, 2020.

[26] M. Asheuer, F. Pflumio, S. Benhamida et al., "Human cd34+ cells differentiate into microglia and express recombinant therapeutic protein," *Proceedings of the National Academy of Sciences of the United States of America*, vol. 101, pp. 3557–3562, 2004.

[27] R. Ladeby, M. Wirenfeldt, I. Dalmau et al., "Proliferating resident microglia express the stem cell antigen cd34 in response to acute neural injury," *Glia*, vol. 50, pp. 121–131, 2005.

[28] J. Jang, S. Lee, H. J. Oh et al., "Fluorescence imaging of in vivo mir-124a-induced neurogenesis of neuronal progenitor cells using neuron-specific reporters," *EJNMMI Research*, vol. 6, no. 1, pp. 016–0190, 2016.

[29] O. S. Manoukian, S. Stratton, M. R. Arul et al., "Polymeric ionically conductive composite matrices and electrical stimulation strategies for nerve regeneration: in vitro characterization," *Journal of Biomedical Materials Research. Part B, Applied Biomaterials*, vol. 107, pp. 1792–1805, 2019.

[30] S. S. Schultz and P. A. Lucas, "Human stem cells isolated from adult skeletal muscle differentiate into neural phenotypes," *Journal of Neuroscience Methods*, vol. 152, pp. 144–155, 2006.

[31] S. Zhang, M. Wu, C. Peng, G. Zhao, and R. Gu, "Gfap expression in injured astrocytes in rats," *Experimental and Therapeutic Medicine*, vol. 14, pp. 1905–1908, 2017.

[32] M. Brenner, "Role of GFAP in CNS injuries," *Neuroscience Letters*, vol. 565, pp. 7–13, 2014.

Hindawi
Neural Plasticity
Volume 2022, Article ID 7605046, 7 pages
https://doi.org/10.1155/2022/7605046

Research Article

Temporal Interference (TI) Stimulation Boosts Functional Connectivity in Human Motor Cortex: A Comparison Study with Transcranial Direct Current Stimulation (tDCS)

Zhiqiang Zhu,[1,2] Yiwu Xiong,[1] Yun Chen,[1] Yong Jiang,[1] Zhenyu Qian,[1] Jianqiang Lu,[1] Yu Liu,[1] and Jie Zhuang[1,3]

[1]*The Research Group of "The Effects of Non-Invasive Deep Brain Stimulation on Improving Human Performance and Its Mechanisms", Shanghai University of Sport, Shanghai 200438, China*
[2]*Faculty of Education of Shenzhen University, Shenzhen 518061, China*
[3]*School of Psychology, Shanghai University of Sport, Shanghai 200438, China*

Correspondence should be addressed to Yu Liu; yuliu@sus.edu.cn and Jie Zhuang; jzhuang255@163.com

Received 25 June 2021; Revised 30 November 2021; Accepted 14 December 2021; Published 31 January 2022

Academic Editor: Mou-Xiong Zheng

Temporal interference (TI) could stimulate deep motor cortex and induce movement without affecting the overlying cortex in previous mouse studies. However, there is still lack of evidence on potential TI effects in human studies. To fill this gap, we collected resting-state functional magnetic resonance imaging data on 40 healthy young participants both before and during TI stimulation on the left primary motor cortex (M1). We also chose a widely used simulation approach (tDCS) as a baseline condition. In the stimulation session, participants were randomly allocated to 2 mA TI or tDCS for 20 minutes. We used a seed-based whole brain correlation analysis method to quantify the strength of functional connectivity among different brain regions. Our results showed that both TI and tDCS significantly boosted functional connection strength between M1 and secondary motor cortex (premotor cortex and supplementary motor cortex). This is the first time to demonstrate substantial stimulation effect of TI in the human brain.

1. Introduction

The neuromodulation effects of noninvasive brain stimulation technologies on neurorehabilitation have gained great attention in scientific and clinical communities. It has a significant effect and is widely used to optimize motor control, motor learning, and treat a motor-related neuropsychiatric disorder, such as Parkinson's disease and poststroke rehabilitation [1–5]. The prevalent noninvasive brain stimulation approaches include transcranial magnet stimulation (TMS), transcranial direct current stimulation (tDCS), and transcranial alternating current stimulation (tACS). For example, tDCS has been considered as a promising ergogenic potential method in neuromodulation [6–8]. A brand-new noninvasive neural stimulation method—temporal interference (TI)—was developed recently, but its practical effects still need to be tested widely and intensively before it is broadly accepted. To this end, here, we aim to investigate whether TI is effective in boosting the human motor cortex, compared with tDCS.

Previous studies have demonstrated that tDCS produced effective neuromodulation by applying a low-intensity current (1-2 mA) delivered to the scalp. The neuromodulation effects are highly polarity-dependent. Anodal tDCS functions increase cortical excitability in the primary motor cortex (M1), whereas cathodal tDCS leads to decreasing cortical excitability by alternating the resting membrane potential [9, 10]. In line with the modulation in cortical excitability, anodal tDCS stimulating M1 improved motor behavior in the contralateral hand, while cathodal tDCS stimulating M1 resulted in contralateral hand functionally ineffective [3, 11].

The functional magnetic resonance imagining (fMRI) technique provides critical insight in exploring the mechanisms of tDCS effects on brain function [11, 12]. Recent

studies showed that tDCS increased resting-state functional connectivity during and post stimulation [13, 14]. Mondino and his colleagues [13] compared the neuromodulation effect of tDCS with the sham condition and found that tDCS increased resting-state functional connectivity between the left dorsolateral prefrontal cortex and bilateral parietal region. Moreover, Polania et al. [14] applied anodal tDCS to each individual's left M1 and found that the functional connectivity was enhanced between the left somatomotor cortex (SM1) and premotor and superior parietal region. These functional connectivity changes induced by tDCS might be related to neuroplastic alteration of relevant brain regions. In addition, the study of Sehm et al. [11] suggested that tDCS might modulate both intracortical and interhemispheric connections with M1 using a seed-based analysis. However, the current tDCS techniques are limited to low-intensity current by the safety guideline [15, 16] and cannot focally stimulate deeper brain regions.

To solve this issue, Grossman and his colleagues discovered a new noninvasive neural stimulation strategy, called "temporal interference (TI)." It could achieve much deeper and focal stimulation without affecting adjacent brain regions. This strategy applied two channels with slightly different high-frequency alternating currents. The frequency of single channel is too high to activate neural firing, but the frequency of the envelope electrical field generated by two channels is lower enough to focally activate neural activity. For instance, Grossman and colleagues applied 2 kHz and 2.01 kHz stimuli on the motor cortex of mice. The two channels generated a low-frequency (10 Hz) envelope electrical field which triggered neural firing and the movement of mice's forepaws and whiskers [15–17]. However, to our knowledge, there is still a lack of research publication about TI study on healthy human adults now. To fill this gap, we design this study to compare the neuromodulation effects of TI and tDCS in stimulating M1 in healthy adults and analyze the online effects of TI and tDCS on brain functional connectivity in the whole brain scale. The reason for choosing tDCS as a baseline is that tDCS is a reliable and robust stimulation technique that has been widely reported in the literature. We hypothesize that TI and tDCS stimulus will both enhance functional connectivity between the M1 and related brain regions.

2. Methods

2.1. Participants. Forty healthy young adults (31 males, age: 25.97 ± 3.53 years; 9 females, age: 24.11 ± 0.93 years) were recruited in this study. The inclusion criteria are as follows: (1) all participants should be right-handed (Edinburgh Handedness Inventory; Oldfield, 1971) (2) age: 18-35 years old; and (3) no history of neurological, psychological disorder, or motor dysfunction. The exclusion criteria are as follows: (1) individuals who have contraindications with respect to the use of tDCS and (2) participants who had metallic implants/implanted electric devices were excluded. All participants have been informed of all aspects of this experiment and provided informed consent before participation. The experimental procedures were approved by the institutional review board of shanghai university of sport (102772020RT116). The Registered Clinical Trial number of this study is ChiCTR2100052866.

2.2. Experimental Protocol. This study is a randomized crossover, double-blinded design. Each participant completed two visits to accepted different types of stimulation (TI, tDCS). The time interval between the two tests was at least 48 hours. Before each test started, the stimulation target brain area of each participant was tested and located via TMS using software "STIMWEAR," which was located in FDI's "Hot Point." Afterward, each participant received two functional scanning sessions, one before stimulation and one during stimulation, in each visit. In the second scanning session, participants received one type of stimulation randomly. A structural scanning session was also performed in the first visit (see Figure 1).

2.3. TI. "Hot Point" is the target area of TI stimulation. The representational field of right FDI was determined by a single-pulse interferential TMS stimulator (Soterix medical, New Jersey, USA). Based on the center of "hot point," two channels of high-frequency alternating current were placed in parallel to the connection line between the eyebrow center and occipital tuberosity. We made a TI stimulation cap on which electrodes could be fixed. As shown in Figure 2, "O" is the position of "hot point". A1, A2, B1, and B2 are the position of 4 electrodes, and the distance of four two-point pairs (A1-A2, A1-B1, B1-B2, A2-B2) is 4 cm. A1-A2 is one channel, and its frequency is 2000 Hz. B1-B2 is another channel, and its frequency is 2020 Hz. The frequency difference between these two channels is 20 Hz (2020 Hz-2000 Hz). The current intensity is 2 mA in each channel, and the total current intensity is 4 mA. The stimulation duration is 20 min, with two short periods of 30s ramp-up and ramp-down stimulation.

2.4. tDCS. The "STIMWEAR" software provided a neuroelectric's online target editor. In this editor, we set the stimulation target area as the brain location of the right FDI, with the maximum stimulation intensity of 2 mA and the maximum stimulation electrode number of 4. The simulated result included each electrode position (10-20 electroencephalogram system) and intensity (C3: 2000 uA, P3: -774 uA, T7: -684 uA, Cz: -542 uA) (Figures 3 and 4).

The stimulator was MR-compatible DC-STIMULATOR PLUS (neuroCnn, Ilmenau, Germany). Further details of the stimulator setting can be found in the study of Esmaeilpouret al. [18]. Four rectangles MRI compatible rubber electrodes ($1.5\,\text{cm} \times 2\,\text{cm}$) were used to deliver continuously direct current. The resistance of each rubber electrode was below $30\,\Omega$. The stimulation duration at goal intensity was 20 min. The ramp-up and ramp-down duration were both 30s.

2.5. MRI Acquisition and Statistical Analysis. All participants were scanned in a 3.0 Tesla Siemens MAGNETOM Prisma whole-body MRI scanner equipped with a 64-channel head coil for radio frequency (RF) reception (Siemens, Munich, Germany). Two sessions of functional images were collected

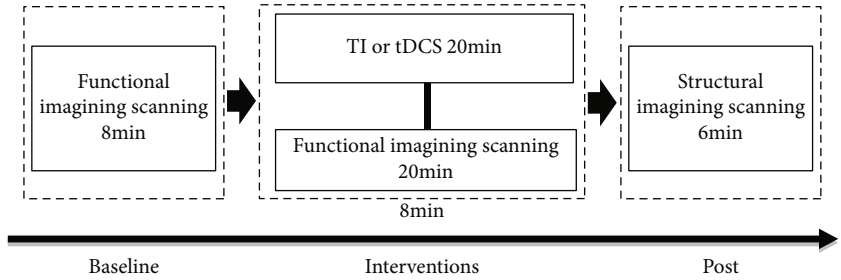

Figure 1: Experimental protocol. The experiment consists of baseline, intervention, and postphase. In the baseline, participants attended an 8 min functional scanning session. In the interventions phase, participants attended 20 min TI or tDCS stimulation and functional scanning simultaneously. In the post phase, participants were scanned 6 min for structural images.

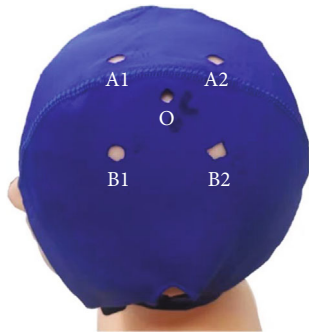

Figure 2: TI stimulation cap. O is the position of hot point. A1-A2 are the positions of two electrodes of one tACS channel in which the peak to peak stimulation intensity is 2 mA, and the frequency is 2000 Hz. B1-B2 are the positions of two electrodes of another tACS channel in which the peak to peak stimulation intensity is 2 mA, and the frequency is 2020 Hz. The distance between the position centers of every two electrodes is 4 cm.

during resting state, in which all participants were asked to stare at a figure of a black cross on a white screen while relaxing, not to fall asleep, and not to think anything particularly difficult, such as mathematically calculation. The blood oxygen level-dependent (BOLD) was acquired using a gradient-echo EPI sequence (TR = 1000 ms; TE = 30 ms; FOV = 240 × 240 mm^2; flip angle = 100°; voxel size = 3 × 3 × 3 mm^3; 48 contiguous oblique axial slices, parallel to the AC-PC line, simultaneous multislice acquisition, three runs function scanning). The first scanning session was composed of the acquisition of a time series of 488 brain volumes, which last for 8 minutes and 8 seconds. The second session consisted of the acquisition of a time series of 1268 brain volumes, which last for 21 minutes and 8 seconds. 8 initial RF excitations were performed to achieve steady state equilibrium and were subsequently removed for each session. In the second session, the initial 30 and last 30 brain volumes were also disregarded to account for the ramp-up and ramp-down period. These factors resulted in 480 and 1200brain volumes for the first and second session, respectively, for each participant. High-resolution structural images were acquired using a 3D MP2RAGE (magnetization-prepared 2 rapid acquisition gradient echoes) pulse sequence (TR = 3130 ms; TE = 2.98 ms; flip angle = 12°; FOV = 256 × 256 mm^2; voxel size = 1 × 1 × 1mm^3; 166 contiguous slices).

We performed preprocessing and statistical analyses on these imaging data in DPABI (http://rfmri.org/DPABI) and SPM12 (Institute of Cognitive Neurology, London, UK. http://www.fil.ion.ucl.ac.uk), under MATLAB (Mathworks Inc., Natick, MA, USA). Default settings were chosen in the stages of early steps including preprocessing. We chose the left M1 as a seed region, extracted the time series of this seed region in each session and for each participant, then correlated with all voxels across the whole brain, and generated a correlational map for each condition. We further performed between conditions and between-group comparisons.

Activations were thresholded at $p < 0.001$, voxel-level uncorrected, and significant clusters were identified only when they also survived a $p < 0.05$, cluster-level correction for multiple comparisons, and all other clusters were filtered out. Coordinates of significant clusters peaks and subpeaks in each effect were listed in the Tables in standard MNI space. Regions were identified using the AAL atlas [19] and Brodmann templates as implemented in MRIcron (http://www.MRicro.com/MRicron).

3. Results

A two-way repeated ANOVA (2 × 2) was used to investigate the main effects of stimulation types (TI, tDCS), stimulation phases (baseline, online stimulation), and their interaction in the brain. There was no significant main effect of stimulation types, indicating that TI and tDCS stimulation did not produce any significant difference. A significant main effect of stimulation phase was found mainly in the left precentral, paracentral lobule, SFG, SMA, SMFG, MFG, MCG (BA 4, 6, 8, 9, 32, 46), precentral, postcentral, paracentral lobule, and SPL (BA 2, 3, 4, 6, 7, 40) (Table 1 and Figure 5). TI and tDCS stimulation generated greater activation in these brain regions than the baseline. There was no significant interaction between stimulation types and phases, indicating that the TI stimulation effect was equivalent to the tDCS stimulation effect.

4. Discussion

To our knowledge, this is the first study to compare online effects of TI and tDCS using a seed-based whole brain functional connectivity method. Our results demonstrated that

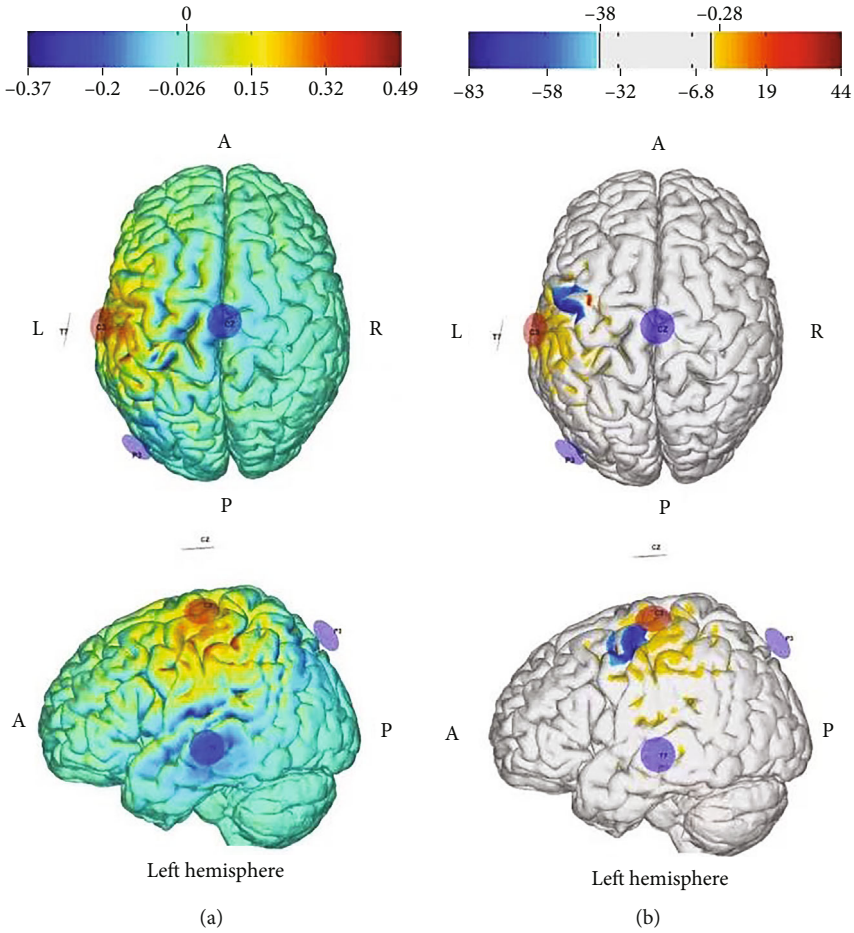

Figure 3: Simulated electrical field. L: left; A: anterior. The total stimulation intensity is 2 mA. The position of anodal electrode is at C3. The positions of cathodal electrodes are at CZ, T7, and P3. (a) is the normal electric field component in target region (v/m) for grey matter. (b) is the error with respect to no intervention (mv^2/m^2) for grey matter.

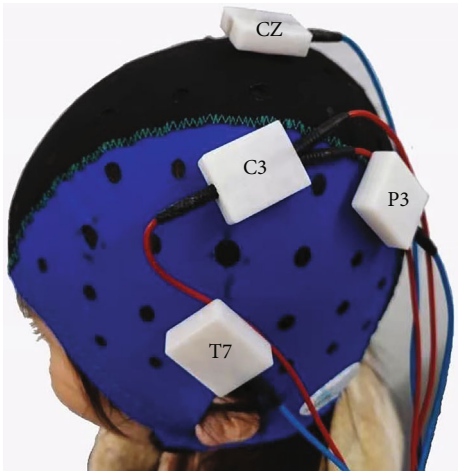

Figure 4: tDCS stimulation montage. Three anodal electrodes were connected to C3 silicone, and each cathodal electrode was connected to CZ, T7, and P3 silicone.

no difference existed between TI and tDCS in functional connectivity effects. Both TI and tDCS stimulation could boost functional connectivity strength between the seed M1 region and corresponding regions, and there is no difference between these two approaches.

4.1. Effects of TI and tDCS. Between-group analysis, our results observed that no difference between tDCS and TI on seed-based functional connectivity. This finding was also demonstrated within-group analyses. Comparing to the prestimulation, online TI and tDCS both increase the ipsilateral functional connectivity in MFG, MSFG, SFG, and SMA. To our knowledge, there is no record of TI effects in healthy human beings. Previous studies investigated the tDCS effect on resting-state functional connectivity, and their results are similar to our results to some extent. In the study of Sehm et al. [11], they found that tDCS induced online and afterward effects on seed-based functional connectivity, and after the termination of the intervention, and induced an increase in functional connectivity within ipsilateral hemispheric. Moreover, the results of Polania's study [14] showed that tDCS induced functional connectivity increased in ipsilateral M1, premotor cortex, and sensorimotor area. However, in

Table 1: Activated brain regions in the functional connectivity analysis.

Contrast	Cluster regions	p	Cluster size	Peak Z value	Peak MNI coordinates		
					X	Y	Z
Main effect of condition	L: precentral, paracentral lobule, SFG, SMA, SMFG, MFG, MCG	<0.001	1078	4.4	-33	-1	53
	L: precentral, postcentral, paracentral lobule, SPL	<0.001	218	4.13	-27	-37	65

L: left; MCG: middle cingulate gyrus; MFG: middle frontal gyrus; SMA: supplementary motor area; SFG: superior frontal gyrus; SMFG: superior medial frontal gyrus; SPL: superior parietal lobule.

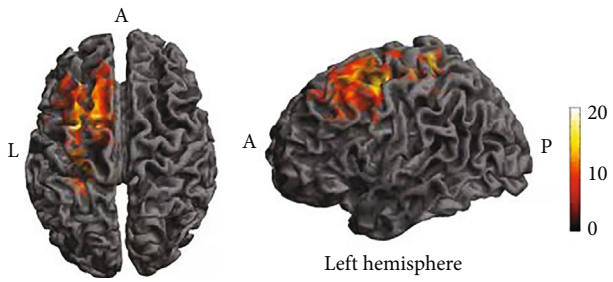

Figure 5: Activated brain regions in the main effect of condition. L: left; A: anterior. The color bar shows the F value.

contrast to Polania's study, the functional connectivity increased area in our study only lie in MFG, MSFG, SFG, and SMA, which are involved in motor planning and motor learning. This difference may cause by the stimulation montage that we choose. Based on the current field simulation, we used multifocal stimulation montage to optimize the stimulation effects. But in Polania's study, they used electrodes on a 5×7 cm area, which covered many brain regions, to deliver current to the scalp. A previous study showed that the size of the electrodes is a factor in modulating the stimulation effect [20]. In the study of Ho [21], they found that stimulated with a larger size induced a cumulative enhance in cortical excitability, but not a smaller electrode.

The tDCS and TI induced seed-based functional connectivity increased with MFG, MSFG, SFG, and SMA areas. Those areas may be related to motor function. In the studyof Rosse [22], they demonstrated that the functional connectivity between premotor cortex and M1 has a negative relationship with resting motor threshold in M1. The lower resting motor threshold in M1 means higher cortical excitability. Thus, the study of Rosse et al. provided support to the notion that the functional connectivity between premotor cortex and M1 has a positive relationship with cortical excitability. It means that the increasing cortical excitability would enhance human performance [23–26]. Cogiamanian's study reported that anodal tDCS improve muscle endurance by improving cortical excitability [27]. Therefore, TI and tDCS induce the modulation coupling of the functional network, which may enhance human performance.

4.2. Comparing the Neurophysiological Mechanism TI and tDCS. Although TI and tDCS online effects are similar, the underlying mechanisms of these two types of stimulation may be different. In tDCS, anodal tDCS may restrain the inhibitory synaptic to increase the resting-state functional connectivity. Previous studies showed that anodal tDCS decreased the gamma-aminobutyric acid (GABA) concentration [28–30]. The GABA concentration was negatively correlated with the strength of resting-state functional connectivity within the motor network [28, 29]. In the study of Bachtiar et al. [28] and Stagg et al. [29], they both demonstrated that the anodal tDCS decreased GABA concentration and increases functional connectivity in the stimulated motor cortex. In the TI, it may modulate the brain oscillation to change the resting-state functional connectivity. Grossman's study [17] showed that TI impacts mice's brain function via a temporal interference field, which was produced by a high-frequency field with slightly different frequencies. The effect of a lower frequency interference field is similar to lower frequency transcranial alternating current stimulation, which mainly depends on the current frequency [31]. In previous studies, 20 Hz-tACS stimulation was applied over M1 that modulation the brain oscillation to increase the excitability of M1 and optimize the participant's performance [31–33]. In our study, we used an interference frequency of 20 Hz (2020 Hz minus 2020 Hz). 20 Hz-TI may change the brain oscillation and increase the resting-state functional connectivity between M1 and secondary motor cortex to improve human performance. Therefore, TI and tDCS may modulate brain function via different neurophysiology mechanisms.

4.3. Limitation. Although we carefully designed the study, there are still many caveats. Overcoming those caveats may be helpful for future studies. (1) The stimulation intensity is too low to induce sufficient effects. TI applied high-frequency current intensity attenuate rapidly in human deep tissue [17]. In our study, the stimulation intensity is 2 mA. The intensity is not high enough to induce the interaction effect of intervention by time. Therefore, in the future study, it can apply much higher current intensity within the ethical limits. (2) It is a lack of a tACS group. TI may impact brain function by modulating brain oscillation, which is similar to tACS. Adding a tACS group may be better to compare the effects and better understand the neurophysiological mechanisms of TI, tDCS, and tACS. (3) In the current study, we did not provide an effective method in simulating the charge density of TI. In the future, TI electric field could be simulated to confirm whether the charge density is equal in different stimulation montages.(4) Forty-eight hours may not be long enough to wash out the posteffect, and longer time intervals are recommended for future studies. (5) The current study did not investigate the long-term effect of TI and tDCS. It could be examined in the future study.

5. Conclusion

TI and tDCS both increased resting-state functional connectivity between M1 and secondary motor cortex (premotor cortex and supplementary motor cortex), and the enhancement of functional connectivity may be related to motor functions.

Data Availability

All experimental data, together with relevant analysis scripts and files, are available upon request from the corresponding author (e-mail: jzhuang255@163.com).

Ethical Approval

This research has been approved by the Shanghai University of Sport Institutional Review Board.

Conflicts of Interest

The authors declare that they have no conflicts of interest.

Authors' Contributions

Zhiqiang Zhu and Yiwu Xiong contributed equally. All authors have reviewed the contents of the manuscript, approved its contents, and validated the accuracy of the data.

Acknowledgments

This study was funded by the National Natural Science Foundation of China (11932013, 31971102), National Key Research and Development Program of China (2018YFF0300500), and the Program for Professor of Special Appointment (Eastern Scholar) at Shanghai Institutions of Higher Learning (No. TP2018056).

References

[1] P. L. Chen, A. Stenling, and L. Machado, "Evidence transcranial direct current stimulation can improve saccadic eye movement control in older adults," *Vision*, vol. 2, no. 4, p. 42, 2018.

[2] S. Furuya, M. Klaus, M. A. Nitsche, W. Paulus, and E. Altenmüller, "Ceiling effects prevent further improvement of transcranial stimulation in skilled musicians," *The Journal of Neuroscience*, vol. 34, no. 41, pp. 13834–13839, 2014.

[3] J. Lee, Y. Jin, and B. Yoon, "Bilateral transcranial direct stimulation over the primary motor cortex alters motor modularity of multiple muscles," *Journal of Motor Behavior*, vol. 52, no. 4, pp. 474–488, 2020.

[4] C. D. Solomons and V. Shanmugasundaram, "A review of transcranial electrical stimulation methods in stroke rehabilitation," *Neurology India*, vol. 67, no. 2, pp. 417–423, 2019.

[5] J. B. Pereira, C. Junqué, D. Bartrés-Faz et al., "Modulation of verbal fluency networks by transcranial direct current stimulation (tDCS) in Parkinson's disease," *Brain Stimulation*, vol. 6, no. 1, pp. 16–24, 2013.

[6] K. S. Chen and R. Chen, "Invasive and noninvasive brain stimulation in parkinson's disease: clinical effects and future perspectives," *Clinical Pharmacology and Therapeutics*, vol. 106, no. 4, pp. 763–775, 2019.

[7] K. Dunlop, C. A. Hanlon, and J. Downar, "Noninvasive brain stimulation treatments for addiction and major depression," *Annals of the New York Academy of Sciences*, vol. 1394, no. 1, pp. 31–54, 2017.

[8] M. A. Halko, M. C. Eldaief, and A. Pascual-Leone, "Noninvasive brain stimulation in the study of the human visual system," *Journal of Glaucoma*, vol. 22, pp. S39–S41, 2013.

[9] V. Rawji, M. Ciocca, A. Zacharia et al., "tDCS changes in motor excitability are specific to orientation of current flow," *Brain Stimulation*, vol. 11, no. 2, pp. 289–298, 2018.

[10] A. Jamil, G. Batsikadze, H. I. Kuo et al., "Current intensity- and polarity-specific online and aftereffects of transcranial direct current stimulation: an fMRI study," *Human Brain Mapping*, vol. 41, no. 6, pp. 1644–1666, 2020.

[11] B. Sehm, J. Kipping, A. Schäfer, A. Villringer, and P. Ragert, "A comparison between uni- and bilateral tDCS effects on functional connectivity of the human motor cortex," *Frontiers in Human Neuroscience*, vol. 7, p. 183, 2013.

[12] C. M. Cummiford, T. D. Nascimento, B. R. Foerster et al., "Changes in resting state functional connectivity after repetitive transcranial direct current stimulation applied to motor cortex in fibromyalgia patients," *Arthritis Research & Therapy*, vol. 18, no. 1, 2016.

[13] M. Mondino, S. Ghumman, C. Gane, E. Renauld, K. Whittingstall, and S. Fecteau, "Effects of transcranial stimulation with direct and alternating current on resting-state functional connectivity: an exploratory study simultaneously combining stimulation and multiband functional magnetic resonance imaging," *Frontiers in Human Neuroscience*, vol. 13, 2020.

[14] R. Polanía, W. Paulus, A. Antal, and M. A. Nitsche, "Introducing graph theory to track for neuroplastic alterations in the resting human brain: a transcranial direct current stimulation study," *NeuroImage*, vol. 54, no. 3, pp. 2287–2296, 2011.

[15] N. Grossman, "Modulation without surgical intervention," *Science*, vol. 361, no. 6401, pp. 461-462, 2018.

[16] A. M. Lozano, "Waving hello to noninvasive deep-brain stimulation," *The New England Journal of Medicine*, vol. 377, no. 11, pp. 1096–1098, 2017.

[17] N. Grossman, D. Bono, N. Dedic et al., "Noninvasive deep brain stimulation via temporally interfering electric fields," *Cell*, vol. 169, no. 6, pp. 1029–41.e16, 2017.

[18] Z. Esmaeilpour, A. D. Shereen, P. Ghobadi-Azbari et al., "Methodology for tDCS integration with fMRI," *Human Brain Mapping*, vol. 41, no. 7, pp. 1950–1967, 2020.

[19] N. Tzourio-Mazoyer, B. Landeau, D. Papathanassiou et al., "Automated anatomical labeling of activations in SPM using a macroscopic anatomical parcellation of the MNI MRI single-subject brain," *NeuroImage*, vol. 15, no. 1, pp. 273–289, 2002.

[20] M. M. Chan and Y. M. Han, "The effect of transcranial direct current stimulation in changing resting-state functional connectivity in patients with neurological disorders: A Systematic review," *Journal of central nervous system disease*, vol. 12, 2020.

[21] K. A. Ho, J. L. Taylor, T. Chew et al., "The effect of transcranial direct current stimulation (tDCS) electrode size and current intensity on motor cortical excitability: evidence from single and repeated sessions," *Brain Stimulation*, vol. 9, no. 1, pp. 1–7, 2016.

[22] C. Rosso, V. Perlbarg, R. Valabregue et al., "Anatomical and functional correlates of cortical motor threshold of the dominant hand," *Brain Stimulation*, vol. 10, no. 5, pp. 952–958, 2017.

[23] D. J. Kidgell, A. M. Goodwill, A. K. Frazer, and R. M. Daly, "Induction of cortical plasticity and improved motor performance following unilateral and bilateral transcranial direct current stimulation of the primary motor cortex," *BMC Neuroscience*, vol. 14, no. 1, 2013.

[24] C. J. Stagg, A. Antal, and M. A. Nitsche, "Physiology of transcranial direct current stimulation," *The Journal of ECT*, vol. 34, no. 3, pp. 144–152, 2018.

[25] T. Yamaguchi, K. Moriya, S. Tanabe, K. Kondo, Y. Otaka, and S. Tanaka, "Transcranial direct-current stimulation combined with attention increases cortical excitability and improves motor learning in healthy volunteers," *Journal of Neuroengineering and Rehabilitation*, vol. 17, no. 1, p. 23, 2020.

[26] S. Bashir, D. Aisha, A. Hamza, F. al-Hussain, and W. K. Yoo, "Effects of transcranial direct current stimulation on cortex modulation by stimulation of the primary motor cortex and parietal cortex in humans," *The International Journal of Neuroscience*, vol. 131, no. 11, pp. 1107–1114, 2021.

[27] F. Cogiamanian, S. Marceglia, G. Ardolino, S. Barbieri, and A. Priori, "Improved isometric force endurance after transcranial direct current stimulation over the human motor cortical areas," *The European Journal of Neuroscience*, vol. 26, no. 1, pp. 242–249, 2007.

[28] V. Bachtiar, J. Near, H. Johansen-Berg, and C. J. Stagg, "Modulation of GABA and resting state functional connectivity by transcranial direct current stimulation," *eLife*, vol. 4, 2015.

[29] C. J. Stagg, V. Bachtiar, U. Amadi et al., "Local GABA concentration is related to network-level resting functional connectivity," *eLife*, vol. 3, 2014.

[30] C. J. Stagg, V. Bachtiar, and H. Johansen-Berg, "The role of GABA in human motor learning," *Current Biology: CB*, vol. 21, no. 6, pp. 480–484, 2011.

[31] L. Schilberg, T. Engelen, S. ten Oever et al., "Phase of beta-frequency tACS over primary motor cortex modulates corticospinal excitability," *Cortex*, vol. 103, pp. 142–152, 2018.

[32] V. Krause, A. Meier, L. Dinkelbach, and B. Pollok, "Beta band transcranial alternating (tACS) and direct current stimulation (tDCS) applied after initial learning facilitate retrieval of a motor sequence," *Frontiers in Behavioral Neuroscience*, vol. 10, p. 4, 2016.

[33] M. Wischnewski, M. Engelhardt, M. A. Salehinejad, D. J. L. G. Schutter, M. . F. Kuo, and M. A. Nitsche, "NMDA receptor-mediated motor cortex plasticity after 20 Hz transcranial alternating current stimulation," *Cerebral cortex*, vol. 29, no. 7, pp. 2924–2931, 2019.

Hindawi
Neural Plasticity
Volume 2022, Article ID 1588090, 10 pages
https://doi.org/10.1155/2022/1588090

Research Article

Proprioceptive Training with Visual Feedback Improves Upper Limb Function in Stroke Patients: A Pilot Study

Jieying He,[1,2] **Chong Li**,[1,2] **Jiali Lin**,[1,2] **Beibei Shu**,[3] **Bin Ye**,[4] **Jianhui Wang**,[5] **Yifang Lin**,[1,2] **and Jie Jia**[1,2]

[1]*Department of Rehabilitation Medicine, Huashan Hospital, Fudan University, Shanghai 200040, China*
[2]*National Clinical Research Center for Aging and Medicine, Huashan Hospital, Fudan University, Shanghai 200040, China*
[3]*Department of Rehabilitation Medicine, Shanghai Jing'an District Central Hospital, Shanghai 200040, China*
[4]*Department of Rehabilitation Medicine, The Shanghai Third Rehabilitation Hospital, Shanghai 200040, China*
[5]*Department of Rehabilitation Medicine, Nanshi Hospital Affiliated to Henan University, Nanyang 473000, China*

Correspondence should be addressed to Jie Jia; shannonjj@126.com

Received 22 June 2021; Revised 30 October 2021; Accepted 9 December 2021; Published 15 January 2022

Academic Editor: Jia-Jia Wu

Proprioceptive deficit is one of the common sensory impairments following stroke and has a negative impact on motor performance. However, evidence-based training procedures and cost-efficient training setups for patients with poststroke are still limited. We compared the effects of proprioceptive training versus nonspecific sensory stimulation on upper limb proprioception and motor function rehabilitation. In this multicenter, single-blind, randomized controlled trial, 40 participants with poststroke hemiparesis were enrolled from 3 hospitals in China. Participants were assigned randomly to receive proprioceptive training involving passive and active movements with visual feedback (proprioceptive training group [PG]; $n = 20$) or nonspecific sensory stimulation (control group [CG]; $n = 20$) 20 times in four weeks. Each session lasted 30 minutes. A clinical assessor blinded to group assignment evaluated patients before and after the intervention. The primary outcome was the change in the motor subscale of the Fugl-Meyer assessment for upper extremity (FMA-UE-M). Secondary outcomes were changes in box and block test (BBT), thumb localization test (TLT), the sensory subscale of the Fugl-Meyer assessment for upper extremity (FMA-UE-S), and Barthel Index (BI). The results showed that the mean change scores of FMA-UE were significantly greater in the PG than in the CG ($p = 0.010$ for FMA-UE-M, $p = 0.033$ for FMA-UE-S). The PG group was improved significantly in TLT ($p = 0.010$) and BBT ($p = 0.027$), while there was no significant improvement in TLT ($p = 0.083$) and BBT ($p = 0.107$) for the CG group. The results showed that proprioceptive training was effective in improving proprioception and motor function of the upper extremity in patients with poststroke. This trial is registered in the Chinese Clinical Trial Registry (ChiCTR2000037808).

1. Introduction

Proprioception derived from the skin, joints, tendons, and muscle spindle receptors allows us to perceive the movement and position of the body, sense of force, and heaviness [1]. During voluntary movement, the brain integrates the afferent proprioception signals to generate an efficient motor plan and adjust motor performance constantly based on proprioceptive feedback [2]. This process involves the somatosensory and motor systems, which are commonly impaired after stroke. Approximately 50% of patients experience upper limb proprioception deficits after stroke [3, 4], which negatively affect their motor control [5], functional learning [6], daily activity, and participation [7].

Intact proprioception is a critical element to facilitate functional recovery [6]. However, the effectiveness of sensory training for improving upper limb function remains controversial due to the limited studies and heterogeneity of interventions and measures [8–11]. There are limited studies focused on upper limb proprioceptive training in stroke patients compared with the number of studies focused on motor task interventions. Several studies have proposed active

multisensory retraining programs that focus on intensive and repetitive sensory tasks with feedback to improve sensory impairment after stroke [12–15]. These training methods generally involve proprioception and tactile discrimination [10]. Furthermore, recent studies have started to investigate the effectiveness of pure proprioception training on patients' outcomes with poststroke [16–18]. Öcal et al. [16] found improved upper extremity motor function in stroke patients after six weeks of proprioceptive training, including the rhythmic stabilization method and active joint position sense training. Vahdat et al. [17] designed robot training techniques with verbal feedback to train the joint position sense of patients with poststroke and demonstrated that it could induce functional connectivity changes in sensorimotor networks. While these studies have shown promising results, Chanubol et al. [19] compared the effectiveness of Perfetti's cognitive sensory motor training therapy, which mainly focuses on active joint position and movement training and tactile training, to conventional treatment. The result showed both groups of patients had significant improvement in hand and arm function, but no significant differences were found between groups.

The conflicting results from previous studies indicate the need for developing a more well-designed approach of proprioception training. Systematic reviews recommend that proprioceptive training involving passive and active movements with or without visual feedback might be more beneficial for improving sensorimotor function [20]. Currently, most proprioceptive interventions focused on active position sense and movement discrimination tasks, but rarely involved passive movement. In addition, most sensory trainings focused on increasing sensory input in the affected side, ignoring or restricting the use of the unaffected side [12, 17]. Recent studies indicate bimanual movements training improves the motor impairments of the affected upper limbs in stroke patients by facilitating cortical and neurologic plasticity [21, 22]. Bimanual movements training is a treatment approach that involves performing repeating tasks with both upper limbs of patients. The training protocol in our study combined passive movement with bimanual movements training. Therapists mobilized both hands of patients in a mirror-symmetrical pattern. Hypothetically, simultaneous passive movement of patients' hands might activate bilateral sensory and motor areas, which improve the sensory performance on the affected limb [23, 24].

Another limitation of previous studies is that they usually used eye masks or verbal instructions to control patients' vision, which was inconvenient for both researchers and patients and affected the efficiency of training [12, 16, 19]. The use of vision is essential in improving the function of the affected hand during training, which includes providing feedback and observing actions. Highly repetitive sensory tasks accompanied by visual feedback in every performance could enhance the training effects [25, 26]. In addition, observing movement or stimulation could modulate the activation of the sensory cortex [27, 28]. Further study is needed to optimize the visual feedback in upper limb proprioceptive training for clinical practice.

In the present study, we developed a proprioceptive training that includes passive and active movements and designed a visual-based sensory training setup to provide manipulable visual feedback. This setup enriches traditional sensory training by enhancing the fundamental role of repetitive visual feedback on sensory tasks. The study is aimed at investigating the feasibility and effectiveness of the proposed proprioception training on upper limb function in patients with poststroke.

2. Materials and Methods

2.1. Visual-Based Sensory Training Setup. The visual-based sensory training setup (700 mm × 800 mm × 1050 mm), also referred to as the perception window, used a smart window to provide manipulable visual feedback (Figure 1(a)). The smart window was fixed on the top of the setup at an angle of approximately 45° with the patient's hands placed naturally under the smart window. The smart window uses electrochromatic technology which allows changing between transparent and opaques modes by applying voltage. A footswitch, mounted under the setup, was used to switch between modes. When therapists depressed the pedal, the power was on and the smart window was transparent. Patients could observe their hands clearly through the window. When therapists removed their feet from the pedal, the power was cut off and the smart window was in opaque mode. At this point, the vision of patients was blocked by the window. During proprioception training, patients did not have to close their eyes but instead watched the smart window in front of them. Therapists conducted proprioceptive training with their hands on the table while modulating the smart window with their feet to control the patient's vision. Instead of giving verbal instructions ("eyes open" and "eyes closed") or using an eye mask, this setup made it easier to present visual feedback and facilitated patients in achieving a better sense of engagement.

2.2. Participants. Participants were recruited from three inpatient rehabilitation departments: Shanghai Jing'an District Central Hospital, Nanshi Hospital Affiliated to Henan University, and Shanghai Third Rehabilitation Hospital. The inclusion criteria were as follows: (1) first-time stroke at least three months ago, (2) age between 18 and 85 years, and (3) unilateral hemiparesis. Patients were excluded if they had one of the following: (1) history of other neurologic diseases and (2) severe visual impairments or aphasia per National Institute of Health Stroke Scale (NIHSS). All patients understood the procedure of the study and signed informed consent forms, which were approved by the ethical committee of Shanghai Jing'an District Central Hospital.

2.3. Sample Size. The sample size was calculated by GPower V.3.1.9 (University of Kiel, Kiel, Germany) software. Based on a previous study, a sample size of 18 patients per group was required to achieve 5% alpha and 90% power with the standardized effect size of 1.142 [12]. Considering the possible loss rate of 20%, 20 patients per group were needed to enroll in this study.

2.4. Experimental Design. A multicenter, single-blinded, prospective parallel-group controlled trial was completed in this

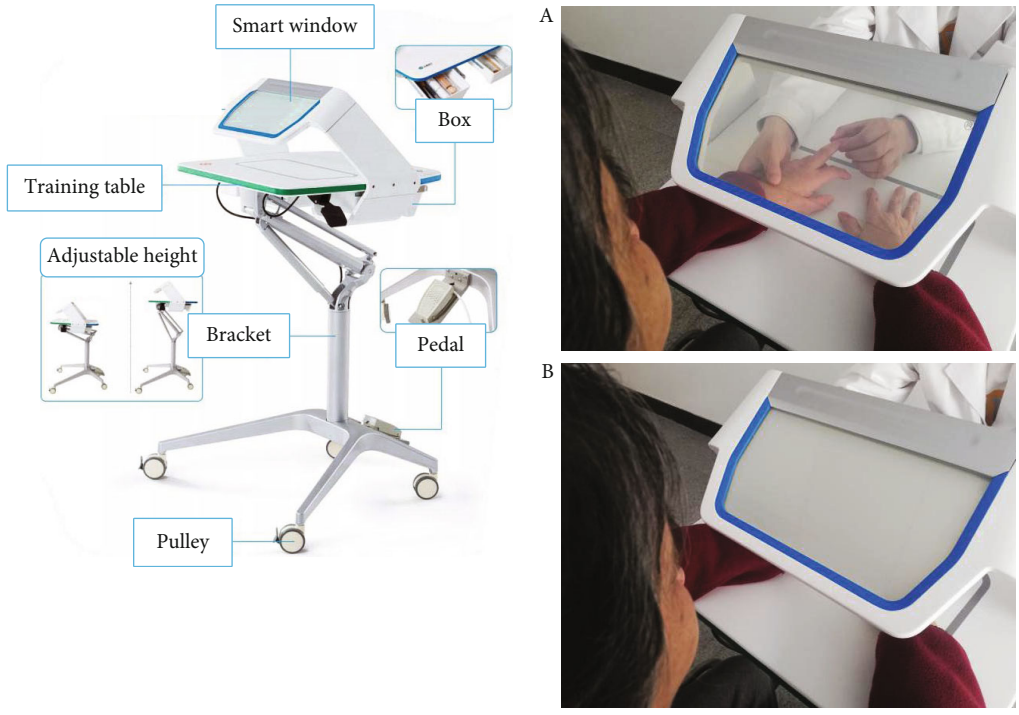

Figure 1: The visual-based sensory training setup. (a) The appearance and composition of the setup. (b) The smart window is in the transparent mode (A) and the opaque mode (B).

study. Before the start of recruitment, treating therapists received uniform training to ensure the consistency of intervention. An independent therapist blinded to the allocation conducted baseline and outcome assessments. All patients were stratified based on the motor subscale of the Fugl-Meyer assessment for upper extremity (FMA-UE-M) (cutoff score was 28) and sex. According to the computer-generated randomization sequence, participants were randomly assigned to the proprioceptive training group (PG) or the control group (CG). The researcher performed randomization by giving treating therapists a sealed opaque envelope when the participant was enrolled. Patients did not contact the allocation researcher, which ensured that the assessment therapist was blinded to the allocation sequence (Figure 2).

The patients assigned to PG received proprioceptive training conducted with the perception window. Before proprioceptive training, the therapist performed stretching and pressure at joints in the upper limb to help patients relax and reduce muscle tone. Both hands of patients were placed on the table. The therapist sat opposite to patients and adjusted the height of the table to ensure that patients could see their hands, wrist, and part of the forearm when the window was transparent. Depending on the patient's somatosensory function status, the therapist tailored individual training with the perception window. In the beginning, the therapist conducted flexion-extension in both upper limbs of patients with the same rhythm and instructed patients to observe and focus on the sensory input on both hands. When the patients reported their perception of the movement in both upper limbs, the therapist switched the smart window to opaque mode, still performing the same movements, and instructed patients to imagine that feeling. If patients could reliably perceive the movement of affected limbs, they were instructed to discriminate the direction of movement in fingers or wrist. Then, patients were instructed to answer which finger was moved or touched by the therapist with their vision occluded. During the training, patients were requested to relax and focus on the sensation that therapists applied with vision occluded. After each movement, the therapist asked patients what they felt and gave them visual feedback by switching the smart window into transparent mode. Based on the performance of the patient, the therapist was able to increase the difficulty of training stage-by-stage, i.e., decreasing the range of limb movement or moving two fingers simultaneously. In the last stage of training, therapists moved the unaffected limb of patients to different positions and requested patients to imitate the position of the unaffected limb with the affected limb. If patients could not match the position, therapists switched the smart window into transparent mode and repeated the training. At the end of the proprioceptive training, the therapist conducted some stretching and pressure in the upper limb again. Every patient in the PG received a 30-minute proprioceptive training per day, five days a week, for four weeks.

Patients allocated to the CG received a 30-minute control sensory intervention (5 times per week for four weeks) provided by experienced therapists. During the sensory control intervention, the smart window was maintained in transparent mode and patients could see their arms under

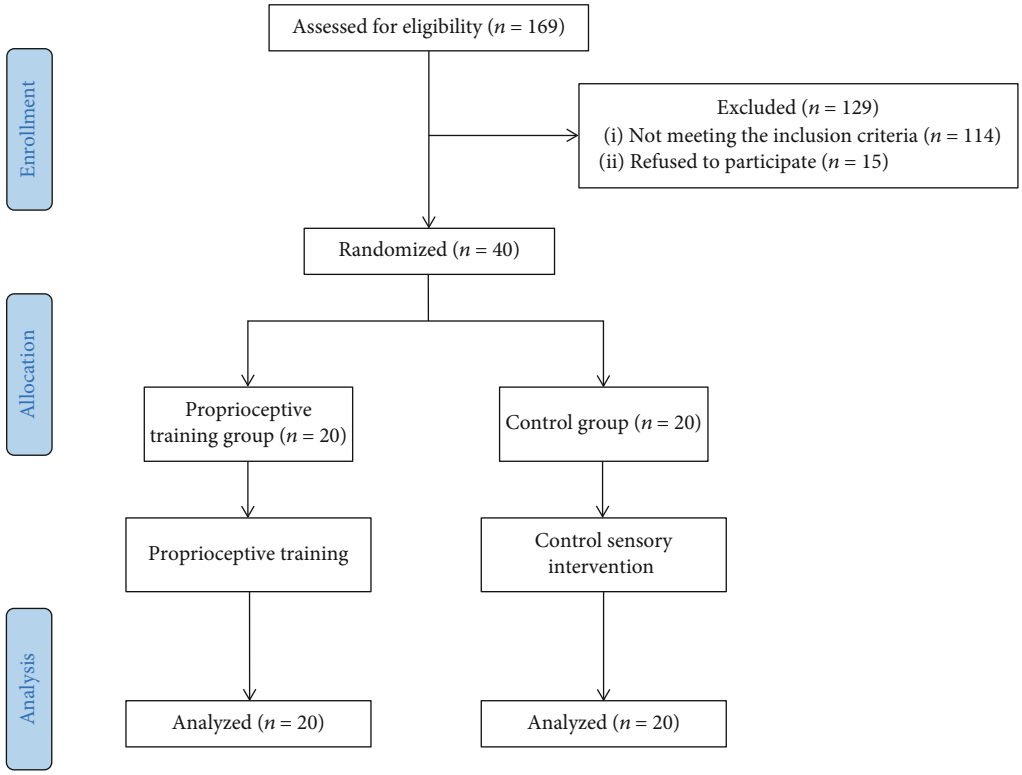

Figure 2: Flow chart of the participant selection and assignment in this study.

the window. The therapist conducted some pressure and passive movement in the upper limb of patients. In addition, patients were exposed to nonspecific sensory stimulation by grasping objects of different shapes, textures, weights, and sizes. During training, the therapist did not provide verbal instruction, and patients could open or close their eyes according to their wishes. Exposure was taken as a control intervention in a previous study since it was similar to activities of daily living and would not provide extra benefit in most patients with poststroke.

Both groups of patients underwent a 4-hour rehabilitation program (5 times per week for four weeks) provided by experienced therapists. This rehabilitation involved conventional physical and occupational therapy as deemed necessary to address the functional impairment of patients.

2.5. Outcome Measures. Patients were assessed at baseline and after four weeks of intervention. The primary outcome was the change in the motor subscale of the Fugl-Meyer assessment for upper extremity (FMA-UE-M), which is a highly reliable and valid assessment that measures motor recovery of the upper limb after stroke [29, 30]. It consists of 33 items, which can be divided into 4 subsections: shoulder-arm, wrist, hand, and upper limb coordination. Each item is scored by a 3-point ordinal scale (0, absent; 1, partial impairment; 2, no impairment). The total score range is from 0 to 66 points [31]. A higher score indicates a better functional performance. The minimal clinically important differences (MCID) of FMA-UE is 9 points in patients with poststroke [32].

Secondary outcomes included changes in the thumb localization test (TLT), the sensory subscale of the Fugl-Meyer assessment for upper extremity (FMA-UE-S), box and block test (BBT), and Barthel Index (BI). TLT was used to assess proprioception. Patients closed their eyes, and the examiner moved the affected upper limb of patients to three different positions and asked patients to pinch the thumb with the unaffected hand. Scoring for each test was based on the patient's performance (0, pinch the thumb accurately; 1, miss the thumb by several centimeters and immediately correct; 2, find the arm and pinch the thumb by tracing from arm; 3, unable to find the thumb). The worst performance of the three tests was the final score [33, 34]. The assessment has established high interrater reliability [35]. FMA-UE-S is scored on a 3-point ordinal scale (0-2) scored to measure light touch and proprioception on the upper extremity [31]. The light touch was tested on the patient's arms and the palmar surface of the hands. The proprioception was tested on the shoulder, elbow, wrist, and thumb of patients. The patient was blindfolded and asked whether they felt the light touch or the position of joints. The total score of FMA-UE-S is 12 [36, 37]. BBT was used to measure gross manual hand dexterity, which is a highly reliable test [38]. The test involves 150 colored cubes and one wooden box divided by a partition into two separate compartments. Patients were instructed to grasp the cube from one compartment and release it into the opposite compartment one by one. The number of cubes patients transferred with their affected hands in one minute was recorded as the score [39]. The performance of basic activities in daily living was assessed

with the Barthel Index (BI) [40], which is a reliable measurement [41]. The scale consists of 10 activity items, and the score for each item is based on the patient's degree of independence. Score ranges from 0 (total dependence) points to 100 points (total independence).

The experience of the patient was assessed with the meCUE (modular evaluation of key Components of User Experience, http://www.mecue.de), which has been used in several studies [42, 43]. The questionnaire has four validated modules: product perceptions, user emotions, consequences of use, and overall evaluation [44]. In the modules of product perceptions, user emotions, and consequences of use, each item has three concerning statements evaluated by a 7-point Likert scale with scores ranging from 1 (strongly disagree) to 7 (strongly agree). Considering the characteristics of the perception window, items on "commitment, status, product loyalty" in the original scale were removed in this study. In the module of the overall evaluation, the scale ranges from −5 (bad) to 5 (good), which evaluated the overall experience of the product.

2.6. Statistical Analyses. Statistical analyses were processed using SPSS version 26 (IBM Inc., Chicago, IL, USA). We analyzed the normality of the patients' demographic and clinical characteristics with the Shapiro-Wilk test. Data are presented as the mean ± standard deviation (SD) for normally distributed continuous variables. Nonnormally distributed variables or ranked variables are expressed as medians (interquartile ranges, IQRs). The chi-square test was used to compare sex, side of the lesion, and type of stroke between the two groups. The independent Student t-test was used to compare age between the two groups, and the independent Mann–Whitney U test was used to compare time from stroke and Brunnstrom stages for upper limb and hand. The paired Student t-test and Wilcoxon signed-rank test were used for analyzing the pretest and posttest scores in clinical outcomes of both groups. To compare the effect of PG with CG, the changes in continuous outcomes between groups were analyzed by Mann–Whitney U test. For the modified meCUE, the results of each subscale were calculated by the mean scores of patients. A p value of 0.05 was set for the level of statistical significance.

3. Results

From October 2020 through May 2021, forty patients who met the inclusion criteria were enrolled. The flow chart of the participant selection and assignment is shown in Figure 2. Patients were randomly allocated to the PG ($N = 20$) and CG ($N = 20$). There were no adverse events during the intervention. The demographic characteristics of participates are shown in Table 1. The mean age was 59.1 years, and the median time from stroke was 21 weeks. There were no differences in age, sex, side of stroke, time poststroke, stroke type, Brunnstrom stage, or somatosensory performance between groups at baseline.

3.1. Effects of Intervention. In the PG group, patients showed a significant improvement in FMA-UE-M ($p < 0.001$), FMA-UE-S ($p = 0.001$), BBT ($p = 0.027$), TLT ($p < 0.001$), and BI ($p < 0.001$). In the CG group, patients showed a significant improvement in FMA-UE-M ($p < 0.001$), FMA-UE-S ($p = 0.006$), and BI ($p < 0.001$), but there was no significant improvement in TLT ($p = 0.083$) and BBT ($p = 0.107$). These results are shown in Figure 3.

Table 1: Demographics and characteristics at baseline of the patients with poststroke.

Characteristics	Total group ($N = 40$)	PG ($N = 20$)	CG ($N = 20$)	p value
Age (years)				
Mean ± SD	59.1 ± 11.4	58.4 ± 10.5	59.8 ± 12.5	0.704
Gender (n)				0.744
Male	25	13	12	
Female	15	7	8	
Time form stroke (weeks)				
Median (IQRs)	21 (31)	19 (30)	22 (33)	0.779
Side of lesion (n)				1.000
Left	16	8	8	
Right	24	12	12	
Type of stroke (n)				0.113
Hemorrhagic	19	12	7	
Ischemic	21	8	13	
Brunnstrom—upper extremity				
Median (IQRs)	3 (2)	3 (1)	2.5 (2)	0.947
Brunnstrom—hand				
Median (IQRs)	2 (3)	2 (3)	2 (3)	0.989
Somatosensory impairment (%)				
TLT	90	90	90	1.000
FMA-UE-S	85	90	80	0.658

The average FMA-UE-M scores improved from 25.0 ± 14.6 to 34.3 ± 16.8 in the PG group and from 23.5 ± 13.3 to 28.5 ± 14.4 in the CG group. In comparison, the mean score changes of FMA-UE-M improved more in the PG than in the CG group ($p = 0.010$), and the percentages of patients who achieved the MCID of the FMA-UE-M were higher in the PG than in the CG group ($p = 0.001$) (Figure 4). The average TLT scores improved from 2.3 ± 0.7 to 1.2 ± 1.0 in the PG group but only from 2.0 ± 0.6 to 1.9 ± 0.8 in the CG group. The average of the FMA-UE-S improved from 4.7 ± 4.5 to 7.6 ± 4.1 in the PG group and from 7.0 ± 13.3 to 8.1 ± 3.6 in the CG group. Compared to the CG group, the PG group showed more improvement in the mean score changes of the TLT ($p < 0.001$) and the FMA-UE-S ($p = 0.033$). Besides, in the PG group, the average BBT scores improved from 2.7 ± 4.9 to 4.8 ± 8.6 and the average BI scores improved from 54.0 ± 11.7 to 65.8 ± 13.9. In the CG

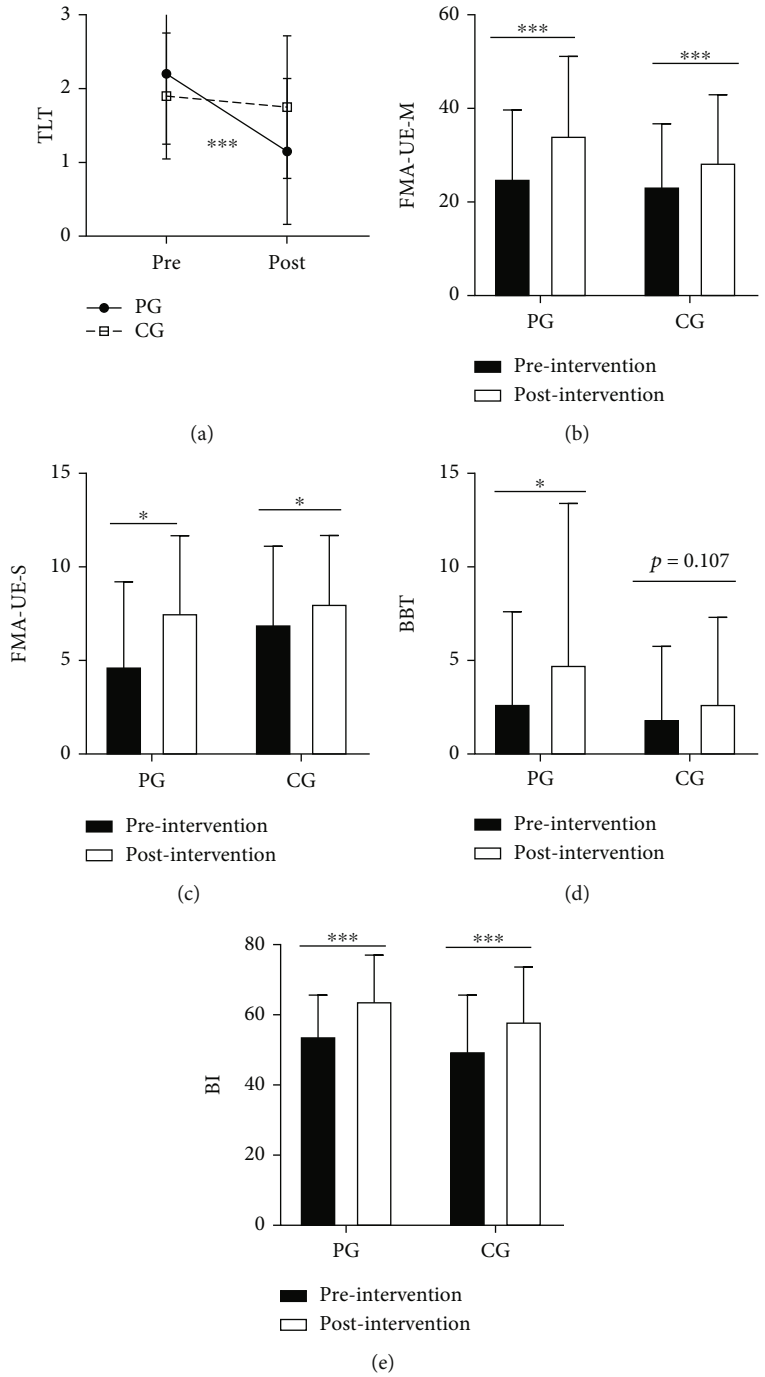

Figure 3: Group differences in clinical measurements. (a) The scores of the thumb localizing test (TLT) in the two groups before (pre) and after (post) intervention. (b) The scores of the motor subscale of Fugl-Meyer assessment for upper extremity (FMA-UE-M) in the two groups before (pre) and after (post) intervention. (c) The scores of the sensory subscale of Fugl-Meyer assessment for upper extremity (FMA-UE-S) in the two groups before (pre) and after (post) intervention. (d) The scores of box and block test (BBT) in the two groups before (pre) and after (post) intervention. (e) The scores of Barthel Index (BI) in the two groups before (pre) and after (post) intervention ($^{*}p < 0.05$ and $^{***}p < 0.001$).

group, the average BBT scores improved from 1.9 ± 3.9 to 2.7 ± 4.6, and the average BI scores improved from 50.3 ± 15.5 to 58.3 ± 15.4. We found no significant differences in the mean score changes of BBT ($p = 0.640$) and BI ($p = 0.134$) between the two groups.

3.2. Patient Experience. After the last treatment session, patients in the PG completed the modified meCUE to express their experience. The rates of usefulness, usability, and visual aesthetics in product perception were high. For emotion, positive emotion was rated higher than negative

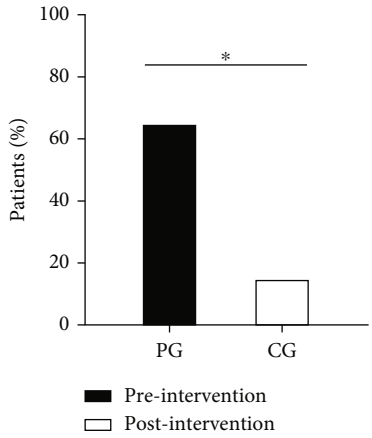

Figure 4: Comparison of the percentages of patients who achieved the minimal clinically important differences (MCID) of the FMA-UE-M between groups after intervention.

Table 2: Modified meCUE.

Modules	Patients rating ($N = 20$) (mean ± SD)
Product perception	
Usefulness	5.12 ± 0.82
Usability	5.32 ± 1.28
Visual aesthetics	5.44 ± 0.93
Emotions	
Positive emotions	4.24 ± 0.88
Negative emotions	2.61 ± 1.13
Consequences of use	
Intention to use	4.95 ± 1.35
Overall evaluation	2.53 ± 1.57

emotion. None of the patients felt uncomfortable or pain during the training. Most of the patients indicated that they were willing to carry out the treatment with the setup. The median rate for overall evaluation rated was "3", which suggested that most patients were satisfied with the treatment (Table 2).

4. Discussion

Our results showed that proprioceptive training is effective in improving upper extremity sensorimotor function in patients with poststroke. In addition, most patients in the PG were satisfied with the proposed visual-based sensory training setup. We suggest that proprioceptive training including both passive and active movements with a visual-based sensory training setup is a feasible treatment and could be an adjunct therapy in clinical intervention.

The PG showed a significant improvement in proprioception following training compared with the CG. This finding is in line with results from other studies [12, 13]. It is well known that sensory stimuli are involved in preparing motor plans and monitoring motor performance [2]. Somatosensory deficits impact the motor output of the patient [5–7]. Therefore, the patient needs to receive continuous and systematic proprioceptive training. In this study, FMA-UE-M and BBT data demonstrated that proprioception training was effective in recovering upper limb motor function after stroke. Emerging evidence indicates that proprioceptive training could improve somatosensory and motor function after stroke [20, 45]. Vahdat et al. [17] observed that even a single session of proprioceptive training could modulate functional connectivity in the sensorimotor network, which might be one of the mechanisms for which proprioceptive training improves motor function following stroke. However, there was no significant difference in the improvement of BI between the two groups. The Barthel Index measures the functional ability of a patient in performing daily activities, which require the involvement of upper or lower limb function. In this study, we only applied different interventions on the upper limbs between the two groups, but interventions for lower limb function were not restricted. In addition, most patients enrolled in this study presented with moderate to severe motor impairment, which might limit their improvement in functional independence of ADL [46].

In this study, the proprioceptive program combined passive and active movements with visual feedback. We conducted passive bimanual repetitive flexion-extension in the upper limbs of patients in a mirror-symmetrical pattern. Passive movements of unilateral upper limb could elicit brain activity in bilateral sensorimotor areas [47]. There are neural connections in the bilateral somatosensory cortex, which allow sensory information from both hands to transfer between hemispheres [48]. The level of brain activity of the affected side was decreased due to the inhibitory imbalance after stroke. Some studies have suggested that using mirror-symmetric bilateral movements as a priming approach could enhance the recovery of upper limb function by rebalancing the excitability of cortical activity [49, 50]. In these studies, patients were instructed to actively flex and extend their unaffected wrist, with a customized device driving their affected wrist in a synchronized mirror-symmetric or parallel movement pattern [51, 52]. While robot-assisted training could provide systematic procedures and various feedback, they are often customized for single-joint and the high cost may limit its application to clinical therapy. Compared with robot-assisted training, sensory training with guidance from therapists might be more feasible and suitable for clinical practice. Kiper et al. [18] reported that patients with stroke had significant improvement in muscle force after bilateral flexion-extension movements training mobilized by the therapist.

In addition to passive movement, we also applied active movement in our training procedure, which increased the challenge of training and patient engagement. Compared with passive proprioceptive training, active proprioceptive training with visual feedback allowed participants to update the internal model of the current state by constantly performing error detection and correction [25]. The common principles of active somatosensory interventions in previous

studies were high intensity, repetitive, and attentive discrimination on the graded difficulty of sensory tasks with feedback [10]. Eye masks and verbal instructions were regularly used to provide feedback during training. However, frequent wearing and taking off the eye mask may make the patient lose patience and influence their sense of immersion and engagement. Some patients in the CG group also complained that closing their eyes for a long time made them feel tired and distracted. To overcome these limitations, we developed a visual-based sensory training setup that enabled therapists to switch the vision of patients instantly. The mode of the smart window can be converted in one second, which is convenient for therapists and patients. Patients were trained to actively discriminate different positions or movements of the affected limb when their vision was blocked and then receive visual feedback for self-checking. Moreover, patients were instructed to observe and sense the stimulation on their hands when the visual-based sensory training setup was in transparent mode. Previous studies have demonstrated that looking at the stimulated body part might induce short-term activation in somatosensory cortices [53]. With the help of immediate enhancement, patients could still sense proprioceptive stimuli without visual input for a while. Repeating the process might facilitate neural plasticity by enhancing experience-dependent synaptic connections. In our study, the visual-based sensory training setup provided a perceptual context in which the patient received visuo-proprioceptive stimulation and feedback. According to the result of "intention to use" in the modified meCUE, most patients were willing to use this setup for daily training.

Since patients had rarely received sensory training before, they were attracted by the setup. As indicated by the modified meCUE results, patients had positive product perceptions of usefulness, usability, and visual aesthetics. However, some patients indicated that the setup could be improved by increasing the space of the training platform and the size of the smart window. In our study, the setup only allowed patients to place their hands, wrists, and part of the forearms on the training platform, which limited the training on the rest of the upper limb. Future studies should consider developing a moveable smart window to make the setup more flexible.

There are some limitations to our study. First, the sample size was still small in this study, which affects the generalizability of the results. Second, the method of application of the setup and the training tasks was different between the two groups. There is no conclusive enough evidence that the visual feedback have some effect on the proprioceptive training in the present study. We could only provide preliminary results for it. In addition, patients were not blind to the assignment group, which might result in a placebo effect in this study.

In conclusion, we investigated the effectiveness and feasibility of the proposed proprioceptive training using visual-based sensory training setup in patients with post-stroke. We found that proprioceptive training effectively improved the upper extremity sensorimotor function in stroke patients.

Data Availability

The data used to support the findings of this research are available from the corresponding author.

Conflicts of Interest

The authors declare that they have no conflicts of interest.

Authors' Contributions

Jie Jia and Jieying He designed the experiment. Jieying He recruited the patients. Chong Li conducted the baseline and outcome assessments. Jiali Lin and Beibei Shu conducted the interventions. Yifang Lin performed the data analysis. Jieying He wrote the manuscript. Bin Ye and Jianhui Wang reviewed and edited the manuscript.

Acknowledgments

The study was supported by the National Key Research & Development Program of the Ministry of Science and Technology of the People's Republic of China under Grants 2018YFC2002300 and 2018YFC2002301.

References

[1] C. S. Sherrington, "On the proprio-ceptive system, especially in its reflex aspect," *Brain*, vol. 29, no. 4, pp. 467–482, 1907.

[2] L. L. Edwards, E. M. King, C. M. Buetefisch, and M. R. Borich, "Putting the "sensory" into sensorimotor control: the role of sensorimotor integration in goal-directed hand movements after stroke," *Frontiers in Integrative Neuroscience*, vol. 13, 2019.

[3] J. A. Semrau, T. M. Herter, S. H. Scott, and S. P. Dukelow, "Robotic identification of kinesthetic deficits after stroke," *Stroke*, vol. 44, no. 12, pp. 3414–3421, 2013.

[4] S. Meyer, N. de Bruyn, C. Lafosse et al., "Somatosensory impairments in the upper limb poststroke," *Neurorehabilitation and Neural Repair*, vol. 30, no. 8, pp. 731–742, 2016.

[5] H. Carlsson, G. Gard, and C. Brogårdh, "Upper-limb sensory impairments after stroke: self-reported experiences of daily life and rehabilitation," *Journal of Rehabilitation Medicine*, vol. 50, no. 1, pp. 45–51, 2018.

[6] M. L. Ingemanson, J. R. Rowe, V. Chan, E. T. Wolbrecht, D. J. Reinkensmeyer, and S. C. Cramer, "Somatosensory system integrity explains differences in treatment response after stroke," *Neurology*, vol. 92, no. 10, pp. e1098–e1108, 2019.

[7] L. M. Carey, T. A. Matyas, and C. Baum, "Effects of somatosensory impairment on participation after stroke," *The American Journal of Occupational Therapy*, vol. 72, no. 3, pp. 7203205100p1–7203205100p10, 2018.

[8] C. Yilmazer, L. Boccuni, L. Thijs, and G. Verheyden, "Effectiveness of somatosensory interventions on somatosensory, motor and functional outcomes in the upper limb post-stroke: a systematic review and meta-analysis," *NeuroRehabilitation*, vol. 44, no. 4, pp. 459–477, 2019.

[9] I. Serrada, B. Hordacre, and S. L. Hillier, "Does sensory retraining improve sensation and sensorimotor function following stroke: a systematic review and meta-analysis," *Frontiers in Neuroscience*, vol. 13, p. 402, 2019.

[10] M. L. Turville, L. S. Cahill, T. A. Matyas, J. M. Blennerhassett, and L. M. Carey, "The effectiveness of somatosensory retraining for improving sensory function in the arm following stroke: a systematic review," *Clinical Rehabilitation*, vol. 33, no. 5, pp. 834–846, 2019.

[11] S. Doyle, S. Bennett, S. E. Fasoli, and K. T. McKenna, "Interventions for sensory impairment in the upper limb after stroke," *Cochrane Database of Systematic Reviews*, vol. 16, no. 6, article D6331, 2010.

[12] C. de Diego, S. Puig, and X. Navarro, "A sensorimotor stimulation program for rehabilitation of chronic stroke patients," *Restorative Neurology and Neuroscience*, vol. 31, no. 4, pp. 361–371, 2013.

[13] L. Carey, R. Macdonell, and T. A. Matyas, "SENSe: study of the effectiveness of neurorehabilitation on Sensation," *Neurorehabilitation and Neural Repair*, vol. 25, no. 4, pp. 304–313, 2011.

[14] N. Byl, J. Roderick, O. Mohamed et al., "Effectiveness of sensory and motor rehabilitation of the upper limb following the principles of neuroplasticity: patients stable poststroke," *Neurorehabilitation and Neural Repair*, vol. 17, no. 3, pp. 176–191, 2003.

[15] N. Smania, B. Montagnana, S. Faccioli, A. Fiaschi, and S. M. Aglioti, "Rehabilitation of somatic sensation and related deficit of motor control in patients with pure sensory stroke," *Archives of Physical Medicine and Rehabilitation*, vol. 84, no. 11, pp. 1692–1702, 2003.

[16] N. M. Öcal, N. Alaca, and M. K. Canbora, "Does upper extremity proprioceptive training have an impact on functional outcomes in chronic stroke patients?," *Medeniyet Medical Journal*, vol. 35, no. 2, pp. 91–98, 2020.

[17] S. Vahdat, M. Darainy, A. Thiel, and D. J. Ostry, "A single session of robot-controlled proprioceptive training modulates functional connectivity of sensory motor networks and improves reaching accuracy in chronic stroke," *Neurorehabilitation and Neural Repair*, vol. 33, no. 1, pp. 70–81, 2019.

[18] P. Kiper, A. Baba, M. Agostini, and A. Turolla, "Proprioceptive based training for stroke recovery. Proposal of new treatment modality for rehabilitation of upper limb in neurological diseases," *Archives of Physiotherapy*, vol. 5, no. 1, p. 6, 2015.

[19] R. Chanubol, P. Wongphaet, N. Chavanich et al., "A randomized controlled trial of cognitive sensory motor training therapy on the recovery of arm function in acute stroke patients," *Clinical Rehabilitation*, vol. 26, no. 12, pp. 1096–1104, 2012.

[20] J. E. Aman, N. Elangovan, I.-L. Yeh, and J Ã.¼r. Konczak, "The effectiveness of proprioceptive training for improving motor function: a systematic review," *Frontiers in Human Neuroscience*, vol. 8, 2015.

[21] P.-m. Chen, P. W. H. Kwong, C. K. Y. Lai, and S. S. M. Ng, "Comparison of bilateral and unilateral upper limb training in people with stroke: a systematic review and meta-analysis," *PLoS One*, vol. 14, no. 5, article e216357, 2019.

[22] J. H. Cauraugh and J. J. Summers, "Neural plasticity and bilateral movements: a rehabilitation approach for chronic stroke," *Progress in Neurobiology*, vol. 75, no. 5, pp. 309–320, 2005.

[23] Y. Iwamura, M. Tanaka, and A. Iriki, "Bilateral hand representation in the postcentral somatosensory cortex," *Nature (London)*, vol. 369, no. 6481, pp. 554–556, 1994.

[24] M. Osumi, M. Sumitani, Y. Otake, and S. Morioka, "A hypothetical explanatory sensorimotor model of bilateral limb interference," *Medical Hypotheses*, vol. 122, pp. 89–91, 2019.

[25] I. A. M. Beets, M. Macé, R. L. J. Meesen et al., "Active versus passive training of a complex bimanual task: is prescriptive proprioceptive information sufficient for inducing motor learning?," *PLoS One*, vol. 7, no. 5, article e37687, 2012.

[26] N. Elangovan, L. Cappello, L. Masia, J. Aman, and J. Konczak, "A robot-aided visuo-motor training that improves proprioception and spatial accuracy of untrained movement," *Scientific Reports*, vol. 7, no. 1, p. 17054, 2017.

[27] C. Fritzsch, J. Wang, L. F. D. Santos, K.-H. Mauritz, M. Brunetti, and C. Dohle, "Different effects of the mirror illusion on motor and somatosensory processing," *Restorative Neurology and Neuroscience*, vol. 32, no. 2, pp. 269–280, 2014.

[28] H. G. Kwon, S. H. Jang, and M. Y. Lee, "Effects of visual information regarding tactile stimulation on the somatosensory cortical activation: a functional MRI study," *Neural Regeneration Research*, vol. 12, no. 7, pp. 1119–1123, 2017.

[29] J. Sanford, J. Moreland, L. R. Swanson, P. W. Stratford, and C. Gowland, "Reliability of the Fugl-Meyer assessment for testing motor performance in patients following stroke," *Physical Therapy*, vol. 73, no. 7, pp. 447–454, 1993.

[30] D. J. Gladstone, C. J. Danells, and S. E. Black, "The Fugl-Meyer assessment of motor recovery after stroke: a critical review of its measurement properties," *Neurorehabilitation and Neural Repair*, vol. 16, no. 3, pp. 232–240, 2002.

[31] A. R. Fugl-Meyer, L. Jääskö, I. Leyman, S. Olsson, and S. Steglind, "The post-stroke hemiplegic patient. 1. A method for evaluation of physical performance," *Scandinavian Journal of Rehabilitation Medicine*, vol. 7, no. 1, pp. 13–31, 1975.

[32] K. N. Arya, R. Verma, and R. K. Garg, "Estimating the minimal clinically important difference of an upper extremity recovery measure in subacute stroke patients," *Topics in Stroke Rehabilitation*, vol. 18, Suppl 1, pp. 599–610, 2011.

[33] D. Rand, "Proprioception deficits in chronic stroke-upper extremity function and daily living," *PLoS One*, vol. 13, no. 3, article e195043, 2018.

[34] K. Hirayama, T. Fukutake, and M. Kawamura, "'Thumb localizing test' for detecting a lesion in the posterior column-medial lemniscal system," *Journal of the Neurological Sciences*, vol. 167, no. 1, pp. 45–49, 1999.

[35] E. Otaka, Y. Otaka, S. Kasuga et al., "Reliability of the thumb localizing test and its validity against quantitative measures with a robotic device in patients with hemiparetic stroke," *PLoS One*, vol. 15, no. 7, article e236437, 2020.

[36] J.-H. Lin, I.-P. Hsueh, C.-F. Sheu, and C.-L. Hsieh, "Psychometric properties of the sensory scale of the Fugl-Meyer assessment in stroke patients," *Clinical Rehabilitation*, vol. 18, no. 4, pp. 391–397, 2004.

[37] K. J. Sullivan, J. K. Tilson, S. Y. Cen et al., "Fugl-Meyer assessment of sensorimotor function after stroke," *Stroke*, vol. 42, no. 2, pp. 427–432, 2011.

[38] J. Desrosiers, G. Bravo, R. Hebert, E. Dutil, and L. Mercier, "Validation of the box and block test as a measure of dexterity of elderly people: reliability, validity, and norms studies," *Archives of Physical Medicine and Rehabilitation*, vol. 75, no. 7, pp. 751–755, 1994.

[39] V. Mathiowetz, G. Volland, N. Kashman, and K. Weber, "Adult norms for the box and block test of manual dexterity," *American Journal of Occupational Therapy*, vol. 39, no. 6, pp. 386–391, 1985.

[40] F. I. Mahoney and D. W. Barthel, "Functional evaluation: the Barthel index," *Maryland State Medical Journal*, vol. 14, pp. 61–65, 1965.

[41] C. Collin, D. T. Wade, S. Davies, and V. Horne, "The Barthel ADL index: a reliability study," *International Disability Studies*, vol. 10, no. 2, pp. 61–63, 1988.

[42] S. Hoermann, L. F. D. Santos, N. Morkisch et al., "Computerised mirror therapy with augmented reflection technology for early stroke rehabilitation: clinical feasibility and integration as an adjunct therapy," *Disability and Rehabilitation*, vol. 39, no. 15, pp. 1503–1514, 2017.

[43] L. Ding, L. Li, X. Zhimin et al., "Computer vision technology-based face mirroring system providing mirror therapy for Bell's palsy patients," *Disability and Rehabilitation*, vol. 42, no. 6, pp. 833–840, 2020.

[44] M. Minge, M. Thüring, I. Wagner, and C. V. Kuhr, "The meCUE questionnaire: a modular tool for measuring user experience," *Paper Presented at the Applied Human Factors and Ergonomics Society (AHFE)*, 2017.

[45] S. E. Findlater and S. P. Dukelow, "Upper extremity proprioception after stroke: bridging the gap between neuroscience and rehabilitation," *Journal of Motor Behavior*, vol. 49, no. 1, pp. 27–34, 2017.

[46] E. J. Woytowicz, J. C. Rietschel, R. N. Goodman et al., "Determining levels of upper extremity movement impairment by applying a cluster analysis to the Fugl-Meyer assessment of the upper extremity in chronic stroke," *Archives of Physical Medicine and Rehabilitation*, vol. 98, no. 3, pp. 456–462, 2017.

[47] J. M. Kenzie, S. E. Findlater, D. J. Pittman, B. G. Goodyear, and S. P. Dukelow, "Errors in proprioceptive matching post-stroke are associated with impaired recruitment of parietal, supplementary motor, and temporal cortices," *Brain Imaging and Behavior*, vol. 13, no. 6, pp. 1635–1649, 2019.

[48] M. Blatow, E. Nennig, A. Durst, K. Sartor, and C. Stippich, "FMRI reflects functional connectivity of human somatosensory cortex," *NeuroImage*, vol. 37, no. 3, pp. 927–936, 2007.

[49] W. D. Byblow, C. M. Stinear, M.-C. Smith et al., "Mirror symmetric bimanual movement priming can increase corticomotor excitability and enhance motor learning," *PLoS One*, vol. 7, no. 3, article e33882, 2012.

[50] C. M. Stinear, P. Alan Barber, J. P. Coxon, M. K. Fleming, and W. D. Byblow, "Priming the motor system enhances the effects of upper limb therapy in chronic stroke," *Brain*, vol. 131, no. 5, pp. 1381–1390, 2008.

[51] C. M. Stinear, M. A. Petoe, S. Anwar, P. A. Barber, and W. D. Byblow, "Bilateral priming accelerates recovery of upper limb function after stroke: a randomized controlled trial," *Stroke*, vol. 45, no. 1, pp. 205–210, 2014.

[52] C. T. Shiner, W. D. Byblow, and P. A. McNulty, "Bilateral priming before Wii-based movement therapy enhances upper limb rehabilitation and its retention after stroke: a case-controlled study," *Neurorehabilitation and Neural Repair*, vol. 28, no. 9, pp. 828–838, 2014.

[53] A. Serino, A. Farnè, M. L. Rinaldesi, P. Haggard, and E. Làdavas, "Can vision of the body ameliorate impaired somatosensory function?," *Neuropsychologia*, vol. 45, no. 5, pp. 1101–1107, 2007.

Hindawi
Neural Plasticity
Volume 2022, Article ID 5241449, 13 pages
https://doi.org/10.1155/2022/5241449

Research Article

Treatment Combining Focused Ultrasound with Gastrodin Alleviates Memory Deficit and Neuropathology in an Alzheimer's Disease-Like Experimental Mouse Model

Kaixuan Luo,[1] **Yuhong Wang**,[1] **Wen-Shiang Chen**,[2] **Xiangjun Feng**,[1] **Yehui Liao**,[1] **Shaochun Chen**,[1] **Yao Liu**,[1] **Chengde Liao**,[3] **Moxian Chen**,[1] **and Lijuan Ao**[1]

[1]*School of Rehabilitation, Kunming Medical University, Kunming, Yunnan Province, China*
[2]*Department of Physical Medicine and Rehabilitation, National Taiwan University Hospital & National Taiwan University College of Medicine, Taipei City, Taiwan*
[3]*Department of Radiology, The Third Affiliated Hospital of Kunming Medical University, Yunnan Cancer Hospital & Cancer Center, Kunming, Yunnan, China*

Correspondence should be addressed to Moxian Chen; chenmoxian@kmmu.edu.cn and Lijuan Ao; 13508710081@qq.com

Received 18 September 2021; Revised 25 November 2021; Accepted 16 December 2021; Published 13 January 2022

Academic Editor: Rongrong Lu

Alzheimer's disease (AD) is the most common type of dementia but lacks effective treatment at present. Gastrodin (GAS) is a phenolic glycoside extracted from the traditional Chinese herb—Gastrodia elata—and has been reported as a potential therapeutic agent for AD. However, its efficiency is reduced for AD patients due to its limited BBB permeability. Studies have demonstrated the feasibility of opening the blood-brain barrier (BBB) via focused ultrasound (FUS) to overcome the obstacles preventing medicines from blood flow into the brain tissue. We explored the therapeutic potential of FUS-mediated BBB opening combined with GAS in an AD-like mouse model induced by unilateral intracerebroventricular (ICV) injection of $A\beta_{1\text{-}42}$. Mice were divided into 5 groups: control, untreated, GAS, FUS and FUS+GAS. Combined treatment (FUS+GAS) rather than single intervention (GAS or FUS) alleviated memory deficit and neuropathology of AD-like mice. The time that mice spent in the novel arm was prolonged in the Y-maze test after 15-day intervention, and the waste-cleaning effect was remarkably increased. Contents of $A\beta$, tau, and P-tau in the observed (also the targeted) hippocampus were reduced. BDNF, synaptophysin (SYN), and PSD-95 were upregulated in the combined group. Overall, our results demonstrate that FUS-mediated BBB opening combined with GAS injection exerts the potential to alleviate memory deficit and neuropathology in the AD-like experimental mouse model, which may be a novel strategy for AD treatment.

1. Introduction

Dementia, a syndrome characterized by dysfunction in memory, thinking, behavior, and the ability to perform daily activities, is affecting 50 million people globally. There are continuing nearly 10 million new cases each year. Alzheimer's disease (AD) is the most common type of dementia, contributing to 60-70% of cases [1], generating physical, psychological, social, and economic impacts on patients, families, and society. AD is a neurodegenerative and one of the protein-conformation diseases [2, 3], pathologically characterized by extracellular beta-amyloid ($A\beta$) deposition, intracellular aggregation of neurofibrillary tangles (NFTs), and extensive loss of neurons [4, 5]. Under the pathological conditions, $A\beta$ promotes the increase of glycogen synthase kinase 3β, which phosphorylates tau into phosphorylated tau (P-tau) [6]. $A\beta$ depositions also contribute to proinflammation responses such as activation of microglia and astrocyte, synaptic dysfunction, and abnormal cell death [7, 8].

There are symptom-relief medications for AD, but no curative approaches available at present [4, 9]. Several AD medications, including Cholinesterase inhibitors (ChEIs) and the N-methyl-d-aspartate (NMDA) antagonist memantine, have been approved by the US Food and Drug

Administration (FDA). Despite the limited clinical benefit, side effects such as nausea, vomiting, diarrhea, and severe cardiovascular response have been reported [6, 9, 10]. Aduhelm (aducanumab) is directed at the underlying Aβ pathology of AD and has been approved by the FDA recently through the accelerated approval pathway. The clinical benefit, however, remains unclear [11]. The treatment of AD continues to be an intractable problem to modern medicine, and the development of new therapies meets current urgent needs.

Gastrodin (GAS) is a phenolic glycoside extracted from the traditional Chinese herb—Gastrodia elata—and is considered the primary active constituent of rhizoma gastrodiae. GAS was traditionally used as a therapeutic agent for ailments such as dizziness, headache, convulsions, hypertension, and cardiovascular diseases [12, 13]. Besides, studies have demonstrated the potential of treating AD with GAS both in vitro and in vivo. GAS may be beneficial for Aβ pathology and symptom of AD via antioxidative effect [14], anti-inflammatory effect [13], antiapoptosis effect [12], and reducing the activity of β [15] as well as γ-secretase [16]. GAS can pass through the BBB with limited permeability [17], which reduces its treatment efficiency despite the promising therapeutic potential for AD.

Barriers between circulation and tissue, such as the blood-brain and blood-cerebral spinal fluid barriers (BBB and BCSFB), are responsible for protecting the central nervous system (CNS) from pathogens as well as toxins. According to the statistics, 98% of small molecules whose size are less than 400 Da and almost 100% of large molecules whose size are above 500 Da cannot pass through the BBB, which hinders therapeutic agents into the brain and becomes an obstacle of CNS disease treatment [18]. Focused ultrasound (FUS), namely, the ultrasound that works in a focused way, is an early-stage, noninvasive method to open the blood-brain barrier locally, transiently, and safely, which facilitates delivery of anticancer drugs [19], gene [20], and immune cells [21] into the brain. Cavitation plays a vital role in BBB opening via FUS. Firstly, the microbubbles were usually preinjected into the blood vessel and circulated through the sonicated region. Then, the FUS activates microbubbles to grow, oscillate (stable cavitation), and even collapse (inertial cavitation), affecting the cellular structure and leading to the opening of tight junctions in BBB [22, 23]. Opening the BBB by FUS has exerted its therapeutic potential for AD [24, 25]. A study [26] provided evidence that BBB opening via MRI-guided FUS enhanced the delivery of intravenously administered antibodies, and β-amyloid (Aβ) plaque pathology was reduced in an AD mouse model. Subsequently, Jordão et al. [24] carried out transcranial FUS BBB opening in the TgCRND8 mouse model; a reduction of plaque pathology was observed without additional therapeutic agents administered. Endogenous antibodies are found to bind to Aβ plaques, and glia activation was enhanced, which may contribute to the internalization of Aβ. The therapeutic effect of combining BBB opening with GAS on brain disorders has been demonstrated before. A study shows an antiepileptic effect by elevating GAS concentration in the cerebral spinal fluid after a single focused shockwave treatment [27].

The present study was directed to investigate the therapeutic potential of the combined treatment (BBB opening via FUS and GAS administration) on AD. What is more, we try to explain the mechanism behind from a relatively new point of view, that is, from a perspective of the waste-cleaning function of the brain. We first explored the safety of BBB opening on male Kunming mice via FUS and microbubbles. The therapeutic effect of FUS-mediated BBB opening combined with GAS treatment was investigated in an A$\beta_{1\text{-}42}$-induced AD-like experimental mouse model. Unilateral A$\beta_{1\text{-}42}$ intracerebroventricular (ICV) injection was carried out on male Kunming mice to establish the AD-like model. BBB openings of the left hippocampus and intraperitoneal (i.p.) GAS injections were performed within treatment duration.

2. Materials and Methods

2.1. Animals. A total of 60 male Kunming mice (KM mice, weight, 28-30 g) were obtained from Kunming Laboratory Animal Center (Kunming, China) for use in the experiment. All mice were housed as five per cage in controlled temperature ($24 \pm 2^{\circ}$C) and humidity ($50 \pm 5\%$) on a 12 h reverse light/dark cycle with food and water ad libitum. All animal protocols were approved by the Animal Ethics Committee of Kunming Medical University (No. KMMU2019078).

2.2. Experimental Design. At the very beginning, we assessed the safety of BBB opening mediated by FUS. We observed its reversibility ($n = 3$ per time point) and performed H&E ($n = 3$ per time point) as well as TUNNEL ($n = 3$ per time point) staining of the targeted brain region before and 4 h, 24 h, 48 h, and 72 h after FUS sonication on normal KM mice. Influence on the safety by AD pathologic condition in the experimental procedure was hypothesized tiny and neglected. Then, mice were randomly allocated into five groups ($n = 6$ per group) after adaptation of 7 days: Group I, control: mice in this group were given ICV injection of saline rather than A$\beta_{1\text{-}42}$ peptide and received placebo interventions within treatment duration; Group II, untreated: mice were intracerebroventricularly injected with A$\beta_{1\text{-}42}$ peptide and given placebo treatment; Group III, GAS, all animals were intracerebroventricularly injected with A$\beta_{1\text{-}42}$ peptide and received i.p. injection of GAS (100 mg/kg, qd.) daily; Group IV, FUS, mice were intracerebroventricularly injected with A$\beta_{1\text{-}42}$ peptide and received FUS-mediated BBB opening every three days once for a total of 5 times; and Group V, FUS+GAS, mice that received ICV injection of A$\beta_{1\text{-}42}$ peptide were given GAS treatment with a dose of 100 mg/kg once a day as well as FUS-mediated BBB opening every three days once for a total of 5 times. In general, mice were given ICV injection of A$\beta_{1\text{-}42}$ peptide to establish an AD-like model at day 0 after one week of adaptation and were allowed a 3-day interval for recovery. Subsequently, treatments were given corresponding to grouping within the treatment duration (from days 3 to 17). Y-maze was carried out on day 18 to evaluate short-term memory, and mice were sacrificed with the left hippocampus collected for protein analysis on day 19 (Figure 1).

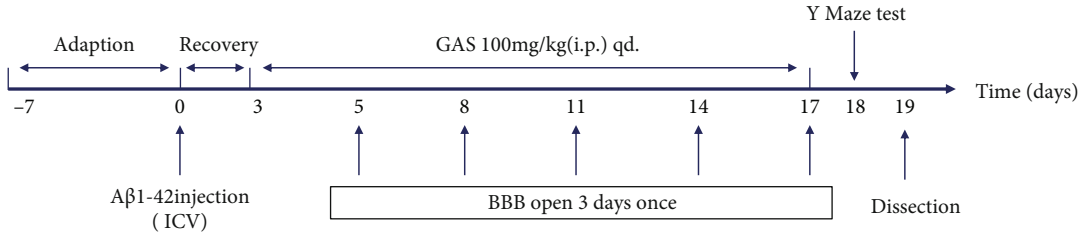

Figure 1: Timeline of the experimental protocol.

2.3. Safety of BBB Opening Mediated by FUS. We explored the reversibility of BBB opening mediated via FUS. To visualize the reversibility, 2% Evans Blue (EB, Millipore-Sigma, Burlington, MA, USA) was injected via the tail vein (2.5 μl/g) immediately after BBB opening mediated by FUS (the procedure is presented in 2.5) and allowed to circulate for 4 hours before sacrifice. The whole brain of mice was harvested. The upper surface and coronal plane of the sonicated brain region were pictured; then, the leakage of EB was observed.

H&E and TUNNEL staining was performed as a part of evidence regarding safety. For H&E staining, a set of HE dye solution (Servicebio G1003, Wuhan, Hubei, China) was used. Paraffin sections of the sonicated region were dewaxed through the following steps: incubate sections in 2 changes of xylene for 20 minutes each, 2 changes of 100% ethanol for 5 minutes each, and 75% ethanol for 5 minutes, then rinse with tap water. After dewaxing, sections were stained with hematoxylin solution for 3 to 5 minutes and rinsed with tap water. Then, sections were treated with hematoxylin differentiation solution and rinsed with tap water. Treat the sections with Hematoxylin Scott Tap Bluing, and rinse sections with tap water. Sections were dipped in 85% and 95% ethanol for 5 min, respectively. Then, stain sections with eosin dye for 5 min. Sections were dehydrated via 3 changes of 100% ethanol and 2 changes of xylene for 5 minutes each; finally, sections were sealed with neutral gum. We observed and photographed sections with a digital microscope. For TUNNEL staining, sections of the sonicated brain region were deparaffinized and rehydrated through a graded series of xylene to distilled water. To detect apoptosis of the sonicated brain tissue, a TUNNEL kit (Servicebio G1501, Wuhan, Hubei, China) was used to stain sections following the manufacturer's instructions. Sections were observed and photographed with a digital microscope.

2.4. Establishment of the AD-Like Experimental Mouse Model. We established an AD-like experimental mouse model via ICV injection of $A\beta_{1\text{-}42}$. The surgical procedure was adapted from the literature [28]. $A\beta_{1\text{-}42}$ (Millipore-Sigma, Burlington, MA, USA) was dissolved in normal saline to prepare a stock solution with a final concentration of 1 μg/μl and then incubated at 37°C for 5 days to gain the fibrillized form. Mice were anesthetized by i.p. injection of 2% sodium pentobarbital (45 mg/kg). An incision of the scalp was made, and a total of 2 μl incubated $A\beta_{1\text{-}42}$ (1 μg/μl) was injected into the left lateral ventricle (coordinates from bregma: -0.94 mm anterior/posterior, 1.80 mm medial/lateral, and -2.40 mm dorsal/ventral) via a 5 μl microsyringe with a speed of 0.2 μl/min using a stereotaxic apparatus (RWD D02967, Shenzhen, Guangdong, China). The needle was left at the injected site for an additional five minutes, then withdrawn slowly (1 mm per minute) until complete removal from the brain. The incision of the scalp was sutured at last. Animal body temperature was maintained by an electric heating pad during and after the surgical procedure until the mouse got completely awake.

2.5. GAS Treatment and BBB Opening via FUS. Mice were administrated GAS via i.p. injection once a day (100 mg/kg) for a total of 15 days (from day 3 to day 17). BBB opening mediated by FUS was performed three days once for a total of 5 times (day 5, 8, 11, 14, and 17) within treatment duration to prevent adverse events such as phlebitis of the caudal vein. To facilitate the opening of mice BBB, the fur on the scalp was removed before any treatment with a depilatory cream. A transducer adaptor was 3D printed to guide ultrasound focus to the left hippocampus. FUS transducer was loaded into the adaptor with ultrasound couplant filled in between and was preprepared before the FUS procedure. The transducer was driven by a waveform generator (RIGOL DG4202, Suzhou, Jiangsu, China) and a power amplifier (Mini-Circuits LZY-22+, New York, USA) to generate FUS. The total exposure time of sonication lasts for 120 seconds, and other parameters are as follows: fundamental frequency, 1 MHz; burst duration, 10 ms; pulse repetition frequency, 1 Hz (Figure 2); and microbubbles, SonoVue®, 2.5 μl/g, with output voltage from the waveform generator set to 200 mV. FUS-mediated BBB opening or placebo operation was carried out immediately once GAS was injected. In summary, the mice were anesthetized with 1.5% isoflurane/oxygen using an isoflurane vaporizer (RWD R500, Shenzhen, Guangdong, China) and were fixed by using a mouse brain fixator with continuous anesthesia. Ultrasound couplant was filled between the transducer and mouse scalp, and the center of the transducer was aligned to the sonication site (coordinates from bregma: -2.70 mm anterior/posterior, 2.50 mm medial/lateral) via iron support. Microbubbles (SonoVue®) were diluted in normal saline then injected intravenously into the tail vein (2.5 μl/g) 10 seconds prior to FUS sonication (Figure 3). Mice were put on an electric heating pad after the sonication to recover.

2.6. Y-Maze Test. Y-maze test was performed on day 18 to evaluate the working memory performance of mice. The apparatus is Y-shaped, consisting of 3 light-blue, opaque

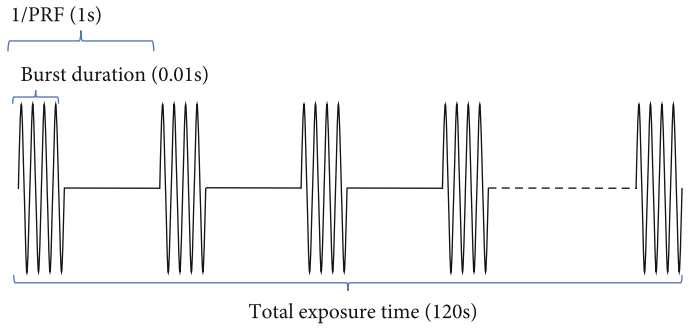

Figure 2: Schematic FUS parameters with 1 Hz pulse repetition frequency (PRF) and 1% duty cycle (DC).

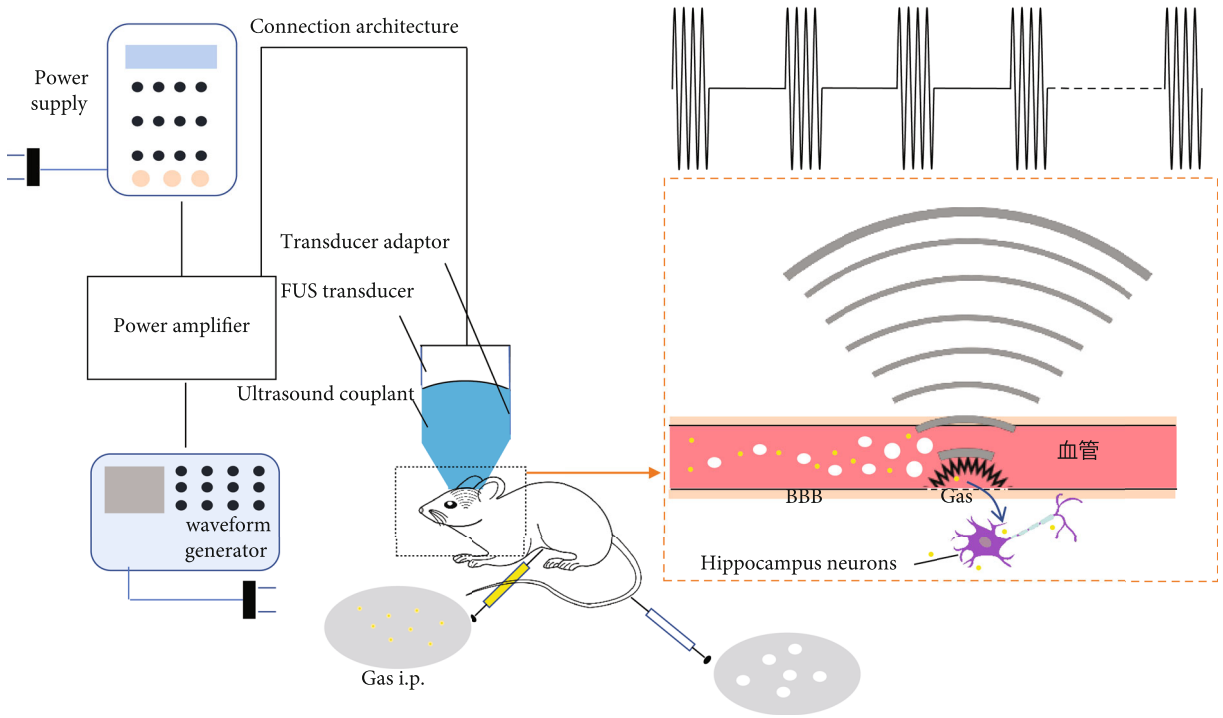

Figure 3: (a) Flow chart of combined treatment (BBB opening via FUS and GAS treatment). (b) Schematic diagram of BBB opening via FUS with the presence of microbubbles.

arms (30 cm long × 8 cm wide × 15 cm high), orientated at 120° from each other, connected by an intersection. A camera was fixed above the maze and videoed the activities of mice for analysis. One of the three arms was blocked to be the novel arm, and the arm that mice were placed in the beginning was recognized as the start arm. The training and testing section lasted 3 minutes with a 1-hour interval between each section. In the training section, the novel arm was blocked. The mice were introduced to the distal end of the start arm and allowed to explore the maze freely. In the testing section, the blockage of the novel arm was removed, and mice were introduced at the same position for testing. The time that mice spent in the novel arm was calculated.

2.7. Tissue Preparation. After the behavior test, mice were dealt with an overdose of 2% sodium pentobarbital i.p. and were perfused transcardially with prechilled saline (4°C). The left hippocampus was harvested ($n = 5$) rapidly for western blotting (WB) analysis and stored at −80°C immediately after collection until use.

2.8. Western Blotting Analysis. Tissue was weighed and dissected; then, radioimmunoprecipitation assay (RIPA) buffer (-
RIPA : phenylmethylsulfonyl fluoride (PMSF) = 1 ml : 10 μl
) was added. The tissue was homogenized via ultrasound and lysed on ice for 30 minutes, then centrifuged at 12000 r/min for 30 min at 4°C, and the supernatant was collected. The concentration of total protein was quantitated by an enhanced bicinchoninic acid (BCA) protein assay kit (Beyotime, China) and equalized to 30 μg/10 μl. Samples that contain a total of 30 μg protein were resolved by 10% sodium dodecyl sulfate-polyacrylamide gel electrophoresis

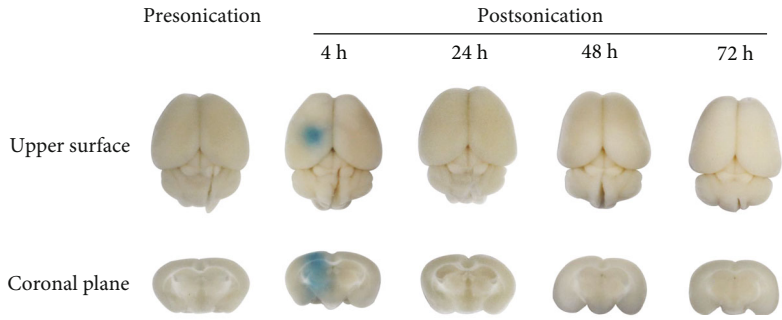

Figure 4: EB staining of mouse brain before/after FUS sonication. Obvious EB leakage is shown in the figure at 4 h after FUS sonication, while there is no EB staining presonication and at 24, 48, and 72 h postsonication.

(SDS-PAGE) and transferred to polyvinylidene difluoride (PVDF) membranes (MilliporeSigma, Burlington, MA, USA). The membranes were blocked in 5% skim milk (taking Tris-buffered saline containing Tween 20 (TBST) as solvent) at room temperature, then incubated with appropriate primary antibodies at 4°C and were shaken gently. The primary antibodies used were monoclonal antibodies (mAbs) against Aβ (1 : 1000; Proteintech, China), tau (1 : 1000; Proteintech, China), BDNF (1 : 1000; Proteintech, China), synaptophysin (1 : 1000; Proteintech, China), β-actin (1: 2000; Santa Cruz Biotechnology, Dallas, TX, USA), polyclonal antibodies against P-tau (1 : 1000; Proteintech, China), AQP4 (1 : 1000; Proteintech, China), and PSD-95 (1 : 1000; Proteintech, China). Subsequently, we washed the membranes with TBST three times (15 minutes per time). Membranes were then incubated with horseradish peroxidase- (HRP-) conjugated goat anti-rabbit/mouse immunoglobulin G (IgG) secondary antibody (1 : 2000; Cell Signaling Technology, Danvers, MA, USA) for 2 hours at room temperature and washed three times with TBST. An enhanced chemiluminescence kit (ECL; Tanon, Shanghai, China) and Amersham Imager 600 (GE Healthcare Life Science, USA) were used to visualize and capture protein bands. A software—ImageJ (US National Institutes of Health, Bethesda, MD, USA)—was used to normalize the protein concentration, taking β-actin as reference.

2.9. Statistical Analysis. Results are presented as mean ± standard deviation (SD). SPSS version 20.0 (IBM Corp., Armonk, NY, USA) was used for all statistical analyses, and graphs were generated by GraphPad Prism software version 7.0 (GraphPad Software, Inc., San Diego, CA, USA). One-way analysis of variance (ANOVA) and two-factor ANOVA were used to process the time that mice spent in the novel arm and WB results. $P < 0.05$ was considered statistically significant.

3. Results

3.1. Safety of BBB Opening Mediated by FUS. We photographed the upper surface of mice's brains and the coronal plane of the sonicated region to observe the leakage of EB from the blood circulation. For mice that were sacrificed at 4 h after FUS sonication, obvious leakage in the brain parenchyma (including the targeted hippocampus) was observed, implying that BBB was effectively opened by FUS. However, there was no EB staining in mouse brains at 24 h, 48 h, and 72 h after FUS sonication (Figure 4), which indicates that FUS-mediated BBB opening in our experiment is reversible and the BBB closed within 24 h, avoiding the infectious risk of the central nervous system induced by long-term BBB opening.

H&E staining showed no bleeding, cellular edema, nuclear fragmentation, or neutrophil infiltration in the sonicated region at 4 h, 24 h, 48 h, and 72 h after FUS-mediated BBB opening (Figure 5). TUNNEL staining of the targeted brain region at the same time points showed no significant apoptosis compared with brains that underwent placebo FUS treatment (Figure 6).

Collectively, the BBB of the sonicated brain region was effectively opened by FUS technology in our experiment and restored to the close state within 24 h, causing no bleeding and apoptosis until the next round of treatment.

3.2. FUS-Mediated BBB Opening Combined with GAS Treatment Increased the Time That AD-Like Mice Spent in the Novel Arm. As shown in Figure 7, the time that untreated mice spent in the novel arm was significantly decreased in comparison to the control group ($P < 0.05$), implying that short-term memory was lesioned in ICV A$\beta_{1\text{-}42}$-injected AD-like mouse model. On the other hand, FUS+GAS treatment statistically increased the time that mice spent in the novel arm compared with that of untreated mice ($P < 0.01$). For GAS and FUS groups, the mean time that mice spent in the novel arms was longer than that in untreated mice, but there was no significance (NS) between groups ($P > 0.05$).

3.3. FUS-Mediated BBB Opening Combined with GAS Treatment Reduced Contents of AD Biomarkers in the Observed (the Left) Hippocampus. We explored the level of Aβ, tau, and P-tau in the observed (the left) hippocampus of mice from different groups. For Aβ, the WB results (Figures 8(a) and 8(b)) revealed that ICV injection of A$\beta_{1\text{-}42}$ significantly increased Aβ level in the observed hippocampus ($P < 0.05$), indicating the mouse model simulated the Aβ pathology of AD. In terms of the Aβ content and the

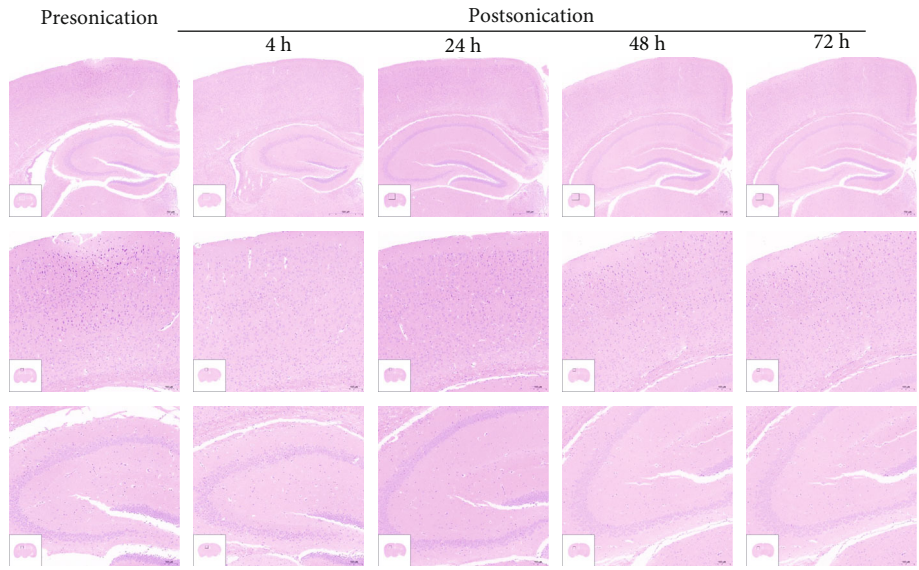

Figure 5: HE staining ((a) ×40, scale bar = 500 μm; (b, c) ×100, scale bar = 100 μm) shows that FUS-mediated BBB opening induced no edema, hemorrhage, or cell necrosis at 4, 24, 48, and 72 h postsonication.

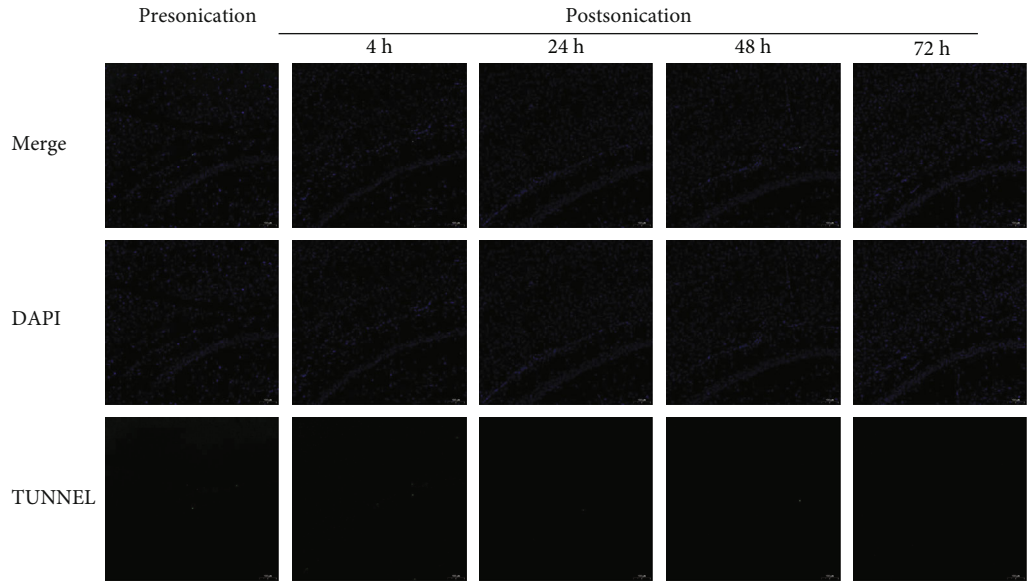

Figure 6: TUNNEL staining (×100, scale bar = 100 μm) shows that there is no significant apoptosis at 4, 24, 48, and 72 h postsonication compared with presonication.

behavioral performance, we successfully established an AD-like mouse model. FUS+GAS reduced the content level of Aβ in comparison to untreated mice ($P < 0.05$), while single GAS/FUS treatment failed to downregulate the Aβ level in the targeted hippocampus ($P > 0.05$). As for tau (Figures 8(c) and 8(d)) and P-tau (Figures 8(e) and 8(f)), combined treatment (FUS+GAS) also exerted an eliminative effect compared with the untreated group ($P < 0.05$). Similarly, single treatment (GAS/FUS treatment) was not enough to reduce the level of tau ($P > 0.05$) as well as P-tau ($P > 0.05$) in the targeted brain region. There was no statistical significance between control and untreated mice ($P > 0.05$) when it came to tau and P-tau.

3.4. FUS-Mediated BBB Opening Combined with GAS Treatment Upregulated the Expression of AQP4 in the Targeted Hippocampus. After a duration of 15-day intervention, FUS+GAS treatment upregulated the expression of AQP4 in the targeted hippocampus compared with untreated mice ($P < 0.05$, Figure 9). There was no significant difference between control and untreated, GAS and untreated, and FUS and untreated groups, respectively ($P > 0.05$).

3.5. FUS-Mediated BBB Opening Combined with GAS Treatment Upregulated BDNF, SYN, and PSD-95 Expressions in the Targeted Hippocampus. In this study, the WB results showed a significant increase of BDNF level in the targeted

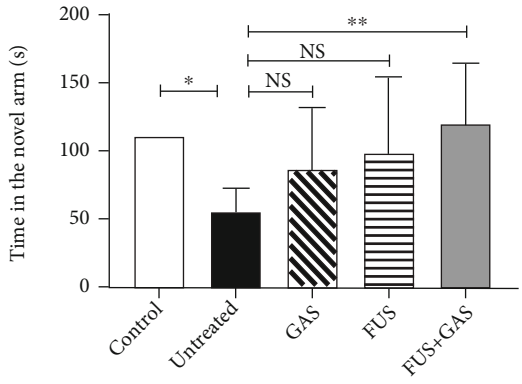

Figure 7: Protective effect of combined treatment (FUS+GAS) on short-term memory of AD-like mice. The time that AD-like mice spent in the novel arm of Y-maze was significantly shortened in comparison to control mice while prolonged via the combined treatment. Each symbol represents the mean ± SD; $^{**}P < 0.01$ against untreated mice; $^{*}P < 0.05$ against untreated mice. One-way ANOVA; $n = 6$ per group.

hippocampus of the FUS+GAS group when compared with untreated mice ($P < 0.01$, Figures 10(a) and 10(b)). In contrast, statistical significance was absent between untreated mice and the remaining groups ($P > 0.05$). For SYN, the combined treatment (FUS+GAS treatment) exerted a promoting effect of expression in comparison to the untreated group ($P < 0.01$, Figures 10(c) and 10(d)). Single GAS/FUS treatment was not enough to induce such an effect of SYN level ($P > 0.05$). There was no statistical significance either between the control and untreated groups ($P > 0.05$). The results of PSD-95 were similar to those of SYN. Combined treatment rather than single GAS/FUS intervention upregulated the expression of PSD-95 in the targeted hippocampus ($P < 0.05$, Figures 10(e) and 10(f)). A significant change was absent between control and untreated mice ($P > 0.05$).

3.6. The Statistic Results Processed by Two-Factor ANOVA. We processed the time that mice spent in the novel arm and the WB results via two-factor ANOVA, trying to make it clear that whether the therapeutic effect of FUS+GAS is a result of additive effect. The P values are all above 0.05 as illustrated in Supplementary table 1.

4. Discussion

In this study, we demonstrated effective BBB disruption without evidence of tissue hemorrhage and apoptosis within the sonicated region on KM mice. EB staining confirmed the disrupted BBB area of the brain (including the left hippocampus) at 4 h after sonication. There was no EB leakage observed at 24 h, 48 h, and 72 h postsonication in the targeted brain region, indicating that the BBB restored automatically within 24 h. Furthermore, HE as well as TUNNEL staining at both early (4 h) and late time points (24, 48, and 72 h) revealed no blood corpuscle and apoptosis within the sonicated brain region. The BBB opening mediated by FUS in the present study is reversible and well tolerated without evidence of tissue damage.

Based on these experimental results, we further reported that FUS-mediated BBB opening combined with GAS treatment rather than single GAS/FUS intervention has multiple anti-AD effects on an AD-like experimental mouse model. We established the model successfully via ICV injection of $A\beta_{1\text{-}42}$, in which the time that mice stayed in the novel arm of Y-maze is statistically shortened, and the $A\beta$ level increased in the observed hippocampus. The combined treatment of BBB opening via FUS and GAS alleviates neuropathology of the AD-like mice by reducing the content of $A\beta$ in the targeted hippocampus and attenuating the level of tau as well as P-tau in the same region.

$A\beta$, tau, and P-tau are biomarkers of AD and have been explored as diagnostic markers in blood and cerebrospinal fluid [29]. In AD, $A\beta$ fibrils polymerize into insoluble amyloid fibrils that aggregate into senile plaques, which activate kinases, leading to hyperphosphorylation of tau and its polymerization into insoluble neurofibrillary tangles. The plaques and neurofibrillary tangles activate microglia and promote local inflammation, contributing to neurotoxicity [4]. Several studies take inhibiting $A\beta$ synthesis as a therapeutic strategy for AD. It is well learned that GAS has the potential to suppress the activities of β-secretase (BACE) [15, 16] and γ-secretase [16]. Both secretases facilitate the synthesis of $A\beta$. Lim et al. reported decreased $A\beta$ aggregation as well as the inhibition of BACE activity in $A\beta$-injected AD-like mice under the treatment of bojungikgi-tang (a traditional herbal formula), which ameliorates memory impairment and protects neurons [30]. In the present study, we found that not only $A\beta$ but also tau as well as P-tau were markedly decreased under the combined treatment. The possible mechanism, an enhanced waste-cleaning function of the brain, is much less reported. Evidence suggests that abnormal aggregation of tau, combined with its decreased clearance, intensifies neurotoxicity in AD [31]. The imbalance of production and clearing of substances such as $A\beta$ and tau is closely linked to the progression of AD pathology [31, 32]. The paravascular pathways in which AQP4 plays an important role are largely involved in the waste-cleaning effect [33]. Studies have shown that the exogenous $A\beta$ which was injected into the brain can be cleared via the paravascular pathways [34, 35]. Accumulated evidence has shown that AQP4 is involved in the pathogenesis of AD. AQP4 is the most extensively expressed aquaporin on astrocytic endfeet in the brain [36], functions as a water channel, and is of great significance in maintaining brain homeostasis [37]. AQP4 is vital for waste clearance including $A\beta$. In the AQP4-null mice, 55% of $A\beta$ clearance was blocked [35]. Another research demonstrated that tau can be cleaned from the brain through the paravascular pathway too, and the deletion of the AQP4 gene led to decreased waste-cleaning function, and elevated P-tau level in traumatic brain injury mice, increased axonal degeneration, neuroinflammation, and exacerbation of posttraumatic cognitive deficits were observed [33]. In our study, the pronounced elevation of AQP4 level was detected in the targeted hippocampus after 15-day combined treatment in AD-like mouse, implying that FUS-mediated BBB opening combined with GAS treatment enhanced the waste-cleaning function of the brain,

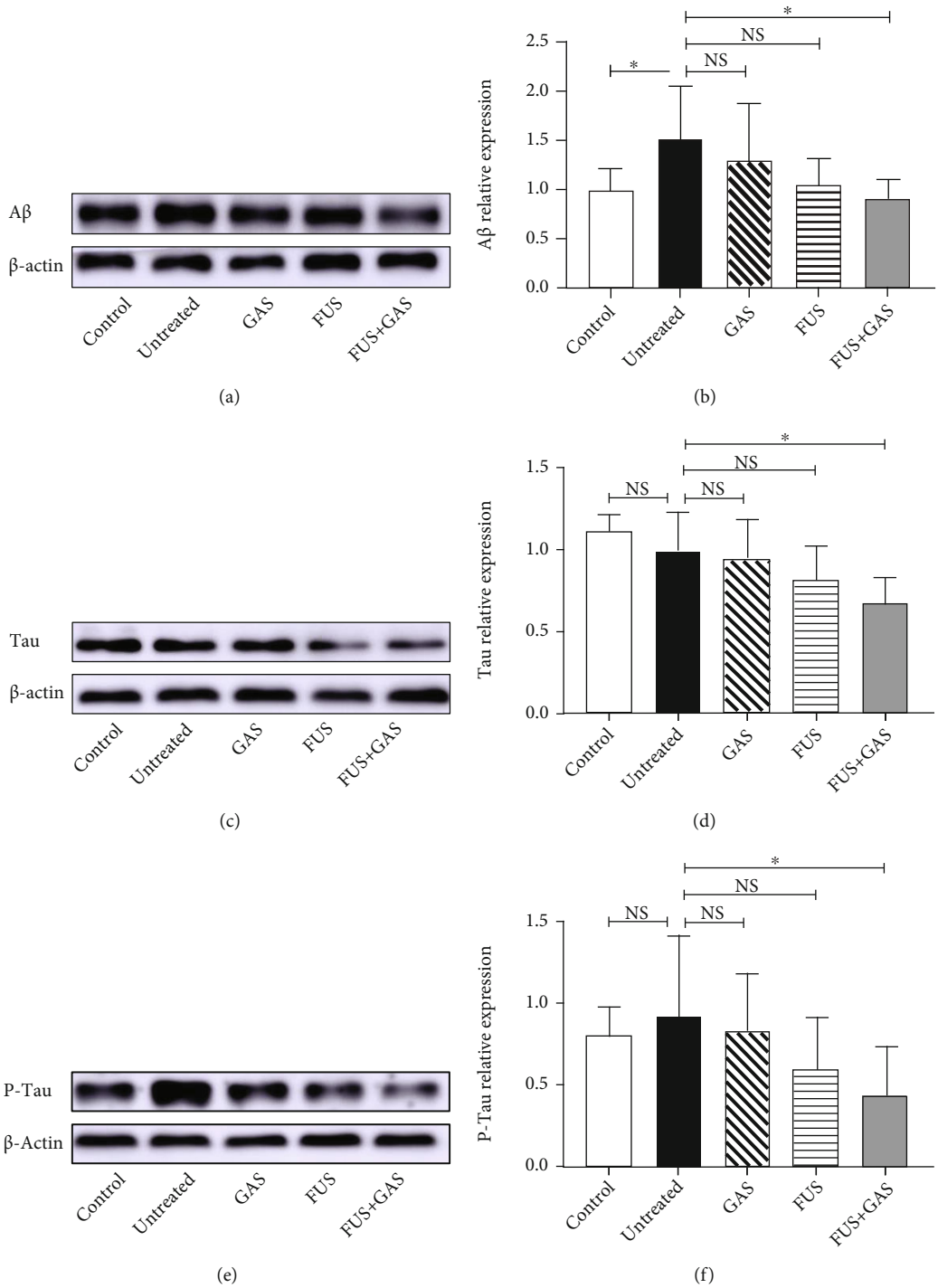

Figure 8: The effects of combined treatment (FUS+GAS) on the level of Aβ (a, b), tau (c, d), and P-tau (e, f) in the left hippocampus. The content of Aβ was increased markedly in the untreated group. Combined treatment reduced the content of Aβ, tau, and P-tau in the targeted hippocampus. Each symbol represents the mean ± SD; $^*P < 0.05$ against untreated mice. One-way ANOVA; $n = 5$ per group.

which may explain the neuropathological improvement of AD-like mice. In this study, we find remarkable therapeutic efficiency of combined treatment rather than single GAS/FUS intervention on AD-like mice, implying that a combination of BBB opening via FUS and GAS treatment may be an advisable strategy to deal with AD.

AD is characterized by aggravating cognitive deficits [38], which benefit little from current medications. One of the vital findings in the present study is that FUS+GAS treatment prolonged the time that AD-like mouse spent in the novel arm as measured by the Y-maze test, indicating that FUS-mediated BBB opening of the targeted (the left)

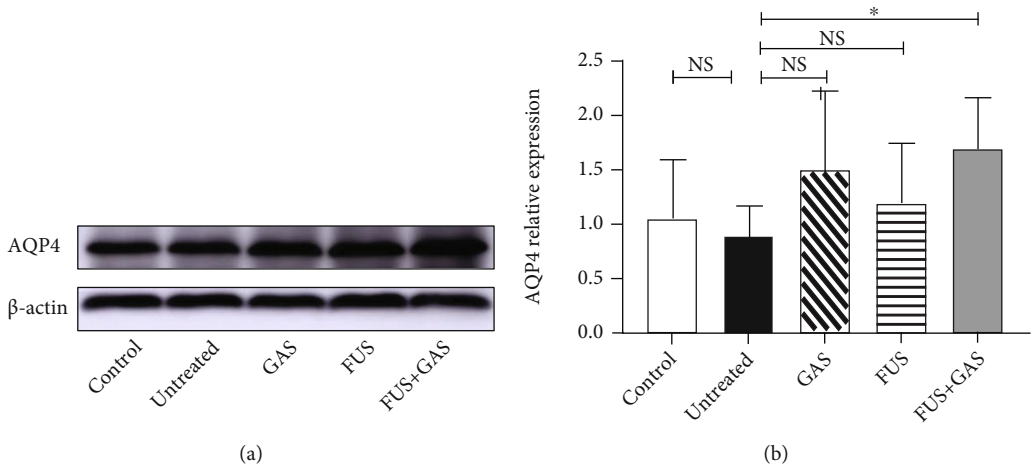

Figure 9: WB analysis of AQP4 level in sonicated hippocampus 15-days after interventions. The combined treatment of BBB opening via FUS and GAS remarkably increased the content of AQP4 in the targeted hippocampus, indicating a stronger waste-cleaning function. Each symbol represents the mean ± SD; $^*P < 0.05$ against untreated mice. One-way ANOVA; $n = 5$ per group.

hippocampus combined with GAS treatment exerts an ameliorative effect on short-term memory function in the AD-like mouse model. It has been suggested that the right hippocampus plays a more important role in spatial-related short-term memory in respect of human [39], and there have been lasting explorations about functional lateralization of the hippocampus in rodents. Results from Sakaguchi and Sakurai suggest that the bilateral hippocampus of Wistar albino rats is involved in short-term memory. The right hippocampus plays a facilitating role while the left exerts the opposite, that is, a suppressive effect [40]. It appears [41] that when it comes to short-term memory, the right hippocampus plays a predominant role. The results from Shipton *et al.* [42], however, provide evidence that an intact left hippocampus is essential for the short-term memory. The study reported that unilateral silencing of either the left or right CA3 was sufficient to impair short-term memory (as measured by Y-maze and T-maze), whereas the left rather than the right CA3 silencing impaired performance on an associative spatial long-term memory task, suggesting a significant role of the left hippocampus on both long- and short-term memory, which may explain the discovery in our study; that is, FUS-mediated BBB opening of the left hippocampus combined with GAS treatment improved short-term memory function as measured by Y-maze.

Studies have revealed that the loss of synapses is the most relevant neurobiological basis of AD's cognitive impairment [43]. In AD, disabled plasticity impacts negatively on synaptic remodeling, axonal sprouting, neurogenesis, synaptogenesis, and long-term potentiation (LTP) [44], which enhances the efficiency of synapses and is thought to underlie memory and learning [45]. The hippocampus is a brain area critical for learning and memory, which is well-established vulnerable to damages such as synapse loss at the early age of AD [46, 47]. To explore whether the combined treatment has an impact on plasticity of the sonicated hippocampus, we evaluated the level of BDNF, SYN, and PSD-95 via WB.

As an important neurotrophin, BDNF is highly expressed in the brain and exerts vital effects on regulating synapses both structurally and functionally. BDNF is an ideal and essential regulator of cellular processes underlying cognition [45]. Numerous studies have demonstrated the critical role of BDNF in terms of hippocampal LTP. Deletion of the BDNF gene in mice causes impaired LTP, which was rescued by recombinant BDNF [48, 49]. SYN is the most abundant integral membrane protein of small synaptic vesicles, constituting 6% to 8% of the synaptic vesicle membrane protein [50]. Involved in the secretion, recycling of synaptic vesicles, and neurotransmitter releasing, SYN continues to be the most widely used marker for synapse density [51], and a great number of papers quote SYN as a synaptic marker [44, 51]. As a postsynaptic marker [44], PSD-95 is an abundant scaffold protein of postsynaptic density, regulates synaptic transmission, and plays an important role in synaptic plasticity, learning, and memory [52].

Our results showed that the combined treatment of FUS-mediated BBB opening and GAS administration remarkably elevated the level of a neurotrophin (BDNF), a presynaptic marker (SYN), and a postsynaptic marker (PSD-95) in the targeted hippocampus, indicating a BDNF-stimulating effect and better neuroplasticity resulting from the combined intervention, which may be the underlying mechanism of behavioral improvement that AD-like mice presented in the Y-maze. In our study, the level of SYN and PSD-95 from control to untreated mice seems to be a rising trend, which may be possibly explained by the transient adaptive synaptic response in the pathologic process of AD [53, 54].

Gastrodia elata Blume (Orchidaceae) has been long used for its anticonvulsant, analgesic, and sedative effect in countries such as China [55]. As a phenolic glycoside extracted from traditional Chinese herb, Gastrodia elata, GAS is a main active constituent of rhizoma gastrodiae. The action mechanism of GAS has been studied for more than 40 years since its isolation in 1978 [17]. Investigations reveal that GAS suppresses γ-aminobutyric acid (GABA) transaminase

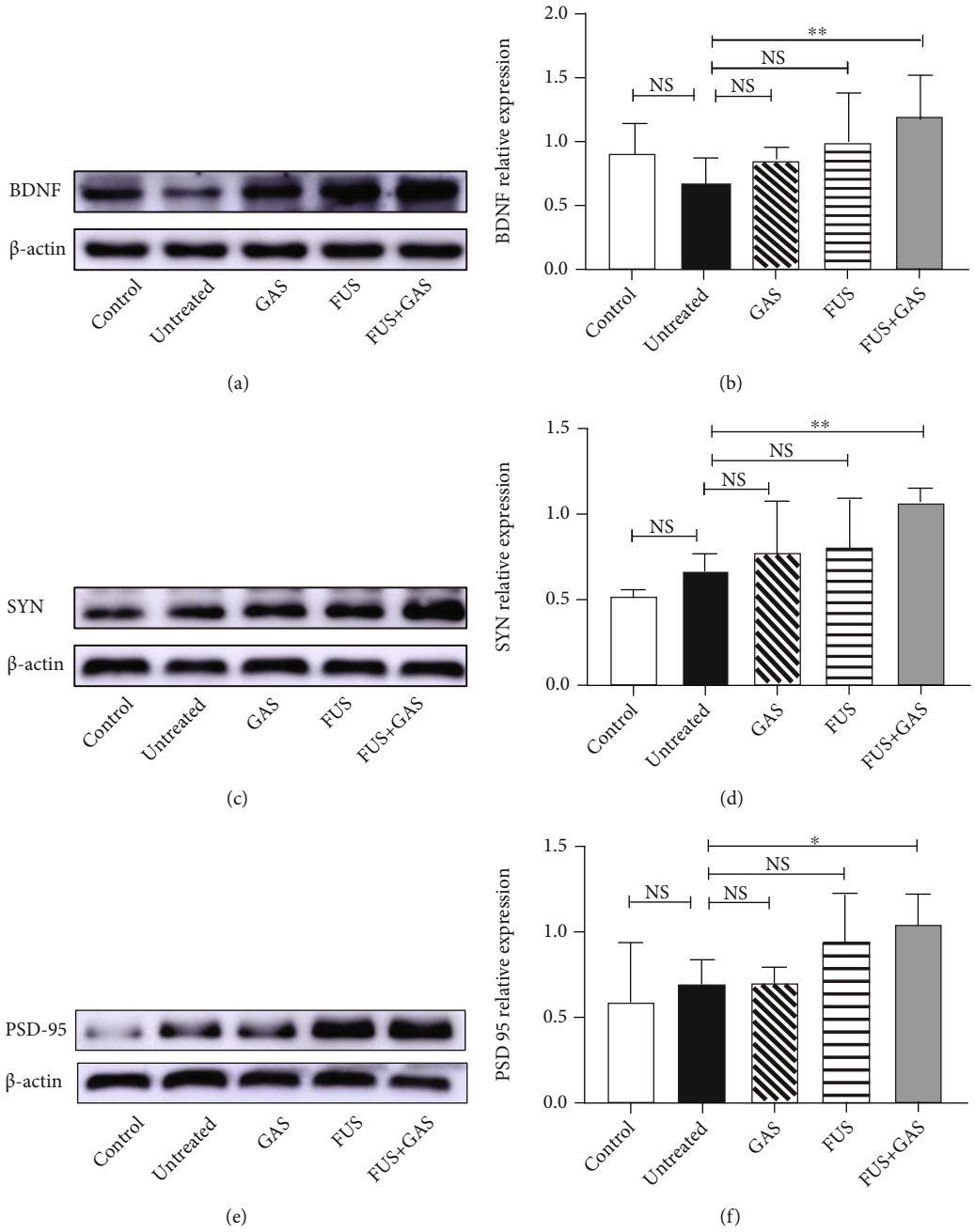

Figure 10: Relative concentrations of BDNF (a, b), SYN (c, d), and PSD-95 (e, f) in the sonicated hippocampus of all groups. Combined treatment (GAS+FUS) statistically upregulated the level of BDNF, SYN, and PSD-95 while single treatment (GAS/FUS alone) failed to. Each symbol represents the mean ± SD; $^{**}P < 0.01$ against untreated mice; $^{*}P < 0.05$ against untreated mice. One-way ANOVA; $n = 5$ per group.

to increase GABA concentration [56] and exerts antioxidant and antiapoptotic effect [17], benefiting epilepsy. What is more, by inhibiting the increase of extracellular glutamate level and blocking the elevation of intracellular Ca^{2+} and neuronal NO synthesis, GAS generates a neuroprotective action [57]. The antiamnestic effect has been explored as well [58, 59]. By normalizing the serotoninergic system [60] and the dopaminergic system [61], GAS ameliorates memory deficits in 3,3′-iminodipropionitrile-induced rats. Our present study demonstrates the memory protective effect of BBB opening via FUS combined with GAS treatment in $A\beta_{1\text{-}42}$-induced AD-like mouse, possibly via the BDNF-stimulating and neuroplasticity-promoting effect.

In summary, our results reveal that FUS-mediated BBB opening combined with GAS treatment reduces the content of $A\beta$, tau, and P-tau in the targeted hippocampus in an ICV $A\beta_{1\text{-}42}$-injected AD-like experimental mouse model possibly because of the elevated content of AQP4, which implies a stronger waste-cleaning function. Results demonstrate that the combined treatment upregulated the level of BDNF,

SYN, and PSD-95, which contribute to short-term memory improvement in the AD-like experimental mouse model. Exerting the potential to alleviate memory deficit and neuropathology of the AD-like mouse model, FUS-mediated BBB opening combined with GAS treatment may be a novel strategy for AD treatment.

5. Limitations

There are several limitations in our study. Firstly, we established an AD-like mouse model via ICV injection of $A\beta_{1\text{-}42}$ and explored the anti-AD effects of BBB opening via FUS combined with GAS treatment. The therapeutic effect needs to be verified further on a transgenic model such as APP/PS1 mice. Moreover, we observed that the levels of AQP4, BDNF, SYN, and PSD-95 were elevated after the combined intervention, while the mechanisms by which it affects the expressions of the above proteins are unclear. Investigations are needed, and several issues are required to be addressed further. Given the view of functional lateralization of the hippocampus, BBB opening of the right hippocampus may be carried out to see whether there is any difference in terms of short-term or long-term memory outcome. Although the results suggest that combined treatment of BBB opening via FUS and GAS treatment exerts therapeutic potential of AD treatment in this study, the present statistic failed to clarify whether the therapeutic effect is a result of additive effect induced by BBB opening mediated by FUS combined with GAS treatment (as illustrated in supplementary table 1) possibly owing to influence factors such as sample size, dose, and frequency of GAS administration, which should be confirmed in the next-step study with a refined design.

6. Conclusions

The combined treatment of BBB opening by FUS and GAS exerts a memory protective effect in the $A\beta_{1\text{-}42}$-induced AD-like mouse model. Moreover, the combined treatment alleviates neuropathology; the content of $A\beta$, tau, and P-tau is reduced possibly via a powerful waste-cleaning effect induced by the upregulation of AQP4. The combination of BBB opening via FUS and GAS treatment may be an advisable strategy to deal with AD.

Abbreviations

AD: Alzheimer's disease
AQP4: Aquaporin-4
$A\beta$: Beta-amyloid
BACE: β-Secretase
BBB: Blood-brain barrier
BDNF: Brain-derived neurotrophic factor
ChEIs: Cholinesterase inhibitors
FUS: Focused ultrasound
GABA: γ-Aminobutyric acid
GAS: Gastrodin
ICV: Intracerebroventricular
KM: Kunming
NFTs: Neurofibrillary tangles
NMDA: N-Methyl-d-aspartate
PSD-95: Postsynaptic density protein 95
P-tau: Phosphorylated tau
SYN: Synaptophysin.

Data Availability

The data supporting the findings of present study is available from the corresponding author upon request.

Conflicts of Interest

The authors declare that they have no conflicts of interest.

Authors' Contributions

Kaixuan Luo and Yuhong Wang contributed equally to this manuscript.

Acknowledgments

The authors owe their deepest gratitude to Li Jin and Manxi Huang, who have supported in language, and to Zhicong Jing, who has supported in illustration. This study was aided financially and supported by the National Natural Science Foundation of China (Nos. 81960421, 81660381, and 82060421) and the Science and Technology Innovative Team Grant of Kunming Medical University (CXTD201905).

Supplementary Materials

Supplementary table 1: the statistic results processed by two-factor ANOVA. *(Supplementary Materials)*

References

[1] World Health Organization, *Global action plan on the public health response to dementia 2017-2025*, WHO, 2017.

[2] M. P. Greenwood, M. Greenwood, A. S. Mecawi, J. Antunes-Rodrigues, J. F. R. Paton, and D. Murphy, "Rasd1, a small G protein with a big role in the hypothalamic response to neuronal activation," *Molecular Brain*, vol. 9, no. 1, pp. 1–22, 2016.

[3] P. Leandro and C. Gomes, "Protein misfolding in conformational disorders: rescue of folding defects and chemical chaperoning," *Mini Reviews in Medicinal Chemistry*, vol. 8, no. 9, pp. 901–911, 2008.

[4] S. Tiwari, V. Atluri, A. Kaushik, A. Yndart, and M. Nair, "Alzheimer's disease: pathogenesis, diagnostics, and therapeutics," *International Journal of Nanomedicine*, vol. 14, pp. 5541–5554, 2019.

[5] P. Scheltens, K. Blennow, M. M. B. Breteler et al., "Alzheimer's disease," *Lancet*, vol. 388, no. 10043, pp. 505–517, 2016.

[6] J.-E. Morley, S.-A. Farr, and A.-D. Nguyen, "Alzheimer disease," *Clinical Geriatrics*, vol. 34, no. 4, pp. 591–601, 2018.

[7] S. Jeong, "SR Proteins: Binders, Regulators, and Connectors of RNA," *Molecules and Cells*, vol. 40, no. 1, pp. 1–9, 2017.

[8] S.-H. Barage and K.-D. Sonawane, "Amyloid cascade hypothesis: pathogenesis and therapeutic strategies in Alzheimer's disease," *Neuropeptides*, vol. 52, pp. 1–18, 2015.

[9] A. Atri, "Current and Future Treatments in Alzheimer's disease," *Seminars in Neurology*, vol. 39, no. 2, pp. 227–240, 2019.

[10] J. Montastruc, A. Gallini, and A. Sommet, "Does memantine induce bradycardia ? A study in the French PharmacoVigilance Database," *Pharmacoepidemiology and Drug Safety*, vol. 17, pp. 877–881, 2008.

[11] US Food and Drug Adminstration, *FDA News & Events for Human Drugs: FDA's decision to approve new treatment for Alzheimer's disease*, 2021, https://www.fda.gov/drugs/news-events-human-drugs/whats-new-related-drugs.

[12] M. Li and S. Qian, "Gastrodin protects neural progenitor cells against amyloid β (1–42)-induced neurotoxicity and improves hippocampal neurogenesis in amyloid β (1–42)-injected mice," *Journal of Molecular Neuroscience*, vol. 60, no. 1, pp. 21–32, 2016.

[13] Y. Hu, C. Li, and W. Shen, "Gastrodin alleviates memory deficits and reduces neuropathology in a mouse model of Alzheimer's disease," *Neuropathology*, vol. 34, no. 4, pp. 370–377, 2014.

[14] X. Zhao, Y. Zou, H. Xu et al., "Gastrodin protect primary cultured rat hippocampal neurons against amyloid- beta peptide-induced neurotoxicity via ERK1/2-Nrf2 pathway," *Brain Research*, vol. 1482, pp. 13–21, 2012.

[15] J.-S. Zhang, S. F. Zhou, Q. Wang et al., "Gastrodin suppresses BACE1 expression under oxidative stress condition via inhibition of the PKR/eIF2α pathway in Alzheimer's disease," *Neuroscience*, vol. 325, pp. 1–9, 2016.

[16] R. Zhu, T.-X. Huang, X.-M. Zhao, J.-M. Zhang, and P. Liang, "Screening of 10 types of Chinese herbal compounds inhibiting Aβ and their possible related mechanism in vitro," *Yao xue xue bao= Acta pharmaceutica Sinica*, vol. 49, pp. 800–806, 2014.

[17] Y. Liu, J. Gao, M. Peng et al., "A review on central nervous system effects of gastrodin," *Frontiers in Pharmacology*, vol. 9, p. 24, 2018.

[18] M. Han, Y. Hur, J. Hwang, and J. Park, "Biological effects of blood–brain barrier disruption using a focused ultrasound," *Biomedical Engineering Letters*, vol. 7, no. 2, pp. 115–120, 2017.

[19] H. L. Liu, P. H. Hsu, C. Y. Lin et al., "Focused ultrasound enhances central nervous system delivery of bevacizumab for malignant glioma treatment," *Radiology*, vol. 281, no. 1, pp. 99–108, 2016.

[20] B. Tayier, Z. Deng, Y. Wang, W. Wang, Y. Mu, and F. Yan, "Biosynthetic nanobubbles for targeted gene delivery by focused ultrasound," *Nanoscale*, vol. 11, no. 31, pp. 14757–14768, 2019.

[21] R.-D. Alkins, A. Burgess, M. Ganguly et al., "Focused ultrasound delivers targeted immune cells to metastatic brain tumors," *Cancer Research*, vol. 73, no. 6, pp. 1892–1899, 2013.

[22] D.-B. Miller and J. P. O'Callaghan, "New horizons for focused ultrasound (FUS) - therapeutic applications in neurodegenerative diseases," *Metabolism*, vol. 69, pp. S3–S7, 2017.

[23] D.-P. Darrow, "Focused ultrasound for neuromodulation," *Neurotherapeutics*, vol. 16, no. 1, pp. 88–99, 2019.

[24] J.-F. Jordão, E. Thévenot, K. Markham-Coultes et al., "Amyloid-β plaque reduction, endogenous antibody delivery and glial activation by brain-targeted, transcranial focused ultrasound," *Experimental Neurology*, vol. 248, pp. 16–29, 2013.

[25] A. Burgess, S. Dubey, S. Yeung et al., "Alzheimer disease in a mouse model: MR imaging-guided focused ultrasound targeted to the hippocampus opens the blood-brain barrier and improves pathologic abnormalities and behavior," *Radiology*, vol. 273, no. 3, pp. 736–745, 2014.

[26] J. F. Jordão, C. A. Ayala-Grosso, K. Markham et al., "Antibodies Targeted to the Brain with Image-Guided Focused Ultrasound Reduces Amyloid-β Plaque Load in the TgCRND8 Mouse Model of Alzheimer's Disease," *PLoS One*, vol. 5, no. 5, p. 10549, 2010.

[27] Y. Kung, M. Y. Hsiao, S. M. Yang et al., "A single low-energy shockwave pulse opens blood-cerebrospinal fluid barriers and facilitates gastrodin delivery to alleviate epilepsy," *Ultrasonics Sonochemistry*, vol. 78, article 105730, 2021.

[28] H. Y. Kim, D. K. Lee, B. R. Chung, H. V. Kim, and Y. Kim, "Intracerebroventricular injection of amyloid-β peptides in normal mice to acutely induce Alzheimer-like cognitive deficits," *Journal of Visualized Experiments*, vol. 109, article 53308, 2016.

[29] J. S. Generoso, R. Morales, and T. Barichello, "Biomarkers in Alzheimer disease: are we there yet?," *Brazilian Journal of Psychiatry*, vol. 42, no. 4, pp. 337–339, 2020.

[30] H. S. Lim, Y. J. Kim, E. Sohn, J. Yoon, B. Y. Kim, and S. J. Jeong, "Bojungikgi-tang, a traditional herbal formula, exerts neuroprotective effects and ameliorates memory impairments in Alzheimer's disease-like experimental models," *Nutrients*, vol. 10, no. 12, p. 1952, 2018.

[31] Y. Gao, L. Tan, J. T. Yu, and L. Tan, "Tau in Alzheimer's disease: mechanisms and therapeutic strategies," *Current Alzheimer Research*, vol. 15, no. 3, pp. 283–300, 2018.

[32] S. T. Ferreira and W. L. Klein, "The Aβ oligomer hypothesis for synapse failure and memory loss in Alzheimer's disease," *Neurobiology of Learning and Memory*, vol. 96, no. 4, pp. 529–543, 2011.

[33] J. J. Iliff, M. J. Chen, B. A. Plog et al., "Impairment of glymphatic pathway function promotes tau pathology after traumatic brain injury," *Journal of Neuroscience*, vol. 34, no. 49, pp. 16180–16193, 2014.

[34] K. K. Ball, N. F. Cruz, R. E. Mrak, and G. A. Dienel, "Trafficking of glucose, lactate, and Amyloid-β from the inferior colliculus through perivascular routes," *Journal of Cerebral Blood Flow and Metabolism*, vol. 30, no. 1, pp. 162–176, 2010.

[35] J. J. Iliff, M. Wang, Y. Liao et al., "A paravascular pathway facilitates CSF flow through the brain parenchyma and the clearance of interstitial solutes, including amyloid β," *Science Translational Medicine*, vol. 4, no. 147, p. 147, 2012.

[36] C. Yang, X. Huang, X. Huang et al., "Aquaporin-4 and Alzheimer's Disease," *Journal of Alzheimer's Disease*, vol. 52, no. 2, pp. 391–402, 2019.

[37] S. Mader and L. Brimberg, "Aquaporin-4 water channel in the brain and its implication for health and disease," *Cell*, vol. 8, no. 2, p. 90, 2019.

[38] B. Winblad, P. Amouyel, S. Andrieu et al., "Defeating Alzheimer's disease and other dementias: a priority for European science and society," *Lancet Neurology*, vol. 15, no. 5, pp. 455–532, 2016.

[39] S. Abrahams, R. G. Morris, C. E. Polkey et al., "Hippocampal involvement in spatial and working memory: a structural MRI analysis of patients with unilateral mesial temporal lobe sclerosis," *Brain and Cognition*, vol. 41, no. 1, pp. 39–65, 1999.

[40] Y. Sakaguchi and Y. Sakurai, "Left-right functional difference of the rat dorsal hippocampus for short-term memory and long-term memory," *Behavioural Brain Research*, vol. 382, article 112478, 2020.

[41] S. Klur, C. Muller, A. Pereira de Vasconcelos et al., "Hippocampal-dependent spatial memory functions might be lateralized in rats: an approach combining gene expression profiling and reversible inactivation," *Hippocampus*, vol. 19, no. 9, pp. 800–816, 2009.

[42] O. A. Shipton, M. el-Gaby, J. Apergis-Schoute et al., "Left-right dissociation of hippocampal memory processes in mice," *Proceedings of the National Academy of Sciences*, vol. 111, no. 42, pp. 15238–15243, 2014.

[43] S. Lista and H. Hampel, "Synaptic degeneration and neurogranin in the pathophysiology of Alzheimer's disease," *Expert Review of Neurotherapeutics*, vol. 17, no. 1, pp. 47–57, 2017.

[44] B. Liu, J. Kou, F. Li et al., "Lemon essential oil ameliorates age-associated cognitive dysfunction via modulating hippocampal synaptic density and inhibiting acetylcholinesterase," *Aging*, vol. 12, no. 9, pp. 8622–8639, 2020.

[45] S. D. Skaper, "BDNF and synaptic plasticity, cognitive function, and dysfunction," *Handbook of Experimental Pharmacology*, vol. 220, pp. 223–250, 2014.

[46] Y. Mu and F. H. Gage, "Adult hippocampal neurogenesis and its role in Alzheimer's disease," *Molecular Neurodegeneration*, vol. 6, no. 1, p. 85, 2011.

[47] T. Arendt, "Synaptic degeneration in Alzheimer's disease," *Acta Neuropathologica*, vol. 77, no. 1, pp. 32–42, 2010.

[48] S. L. Patterson, T. Abel, T. A. S. Deuel, K. C. Martin, J. C. Rose, and E. R. Kandel, "Recombinant BDNF rescues deficits in basal synaptic transmission and hippocampal LTP in BDNF knockout mice," *Neuron*, vol. 16, no. 6, pp. 1137–1145, 1996.

[49] M. Korte, P. Carroll, E. Wolf, G. Brem, H. Thoenen, and T. Bonhoeffer, "Hippocampal long-term potentiation is impaired in mice lacking brain-derived neurotrophic factor," *Proceedings of the National Academy of Sciences*, vol. 92, no. 19, pp. 8856–8860, 1995.

[50] G. Thiel, "Synapsin I, synapsin II, and synaptophysin: marker proteins of synaptic vesicles," *Brain Pathology*, vol. 3, no. 1, pp. 87–95, 1993.

[51] F. Valtorta, M. Pennuto, D. Bonanomi, and F. Benfenati, "Synaptophysin: leading actor or walk-on role in synaptic vesicle exocytosis," *BioEssays*, vol. 26, no. 4, pp. 445–453, 2004.

[52] E. Kim and M. Sheng, "PDZ domain proteins of synapses," *Nature Reviews. Neuroscience*, vol. 5, no. 10, pp. 771–781, 2004.

[53] E. B. Mukaetova-Ladinska, F. Garcia-Siera, J. Hurt et al., "Staging of Cytoskeletal and β-Amyloid Changes in Human Isocortex Reveals Biphasic Synaptic Protein Response during Progression of Alzheimer's Disease," *The American Journal of Pathology*, vol. 157, no. 2, pp. 623–636, 2000.

[54] A. Savioz, G. Leuba, and P. G. Vallet, "A framework to understand the variations of PSD-95 expression in brain aging and in Alzheimer's disease," *Ageing Research Reviews*, vol. 157, no. 2, pp. 623–636, 2000.

[55] L. C. Lin, Y. F. Chen, W. C. Lee, Y. T. Wu, and T. H. Tsai, "Pharmacokinetics of gastrodin and its metabolite *p* -hydroxybenzyl alcohol in rat blood, brain and bile by microdialysis coupled to LC-MS/MS," *Journal of Pharmaceutical and Biomedical Analysis*, vol. 48, no. 3, pp. 909–917, 2008.

[56] S. J. An, S. K. Park, I. K. Hwang et al., "Gastrodin decreases immunoreactivities of ?-aminobutyric acid shunt enzymes in the hippocampus of seizure-sensitive gerbils," *Journal of Neuroscience Research*, vol. 71, no. 4, pp. 534–543, 2003.

[57] X. Zeng, S. Zhang, L. Zhang, K. Zhang, and X. Zheng, "A study of the neuroprotective effect of the phenolic glucoside gastrodin during cerebral Ischemiain vivoandin vitro," *Planta Medica*, vol. 72, no. 15, pp. 1359–1365, 2006.

[58] C. R. Wu, M. T. Hsieh, S. C. Huang, W. H. Peng, Y. S. Chang, and C. F. Chen, "Effects ofGastrodia elataand its active constituents on scopolamine-induced amnesia in rats," *Planta Medica*, vol. 62, no. 4, pp. 317–321, 1996.

[59] M. T. Hsieh, C. R. Wu, and C. F. Chen, "Gastrodin and *p* -hydroxybenzyl alcohol facilitate memory consolidation and retrieval, but not acquisition, on the passive avoidance task in rats," *Journal of Ethnopharmacology*, vol. 56, no. 1, pp. 45–54, 1997.

[60] X. Wang, Y. Tan, and F. Zhang, "Ameliorative effect of gastrodin on 3,3′-iminodipropionitrile-induced memory impairment in rats," *Neuroscience Letters*, vol. 594, pp. 40–45, 2015.

[61] X. Wang, S. Yan, A. Wang, Y. Li, and F. Zhang, "Gastrodin ameliorates memory deficits in 3,3′-Iminodipropionitrile-Induced rats: possible involvement of dopaminergic system," *Neurochemical Research*, vol. 39, no. 8, pp. 1458–1466, 2014.

Hindawi
Neural Plasticity
Volume 2021, Article ID 1763533, 14 pages
https://doi.org/10.1155/2021/1763533

Research Article

Early Repetitive Transcranial Magnetic Stimulation Exerts Neuroprotective Effects and Improves Motor Functions in Hemiparkinsonian Rats

Tsung-Hsun Hsieh,[1,2,3] **Xiao-Kuo He**,[4] **Hui-Hua Liu**,[5] **Jia-Jin J. Chen**,[6,7] **Chih-Wei Peng**,[8] **Hao-Li Liu**,[9] **Alexander Rotenberg**,[10] **Ko-Ting Chen**,[11] **Ming-Yuan Chang**,[12,13] **Yung-Hsiao Chiang**,[14] **Pi-Kai Chang**,[1] **and Chi-Wei Kuo**[1]

[1]*School of Physical Therapy and Graduate Institute of Rehabilitation Science, Chang Gung University, Taoyuan, Taiwan*
[2]*Neuroscience Research Center, Chang Gung Memorial Hospital at Linkou, Taoyuan, Taiwan*
[3]*Healthy Aging Research Center, Chang Gung University, Taoyuan, Taiwan*
[4]*Department of Rehabilitation Medicine, Fifth Hospital of Xiamen, Xiamen, China*
[5]*Department of Rehabilitation Medicine, Sun Yat-sen Memorial Hospital, Sun Yat-sen University, Guangzhou, China*
[6]*Department of Biomedical Engineering, College of Engineering, National Cheng Kung University, Tainan, Taiwan*
[7]*Medical Device Innovation Center, National Cheng Kung University, Tainan, Taiwan*
[8]*School of Biomedical Engineering, College of Biomedical Engineering, Taipei Medical University, Taipei, Taiwan*
[9]*Department of Electrical Engineering, National Taiwan University, Taipei, Taiwan*
[10]*Department of Neurology, Boston Children's Hospital, Harvard Medical School, Boston, MA, USA*
[11]*Department of Neurosurgery, Chang Gung Memorial Hospital at Linkou, Taoyuan, Taiwan*
[12]*Division of Neurosurgery, Department of Surgery, Min-Sheng General Hospital, Taiwan*
[13]*Department of Early Childhood and Family Educare, Chung Chou University of Science and Technology, Changhua County, Taiwan*
[14]*Department of Surgery, School of Medicine, College of Medicine, Taipei Medical University, Taipei, Taiwan*

Correspondence should be addressed to Tsung-Hsun Hsieh; hsiehth@mail.cgu.edu.tw

Received 25 June 2021; Revised 31 October 2021; Accepted 13 December 2021; Published 27 December 2021

Academic Editor: Mou-Xiong Zheng

Repetitive transcranial magnetic stimulation (rTMS) is a popular noninvasive technique for modulating motor cortical plasticity and has therapeutic potential for the treatment of Parkinson's disease (PD). However, the therapeutic benefits and related mechanisms of rTMS in PD are still uncertain. Accordingly, preclinical animal research is helpful for enabling translational research to explore an effective therapeutic strategy and for better understanding the underlying mechanisms. Therefore, the current study was designed to identify the therapeutic effects of rTMS on hemiparkinsonian rats. A hemiparkinsonian rat model, induced by unilateral injection of 6-hydroxydopamine (6-OHDA), was applied to evaluate the therapeutic potential of rTMS in motor functions and neuroprotective effect of dopaminergic neurons. Following early and long-term rTMS intervention with an intermittent theta burst stimulation (iTBS) paradigm (starting 24 h post-6-OHDA lesion, 1 session/day, 7 days/week, for a total of 4 weeks) in awake hemiparkinsonian rats, the effects of rTMS on the performance in detailed functional behavioral tests, including video-based gait analysis, the bar test for akinesia, apomorphine-induced rotational analysis, and tests of the degeneration level of dopaminergic neurons, were identified. We found that four weeks of rTMS intervention significantly reduced the aggravation of PD-related symptoms post-6-OHDA lesion. Immunohistochemically, the results showed that tyrosine hydroxylase- (TH-) positive neurons in the substantia nigra pars compacta (SNpc) and fibers in the striatum were significantly preserved in the rTMS treatment group. These findings suggest that early and long-term rTMS with the iTBS paradigm exerts neuroprotective effects and mitigates motor impairments in a hemiparkinsonian rat model. These results further highlight the potential therapeutic effects of rTMS and confirm that long-term rTMS treatment might have clinical relevance and usefulness as an additional treatment approach in individuals with PD.

1. Introduction

Parkinson's disease (PD) is recognized as the second most prevalent age-related neurodegenerative disorder after Alzheimer's disease, affecting approximately 1% of the population over the age of 60 years [1–4]. The major pathological hallmark of the disease results from the degeneration of dopaminergic cells in the substantia nigra *pars compacta* (SNpc), leading to several motor disturbances, e.g., tremor, muscular rigidity, bradykinesia, akinesia, and gait disturbance [5–8]. Currently, mainstream PD treatment is pharmacological management, such as dopamine supplementation (e.g., levodopa), dopamine agonists, catechol-O-methyltransferase inhibitors (COMTIs), or monoamine oxidase type B inhibitors (MAO-BIs) [9–11]. Among them, the dopamine precursor levodopa is the most common and effective antiparkinsonian medicine and remains the mainstay of PD treatment [10–13]. However, with long-term dopaminergic replacement therapy, several complications, mainly motor in nature, such as motor fluctuations, levodopa-induced dyskinesia, freezing, gait disturbance, and postural instability, are common side effects following long-term administration of levodopa [10, 14, 15]. Consequently, a number of alternative nonpharmacological approaches, e.g., deep-brain stimulation (DBS), have been investigated as new therapeutic strategies for PD [16–19]. However, DBS, a stimulation technique that involves implanting electrodes deeply into a selected portion of the basal ganglia, requires an invasive stereotactic approach with intraparenchymal implantation and is a high-cost procedure [20–22]. Furthermore, although DBS may improve some PD symptoms, it cannot modulate disease progression [23, 24]. Therefore, an alternative and better treatment that can modify disease progression is urgently needed for PD.

Recent research suggests that noninvasive repetitive transcranial magnetic stimulation (rTMS) can modulate cortical excitability in the motor cortex via plasticity-like mechanisms [25–27]. Furthermore, the recently developed theta burst stimulation (TBS) scheme of rTMS is capable of modulating motor cortical excitability beyond a short period of stimulation (20-190 sec) and with lower stimulus intensity than conventional low- or high-frequency rTMS [28–30]. Thus, this rTMS-TBS protocol has been considered to have therapeutic potential for PD [31–33]. However, the results among various studies exploring the therapeutic effects of rTMS using the TBS protocol on PD have been inconsistent [34]. Improvements in motor function, such as gross movements of the hand and Unified Parkinson's Disease Rating Scale (UPDRS) motor subscores, in PD after rTMS using TBS have been reported [35]. Conversely, other studies performed in PD patients showed no improvements in gait, bradykinesia, UPDRS scores, or gait freezing using intermittent TBS [33, 36]. Although the exact underlying therapeutic mechanism is still unclear, the controversial results might be due to methodological differences, the heterogeneity of clinical presentations and disease severity, long-lasting pharmacological effects, and protocol variability [37–40].

Animal models of disease may help in exploring the effectiveness and developing the therapeutic strategy of rTMS protocols by eliminating the discrepancy to provide a more stable disease condition [41–43]. A few animal studies found that 4 weeks of low-frequency intervention (500 pulses at 0.5 Hz) or high-frequency (10 Hz for 20 min) rTMS improved locomotor functions, dopaminergic neuron survival, and rotational behavior in a midstage 6-hydroxydopamine- (6-OHDA-) induced hemiparkinsonian rat model [43, 44]. Moreover, based on our previous finding, rTMS-induced motor plasticity was reduced in 6-OHDA-induced hemiparkinsonian rats with advanced disease. Such a reduction in motor plasticity is strongly correlated with dopaminergic cell loss in the substantia nigra and the severity of PD symptoms [45]. However, it remains unclear whether earlier intervention with rTMS using the TBS protocol could lead to improved therapeutic effects on motor function and improved induction of a neuroprotective effect in dopaminergic neurons. Therefore, in the current study, a series of experiments was conducted to test the therapeutic potential of rTMS in a preclinical PD animal model as an early step toward eventual clinical application. We employed our previously developed quantitative motor performance assessment techniques to enhance the understanding of the underlying neuromodulation mechanisms. The effects of rTMS were mainly assessed by behavioral measurements and immunohistochemical analyses, including comprehensive video-based gait analysis, the bar test for akinesia, apomorphine-induced rotational analysis, and tests of the dopaminergic neuron degeneration level. It was hypothesized that long-term rTMS treatment, especially using the TBS protocol, would result in a lasting reduction in motor deficits and have a neuroprotective effect on dopaminergic neurons in 6-OHDA-induced hemiparkinsonian rats. The knowledge obtained in these experiments may have translational relevance for establishing new clinical therapeutic applications of rTMS.

2. Materials and Methods

2.1. Animals. Adult male Wistar rats (350-400 g; $N = 41$) obtained from the Animal Center of Chang Gung University were used for the present study. All rats were housed in a temperature-controlled animal care facility at a temperature of 25°C with a 12 h light/dark cycle. All experimental protocols and surgical procedures were approved and followed the guidelines of the Institutional Animal Care and Use Committee at Chang Gung University (IACUC Approval No. CGU16-031, with validation period 08/01/2016-07/31/2019). In the present study, all efforts were made to minimize animal suffering and the number of animals used.

2.2. Hemiparkinsonian Rat Model. The procedures for the induction of hemiparkinsonian rats were described previously [45–48]. Briefly, animals were deeply anesthetized by Zoletil (50 mg/kg, i.p.; Vibac Laboratories, France) and xylazine (10 mg/kg, Rompun, Bayer, Germany) and then mounted in a stereotaxic apparatus (Stoelting, Wood Dale, IL, USA). A 2 cm incision was made along the midline of the scalp, and the area was carefully cleared to expose the line of bregma. A small hole was drilled in the skull 4.3 mm posterior and 1.6 mm lateral (left side only) to the

midline. A solution of 6-OHDA (8 μg dissolved in 4 μl 0.02% ascorbic saline) was injected into the left medial forebrain bundle (DV: 8.2 mm) at a rate of 0.5 μl/min using a 10 μl Hamilton microsyringe fitted with a 26-gauge steel cannula and mounted vertically on the stereotactic frame [49]. Before being retracted, the needle was left in the brain for 5 min to prevent backfilling along the injection tract [50]. To verify dopamine depletion after unilateral neurotoxin 6-OHDA infusion, a conventional and reliable apomorphine-induced rotation test was adopted [50–52]. In general, hemiparkinsonism induction by 6-OHDA was considered successful in rats with rotational responses of over 120 turns [53]. According to the criteria, at 4 weeks after surgery, all animals ($n = 26$) in both groups were regarded as hemiparkinsonian rats.

2.3. rTMS Treatment. All rTMS treatments were performed using a figure-eight coil (25 mm double small coil, Magstim Co.) connected to a Rapid^2 magnetic stimulator (Magstim Co., Whitland, Carmarthenshire, Wales, UK). To maintain the stability of the rTMS stimulation, the unanesthetized rats were restrained on a platform with four straps with minimal discomfort (Figure 1). The coil was held in the stereotaxic frame and positioned in the midline at the interocular line over the dorsal scalp, a position that can reliably and equally stimulate the bilateral motor cortex of limb and elicit bilateral limb movement [54]. In our experience, a rat can tolerate torso restraint for 5 min, which allows time for one session of TBS treatment [54]. The animals in the rTMS treatment group received the intermittent TBS (iTBS) paradigm (2 seconds of TBS training was repeated every 10 seconds for 20 repetitions for a total of 600 pulses each day for 7 consecutive days per week) under awake conditions for 4 weeks (28 consecutive sessions of iTBS in total) [45]. TBS consists of triplets of pulses at 50 Hz repeated every 200 ms [30]. The intensity of magnetic pulses was set at an 80% resting motor threshold, which was defined as the minimal intensity of magnetic stimulation required for eliciting minimal forelimb muscle twitches. The animals in the sham control group underwent an identical procedure to the experimental group except that rTMS-iTBS was replaced with sham rTMS with the magnetic coil placed 80 mm laterally and above the rat's head [55].

2.4. Behavioral Tests. A well-trained examiner was blinded to group assignment and performed all behavioral examinations before and after treatment. Three motor behavioral tests, i.e., video-based gait analysis, the bar test for akinesia, and an apomorphine-induced rotational behavior test, were performed in the same sequence on the same day to test the changes in functional motor performance in the sham rTMS ($n = 13$) and real rTMS groups ($n = 13$). There was at least a 2-hour break between tests to avoid possible interactions. The video-based gait analysis, bar test, and rotational behavior test were performed at baseline and after every weekly treatment.

2.4.1. Video-Based Gait Analysis. To identify the changes in gait pattern in hemiparkinsonian rats with and without

Figure 1: Setup of repetitive transcranial magnetic stimulation (rTMS) treatment for 6-OHDA-induced hemiparkinsonian rats. Unanesthetized rats were restrained on a platform with 4 straps with minimal discomfort. The figure-8 TMS coil is centered over the dorsal scalp at the interaural line to stimulate the bilateral motor cortex.

rTMS treatment, a walking track equipped with a video-based gait analysis system was applied to obtain the spatiotemporal parameters of the gait pattern. The procedure of video-based gait analysis to measure the gait pattern of hemiparkinsonian rats was described previously [46–48]. Briefly, the walking track equipment consisted of an enclosed walkway made of transparent Plexiglas (80 cm L $\times$ 6 cm W $\times$ 12 cm H) with a 45° tilting mirror positioned underneath the walkway. A high-speed and high-resolution camera (EX-F1, Casio, Japan) was positioned on the side of the walkway to capture the sagittal view and the reflected bottom view from the mirror. Before the experiment, all animals were acclimated to the walkway by allowing them to walk freely on the track for 20 min. Then, animals were trained to walk steadily on the Plexiglas walking track five times before formal recording. During the measurement, the rats were allowed to walk freely on the walking track at their own speed. The walking task was repeated in both directions for recording the movement of each hind limb. The walking task was repeated until five satisfactory walking trials were considered successful, meaning that at least four steps without pause were obtained during each test [46, 47]. The whole process for walking trials took approximately 30 minutes, and there was at least a 2-hour break between tests to prevent possible interactions. After recording, the image data captured from each trial were processed semiautomatically to identify the sequential footprints by MATLAB software (MathWorks, version 7.6., R2008a) [47]. Two spatial parameters (i.e., step length and stride length) and three temporal gait parameters (i.e., walking speed, stance phase time, and swing phase time) were determined in bilateral hind limbs of each group [46–48, 56].

2.4.2. Bar Test. Akinesia is a typical symptom in PD. The bar test was adopted in this study to detect forelimb akinesia in hemiparkinsonian rats [46, 57]. During the bar test, each rat was placed gently on a table, and the affected forepaw (the paw contralateral to the 6-OHDA lesion) was placed on a horizontal acrylic bar (0.7 cm diameter), positioned 9 cm above the table surface. The duration of time (in sec) spent from placing the affected forepaw on the bar to the first complete removal from the support bar was recorded [46, 48]. The animals were subjected to five subsequent trials, which were video recorded, and the duration was averaged over these five trials.

2.4.3. Apomorphine-Induced Spontaneous Rotation Test. Conventional and reliable apomorphine-induced contraversive rotational behavior was measured every week after the 6-OHDA injection to estimate the severity of dopamine depletion [46, 58, 59]. After the injection of apomorphine (0.5 mg/kg in 0.1% ascorbic acid, s.c.; Sigma), the hemiparkinsonian rats were placed in a round bowl (40 cm in diameter). Apomorphine-induced rotational behavior was recorded by a digital video camera for a 60 min period. For precise calculation of the number of rotations after apomorphine injection, the net number of rotations was manually calculated as the difference between the number of contralateral rotations and the number of ipsilateral rotations to the 6-OHDA lesion side (total right-total left 360° turns) after apomorphine injection from the 60-minute video recording.

2.5. Immunohistochemistry Investigation. After behavioral tests were performed on days 7 and 28 postlesion, animals were sacrificed for tyrosine hydroxylase (TH) staining. TH staining analysis was carried out according to a previously employed protocol [45, 48, 60]. Briefly, animals were deeply anesthetized with an overdose of pentobarbital (60 mg/kg i.p., Apoteksbolaget, Sweden) and perfused transcardially with phosphate-buffered saline (PBS) and 4% paraformaldehyde solution (PFA). Brains were carefully removed, postfixed for 3 days, and cryoprotected in 30% sucrose solution at 4°C until the brain sank. The brains were sectioned into coronal blocks at a thickness of 30 μm on a cryostat (Leica CM3050 S Cryostat, FL, USA), and the areas of the SNpc and striatum were selected [48]. The free-floating sections were quenched with 0.3% H_2O_2/PBS for 10 min and 10% milk (ANCHOR SHAPE-UP, New Zealand) for 1 hour to block nonspecific antibody binding. Sections were then incubated with rabbit primary anti-TH (1 : 1000, AB152, Millipore, USA) for 1 hour at room temperature. Thereafter, sections were washed in PBS and incubated for 1 h with the secondary anti-rabbit antibody (1 : 200, MP-7401, Vector Labs, USA) in PBS. After rinsing, sections were placed in 3,3-diaminobenzidine (DAB, SK-4105, Vector Labs, USA) for 3-5 min. Finally, the sections were mounted on slides, dehydrated in a series of alcohols, cleared in xylene, and cover-slipped in DPX. The mounted coronal sections were digitally scanned at 40x magnification (0.25 μM/pixel) using a digital pathology slide scanner (Aperio CS2, Leica Biosystems Inc. Buffalo Grove, IL, USA) and viewed with Aperio ImageScope software. The obtained images were converted into binary (8-bit black-and-white) images. The binary threshold was determined to capture the TH-positive cells in the regions of interest while minimizing background staining and was kept constant for all images. The numbers of TH-positive cells in each region were counted by means of particle analysis using computer-based image analysis software (Image-Pro Plus 6.0, Media Cybernetics, Bethesda, MD, USA), and these values were then manually validated by two investigators to ensure the correct identification of immunoreactivity patterns. The percentage loss of TH-positive cells was calculated in the ipsilateral hemisphere and normalized with respect to the contralateral side. With regard to the striatal TH-positive fibers, the optical density of TH-positive fibers in the striatal sections was analyzed using Image-Pro Plus 6.0 software (Media Cybernetics, USA) with correction for nonspecific background density measured at the corpus callosum. The percentage loss of dopaminergic fibers on the ipsilateral side was normalized and presented with respect to the contralateral side.

2.6. Experimental Design. To verify the therapeutic effects of long-term rTMS intervention in hemiparkinsonian rats, the experimental hemiparkinsonian rats were randomly divided into a 6-OHDA+rTMS treatment group ($n = 22$) and a 6-OHDA+sham treatment group ($n = 19$). For the early and long-term rTMS intervention, hemiparkinsonian rats were randomly assigned to receive sham or real rTMS intervention. Starting 24 h after 6-OHDA injection, neurotoxic PD rats received daily sham or real rTMS under awake conditions for 7 consecutive days/week for 4 weeks (Figure 2). Behavioral tests, including detailed video-based gait analysis and the bar test, were performed at baseline and every week after 6-OHDA was injected until the end of the rTMS intervention. Apomorphine-induced rotational behavior was measured every week after 6-OHDA through 4 weeks of rTMS treatment. Tyrosine hydroxylase (TH) staining was assessed in randomly selected hemiparkinsonian rats after behavioral tests at 1 week ($n = 9$ in the 6-OHDA+rTMS group; $n = 6$ in the 6-OHD+sham treatment group) and 4 weeks ($n = 9$ in the 6-OHDA+rTMS group; $n = 6$ in the 6-OHD+sham treatment group) post-6-OHDA lesion.

2.7. Data Analysis

2.7.1. Statistical Analysis. Data were analyzed using SPSS version 17.0 with the significance level set as $P < 0.05$ for each assessment. All data are presented as the average ± standard error of the mean (SEM). The effect of rTMS on the behavioral test performance was evaluated by a two-way repeated-measures analysis of variance (ANOVA) with protocol (real vs. sham) as the between-subject factor and time (pre, every week during intervention) as the within-subject factor. No preintervention data were included for apomorphine-induced rotation in the early intervention session because there was no rotation before 6-OHDA was injected. Unpaired t -tests were performed to compare groups at each time point when the main effect of the group was significant. Furthermore, a separate one-way ANOVA followed by post hoc Fisher's LSD tests was used to compare

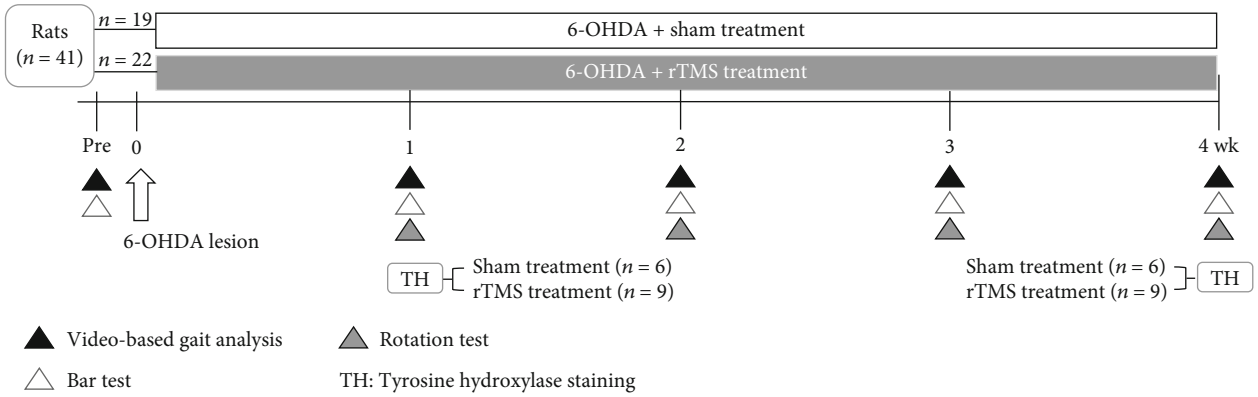

Figure 2: Design of the study of the long-term treatment effects of rTMS on rats with 6-OHDA-induced PD. rTMS and sham control treatments were performed daily over 4 successive weeks. Behavioral tests, including gait analysis, the bar test, and apomorphine-induced rotation tests, were performed every week to investigate the time-course treatment effects. Immunohistochemistry tests were performed at week 1 and week 4 post-6-OHDA lesion to identify the neuroprotective effects rTMS treatment on dopaminergic neurons and fibers.

behavioral and immunohistochemical data between time points when needed.

3. Results

3.1. Effect of rTMS Intervention on Behavioral Assessments. Performances in the detailed video-based gait analysis and bar test were assessed in the 6-OHDA+rTMS treatment group ($n = 13$) and 6-OHDA+sham treatment group ($n = 13$) at baseline and every week after the 6-OHDA lesion until the end of the rTMS intervention. The rotation test was performed every week after 6-OHDA until 4 weeks of rTMS treatment in both groups ($n = 13$ in each group). The descriptive and inferential statistics of the primary outcomes for all the behavioral tests are shown in Supplementary Table S1. Figure 3(a) shows the time-course changes in the apomorphine-induced rotation response (net of contralateral rotations/hour) after lesion induction. Two-way repeated-measures ANOVA showed significant main effects in time ($F_{3,72} = 18.94$, $p < 0.001$) and in protocol ($F_{1,24} = 5.875$, $p = 0.023$). The post hoc t-tests between the two groups revealed that the rotation number reached significant differences at 1 week ($t = 2.771$; $p = 0.011$) and 2 weeks ($t = 2.595$; $p = 0.016$) posttreatment but not at 3 weeks ($t = 1.300$; $p = 0.206$) or 4 weeks post-6-OHDA lesion ($t = 0.258$; $p < 0.799$). Figure 3(b) shows the time-course changes in the performance in the bar test for akinesia in the 6-OHDA+rTMS- and 6-OHDA+sham-treated rats over a 4-week observation period. Two-way repeated-measures ANOVA revealed significant effects of time ($F_{4,96} = 24.879$, $p < 0.001$) and group ($F_{1,24} = 18.434$, $p < 0.001$) on the contralateral (affected) limb. Subsequent post hoc t-tests between the groups showed that the bar test scores reached significant differences at 1 week ($t = 2.341$; $p = 0.032$), 2 weeks ($t = 2.573$; $p = 0.017$), 3 weeks ($t = 2.182$; $p = 0.039$), and 4 weeks post-6-OHDA lesion ($t = 3.322$; $p = 0.004$).

For the results of gait analysis, Figure 4(a) shows typical footprint images recorded from a sham PD rat and real PD treatment rat in the early intervention group. Two-way repeated-measures ANOVA showed significant main effects of group in walking speed ($F_{1,24} = 11.57$, $p = 0.002$), step length ($F_{1,24} = 8.84$, $p = 0.007$ on the affected side; $F_{1,24} = 11.93$, $p = 0.002$ on the unaffected side), stride length ($F_{1,24} = 15.56$, $p = 0.001$ on the affected side; $F_{1,24} = 13.46$, $p = 0.001$ on the unaffected side), and stance phase time ($F_{1,24} = 10.12$, $p = 0.004$ on the affected side) but not in swing phase time ($F_{1,24} = 0.13$, $p = 0.722$ on the affected side), suggesting less impairment of gait pattern in the real treatment group than in the sham group. Subsequent post hoc t-tests between groups at each time point showed that this difference was largely driven by rTMS treatment effects observed starting at the first week of treatment on walking speed ($t = 2.38$, $p = 0.025$), step length ($t = 2.16$, $p = 0.041$ on the affected side; $t = 2.18$, $p = 0.039$ on the unaffected side), stride length ($t = 2.81$, $p = 0.01$ on the affected side; $t = 2.20$, $p = 0.038$ on the unaffected side), and stance phase time ($t = 2.86$, $p = 0.009$) (Figures 4(b)–4(g)). All these differences remained statistically significant at the end of the 4-week intervention (unpaired t-tests, $p < 0.05$).

3.2. Effects of rTMS Intervention Assessed by Immunohistochemistry. With regard to the effects of long-term rTMS intervention on dopaminergic neurons, the results of TH immunohistochemistry in the SNpc and striatum in rats at 1 wk and 4 wk post-6-OHDA lesion are shown in Figures 5(a)–5(d). The quantification of TH-positive cell loss in the substantia nigra and TH-positive fiber loss in the striatum at 1 week and 4 weeks post-6-OHDA lesion is presented in Figures 5(e) and 5(f). Rats that received rTMS intervention showed a preservation of TH-positive neurons in the SN ($t = 2.338$, $p = 0.035$ at week 1; $t = 2.396$, $p = 0.031$ at week 4) and TH-positive fibers in the striatum ($t = 2.886$, $p = 0.012$ at week 1; $t = 2.837$, $p = 0.013$ at week 4) compared to those that received sham stimulation.

4. Discussion

In the present study, we explored the hypothesis that long-term rTMS treatment with TBS would mitigate 6-OHDA-induced motor dysfunction and has a neuroprotective effect

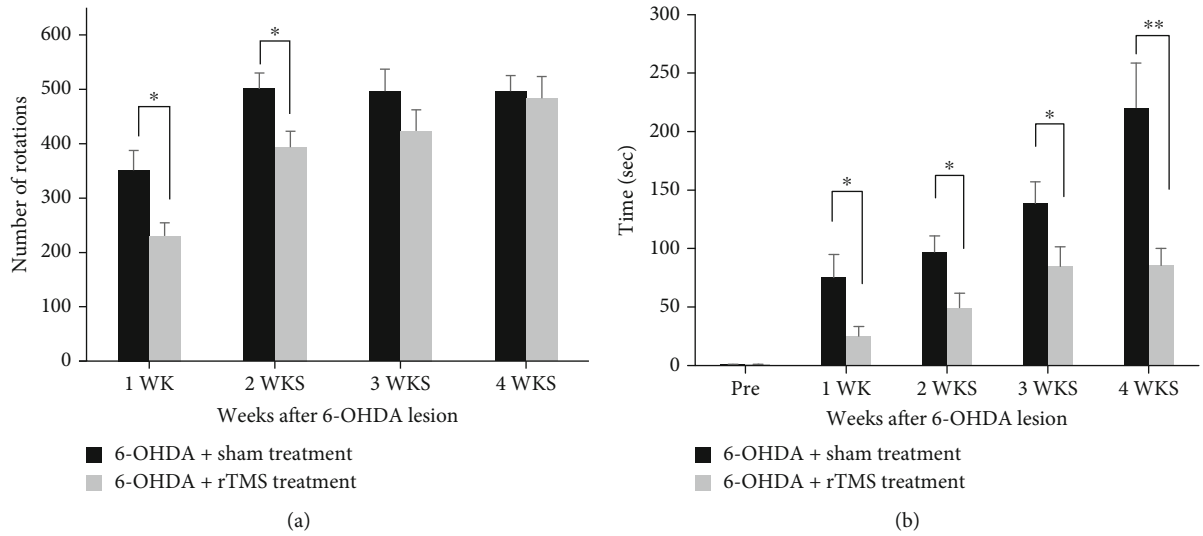

Figure 3: Time-course analysis of apomorphine-induced rotational behavior (a) and duration of bar test for akinesia (b) observed over 4 weeks in the sham- and rTMS-treated groups. Error bars = SEM; $^{*}p < 0.05$ and $^{**}p < 0.01$, significant difference between the two groups.

on dopamine neurons. We found that long-term rTMS intervention ameliorated progressive motor disturbances such as gait impairments (e.g., lower walking speed, shorter step/stride length, and longer stance phase time) and akinesia following 6-OHDA administration, indicating that early and long-term rTMS can suppress neurotoxin-induced motor impairments over repeated sessions of stimulation. Histological investigation revealed more preserved dopaminergic neurons in the SNpc and striatal fibers in the rTMS treatment group than in the sham group, suggesting a neuroprotective effect of rTMS.

Until now, the therapeutic efficacy and the detailed mechanisms of rTMS treatment for PD have remained inconsistent and unclear [33, 61–64]. For example, an improvement in motor symptoms in PD patients after rTMS treatment was reported, showing improvements in walking speed [65], Unified Parkinson's Disease Rating Scale part III (UPDRS-III) scores [66–71], 10 m walking test performance [68, 71], timed up-and-go test performance [69, 72], and freezing of gait (FOG) [69, 70, 73]. In contrast, some studies showed no significant improvement in rigidity, bradykinesia, tremor [74], functional performance of the hand [75], UPDRS-III scores [33, 76, 77], FOG [36, 78], gait, or bradykinesia [33, 77]. Although the exact underlying therapeutic mechanism is still unclear, the controversial results might be due to the variability of protocols, long-term pharmacological effects, clinical heterogeneity, and different severities of disease [37–40]. The use of an animal model could help in the control of confounding factors and may provide more information for clarifying the benefits of rTMS in PD and the underlying mechanisms its effects. Earlier animal studies have reported that rTMS treatment improved treadmill locomotor function and apomorphine/amphetamine-induced rotational behavior [43, 44]. In the present study, in addition to evaluations of rotational behavior, we performed comprehensive and quantitative assessments of gait and akinesia, which are the symptoms commonly observed in PD patients, to investigate the beneficial effects during and after four weeks of rTMS intervention. Moreover, our data show that long-term rTMS treatment has an accumulated effect on gait function. The time-course observation of such a comprehensive mean of behavioral tests is helpful for determining behavioral compensation and for quantifying the relative degeneration in dopaminergic neurons with disease progression. After hemiparkinsonian rats were treated with rTMS or sham treatment for four weeks, clear alleviation of gait dysfunction (e.g., lower walking speed, short step/stride length) was observed in the rTMS-treated group. When compared with the sham rTMS treatment group, we found that 4 weeks of rTMS treatment postponed disease progression after 6-OHDA injection. To the best of our knowledge, this is the first study confirming the therapeutic effects on gait disturbances and akinesia symptoms in hemiparkinsonian rats. This finding may also support clinical observations showing prolonged positive effects on gait function after rTMS treatment [40, 65, 79] and augments the growing amount of basic research and clinical literature on the efficacy of rTMS in PD treatment.

With regard to the effect of rTMS on akinesia, we found that four weeks of rTMS in hemiparkinsonian rats led to a reduction in akinesia. These results parallel PD human and animal studies showing a reduction in bradykinesia or forelimb akinesia after rTMS treatment, encouraging further research into the therapeutic potential of rTMS [79, 80]. The mechanisms by which rTMS improves several aspects of motor function in PD are still unclear. Evidence possibly supporting the efficacy of rTMS in PD is related to the release of dopamine induced by rTMS [81–84]. The widespread activation of dopaminergic neuronal systems or the elevation of serum dopamine concentration after repeated rTMS sessions could be one of the mechanisms for delaying the deterioration of motor dysfunction and may have contributed to the improvements in motor functions after daily

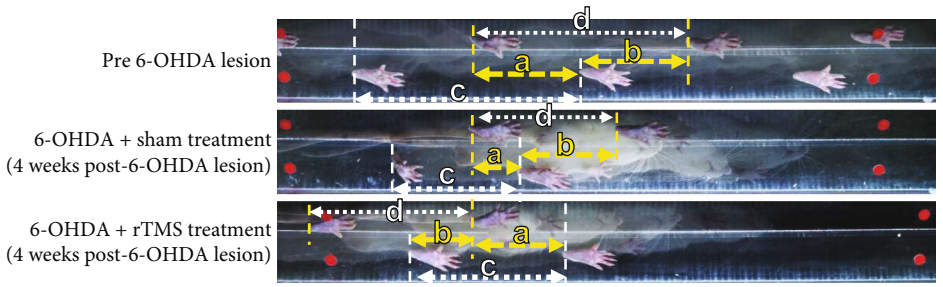

a: Step length in right (affected) hindlimb
b: Step length in left (unaffected) hindlimb
c: Stride length in right (affected) hindlimb
d: Stride length in left (unaffected) hindlimb

(a)

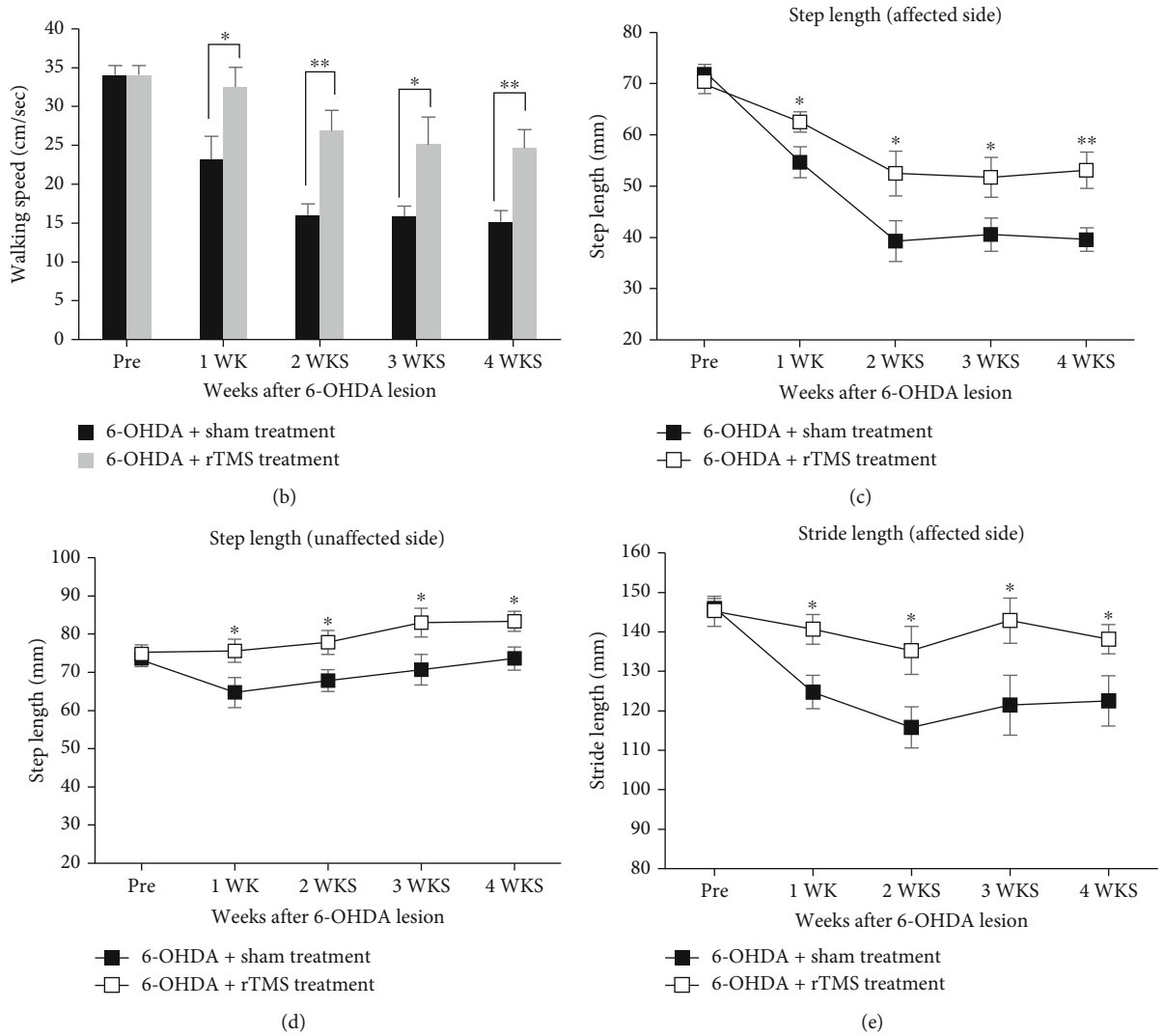

Figure 4: Continued.

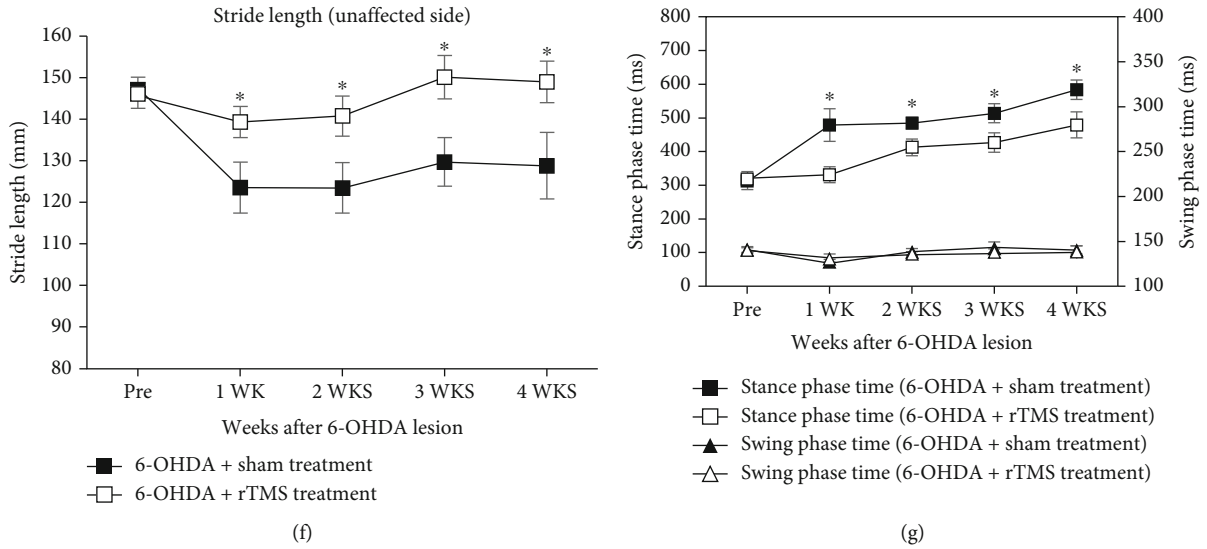

Figure 4: Characteristics of stepping footprint during 1 sec walkway locomotion in a rate pre-6-OHDA lesion, in a sham-treatment rat 4 weeks post-6-OHDA lesion, and in an rTMS-treated rat 4 weeks post-6-OHDA lesion (a). Time-course changes in walking speed (b), step length in the affected limb (c) and unaffected limb (d), stride length in the affected limb (e) and unaffected limb (f), and stance/swing phase time (g) in the sham- and rTMS-treated PD rats over 4 weeks of observation. Note that the step and stride lengths decreased significantly in the sham rTMS treatment group but decreased less in the rTMS treatment group. Gradual increases in the stance phases were found in both groups, but the sham treatment group showed a higher trend than the rTMS treatment group. No significant difference was found in swing phase duration. $^{*}p < 0.05$ and $^{**}p < 0.01$, significant post hoc Fisher's LSD differences when compared between the two groups at each time point.

sessions of rTMS observed in hemiparkinsonian rats [80, 85]. Another possible mechanism for the improvements in motor function following long-term rTMS treatment in PD could be related to the modulation of motor cortical plasticity induced by rTMS. In the classic complex cerebro-basal ganglia network, the usual facilitating effect of thalamic projections to the motor cortex is reduced in PD, resulting in the deactivation or hypoactivation of motor cortical areas and thus leading to reduced motor output during movement [86, 87]. Similar to the human TBS protocol, our earlier study indicated that rTMS with the iTBS protocol might be useful to promote motor cortical plasticity in healthy rats [45]. Furthermore, we previously demonstrated that rTMS-induced motor plasticity was reduced with time as the disease progressed in 6-OHDA-induced hemiparkinsonian rats, indicating that the change in motor plasticity is highly correlated with the degree of dopaminergic cell loss after PD lesions form [45]. Similarly, the impairments in the induction of the two forms of corticostriatal plasticity, long-term potentiation (LTP) and long-term depression (LTD), have been found to correlate with dopamine depletion and the onset of symptoms in the experimental parkinsonism rat model induced by 6-OHDA [88]. These impairments of bidirectional corticostriatal plasticity can be rescued by rTMS, which is linked to the increase in striatal dopamine levels produced by rTMS treatment [80]. Although we did not investigate the motor plasticity changes assessed by electrophysiological measures (e.g., motor evoked potential (MEP) elicited by TMS) in the current study, the possible mechanisms underlying the therapeutic effect in the improvement of motor functions could be via plasticity-like effects induced by long-term rTMS intervention in 6-OHDA-induced hemiparkinsonian rats when dopaminergic cells were preserved in the early stage after 6-OHDA injection.

Apomorphine-induced rotational behavior is a common method used to explore the level of dopamine depletion in 6-OHDA-induced hemiparkinsonian rats [45, 46, 89]. The time-course observations in the rotation test showed that the number of rotations observed in an hour gradually increased over the 4 weeks post-6-OHDA lesion in the sham-rTMS group, indicating a progressive increase in dopamine depletion with the increasing sensitization of the denervated dopaminergic receptors in the observation stage [89, 90]. However, the rotational response was reduced in the first and second weeks in rats that received rTMS treatment compared with rats that received sham treatment. These results indicated that early and intermittent high-frequency rTMS treatment could suppress the progression of dopamine depletion post-6-OHDA lesion over repeated sessions of stimulation. The effect of long-term rTMS treatment on the mitigation of 6-OHDA-induced progressive dopamine depletion in the early stage (i.e., 1-2 weeks post-PD lesion) was parallel with the histological observations, which showed neuroprotective effects against neurotoxin-induced damage to dopaminergic neurons and fibers in the SNpc and striatum, respectively. However, our findings revealed that 4 weeks of rTMS showed a neuroprotective effect in nigrostriatal dopaminergic neurons in histological analyses but not in rotational behavior tests since the rotation tests indicated that there were no differences between the rTMS and sham treatment groups in the number of rotations at weeks 3 and 4 post-6-OHDA lesion. No differences were observed between two groups in the number of

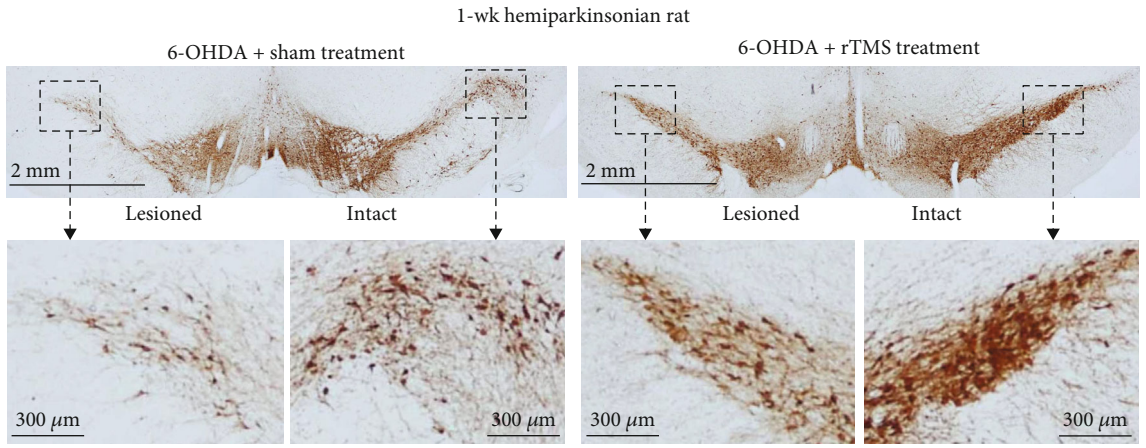

(a)

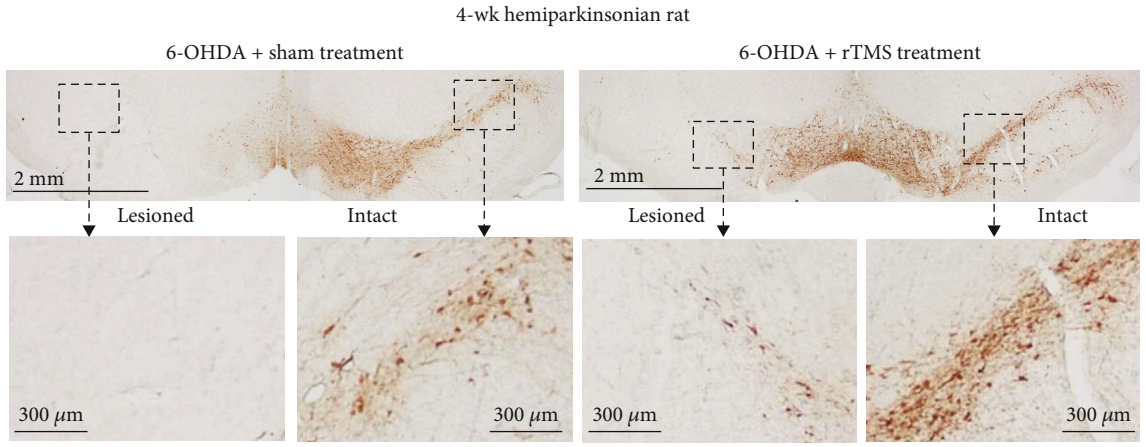

(b)

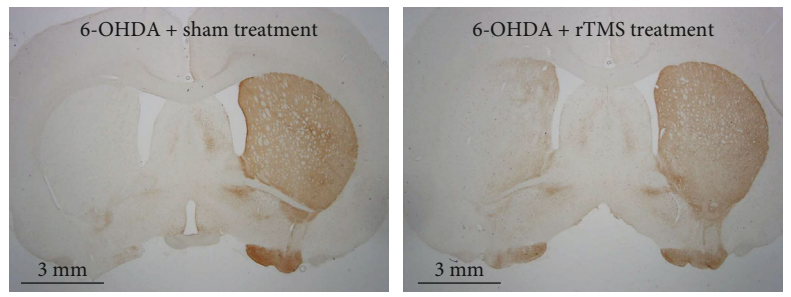

(c)

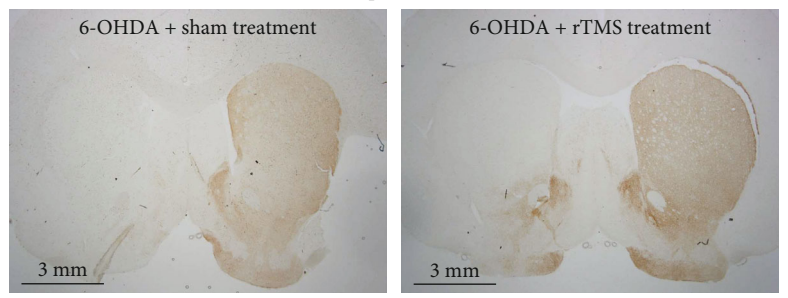

(d)

Figure 5: Continued.

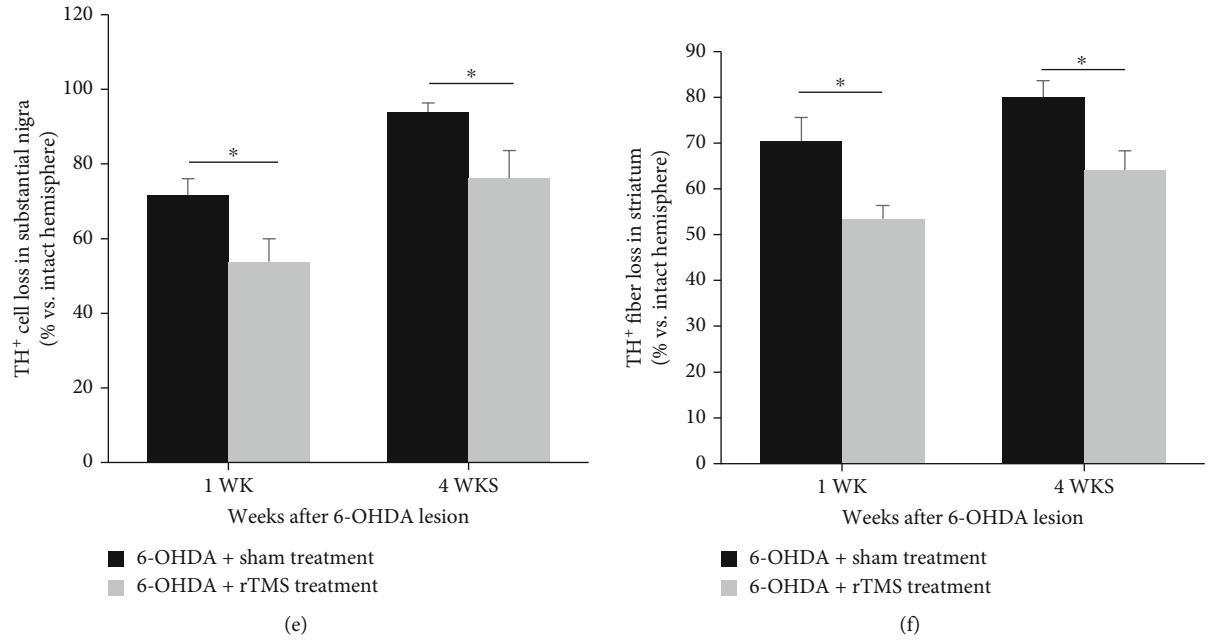

Figure 5: Representative TH-positive neurons in the substantia nigra pars compacta (a, b) and TH-positive fibers in the striatum (c, d) from sham control and rTMS-treated animals sacrificed at 1 week and 4 weeks post-6-OHDA lesion. Note the obvious reduction in TH-positive neurons or fibers in the lesioned hemisphere (left side) of the rTMS group at 1 week and 4 weeks post-6-OHDA lesion when the percentages of TH-positive neuron loss in the substantia nigra (e) and TH-positive fiber loss in the striatum (d) were compared to those in the sham treatment group. $^*p < 0.05$ (unpaired t-test).

rotations could be due to the dose of apomorphine for inducing spontaneous rotation being too high to show supersensitivity differences [91, 92]. In the current study, the dose of apomorphine was 0.5 mg/kg, a relatively high dose of apomorphine, which could easily lead to a plateau in rotational behavior [91]. To overcome this possible limitation, lower doses of apomorphine (0.05–0.1 mg/kg) may be more appropriate to detect the degree of dopamine receptor supersensitivity and maximize the difference between the rTMS and sham treatment groups [48, 91, 93].

The histological investigation showed that more dopaminergic cells survived in the group that received rTMS treatment than in the group that received sham rTMS stimulation. Such results suggest that daily rTMS intervention may not only improve motor functions but also have neuroprotective effects and mitigate the neurotoxin-induced damage to dopaminergic neurons. Similar neuroprotective results have been reported using low- (0.1 Hz) or high-frequency (10 Hz) rTMS [43, 44]. The neuroprotective effects on dopaminergic cells or fibers could be related to anti-inflammatory factors (e.g., cyclooxygenase-2 (COX-2) or tumor necrosis factor-alpha (TNF-α)); the upregulation of neurotrophic/growth factors such as brain-derived neurotrophic factor (BDNF), glial cell line-derived neurotrophic factor (GDNF), platelet-derived growth factor, and nerve growth factor (NGF); and a reduction in the astrogliosis and microglial activation (e.g., ionized calcium binding adaptor molecule 1 (Iba-1), glial fibrillary acidic protein (GFAP) induced by rTMS) [43, 44, 80]. Similar neuroprotective effects of rTMS were observed in brain injury and stroke animal models [94, 95]. With rTMS intervention using the TBS protocol, rTMS significantly reduced glial activation and neuronal death and improved functional recovery, indicating that rTMS may have potential as an antiapoptotic and anti-inflammatory treatment [94]. Furthermore, in an animal model of stroke, long-term rTMS induces complex changes in gene expression involved in angiogenesis, cellular repair, structural remodeling, neuroprotection, neurotransmission, and neuronal plasticity [95]. Although the underlying mechanisms are still unclear, further investigations are needed to clarify the detailed mechanisms underlying the neuroprotective effects of rTMS in PD.

5. Conclusion

In conclusion, the current study findings provide a clearer picture of progressive symptom changes with and without rTMS treatment and indicate the efficacy of rTMS in preventing motor and dopaminergic system abnormalities in a 6-OHDA hemiparkinsonian rat model. rTMS treatment improved motor functions and had a neuroprotective effect, showing that rTMS treatment preserved the function of dopamine neurons damaged by 6-OHDA administration in a rat model of PD. This long-term rTMS treatment model may serve as a bridge between animal and PD human studies. Future research is still needed to further clarify the underlying mechanisms and will lead to improved rTMS protocols and more effective PD therapies in humans.

Abbreviations

6-OHDA: 6-Hydroxydopamine
BDNF: Brain-derived neurotrophic factor
BOS: Base of support

COX-2: Cyclooxygenase-2
DBS: Deep brain stimulation
GDNF: Glial cell line-derived neurotrophic factor
GFAP: Glial fibrillary acidic protein
Iba-1: Ionized calcium binding adaptor molecule 1
iTBS: Intermittent theta burst stimulation
NGF: Nerve growth factor
NHS: Normal horse serum
PBS: Phosphate-buffered saline
PD: Parkinson's disease
PFA: Paraformaldehyde solution
rTMS: Repetitive transcranial magnetic stimulation
SN: Substantia nigra
TBS: Theta burst stimulation
TH: Tyrosine hydroxylase.

Data Availability

The data generated and analyzed during the current study are available from the corresponding authors on reasonable request.

Disclosure

The preliminary results and findings in this study have been presented via poster and conference abstract at the 45th annual meeting of the Society for Neuroscience (Neuroscience 2015), Chicago, IL, USA.

Conflicts of Interest

The authors declare that they have no conflicts of interest regarding the publication of this paper.

Authors' Contributions

T-HH and J-J.JC conceived and designed the experiments. K-TC and M-YC provided the research theories to support the study. T-HH, X-KH, H-HL, P-KC, and C-WK performed the experiments and collected the data. T-HH, J-J.JC, C-WP, H-LL, and M-YC provided the instrumentation and study materials. T-HH, J-J.J.C, AR, and Y-HC developed the methodology. T-HH, H-HL, and C-WK performed the analysis and interpretation of data. T-HH, X-KH, H-HL P-KC, and C-WK contributed to writing and editing the manuscript.

Acknowledgments

The authors would like to thank Professor Ying-Zu Huang for his helpful advice and are grateful to the Neuroscience Research Center of Chang Gung Memorial Hospital at Linkou, Taiwan. This study was supported by grants from the Ministry of Science and Technology, Taiwan (MOST 109-2314-B-182-029-MY3, MOST 108-2314-B-182-015-MY3 to T-HH, and MOST 109-2221-E-038-005-MY3 to C-WP); Chang Gung Medical Foundation, Taiwan (CMRPD1H0463 and CMRPD1K0671 to T-HH); Industry-Academy Cooperation Project of Chang Gung University (QCRPD657, SCRPD1H0061, SCRPD1K0351, and SCRPD1K0611 to T-HH); and Min-Sheng General Hospital (Grant numbers 1090003 and 2020003 to M-YC).

Supplementary Materials

Supplementary Table S1: the descriptive and inferential statistics of the primary outcomes for all the behavioral tests are shown. *(Supplementary Materials)*

References

[1] L. M. de Lau and M. M. Breteler, "Epidemiology of Parkinson's disease," *The Lancet Neurology*, vol. 5, no. 6, pp. 525–535, 2006.

[2] T. L. Kauffman, J. O. Barr, and M. L. Moran, *Geriatric Rehabilitation Manual*, Churchill Livingstone Elsevier, Edinburgh; New York, 2nd edition, 2007.

[3] A. Reeve, E. Simcox, and D. Turnbull, "Ageing and Parkinson's disease: why is advancing age the biggest risk factor?," *Ageing Research Reviews*, vol. 14, pp. 19–30, 2014.

[4] S. Gilman, *Neurobiology of Disease*, Elsevier Academic Press, Burlington, Mass, 2007.

[5] M. W. Rogers, "Disorders of posture, balance, and gait in Parkinson's disease," *Clinics in Geriatric Medicine*, vol. 12, no. 4, pp. 825–845, 1996.

[6] L. V. Kalia and A. E. Lang, "Parkinson's disease," *The Lancet*, vol. 386, no. 9996, pp. 896–912, 2015.

[7] J. C. Möller, A. Menig, and M. Oechsner, "Neurorehabilitation bei der Parkinson-Krankheit," *Praxis*, vol. 105, no. 7, pp. 377–382, 2016.

[8] S. Sveinbjornsdottir, "The clinical symptoms of Parkinson's disease," *Journal of Neurochemistry*, vol. 139, pp. 318–324, 2016.

[9] T. Nagatsu and M. Sawada, "L-dopa therapy for Parkinson's disease: past, present, and future," *Parkinsonism & Related Disorders*, vol. 15, Supplement 1, pp. S3–S8, 2009.

[10] B. S. Connolly and A. E. Lang, "Pharmacological treatment of Parkinson Disease," *JAMA*, vol. 311, no. 16, pp. 1670–1683, 2014.

[11] J. J. Ferreira, R. Katzenschlager, B. R. Bloem et al., "Summary of the recommendations of the EFNS/MDS-ES review on therapeutic management of Parkinson's disease," *European Journal of Neurology*, vol. 20, no. 1, pp. 5–15, 2013.

[12] Y. Ohno, S. Shimizu, K. Tokudome, N. Kunisawa, and M. Sasa, "New insight into the therapeutic role of the serotonergic system in Parkinson's disease," *Progress in Neurobiology*, vol. 134, pp. 104–121, 2015.

[13] D. Salat and E. Tolosa, "Levodopa in the treatment of Parkinson's disease: current status and new developments," *Journal of Parkinson's Disease*, vol. 3, no. 3, pp. 255–269, 2013.

[14] M. F. Bastide, W. G. Meissner, B. Picconi et al., "Pathophysiology of L-dopa-induced motor and non-motor complications in Parkinson's disease," *Progress in Neurobiology*, vol. 132, pp. 96–168, 2015.

[15] A. J. Espay, F. Morgante, A. Merola et al., "Levodopa-induced dyskinesia in Parkinson disease: current and evolving concepts," *Annals of Neurology*, vol. 84, no. 6, pp. 797–811, 2018.

[16] G. Deuschl, C. Schade-Brittinger, P. Krack et al., "A randomized trial of deep-brain stimulation for Parkinson's disease," *The New England Journal of Medicine*, vol. 355, no. 9, pp. 896–908, 2006.

[17] A. Collomb-Clerc and M. L. Welter, "Effets de la stimulation cerebrale profonde sur l'equilibre et la marche chez les patients atteints de la maladie de Parkinson : une revue systematique neurophysiologique," *Neurophysiologie Clinique*, vol. 45, no. 4-5, pp. 371–388, 2015.

[18] M. Beudel and P. Brown, "Adaptive deep brain stimulation in Parkinson's disease," *Parkinsonism & Related Disorders*, vol. 22, Supplement 1, pp. S123–S126, 2016.

[19] V. Dayal, P. Limousin, and T. Foltynie, "Subthalamic nucleus deep brain stimulation in Parkinson's disease: the effect of varying stimulation parameters," *Journal of Parkinson's Disease*, vol. 7, no. 2, pp. 235–245, 2017.

[20] Y. Kawamoto, M. Mouri, T. Taira, H. Iseki, and K. Masamune, "Cost-Effectiveness Analysis of Deep Brain Stimulation in Patients with Parkinson's Disease in Japan," *World Neurosurgery*, vol. 89, pp. 628–635.e1, 2016.

[21] K. T. Stroupe, F. M. Weaver, L. Cao et al., "Cost of deep brain stimulation for the treatment of Parkinson's disease by surgical stimulation sites," *Movement Disorders*, vol. 29, no. 13, pp. 1666–1674, 2014.

[22] J. Dams and R. Dodel, "An economic evaluation of deep brain stimulation for patients with Parkinson's disease," *Movement Disorders*, vol. 31, no. 8, pp. 1122–1124, 2016.

[23] D. Tarsy, L. Scollins, K. Corapi, S. O'Herron, D. Apetauerova, and T. Norregaard, "Progression of Parkinson's disease following thalamic deep brain stimulation for tremor," *Stereotactic and Functional Neurosurgery*, vol. 83, no. 5-6, pp. 222–227, 2006.

[24] X. Wang, C. Chang, N. Geng et al., "Long-term effects of bilateral deep brain stimulation of the subthalamic nucleus on depression in patients with Parkinson's disease," *Parkinsonism & Related Disorders*, vol. 15, no. 8, pp. 587–591, 2009.

[25] Y. Z. Huang, M. K. Lu, A. Antal et al., "Plasticity induced by non-invasive transcranial brain stimulation: a position paper," *Clinical Neurophysiology*, vol. 128, no. 11, pp. 2318–2329, 2017.

[26] W. He, P. Y. Fong, T. W. H. Leung, and Y. Z. Huang, "Protocols of non-invasive brain stimulation for neuroplasticity induction," *Neuroscience Letters*, vol. 719, p. 133437, 2020.

[27] D. Baur, D. Galevska, S. Hussain, L. G. Cohen, U. Ziemann, and C. Zrenner, "Induction of LTD-like corticospinal plasticity by low-frequency rTMS depends on pre-stimulus phase of sensorimotor μ-rhythm," *Brain Stimulation*, vol. 13, no. 6, pp. 1580–1587, 2020.

[28] P. B. Fitzgerald, S. Fountain, and Z. J. Daskalakis, "A comprehensive review of the effects of rTMS on motor cortical excitability and inhibition," *Clinical Neurophysiology*, vol. 117, no. 12, pp. 2584–2596, 2006.

[29] E. M. Khedr, J. C. Rothwell, M. A. Ahmed, O. A. Shawky, and M. Farouk, "Modulation of motor cortical excitability following rapid-rate transcranial magnetic stimulation," *Clinical Neurophysiology*, vol. 118, no. 1, pp. 140–145, 2007.

[30] Y. Z. Huang, M. J. Edwards, E. Rounis, K. P. Bhatia, and J. C. Rothwell, "Theta burst stimulation of the human motor cortex," *Neuron*, vol. 45, no. 2, pp. 201–206, 2005.

[31] S. Lang, L. S. Gan, E. J. Yoon et al., "Theta-burst stimulation for cognitive enhancement in Parkinson's disease with mild cognitive impairment: a randomized, Double-Blind, Sham-Controlled Trial," *Frontiers in Neurology*, vol. 11, 2020.

[32] J. Trung, A. Hanganu, S. Jobert et al., "Transcranial magnetic stimulation improves cognition over time in Parkinson's disease," *Parkinsonism & Related Disorders*, vol. 66, pp. 3–8, 2019.

[33] D. H. Benninger, B. D. Berman, E. Houdayer et al., "Intermittent theta-burst transcranial magnetic stimulation for treatment of Parkinson disease," *Neurology*, vol. 76, no. 7, pp. 601–609, 2011.

[34] J. P. Lefaucheur, A. Aleman, C. Baeken et al., "Evidence-based guidelines on the therapeutic use of repetitive transcranial magnetic stimulation (rTMS): an update (2014-2018)," *Clinical Neurophysiology*, vol. 131, no. 2, pp. 474–528, 2020.

[35] C. Eggers, M. Gunther, J. Rothwell, L. Timmermann, and D. Ruge, "Theta burst stimulation over the supplementary motor area in Parkinson's disease," *Journal of Neurology*, vol. 262, no. 2, pp. 357–364, 2015.

[36] C. Tard, H. Devanne, L. Defebvre, and A. Delval, "Single session intermittent theta-burst stimulation on the left premotor cortex does not alleviate freezing of gait in Parkinson's disease," *Neuroscience Letters*, vol. 628, pp. 1–9, 2016.

[37] M. Hamada, N. Murase, A. Hasan, M. Balaratnam, and J. C. Rothwell, "The role of interneuron networks in driving human motor cortical plasticity," *Cerebral Cortex*, vol. 23, no. 7, pp. 1593–1605, 2013.

[38] J. F. M. Müller-Dahlhaus, Y. Orekhov, Y. Liu, and U. Ziemann, "Interindividual variability and age-dependency of motor cortical plasticity induced by paired associative stimulation," *Experimental Brain Research*, vol. 187, no. 3, pp. 467–475, 2008.

[39] M. Bologna, A. Conte, A. Suppa, and A. Berardelli, "Motor cortex plasticity in Parkinson's disease: advances and controversies," *Clinical Neurophysiology*, vol. 123, no. 4, pp. 640-641, 2012.

[40] R. Nardone, V. Versace, F. Brigo et al., "Transcranial magnetic stimulation and gait disturbances in Parkinson's disease: a systematic review," *Neurophysiologie Clinique*, vol. 50, no. 3, pp. 213–225, 2020.

[41] T. M. Dawson, T. E. Golde, and C. Lagier-Tourenne, "Animal models of neurodegenerative diseases," *Nature Neuroscience*, vol. 21, no. 10, pp. 1370–1379, 2018.

[42] W. Dauer and S. Przedborski, "Parkinson's disease: mechanisms and models," *Neuron*, vol. 39, no. 6, pp. 889–909, 2003.

[43] J. Y. Lee, S. H. Kim, A. R. Ko et al., "Therapeutic effects of repetitive transcranial magnetic stimulation in an animal model of Parkinson's disease," *Brain Research*, vol. 1537, pp. 290–302, 2013.

[44] X. Yang, L. Song, and Z. Liu, "The effect of repetitive transcranial magnetic stimulation on a model rat of Parkinson's disease," *Neuroreport*, vol. 21, no. 4, pp. 268–272, 2010.

[45] T. H. Hsieh, Y. Z. Huang, A. Rotenberg et al., "Functional dopaminergic neurons in substantia nigra are required for transcranial magnetic stimulation-induced motor plasticity," *Cerebral Cortex*, vol. 25, no. 7, pp. 1806–1814, 2015.

[46] T. H. Hsieh, J. J. Chen, L. H. Chen, P. T. Chiang, and H. Y. Lee, "Time-course gait analysis of hemiparkinsonian rats following 6-hydroxydopamine lesion," *Behavioural Brain Research*, vol. 222, no. 1, pp. 1–9, 2011.

[47] H. Y. Lee, T. H. Hsieh, J. I. Liang, M. L. Yeh, and J. J. Chen, "Quantitative video-based gait pattern analysis for hemiparkinsonian rats," *Medical & Biological Engineering & Computing*, vol. 50, no. 9, pp. 937–946, 2012.

[48] X. J. Feng, Y. T. Huang, Y. Z. Huang et al., "Early transcranial direct current stimulation treatment exerts neuroprotective

effects on 6-OHDA-induced parkinsonism in rats," *Brain Stimulation*, vol. 13, no. 3, pp. 655–663, 2020.

[49] G. Paxinos and C. Watson, *The Rat Brain in Stereotaxic Coordinates*, Elsevier Academic Press, Amsterdam, 5th edition, 2005.

[50] L. Truong, H. Allbutt, M. Kassiou, and J. M. Henderson, "Developing a preclinical model of Parkinson's disease: a study of behaviour in rats with graded 6-OHDA lesions," *Behavioural Brain Research*, vol. 169, no. 1, pp. 1–9, 2006.

[51] F. Blandini, G. Levandis, E. Bazzini, G. Nappi, and M. T. Armentero, "Time-course of nigrostriatal damage, basal ganglia metabolic changes and behavioural alterations following intrastriatal injection of 6-hydroxydopamine in the rat: new clues from an old model," *The European Journal of Neuroscience*, vol. 25, no. 2, pp. 397–405, 2007.

[52] R. Deumens, A. Blokland, and J. Prickaerts, "Modeling Parkinson's disease in rats: an evaluation of 6-OHDA lesions of the nigrostriatal pathway," *Experimental Neurology*, vol. 175, no. 2, pp. 303–317, 2002.

[53] R. J. Su, J. L. Zhen, W. Wang, J. L. Zhang, Y. Zheng, and X. M. Wang, "Time-course behavioral features are correlated with Parkinson's disease-associated pathology in a 6-hydroxydopamine hemiparkinsonian rat model," *Molecular Medicine Reports*, vol. 17, no. 2, pp. 3356–3363, 2018.

[54] T. H. Hsieh, S. C. Dhamne, J. J. Chen, A. Pascual-Leone, F. E. Jensen, and A. Rotenberg, "A new measure of cortical inhibition by mechanomyography and paired-pulse transcranial magnetic stimulation in unanesthetized rats," *Journal of Neurophysiology*, vol. 107, no. 3, pp. 966–972, 2012.

[55] J. Trippe, A. Mix, S. Aydin-Abidin, K. Funke, and A. Benali, "Theta burst and conventional low-frequency rTMS differentially affect GABAergic neurotransmission in the rat cortex," *Experimental Brain Research*, vol. 199, no. 3-4, pp. 411–421, 2009.

[56] J. I. Liang, P. C. Lin, M. Y. Chen, T. H. Hsieh, J. J. Chen, and M. L. Yeh, "The effect of tenocyte/hyaluronic acid therapy on the early recovery of healing Achilles tendon in rats," *Journal of Materials Science Materials in Medicine*, vol. 25, no. 1, pp. 217–227, 2014.

[57] O. S. Mabrouk, M. Marti, S. Salvadori, and M. Morari, "The novel delta opioid receptor agonist UFP-512 dually modulates motor activity in hemiparkinsonian rats via control of the nigro-thalamic pathway," *Neuroscience*, vol. 164, no. 2, pp. 360–369, 2009.

[58] G. A. Metz, A. Tse, M. Ballermann, L. K. Smith, and K. Fouad, "The unilateral 6-OHDA rat model of Parkinson's disease revisited: an electromyographic and behavioural analysis," *The European Journal of Neuroscience*, vol. 22, no. 3, pp. 735–744, 2005.

[59] M. C. Yoon, M. S. Shin, T. S. Kim et al., "Treadmill exercise suppresses nigrostriatal dopaminergic neuronal loss in 6-hydroxydopamine-induced Parkinson's rats," *Neuroscience Letters*, vol. 423, no. 1, pp. 12–17, 2007.

[60] T. H. Hsieh, C. W. Kuo, K. H. Hsieh, M. J. Shieh, C. W. Peng, Y. C. Chen et al., "Probiotics alleviate the progressive deterioration of motor functions in a mouse model of Parkinson's disease," *Brain Sciences*, vol. 10, no. 4, 2020.

[61] A. Degardin, D. Devos, L. Defebvre et al., "Effect of intermittent theta-burst stimulation on akinesia and sensorimotor integration in patients with Parkinson's disease," *The European Journal of Neuroscience*, vol. 36, no. 5, pp. 2669–2678, 2012.

[62] B. Elahi and R. Chen, "Effect of transcranial magnetic stimulation on Parkinson motor function–systematic review of controlled clinical trials," *Movement Disorders*, vol. 24, no. 3, pp. 357–363, 2009.

[63] J. P. Lefaucheur, X. Drouot, F. Von Raison, I. Menard-Lefaucheur, P. Cesaro, and J. P. Nguyen, "Improvement of motor performance and modulation of cortical excitability by repetitive transcranial magnetic stimulation of the motor cortex in Parkinson's disease," *Clinical Neurophysiology*, vol. 115, no. 11, pp. 2530–2541, 2004.

[64] Y. Shirota, H. Ohtsu, M. Hamada, H. Enomoto, Y. Ugawa, and For the Research Committee on rTMS Treatment of Parkinson's Disease, "Supplementary motor area stimulation for Parkinson disease," *Neurology*, vol. 80, no. 15, pp. 1400–1405, 2013.

[65] E. M. Khedr, H. M. Farweez, and H. Islam, "Therapeutic effect of repetitive transcranial magnetic stimulation on motor function in Parkinson's disease patients," *European Journal of Neurology*, vol. 10, no. 5, pp. 567–572, 2003.

[66] P. Arias, J. Vivas, K. L. Grieve, and J. Cudeiro, "Controlled trial on the effect of 10 days low-frequency repetitive transcranial magnetic stimulation (rTMS) on motor signs in Parkinson's disease," *Movement Disorders*, vol. 25, no. 12, pp. 1830–1838, 2010.

[67] E. M. Khedr, J. C. Rothwell, O. A. Shawky, M. A. Ahmed, and A. Hamdy, "Effect of daily repetitive transcranial magnetic stimulation on motor performance in Parkinson's disease," *Movement Disorders*, vol. 21, no. 12, pp. 2201–2205, 2006.

[68] C. W. Yip, P. W. Cheong, A. Green et al., "A prospective pilot study of repetitive transcranial magnetic stimulation for gait dysfunction in vascular parkinsonism," *Clinical Neurology and Neurosurgery*, vol. 115, no. 7, pp. 887–891, 2013.

[69] M. S. Kim, W. H. Chang, J. W. Cho, J. Youn, Y. K. Kim, S. W. Kim et al., "Efficacy of cumulative high-frequency rTMS on freezing of gait in Parkinson's disease," *Restorative Neurology and Neuroscience*, vol. 33, no. 4, pp. 521–530, 2015.

[70] W. H. Chang, M. S. Kim, J. W. Cho et al., "Effect of cumulative repetitive transcranial magnetic stimulation on freezing of gait in patients with atypical parkinsonism: a pilot study," *Journal of Rehabilitation Medicine*, vol. 48, no. 9, pp. 824–828, 2016.

[71] T. Maruo, K. Hosomi, T. Shimokawa et al., "High-frequency repetitive transcranial magnetic stimulation over the primary foot motor area in Parkinson's disease," *Brain Stimulation*, vol. 6, no. 6, pp. 884–891, 2013.

[72] S. Y. Lee, M. S. Kim, W. H. Chang, J. W. Cho, J. Y. Youn, and Y. H. Kim, "Effects of repetitive transcranial magnetic stimulation on freezing of gait in patients with parkinsonism," *Restorative Neurology and Neuroscience*, vol. 32, no. 6, pp. 743–753, 2014.

[73] J. Ma, L. Gao, T. Mi, J. Sun, P. Chan, and T. Wu, "Repetitive transcranial magnetic stimulation does not improve the sequence effect in freezing of gait," *Parkinson's Disease*, vol. 2019, article 2196195, 8 pages, 2019.

[74] S. R. Filipovic, J. C. Rothwell, and K. Bhatia, "Low-frequency repetitive transcranial magnetic stimulation and off-phase motor symptoms in Parkinson's disease," *Journal of the Neurological Sciences*, vol. 291, no. 1-2, pp. 1–4, 2010.

[75] H. Rothkegel, M. Sommer, T. Rammsayer, C. Trenkwalder, and W. Paulus, "Training effects outweigh effects of single-session conventional rTMS and theta burst stimulation in PD patients," *Neurorehabilitation and Neural Repair*, vol. 23, no. 4, pp. 373–381, 2009.

[76] M. F. del Olmo, O. Bello, and J. Cudeiro, "Transcranial magnetic stimulation over dorsolateral prefrontal cortex in Parkinson's disease," *Clinical Neurophysiology*, vol. 118, no. 1, pp. 131–139, 2007.

[77] D. H. Benninger, K. Iseki, S. Kranick, D. A. Luckenbaugh, E. Houdayer, and M. Hallett, "Controlled study of 50-Hz repetitive transcranial magnetic stimulation for the treatment of Parkinson disease," *Neurorehabilitation and Neural Repair*, vol. 26, no. 9, pp. 1096–1105, 2012.

[78] I. Rektorova, S. Sedlackova, S. Telecka, A. Hlubocky, and I. Rektor, "Repetitive transcranial stimulation for freezing of gait in Parkinson's disease," *Movement Disorders*, vol. 22, no. 10, pp. 1518-1519, 2007.

[79] M. P. Lomarev, S. Kanchana, W. Bara-Jimenez, M. Iyer, E. M. Wassermann, and M. Hallett, "Placebo-controlled study of rTMS for the treatment of Parkinson's disease," *Movement Disorders*, vol. 21, no. 3, pp. 325–331, 2006.

[80] F. Cacace, D. Mineo, M. T. Viscomi et al., "Intermittent theta-burst stimulation rescues dopamine-dependent corticostriatal synaptic plasticity and motor behavior in experimental parkinsonism: possible role of glial activity," *Movement Disorders*, vol. 32, no. 7, pp. 1035–1046, 2017.

[81] M. E. Keck, T. Welt, M. B. Müller et al., "Repetitive transcranial magnetic stimulation increases the release of dopamine in the mesolimbic and mesostriatal system," *Neuropharmacology*, vol. 43, no. 1, pp. 101–109, 2002.

[82] M. Kanno, M. Matsumoto, H. Togashi, M. Yoshioka, and Y. Mano, "Effects of acute repetitive transcranial magnetic stimulation on dopamine release in the rat dorsolateral striatum," *Journal of the Neurological Sciences*, vol. 217, no. 1, pp. 73–81, 2004.

[83] A. P. Strafella, T. Paus, J. Barrett, and A. Dagher, "Repetitive transcranial magnetic stimulation of the human prefrontal cortex induces dopamine release in the caudate nucleus," *The Journal of Neuroscience*, vol. 21, no. 15, p. RC157, 2001.

[84] J. Y. Kim, E. J. Chung, W. Y. Lee et al., "Therapeutic effect of repetitive transcranial magnetic stimulation in Parkinson's disease: analysis of [11C] raclopride PET study," *Movement Disorders*, vol. 23, no. 2, pp. 207–211, 2008.

[85] E. M. Khedr, J. C. Rothwell, O. A. Shawky, M. A. Ahmed, N. Foly K, and A. Hamdy, "Dopamine levels after repetitive transcranial magnetic stimulation of motor cortex in patients with Parkinson's disease: preliminary results," *Movement Disorders*, vol. 22, no. 7, pp. 1046–1050, 2007.

[86] T. Wichmann and M. R. DeLong, "Functional and pathophysiological models of the basal ganglia," *Current Opinion in Neurobiology*, vol. 6, no. 6, pp. 751–758, 1996.

[87] J. P. Lefaucheur, "Motor cortex dysfunction revealed by cortical excitability studies in Parkinson's disease: influence of antiparkinsonian treatment and cortical stimulation," *Clinical Neurophysiology*, vol. 116, no. 2, pp. 244–253, 2005.

[88] V. Paille, B. Picconi, V. Bagetta et al., "Distinct levels of dopamine denervation differentially alter striatal synaptic plasticity and NMDA receptor subunit composition," *The Journal of Neuroscience*, vol. 30, no. 42, pp. 14182–14193, 2010.

[89] J. L. Hudson, C. G. van Horne, I. Strömberg et al., "Correlation of apomorphine- and amphetamine-induced turning with nigrostriatal dopamine content in unilateral 6-hydroxydopamine lesioned rats," *Brain Research*, vol. 626, no. 1-2, pp. 167–174, 1993.

[90] J. P. Kostrzewa, R. A. Kostrzewa, R. M. Kostrzewa, R. Brus, and P. Nowak, "Perinatal 6-Hydroxydopamine to produce a lifelong model of severe Parkinson's disease," *Current Topics in Behavioral Neurosciences*, vol. 29, pp. 313–332, 2016.

[91] J. F. Marshall and U. Ungerstedt, "Supersensitivity to apomorphine following destruction of the ascending dopamine neurons: quantification using the rotational model," *European Journal of Pharmacology*, vol. 41, no. 4, pp. 361–367, 1977.

[92] R. J. Mandel, R. E. Wilcox, and P. K. Randall, "Behavioral quantification of striatal dopaminergic supersensitivity after bilateral 6-hydroxydopamine lesions in the mouse," *Pharmacology, Biochemistry, and Behavior*, vol. 41, no. 2, pp. 343–347, 1992.

[93] A. Bjorklund and S. B. Dunnett, "The amphetamine induced rotation test: a re-assessment of its use as a tool to monitor motor impairment and functional recovery in rodent models of Parkinson's disease," *Journal of Parkinson's Disease*, vol. 9, no. 1, pp. 17–29, 2019.

[94] V. Sasso, E. Bisicchia, L. Latini et al., "Repetitive transcranial magnetic stimulation reduces remote apoptotic cell death and inflammation after focal brain injury," *Journal of Neuroinflammation*, vol. 13, no. 1, p. 150, 2016.

[95] M. R. Ljubisavljevic, A. Javid, J. Oommen et al., "The effects of different repetitive transcranial magnetic stimulation (rTMS) protocols on cortical gene expression in a rat model of cerebral ischemic-reperfusion injury," *PLoS One*, vol. 10, no. 10, article e0139892, 2015.

Hindawi
Neural Plasticity
Volume 2021, Article ID 1987662, 7 pages
https://doi.org/10.1155/2021/1987662

Research Article

Effectiveness of Contralaterally Controlled Functional Electrical Stimulation versus Neuromuscular Electrical Stimulation on Upper Limb Motor Functional Recovery in Subacute Stroke Patients: A Randomized Controlled Trial

Songhua Huang,[1,2] **Peile Liu**,[1] **Yinglun Chen**,[1] **Beiyao Gao**,[1] **Yingying Li**,[1] **Chan Chen**,[1,2] **and Yulong Bai**[1,2,3]

[1]*Department of Rehabilitation Medicine, Huashan Hospital, Fudan University, Shanghai 20000, China*
[2]*Department of Rehabilitation Medicine, Huashan Hospital North, Fudan University, Shanghai 20000, China*
[3]*National Center for Neurological Disorder, Shanghai, China*

Correspondence should be addressed to Chan Chen; chanchen09@fudan.edu.cn and Yulong Bai; dr_baiyl@fudan.edu.cn

Received 9 June 2021; Accepted 6 December 2021; Published 22 December 2021

Academic Editor: Jia-Jia Wu

Purpose. To compare the effectiveness of contralaterally controlled functional electrical stimulation (CCFES) versus neuromuscular electrical stimulation (NMES) on motor recovery of the upper limb in subacute stroke patients. *Materials and Methods*. Fifty patients within six months poststroke were randomly assigned to the CCFES group ($n = 25$) and the NMES group ($n = 25$). Both groups underwent routine rehabilitation plus 20-minute stimulation on wrist extensors per day, five days a week, for 3 weeks. Fugl-Meyer Assessment of upper extremity (FMA-UE), action research arm test (ARAT), Barthel Index (BI), and surface electromyography (sEMG) were assessed at baseline and end of intervention. *Results*. After a 3-week intervention, FMA-UE and BI increased in both groups ($p < 0.05$). ARAT increased significantly only in the CCFES group ($p < 0.05$). The changes of FMA-UE, ARAT, and BI in the CCFES group were not greater than those in the NMES group. The improvement in sEMG response of extensor carpi radialis by CCFES was greater than that by NMES ($p = 0.026$). The cocontraction ratio (CCR) of flexor carpi radialis did not decrease in both groups. *Conclusions*. CCFES improved upper limb motor function, but did not show better treatment effect than NMES. CCFES significantly enhanced the sEMG response of paretic extensor carpi radialis compared with NMES, but did not decrease the cocontraction of antagonist.

1. Introduction

Neuromuscular electrical stimulation (NMES) is a modality widely used in stroke rehabilitation for motor impairment by improving or assisting volitional movement [1]. Cyclic NMES offers a preset and passive stimulation on specific muscles with on-off cycles of repetitive mode. The therapeutic effect of NMES for upper limb motor impairment after stroke has been shown in several randomized controlled trials [2]. The repetitive movement training induced by NMES may facilitate motor relearning. However, goal-oriented active repetitive training is not easy to carry out by cyclic NMES in acute or subacute phase after stroke, especially in severe cases. As a kind of physical therapy, NMES consists in evoking contractions by applying an electrical current over the muscle via surface electrodes. It represents an incomplete activation of the neuromuscular system, and the use of submaximal training intensities should partly account for its lower efficiency on muscle strength than resistance training [1]. Some studies found more significant functional improvements by cyclic NMES when paired with simultaneous voluntary effort using residual movement [2].

Contralaterally controlled functional electrical stimulation (CCFES) is a unique stimulation modality using a

motor signal detected from the volitional movement of the nonparetic limb to control the electrical stimulation delivered to the paretic limb, which induces similar movement on the paretic limb [3]. Different with cyclic NMES, CCFES enables active participation of both sides of limb as well as self-control of the timing and intensity of stimulation to the paretic limb, without requirement of residual movement. A small clinical study has reported that CCFES improves hand dexterity in subacute stroke patients [4]. The effect of CCFES on wrist extension (active range of motion) and the improvement of the upper limb function were reported in stroke patients in 3 months and 15 days [5, 6]. The changes of Motricity Index of the upper limb and strength of extensor carpi assessed by the manual muscle power test were also reported. But the Motricity Index was not significantly enhanced along with the improvement of active range of motor of wrist extension. Surface electromyography (sEMG) evaluation may be an appropriate assessment of muscle activation [7, 8].

This study is aimed at comparing the effectiveness of CCFES versus NMES on upper limb function recovery in 6 months poststroke by upper limb and hand functional assessment and surface electromyography (sEMG) evaluation. We hypothesized that CCFES had better effect on the upper limb function and muscle activation than NMES in subacute stroke patients.

2. Materials and Methods

This study was designed as a parallel randomized controlled trial. Doctors who evaluated the outcome assessments were blinded to the allocation. The study protocol was approved by the ethics committee of Huashan Hospital, Fudan University (the approval number 2019-006). This study has been registered with Chinese Clinical Trial Registry (http://www.chictr.org.cn/) (No. ChiCTR1900021770).

2.1. Subjects. Patients admitted to the Department of Rehabilitation Medicine, Huashan Hospital North, Fudan University, from March 2019 to March 2020 were recruited. All patients were given informed consent for this study, and written consents were provided by the patients or their legally authorized representatives.

Inclusion criteria were as follows: (1) diagnosis of a first-ever stroke confirmed by head CT or MRI scanning, (2) well general condition with stabilized vital signs and normal consciousness, (3) age 30~85 years, (4) Brunnstrom recovery stage one to four for the affected upper limb, (5) 7 days to 6 months after stroke onset [9], (6) unilateral lesion indicated by CT or MRI, and (7) voluntary for this study with a signed informed consent.

Exclusion criteria were as follows: (1) reversible stroke; (2) severe visceral organ (e.g., heart, lung, liver, and kidney dysfunction); (3) severe cognitive dysfunction, MMSE < 23; (4) with a history of mental disease and cannot cooperate in rehabilitation treatment; (5) deaf-mutes; (6) unable to receive treatment in designated hospital at specific time or unable to be followed up regularly; (7) implanted with cardiac pacemaker; and (8) with upper limb dysfunction due to other causes.

The administrative assistant of the study who did not participate in the treatment and assessment assigned the patients to either the NMES group or the CCFES group using random number table generated by computer and allocated 1 : 1 by concealed sequentially numbered envelopes.

2.2. Study Protocol. Both groups went through routine rehabilitation (1 hour/day) for 5 days per week over a period of 3 weeks, including posture management (sitting, standing, and sit to stand), abnormal reflex inhibition, proprioceptive neuromuscular facilitation, and occupational therapy. Routine rehabilitation was performed by therapists blinded to group allocation. Both CCFES and NMES were provided in addition to routine rehabilitation training. Accompanying diseases (e.g., hypertension, coronary artery disease, and diabetes) were treated with medicines.

In the CCFES group, contralaterally controlled functional electrical stimulator (DC-L-500, Jiangsu NeuCognic Medical Co., Ltd., Jiangsu, China) was used to stimulate wrist extensors of the paretic side controlled by the nonparetic side. Subjects sit with arm and hand resting at side and forearm pronated. The 2 stimulating electrodes were placed on the muscle belly of extensor carpi radialis of the paretic side. The main controller for detecting nonparetic wrist extension and triggering stimulation on paretic wrist extensors was worn on the back of the nonparetic hand. Before stimulation, subjects were asked to voluntarily extend the nonparetic wrist to certain angle according to the instruction (0, 45, and 20 degrees) and recorded by the main controller. The extension of the paretic wrist was elicited by the electrical stimulation from the main controller when it detected the motion of the nonparetic wrist (at least 20-degree extension). The stimulation is aimed at generating 20-25 degrees of wrist extension on the paretic side. The therapist would instruct the nonparetic wrist extension and adjust the stimulating intensity ensuring to elicit 20–25-degree wrist extension on the paretic side without causing pain or any discomfort (a sensory sustainable range). Subjects were instructed to relax the paretic arm during the treatment. The waveform of stimulation was biphasic rectangular wave with frequency of 35 pps and pulse width of 200 μs. Subjects were asked to maintain the nonparetic wrist extension for 10 s so that the stimulation on the paretic side could last. Once the nonparetic wrist relaxed and went back to 0 degree, the stimulation ceased. The interval of every motion and stimulation was set as 10 s. The CCFES treatment was performed 20 min/session, 1 session/day, 5 consecutive days/week, for 3 weeks. A 5 min practice session was performed in the initial of the CCFES therapy to make sure the subjects know how to accomplish the treatments.

In the NMES group, the stimulation was conducted by the bio-feedback electrical stimulator (MyoNet-BOW, Shanghai Ncc Electronic Co., Ltd., Shanghai, China). Subjects sit with arm and hand resting at side and forearm pronated. The 2 stimulating electrodes were placed on the muscle belly of extensor carpi radialis on the paretic side.

Subjects were instructed to relax the paretic arm during NMES. The waveform of stimulation was biphasic rectangular wave with frequency of 35 pps and pulse width of 200 μs. The stimulation and relaxation time was set as 10 s : 10 s. The stimulation intensity was adjusted to the level of tetanic contraction, which would elicit 20-25 degrees of wrist extension of the paretic hand, without causing any pain sensation. The electrical stimulation treatments were performed 20 min/session, 1 session/day, 5 consecutive days/week, for 3 weeks.

2.3. Outcome Assessment. Functional evaluations were performed by two doctors blinded to group allocation at baseline and after a 3-week intervention.

The primary outcome was action research arm test (ARAT). This test is used to evaluate the motor performance of the arm and hand including 4 subscales (grasp, grip, pinch, and gross movement). The 19 items are rated on a 4-point scale scoring from 0 (no movement) to 3 (normally performed movement). The maximum score is 57. On the basis of clinical experience and estimates reported for similar outcome measures, the minimal clinically important difference (MCID) of ARAT was set at 10% of the total range, which was 5.7 points [10].

The secondary outcomes included the following:

(1) Motor function of Fugl-Meyer Assessment of upper extremity (FMA-UE): the motor function of FMA-UE evaluates the tendon reflexes and the performance of given tasks involving the shoulder, elbow, wrist, and hand. Each item is rated on a 3-point scale scoring from 0 to 2, except for the reflex activity which has only 2 points, scoring 0 or 2. Scoring 0 means no reflex can be elicited or cannot do the given task. Scoring 1 means the task can be performed partially. Scoring 2 means the task can be performed fully. The maximum score of motor function of FMA-UE is 66

(2) Barthel Index: 10 items, including feeding, fecal and urinary incontinence, dressing and undressing, grooming, toilet use, bathing, transfer (e.g., from chair to bed), walking, and climbing stairs. The total score is 100

(3) Surface electromyography (sEMG): the surface electromyographic signals of the extensor carpi radialis and flexor carpi radialis on both side were recorded during active wrist extension by surface electromyography apparatus (MyoMove-EOW, Shanghai Ncc Electronic Co., Ltd., Shanghai, China). The signal was amplified and band pass filtered (5-500 Hz) prior to sampling. The subjects were trained before signal collection to understand the whole procedure. During the collection, the subjects were required to try their best to extend the wrist and maintain for about 3 s and then relax for 5 s, repeating for 3 times. The signals were recorded and generated automatically to the root mean square (RMS) values by the software installed with the surface electromyography apparatus. The RMS of paretic extensor carpi radialis was standardized by calculating sEMG signal ratio in percentage, a ratio of RMS of the paretic side/the nonparetic side. Cocontraction ratio (CCR) of paretic flexor carpi radialis was calculated by the ratio of RMS of flexor carpi radialis/(RMS of flexor carpi radialis + RMS of extensor carpi radialis) [8]. The smaller CCR of paretic wrist flexors indicates the better motor control of voluntary wrist extension

2.4. Statistical Analysis. For baseline demographic and clinical characteristic comparability, chi-square test was used for categorical variables and t-test was used for continuous variables. Two-sample t-test was used to compare the change of each assessment (ARAT, FMA-UE, Barthel Index, and RMS of extensor carpi and CCR of flexor carpi) from baseline to end of intervention between groups. Paired t-test was used for comparison of each assessment between baseline and end of intervention in each group. The significance level is set at 0.05. SPSS 18.0 was used for statistical analysis.

Sample size was estimated according to the MCID of ARAT. SD was 6.0. Sample size was calculated using two-sample estimation at a level of significance of 0.05 with 90% powers.

3. Results

Fifty eligible patients were enrolled and randomly assigned into the NMES group ($n = 25$) and the CCFES group ($n = 25$) (Figure 1). There were no significant differences between groups in gender, type of stroke, side of affected hemisphere, and Brunnstrom recovery stage according to chi-square test ($p > 0.05$), nor in age and course of disease according to t-test ($p > 0.05$) (Table 1).

After a 3-week intervention, FMA-UE and Barthel Index increased significantly in both groups ($p < 0.05$). ARAT increased significantly only in the CCFES group ($p < 0.05$). The change of FMA-UE, ARAT, and Barthel Index from baseline in the CCFES group was not significantly greater than that in the NMES group. For sEMG evaluation, the improvement of RMS of extensor carpi radialis in the CCFES group was greater than that in the NMES group with the difference of 0.09 (95% CI 0.01-0.16, $p = 0.026$). NMES had no effect on RMS of extensor carpi radialis. The CCR of flexor carpi radialis in CCFES did not significantly decrease, and the change of CCR in CCFES was not significantly lower than that in the NMES group (Table 2).

No adverse events were reported during the intervention and follow-up in any of the groups.

4. Discussion

This randomized controlled trial compared the effectiveness of CCFES and NMES on upper limb motor function recovery in patients within 6 months poststroke. At the end of the 3-week intervention, the CCFES group gained greater improvement of RMS of extensor carpi radialis than the NMES group. Treatment effects of ARAT, FMA-UE, Barthel Index, and CCR of flexor carpi radialis were not significantly different between the CCFES and NMES groups. Both

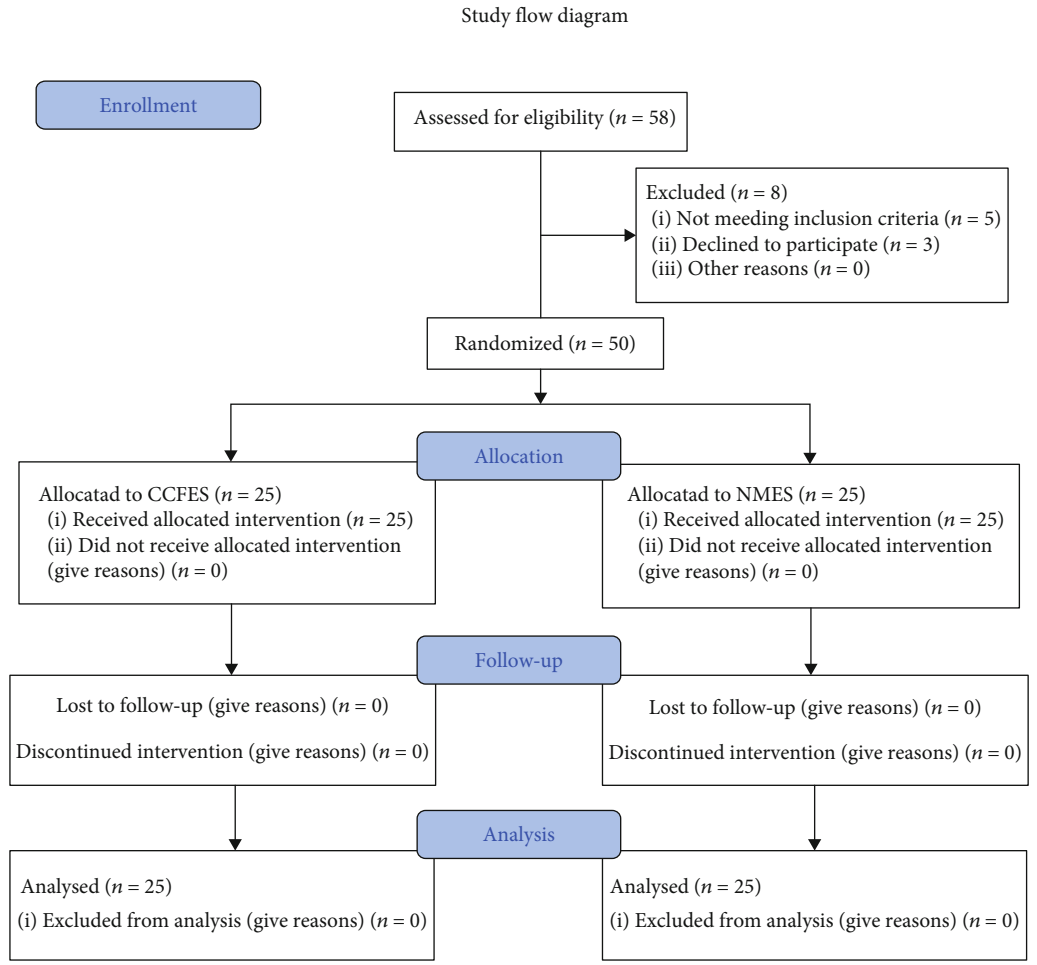

Figure 1: Study flow diagram. CCFES: contralaterally controlled functional electrical stimulation; NMES: neuromuscular electrical stimulation.

groups had greater scores of FMA-UE and BI at the end of intervention, while ARAT increased significantly only in the CCFES group.

CCFES improved upper limb function, but did not show greater treatment effect on assessed upper limb function (FMA-UE and ARAT) in our study. This finding was not consistent with reported studies. An early-phase study reported by Knutson et al. favored 6-week intervention of CCFES over NMES on improvement of FMA, box and block test (BBT), arm motor ability test (AMAT), and the angle of finger extension at the end of treatment and 1 month and 3 months posttreatment in subacute stroke patients [4]. However, the power of this study was limited by the small number of subjects. Later in 2016, Knutson et al. reported results in chronic stroke patients (>6 months) with longer treatment (12 weeks, 10 hours/week). The CCFES group had greater improvement on BBT performance than NMES at 6 months posttreatment but no significant gain on FMA and AMAT [11]. The stimulation duration and sessions were longer compared with our study. Besides, the stimulation was targeted on hand opening, along with functional task training assisted by CCFES, which may explain the greater gain in hand dexterity. In 2015, Shen et al. reported a study comparing the effectiveness of CCFES on wrist extensors versus NMES in patients within 3 months post-stroke. After the 3-week intervention of CCFES, they reported greater improvement of FMA of upper extremity, the Hong Kong version of the Functional Test for the Hemiplegic Upper Extremity (FTHUE-HK), and Active Range of Motion (AROM) of wrist extension than NMES. The gain of FMA was 7.6 (SD1.4) in the CCFES group and 4.9 (SD1.4) in the NMES group, with a mean difference of 2.7 [5]. Our study reported a greater gain of FMA in the NMES group (6.04) and a smaller difference of gain between groups, with 1.76 (95% CI -2.65-6.17). Although our intervention protocol was similar to the study by Shen et al., the subject population might have different characteristics of central plasticity such as cortical excitability, interhemispheric inhibition, and integrity of the corticospinal tract. The central plasticity of subjects would be a confounder of the treatment effect of CCFES on functional assessment.

The recovery of muscle strength was also assessed in previous studies. Zheng et al. found that CCFES had better effect on wrist extensor strength than NMES in acute stroke patients [6]. Shen et al. reported no significant benefit for Motricity Index by CCFES in subacute stroke patients [5]. Our study used sEMG evaluation to measure the paretic muscle activation. The temporal bioelectrical signals of

Table 1: Baseline demographics and clinical characteristics.

Characteristic	CCFES ($n = 25$)	NMES ($n = 25$)	p value
Age (years)	56.2 ± 12.2	60.4 ± 11.3	0.521
Gender			0.544
Male	18 (72%)	16 (64%)	
Female	7 (18%)	9 (36%)	
Course of disease (days since stroke)	43.9 ± 33.4	46.3 ± 33.1	0.662
Type of stroke			0.382
Ischemic	17 (68%)	14 (56%)	
Hemorrhagic	8 (32%)	11 (44%)	
Hemisphere affected			0.571
Left	11 (44%)	13 (52%)	
Right	14 (56%)	12 (48%)	
Brunnstrom recovery stage			
I-III (hand)	18 (72%)	23 (92%)	
IV (hand)	7 (28%)	2 (8%)	0.066
I-III (upper limb)	20 (80%)	23 (92%)	
IV (upper limb)	5 (20%)	2 (8%)	0.22
ARAT	7.36 ± 12.67	3.44 ± 9.59	0.108
FMA of upper limb	19.52 ± 14.39	14.08 ± 10.35	0.091
Barthel Index	51.20 ± 20.93	46.40 ± 16.80	0.376
RMS of paretic extensor carpi radialis	0.13 ± 0.14	0.12 ± 0.15	0.648
CCR of paretic flexor carpi radialis	0.44 ± 0.18	0.46 ± 0.22	0.673

Data are presented with mean ± SD or numbers (%).

Table 2: Changes from baseline to end of intervention in functional assessments and sEMG.

	CCFES ($n = 25$) (mean ± SD)	NMES ($n = 25$) (mean ± SD)	Difference between groups (mean, 95% CI)	p value
ARAT	8.92 ± 12.16^	3.48 ± 10.44	5.44 (-1.0, 11.89)	0.096
FMA-UE	7.8 ± 7.27^	6.04 ± 8.19^	1.76 (-2.65, 6.17)	0.43
Barthel Index	11.80 ± 12.90^	9.80 ± 10.25^	2 (-4.63, 8.63)	0.553
RMS of paretic extensor carpi radialis	0.09 ± 0.16^	0.00 ± 0.09	0.09 (0.01, 0.16)*	0.026
CCR of paretic flexor carpi radialis	−0.02 ± 0.179	0.02 ± 0.21	-0.04 (-0.07, 0.15)	0.491

^The difference between end of treatment and baseline is statistically significant, $p < 0.05$. *The difference between the CCFES and NMES groups is statistically significant.

muscles recorded from the skin surface during muscle activation reflect the recruitment and synchronization of motor units. Although we set the stimulation in a "passive" mode, CCFES had greater treatment effect for extensor carpi radialis than NMES. The cocontraction ratio we used was defined as the proportion of cocontraction muscle forces to total muscle forces. Excessive cocontraction and abnormal muscle recruitment may limit the movement in the central nervous diseases. Studies have indicated higher cocontraction ratio of the affected limb in stroke [7] and cerebral palsy [8]. CCFES also favored decreased cocontraction of flexor carpi radialis, without significant difference with NMES. The results indicated that CCFES had a potential benefit for enhanced voluntary contraction of paralyzed muscle and muscular activation pattern. However, the improvement of muscular activation did not translate to greater functional gain in our study. We assumed longer intervention and combination of functional task training may enhance the translation.

NMES is one rehabilitation treatment option for stroke patients with motor function impairment. The motor learning mechanism is assumed to be the therapeutic effect NMES as it can induce repetitive movement. However, the effectiveness of NMES on function improvement has been questioned. Wilson et al. observed the effectiveness of 3 different modes of electrical stimulation (cyclic NMES, EMG-triggered NMES, and sensory stimulation without motor recruitment) on upper limb functional changes in stroke patients within six months poststroke. Yet they attributed

the results to self-recovery rather than electrical therapies [12]. Combined with task-related training, functional electrical stimulation (FES) has been verified to promote motor recovery by changing the motor networks in the cortex and enhancing synaptic remodeling [13].

CCFES offers a new mode with combination of bilateral symmetrical motor training and self-controlled electrical stimulation. Bilateral symmetrical motor training is assumed to effectively activate the primary motor cortex (M1) ipsilateral to brain damages [14] and further rebuild new task-relevant neural networks based on residual neurons [15, 16]. This intervention may accelerate functional recovery through motor pathway facilitation [17, 18]. Cortical physiological studies conducted by transcranial magnetic stimulation showed that in the acute phase of stroke, patients' performance was limited to corticospinal damage [19]. While at 3 months poststroke or chronic phase, intracortical disinhibition may play a role in reorganization of cortical network and improvement of hand function [19–21]. Some transcallosal nerves that originated from the nonlesion side to lesion side show crucial effect on motor function recovery after neural disconnection [22]. In chronic stroke patients, bilateral arm training led to significantly higher increase in activation in the ipsilesional cortex (the precentral, the anterior cingulate, and the postcentral gyri and the supplementary motor area) and contralesional superior frontal gyrus. Activation change in the contralesional cortex was correlated with improvement in the Wolf Motor Function Test Time [23]. The theoretical model developed by Mudie and Matyas suggested that bilateral symmetric movement could promote interhemispheric disinhibition and allow the ipsilesional hemisphere to share a "template of motor network recruitment" from the contralesional hemisphere [16]. Coupled bilateral movement and EMG-triggered NMES on affected arm enhanced hand function and reaching task performance compared with NMES in chronic stroke [24, 25]. And compared with coupled bilateral movement and placebo stimulation, coupled bilateral movement and FES had better effect on improvement of functional test of upper limb and active range of wrist extension [26, 27]. A recent crossover study showed that CCFES (bilateral symmetric movement) reduced interhemispheric inhibition and maintained ipsilesional output when compared with NMES (unilateral-based therapy) [28]. Besides, the intention-to-control mode of stimulation offered by CCFES enables patients who have no or fewer residual motor function of affected limb to do functional-related repetitive training. By offering the illusion of good motor control to the patient, CCFES may integrate afferent sensory fibers to change the motor network in the cortex and enhance synaptic remodeling to facilitate brain plasticity.

There are several limitations to this study. The central plasticity of subject was not evaluated by electrophysiological or functional imaging investigation at baseline, which could be a confounder of the treatment effect of CCFES. And the effect of CCFES on central plasticity was not measured in this study. The duration of intervention was short, which may reduce the effect of CCFES. The lasting effect of possible central plasticity by CCFES was unable to be explored due to the lack of longer follow-up assessments. The study included patients with different Brunnstrom recovery stages of upper limb, which may lead to confusion as to the best application of CCFES. In the future study, adding a new intervention group of voluntary movement on nonparetic side (without CCFES)+NMES on paretic side as a bilateral movement training may provide more information.

5. Conclusions

CCFES improved upper limb motor function but did not show better therapeutic effect than NMES after the 3-week stimulation on extensor carpi radialis according to functional assessments in subacute stroke patients. CCFES enhanced the sEMG response of paretic extensor carpi radialis better than NMES but did not decrease the cocontraction ratio of flexor carpi radialis.

Data Availability

The demographic data and data of outcome assessment used to support the findings of this study are available from the corresponding author upon request.

Conflicts of Interest

The authors declare that there is no conflict of interest regarding the publication of this paper.

Acknowledgments

The authors thank the staff of the Department of Rehabilitation Medicine, Huashan Hospital, Fudan University, in particular, Yuyuan Wang, Yiming Xu, Tianhao Gao, Xiao Qiu, Yan Hua, Juan Zhao, Erkang Xie, Junqi Ling, Yangyang Cong, and Liujun Jiang. The authors disclosed receipt of the following financial support of the research, authorship, and publication of this article. This work was supported by the suburb tertiary hospital development project of Shanghai Shenkang Hospital Development Center (grant number SHDC12014906), the scientific research project supported by Huashan Hospital North, Fudan University (grant number HSBY2017014), the Science and Technology Commission of Shanghai Municipality (grant number 17511107802), and the National Natural Science Foundation of China (grant number 81601960).

References

[1] A. Bouguetoch, A. Martin, and S. Grospretre, "Insights into the combination of neuromuscular electrical stimulation and motor imagery in a training-based approach," *European Journal of Applied Physiology*, vol. 121, no. 3, pp. 941–955, 2021.

[2] J. S. Knutson, M. J. Fu, L. R. Sheffler, and J. Chae, "Neuromuscular electrical stimulation for motor restoration in hemiplegia," *Physical Medicine and Rehabilitation Clinics of North America*, vol. 26, no. 4, pp. 729–745, 2015.

[3] J. S. Knutson, M. Y. Harley, T. Z. Hisel, and J. Chae, "Improving hand function in stroke survivors: a pilot study of

contralaterally controlled functional electric stimulation in chronic hemiplegia," *Archives of Physical Medicine and Rehabilitation*, vol. 88, no. 4, pp. 513–520, 2007.

[4] J. S. Knutson, M. Y. Harley, T. Z. Hisel, S. D. Hogan, M. M. Maloney, and J. Chae, "Contralaterally controlled functional electrical stimulation for upper extremity hemiplegia: an early-phase randomized clinical trial in subacute stroke patients," *Neurorehabilitation and Neural Repair*, vol. 26, no. 3, pp. 239–246, 2012.

[5] Y. Shen, Z. Yin, Y. Fan et al., "Comparison of the effects of contralaterally controlled functional electrical stimulation and neuromuscular electrical stimulation on upper extremity functions in patients with stroke," *CNS & Neurological Disorders Drug Targets*, vol. 14, no. 10, pp. 1260–1266, 2015.

[6] Y. Zheng, M. Mao, Y. Cao, and X. Lu, "Contralaterally controlled functional electrical stimulation improves wrist dorsiflexion and upper limb function in patients with early-phase stroke: a randomized controlled trial," *Journal of Rehabilitation Medicine*, vol. 51, no. 2, pp. 103–108, 2019.

[7] C. C. Silva, A. Silva, A. Sousa et al., "Co-activation of upper limb muscles during reaching in post-stroke subjects: an analysis of the contralesional and ipsilesional limbs," *Journal of Electromyography and Kinesiology*, vol. 24, no. 5, pp. 731–738, 2014.

[8] K. Xu, J. Mai, L. He, X. Yan, and Y. Chen, "Surface electromyography of wrist flexors and extensors in children with hemiplegic cerebral palsy," *PM & R : The Journal of Injury, Function, and Rehabilitation*, vol. 7, no. 3, pp. 270–275, 2015.

[9] J. Bernhardt, K. S. Hayward, G. Kwakkel et al., "Agreed definitions and a shared vision for new standards in stroke recovery research: the stroke recovery and rehabilitation roundtable taskforce," *Neurorehabilitation and Neural Repair*, vol. 31, no. 9, pp. 793–799, 2017.

[10] J. H. van der Lee, R. C. Wagenaar, G. J. Lankhorst, T. W. Vogelaar, W. L. Devillé, and L. M. Bouter, "Forced use of the upper extremity in chronic stroke patients: results from a single-blind randomized clinical trial," *Stroke*, vol. 30, no. 11, pp. 2369–2375, 1999.

[11] J. S. Knutson, D. D. Gunzler, R. D. Wilson, and J. Chae, "Contralaterally controlled functional electrical stimulation improves hand dexterity in chronic hemiparesis: a randomized trial," *Stroke*, vol. 47, no. 10, pp. 2596–2602, 2016.

[12] R. D. Wilson, S. J. Page, M. Delahanty et al., "Upper-limb recovery after stroke: a randomized controlled trial comparing EMG-triggered, cyclic, and sensory electrical stimulation," *Neurorehabilitation and Neural Repair*, vol. 30, no. 10, pp. 978–987, 2016.

[13] F. Quandt and F. C. Hummel, "The influence of functional electrical stimulation on hand motor recovery in stroke patients: a review," *Experimental & translational stroke medicine*, vol. 6, no. 1, p. 9, 2014.

[14] M. E. Stoykov, E. King, F. J. David, A. Vatinno, L. Fogg, and D. M. Corcos, "Bilateral motor priming for post stroke upper extremity hemiparesis: a randomized pilot study," *Restorative Neurology and Neuroscience*, vol. 38, no. 1, pp. 11–22, 2020.

[15] N. AuYong, M. Malekmohammadi, J. Ricks-Oddie, and N. Pouratian, "Movement-modulation of local power and phase amplitude coupling in bilateral globus pallidus interna in Parkinson disease," *Frontiers in Human Neuroscience*, vol. 12, p. 270, 2018.

[16] M. H. Mudie and T. A. Matyas, "Can simultaneous bilateral movement involve the undamaged hemisphere in reconstruction of neural networks damaged by stroke?," *Disability and Rehabilitation*, vol. 22, no. 1-2, pp. 23–37, 2000.

[17] S. McCombe Waller, J. Whitall, T. Jenkins et al., "Sequencing bilateral and unilateral task-oriented training versus task oriented training alone to improve arm function in individuals with chronic stroke," *BMC Neurology*, vol. 14, no. 1, p. 236, 2014.

[18] J. L. Neva, M. Vesia, A. M. Singh, and W. R. Staines, "Modulation of left primary motor cortex excitability after bimanual training and intermittent theta burst stimulation to left dorsal premotor cortex," *Behavioural Brain Research*, vol. 261, pp. 289–296, 2014.

[19] O. B. Swayne, J. C. Rothwell, N. S. Ward, and R. J. Greenwood, "Stages of motor output reorganization after hemispheric stroke suggested by longitudinal studies of cortical physiology," *Cerebral Cortex*, vol. 18, no. 8, pp. 1909–1922, 2008.

[20] B. Hordacre, M. Lotze, M. Jenkinson et al., "Fronto-parietal involvement in chronic stroke motor performance when corticospinal tract integrity is compromised," *NeuroImage: Clinical*, vol. 29, article 102558, 2021.

[21] Z. Liu, H. Xin, and M. Chopp, "Axonal remodeling of the corticospinal tract during neurological recovery after stroke," *Neural Regeneration Research*, vol. 16, no. 5, pp. 939–943, 2021.

[22] L. J. Carr, L. M. Harrison, and J. A. Stephens, "Evidence for bilateral innervation of certain homologous motoneurone pools in man," *The Journal of Physiology*, vol. 475, no. 2, pp. 217–227, 1994.

[23] J. Whitall, S. M. C. Waller, J. D. Sorkin et al., "Bilateral and unilateral arm training improve motor function through differing neuroplastic mechanisms: a single-blinded randomized controlled trial," *Neurorehabilitation and Neural Repair*, vol. 25, no. 2, pp. 118–129, 2011.

[24] N. Kang and J. H. Cauraugh, "Right hemisphere contributions to bilateral force control in chronic stroke: a preliminary report," *Journal of Stroke and Cerebrovascular Diseases*, vol. 27, no. 11, pp. 3218–3223, 2018.

[25] S. Obayashi, R. Takahashi, and M. Onuki, "Upper limb recovery in early acute phase stroke survivors by coupled EMG-triggered and cyclic neuromuscular electrical stimulation," *NeuroRehabilitation*, vol. 46, no. 3, pp. 417–422, 2020.

[26] M. K. Chan, R. K. Tong, and K. Y. Chung, "Bilateral upper limb training with functional electric stimulation in patients with chronic stroke," *Neurorehabilitation and Neural Repair*, vol. 23, no. 4, pp. 357–365, 2009.

[27] A. Boyaci, O. Topuz, H. Alkan et al., "Comparison of the effectiveness of active and passive neuromuscular electrical stimulation of hemiplegic upper extremities," *International Journal of Rehabilitation Research*, vol. 36, no. 4, pp. 315–322, 2013.

[28] D. A. Cunningham, J. S. Knutson, V. Sankarasubramanian, K. A. Potter-Baker, A. G. Machado, and E. B. Plow, "Bilateral contralaterally controlled functional electrical stimulation reveals new insights into the interhemispheric competition model in chronic stroke," *Neurorehabilitation and Neural Repair*, vol. 33, no. 9, pp. 707–717, 2019.

Hindawi
Neural Plasticity
Volume 2021, Article ID 9955153, 8 pages
https://doi.org/10.1155/2021/9955153

Research Article

Soleus H-Reflex Change in Poststroke Spasticity: Modulation due to Body Position

Wenting Qin[1,2] **Anjing Zhang**[1,3] **Mingzhen Yang**[4] **Chan Chen**[1] **Lijun Zhen**[1] **Hong Yang**[3] **Lingjing Jin**[2] **and Fang Li**[1,5,6]

[1]*Department of Rehabilitation Medicine, Huashan Hospital, Fudan University, Shanghai, China*
[2]*Department of Neurology, Shanghai Tongji Hospital, Tongji University School of Medicine, Shanghai, China*
[3]*Department of Neurorehabilitation Medicine, Kongjiang Branch, the First Rehabilitation Hospital of Shanghai, Yangpu District, Shanghai, China*
[4]*Department of Rehabilitation Medicine, Zhongshan Hospital, Fudan University, Shanghai, China*
[5]*Department of Rehabilitation Medicine, Renhe Hospital, Baoshan District, Shanghai, China*
[6]*National Center for Neurological Disorders NCND, Shanghai, China*

Correspondence should be addressed to Fang Li; fangl@fudan.edu.cn

Received 1 April 2021; Revised 22 October 2021; Accepted 16 November 2021; Published 7 December 2021

Academic Editor: Chun Lei Shan

Purpose. This study is aimed at exploring how soleus H-reflex change in poststroke patients with spasticity influenced by body position. *Materials and Methods*. Twenty-four stroke patients with spastic hemiplegia and twelve age-matched healthy controls were investigated. Maximal Hoffmann-reflex (Hmax) and motor potential (Mmax) were elicited at the popliteal fossa in both prone and standing positions, respectively, and the Hmax/Mmax ratio at each body position was determined. Compare changes in reflex behavior in both spastic and contralateral muscles of stroke survivors in prone and standing positions, and match healthy subjects in the same position. *Results*. In healthy subjects, Hmax and Hmax/Mmax ratios were significantly decreased in the standing position compared to the prone position (Hmax: $p = 0.000$, Hmax/Mmax: $p = 0.016$). However, Hmax/Mmax ratios were increased in standing position on both sides in poststroke patients with spasticity (unaffected side: $p = 0.006$, affected side: $p = 0.095$). The Hmax and Hmax/Mmax ratios were significantly more increased on the affected side than unaffected side irrespective of the position. *Conclusions*. The motor neuron excitability of both sides was not suppressed but instead upregulated in the standing position in subjects with spasticity, which may suggest that there was abnormal regulation of the Ia pathway on both sides.

1. Introduction

Spasticity is defined as velocity-dependent increase in the tonic stretch reflexes (muscle tone) [1], which is one of the positive signs of upper motor neuron syndrome. It can cause continuous contraction of the affected muscles and difficulty in muscle coordination. Spasticity can cause pain, limited active and passive activities, and difficulty in nursing, which will seriously reduce the quality of life of the patient. Notably, as reported by Zorowitz et al. [2], the estimated range of spasticity in stroke survivors ranges from 20% to 40%.

In clinical practice, spasticity is usually measured at rest, based on the combination of physical signs, including increased muscle tone and tendon hyperreflexia. A previous study conducted by our research group showed that from the supine position to standing or sitting position, Modified Tardieu Scale (MTS) and Triple Spasticity Scale (TSS) scores significantly increased in the evaluated muscles of the hemiplegic upper limb in all poststroke patients [3]. Wang et al. observed that the contraction rates of elbow flexors in the affected side increase with the difficulty in different standing postures [4]. De Azevedo et al. found that in SCI patients a change in body position from sitting to supine increased the spastic state in quadriceps femoris during the pendulum test [5]. All above studies indicated that posture plays an important role in the spasticity regulation.

Burke et al. believed that the loss of homosynaptic inhibition between the Ia afferent pathway and motor neurons changes in reflex circuits affecting motoneuron excitability (e.g., Renshaw inhibition, Ib inhibition, and reciprocal Ia inhibition), and the intrinsic property changes of motor neurons and muscles make up the leading causes of increased muscle tone and tendon hyperexcitability in spastic patients [6]. The effect of posture on spasticity suggested that the spinal reflex mechanism in spasticity during motion might not be identical with rest. Importantly, only a few spinal mechanisms can explain the excessive muscle activity at rest, whereas almost all spinal cord circuits participate in defective spinal cord control in the state of motion, however, resulting in dyskinesia [6, 7].

Several studies showed that spastic patients exhibited a larger H-reflex amplitude or Hmax/Mmax ratio than the control group or their unaffected side in the prone position [8], suggesting that spasticity at rest results from the increased excitability of motor neurons in spinal circuits. Cattagni et al. and Kim et al. found that the Hmax/Mmax ratio can be affected by the muscle activity or body position in healthy individuals [9, 10]. This phenomenon may be associated with reciprocal inhibition or other suppression mechanisms in the spinal cord level. A particular study by Katz and Pierrot-Deseilligny investigated the recurrent inhibition by conditioning H-reflex changes in spastic patients during various voluntary and postural contractions. The study concluded that paralysis of the supraspinal control of Renshaw cells might partly account for muscular debilitation and dexterity loss of voluntary movement in spastic patients [11]. Though there are only a few studies on H-reflex in spastic patients at a standing position or movement, the exact pathology of spasticity is still unknown.

Accordingly, the objectives of this study were as follows: (1) if varying posture could influence H-reflex excitability on both sides in stroke patients with lower limb spasticity and (2) to compare changes in reflex behavior in both spastic and contralateral muscles of stroke survivors and match healthy subjects in a standing position. We hypothesized that posture transformation would affect the H-reflex excitability of spastic patients on both sides. Our theory would thus help us understand that the role modulation of afferent Ia spinal cord pathway plays in a standing position. Also, if the hypothesis proves right, it would enable us to explore further the pathophysiological mechanism(s) of spasticity in a standing position. We also hypothesized that unstable posture might acutely increase spinal cord excitability.

2. Materials and Methods

2.1. Participants. We recruited a total of twenty-four hemiparetic spastic stroke survivors in the rehabilitation inpatient department in Huashan Hosipital and twelve age-matched healthy subjects (patient's caregiver) serving as controls. Inclusion criteria for the stroke subjects were (1) hyperactive ankle jerk with clonus and extensor plantar response (Babinski response), (2) present range of motion (ROM) difference between two speed and the quality of ankle joint plantar flexor muscle reaction elicited on the fast passive stretch ≥ 2 according to the Modified Tardieu Scale (MTS), (3) Brunnstrom recovery stage 3 or 4 in the lower limb, (4) the ability to stand independently, and (5) the presence of soleus H-reflex. Exclusion criteria were (1) with history of Parkinson's disease or other neurological diseases; (2) taking any medication that may affect motor control or nerve function, such as Baclofen; (3) medically unstable or concurrent uncontrolled systemic illnesses; (4) skin ulceration, irritation, and inflammation in bilateral calves which influence placing electrodes; and (5) severe disturbance of emotion, visual, and cognitive impairment. All participants gave informed consent via the study protocol approved by the ethics committee of Huashan Affiliated Hospital, Fudan University (ChiCTR-TRC-1800018427).

2.2. Procedures. Before the beginning of this study, demographic information such as gender, age, height, and stroke-related information such as the course of disease, hemiplegic side, and stroke types was also collected.

2.3. Electrophysiologic Evaluation. The H-reflex and M-wave recruitment curves in the soleus muscles of each patient were recorded three times by electrodiagnostic equipment (Shanghai Nuocheng Electrical Co., Ltd.; Shanghai, China) at the fixed time (8 : 00 am-9 : 00 am) before the rehabilitation on the same day. The recruitment curves were carried out in two different body postures: prone position and standing position. In the prone position, the subjects comfortably laid on the treatment bed face down, while a triangular sponge pad was placed under their ankle joint to relax the calf triceps. In standing position, however, participants were asked to stand still, with their head and the upper body in a neutral position, eyes straight ahead, feet apart with the toes facing forward, and the upper limbs hanging on both sides of the torso. The center of gravity of the body is located between the feet and cannot be deflected. The evaluation was as follows: the unaffected side in a prone position, the affected side in a prone position, the unaffected side in a standing position, and the affected side in a standing position. After the tests in a prone position, each participant was given a five minutes break for which the subject's position was then changed. The self-adhesive surface electrodes (2.0 cm Ag-AgCl square electrodes) were attached to the belly of Soleus (active electrode) and the Achilles tendon (reference electrode). A ground electrode (2.0 cm Ag-AgCl square electrode) was attached to the skin between the active electrode and the reference electrode. The tibial nerve was stimulated at the popliteal fossa using a handheld bipolar stimulator (1 ms rectangular pulse), with the cathode was pointing towards the proximal end. Where the stimulator electrodes were to be placed on the skin was marked with an indelible pen to ensure that the same recording site was used in the successive session. The optimal stimulation site of the posterior tibial nerve was identified using the stimulating electrodes.

The H-reflex (Hmax) was determined using many stimuli as required at 0.5 mA, precisely around the intensity eliciting the largest amplitude of the H-reflex. The maximum amplitude of the M-wave (Mmax) was determined as the size

of the response to a stimulus of supramaximal intensity. Amplitude was measured from baseline to the largest negative peak in each series while determining the Hmax/Mmax ratio. Recording parameters settings are as follows: the sensitivity is 2 mV, the scanning speed is 5 ms/cm, and the stimulation intensity duration is 1 ms. The EMG signal was amplified (1 mV/D) and band-pass filtered (2–10,000 Hz).

2.4. Data Analysis. The H-reflex (Hmax, Mmax, Hmax/Mmax ratio) from each subject were presented as mean ± SD. One-way ANOVA was employed to assess the differences in H-reflex data among the affected side, unaffected side in spasticity patients, and the average value of both sides in healthy subjects. The H-reflex results of the same side in stroke patients with spasticity in different positions were tested using a paired-sample t-test (assuming a normal distribution) and using Kruskal-Wallis (nonparametric test) to test if it does not meet the normal distribution.

3. Results

The demographic and clinical characteristics of all participants are summarized in Table 1. In the healthy subjects, the mean age was 55.17 ± 4.67 years, ranging from 41 to 66 years of age. The mean age of stroke patients was 54.54 ± 12.36 years, ranging from 49 to 71 years. The mean time since stroke outset was 6.17 ± 6.72 months, ranging from 1.5 to 30 months. There were no significant differences in age, gender, or height between the two groups.

3.1. Comparison of H-Reflex Results between the Affected Side and the Unaffected Side in the Same Position. In the prone position, post hoc multiple comparisons were used for the H-reflex data of the affected side, the unaffected side, and the healthy group. The mean ± SD of the Hmax for the affected side, the unaffected side, and healthy control groups were 3.75 ± 1.95 mV, 2.96 ± 1.92 mV, and 3.28 ± 1.44 mV, respectively. Significant differences existed between the affected side and the unaffected side ($p = 0.0002$), but the differences between the affected side and the healthy subjects as well as the unaffected side and the healthy subjects were not statistically significant (Figure 1). The Hmax/Mmax ratio of the affected side (37.95 ± 15.16%) was significantly higher than the unaffected side and the healthy subjects (25.91 ± 13.61% and $p = 0.003$ and 26.88 ± 11.88% and $p = 0.006$, respectively). Nevertheless, no statistical difference in the Hmax/Mmax ratio was found between the unaffected side and the healthy subjects.

In the standing position, the mean ± SD of the Hmax for the affected side, the unaffected side, and healthy control groups were 3.46 ± 1.69 mV, 2.88 ± 1.84 mV, and 2.41 ± 0.97 mV, respectively. Significant differences existed between the affected side and the healthy subjects ($p < 0.0001$) and the affected side and the unaffected side ($p = 0.038$). Nevertheless, the differences between the unaffected side and the healthy subjects were not statistically significant. The mean ± SD of the Hmax/Mmax ratio for the affected side, the unaffected side, and healthy control groups were 43.58 ± 19.05%, 32.32 ± 16.23%, and 22.95 ± 9.58%, respectively. The statistical differences for the Hmax/Mmax ratio were found between any two groups in the standing position.

Table 1: Demographic and clinical characteristics of the subjects.

	Stroke group ($n = 24$)	Healthy group ($n = 12$)	p value
Age (years)	54.54 ± 12.36	55.17 ± 4.67	0.868
Gender (M/F)	16/8	5/7	0.635
Height (cm)	168.21 ± 6.30	165.42 ± 6.52	0.227
Affected side (R/L)	10/14		
Time since stroke (months)	6.17 ± 6.72		
(CI/CH)	11/13		

M: male; F: female; CI: cerebral ischemia; CH: cerebral hemorrhage; L: left; R: right.

3.2. Effects of Different Postures on the Results of H-Reflex in Healthy Subjects and Stroke Patients with Spasticity. In healthy subjects, Hmax significantly decreased in standing position compared to the prone position (Figure 2(a)). In stroke patients with spastic hemiplegia, the Hmax, however, did not decrease but somewhat increased in the standing position on both sides in several patients (14/24 for the Hmax) (Figures 2(b) and 2(c)).

In healthy controls (Figure 3), the mean values of the Hmax (e) and the Hmax/Mmax ratio (f) were significantly higher in the prone position than in the standing position ((e): $p = 0.000$, (f): $p = 0.016$). Individual results on the affected side of most stroke patients showed that the data of H-reflex (a, b) in prone position were lower than in the standing position (14/24 for the Hmax and 20/24 for the Hmax/Mmax ratio), however, which showed no statistical difference in the mean value of the Hmax ((a): $p = 0.284$) and the Hmax/Mmax ratio ((b): $p = 0.095$) from the prone position to the standing position in patients. On the unaffected side, the mean value of the Hmax/Mmax ratio was significantly larger in the standing position than in the prone position ((d): $p = 0.006$).

4. Discussion

The primary observation in the present study is that a transformed position can significantly alter spinal cord excitability in stroke patients with spasticity. In neurologically intact individuals, a striking decline could be found in Hmax and Hmax/Mmax ratios from the prone to the standing position. Notably, in the participants with lower limb spasticity, the H-reflex was not suppressed on both sides during postural adjustment. Regardless of the prone and the standing position, the affected sides exhibited distinctly increasing in terms of spinal excitability, and the Hmax/Mmax ratio in the unaffected side was significantly higher in the standing position. It suggests that the neural mechanisms responsible for posture adjustment may be different between stroke patients with spasticity and the healthy subjects.

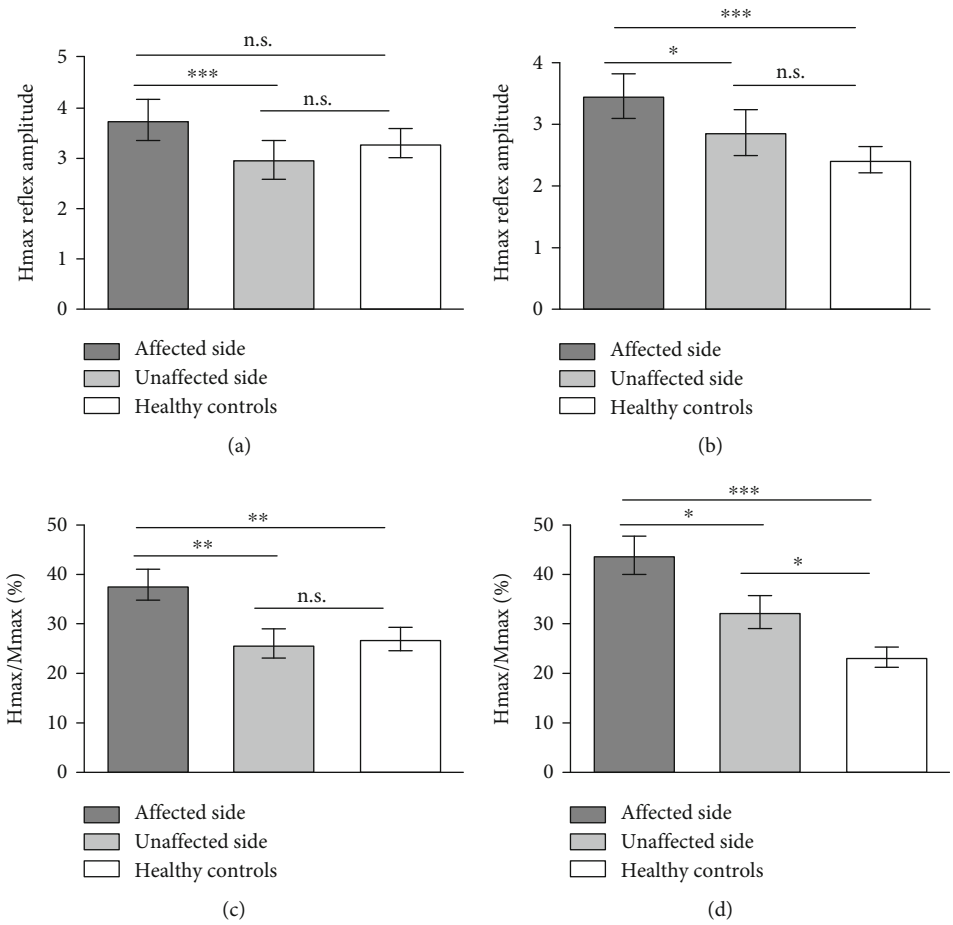

Figure 1: The post hoc multiple comparisons for the H-reflex data of the affected side, the unaffected side, and the healthy control group: (a, c) in the prone position; (b, d) in the standing position. Asterisks indicate significant differences. ns: not significant. $^{*}p < 0.05$; $^{**}p < 0.01$; $^{***}p < 0.001$.

The pathophysiological mechanism of spasticity after stroke is complicated and still being explored. It is currently believed that the cause of stretch reflex hyperexcitability in stroke patients with spasticity is primarily due to abnormal remodeling of the descending conduction pathway above the spinal cord level and error processing within the spinal cord level [12]. All these changes could affect the excitability of alpha motor neurons [13]. The excitability of alpha motor neurons could represent the severity of spasticity to some extent. Thus, H-reflex, reflecting the excitability of alpha motor neurons, has been used to investigate the role of peripheral sensory afferent or supraspinal descending conduction pathway in various aspects of human movements [14].

In the present study (Figure 2), when a healthy person changed from a prone position to a standing position, the Hmax significantly decreased. The results showed that the excitability of the related alpha motor neuron and the Ia afferent pathway were modulated during standing. The study results by Cattagni et.al showed that the Hmax/Mmax ratio in an active sitting was lower than in a passive sitting and lowest in an upright standing position [9]. In another study, H-reflex amplitudes of fibularis longus (FL) and soleus in healthy subjects were significantly lower in the uni-pedal stance than the prone and bipedal positions [10]. We believed that the excitability decrease of H-reflex in healthy people might be associated with reciprocal inhibition in the spinal cord level, which may also involve others spinal cord suppression mechanism [15].

Compared to the healthy subjects in standing positions, the H-reflex amplitude of the affected side distinctly increased in the stroke patients with spasticity (Figures 2 and 3). The present study indicated that the spastic hemiplegic patients had an overall upregulation of the anterior horn cells excitability both in the prone and the standing positions, which is also in line with previously reported findings [16]. Fleuren et al. stated that when the patients changed their body position from a prone position to that of a standing position, their triceps surae muscle was lengthened. The increased muscle length could augment the stretch reflex activity [17]. The tonic activity from the proprioceptors may presynaptically interfere with the effectiveness of the spindle primary afferent synapses on the soleus motor neurons [14]. Importantly, the Hmax/Mmax ratio appears to be exclusively modulated by body position (Figure 3). This body position transition might deteriorate spasticity, which

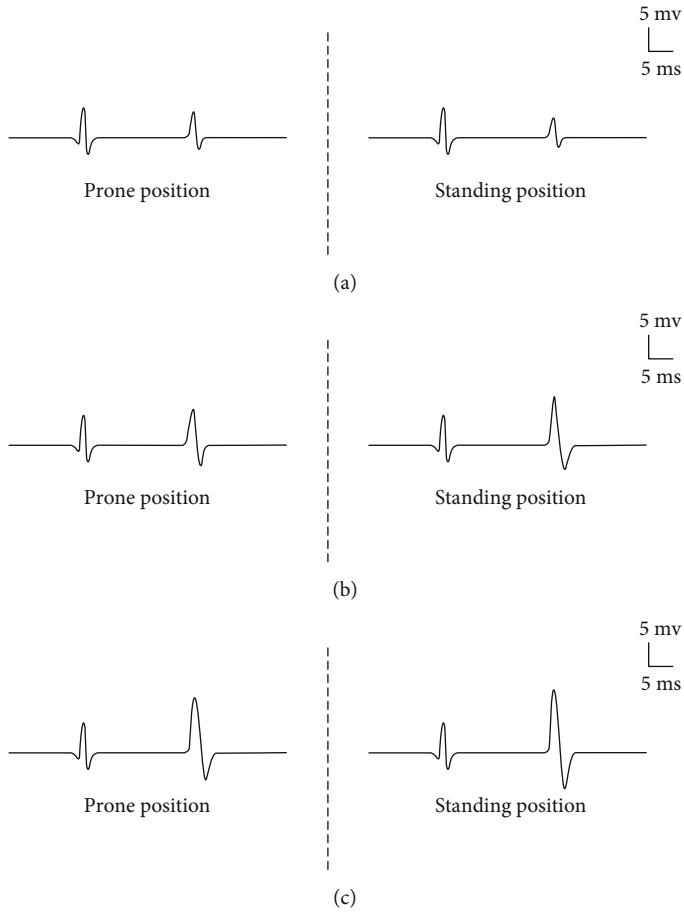

Figure 2: The Hmax in different positions: (a) healthy subject; (b) the unaffected side in a stroke patient; (c) the affected side in the same stroke patient (left: prone position; right: standing position). The first wave means the M-wave, and the second wave represents the Hmax. Note the same amplitude changing trend of the Hmax in the both conditions for the patient.

shows that the abnormal reciprocal inhibition of Ia fiber exists in spastic patients.

In the present study, we found out that the H-reflex excitability was not inhibited on both sides, and the anterior horn cell's excitability of the unaffected side was even enhanced in the standing position in spastic patients. It also indicates that the abnormal Ia reciprocal inhibition in these patients can occur on both sides. The results of the present study are in line with the study by Phadke et al. [18]. On the contrary, Kawashima et al. reported that the soleus H-reflex from sitting to standing was inhibited in patients with complete SCI [19]. In addition to different testing conditions, another critical issue with their study was that it failed to take spasticity into account.

Besides the intraspinal processing, the reticulospinal tract (RST) might be taken into consideration. The RST is best known for playing an essential role in maintaining joint position, posture against gravity, and locomotion [20]. Reticulospinal pathways usually have bilateral projections for head, neck, trunk, and proximal limb movements [21]. The hyperexcitability of RST could be found in the spastic stage but not in recovered nonspastic stages [22, 23]. The increased stretch reflex thresholds of the biceps brachii muscle on both contralateral and affected sides of stroke survivors suggested that RST activation in the spastic stage still have a bilateral descending influence [24]. The increased Hmax/Mmax ratio on bilateral sides in stroke patients with spasticity was observed at rest and during standing in the present study. Motor overflow from the affected limb to contralateral side extended the findings of all abovementioned studies and may further support reticulospinal hyperexcitability at least partially responsible for increased stretch reflex excitability. However, for studies on other pathways within the spinal cord level or supraspinal level during movement, extensive electrophysiological methods are needed.

In healthy people, there may be a positive correlation between the depression or downward modulation of the soleus H-reflex and the degree of the postural instability in which the subjects are placed [25]. The depression modulation of SOL H-reflex under such condition is predominately a result of the presynaptic inhibitory mechanisms for avoiding oversaturation of the spinal motoneurons to obtain more descending commands for postural correction [26]. In spastic patients, the ascending sensory and descending supraspinal tracts are interrupted in different degrees. The decreased suppression of the stretch reflex and the delayed or reduced spinal reflex processing may contribute to impaired balance control [27, 28]. Therefore, the worse

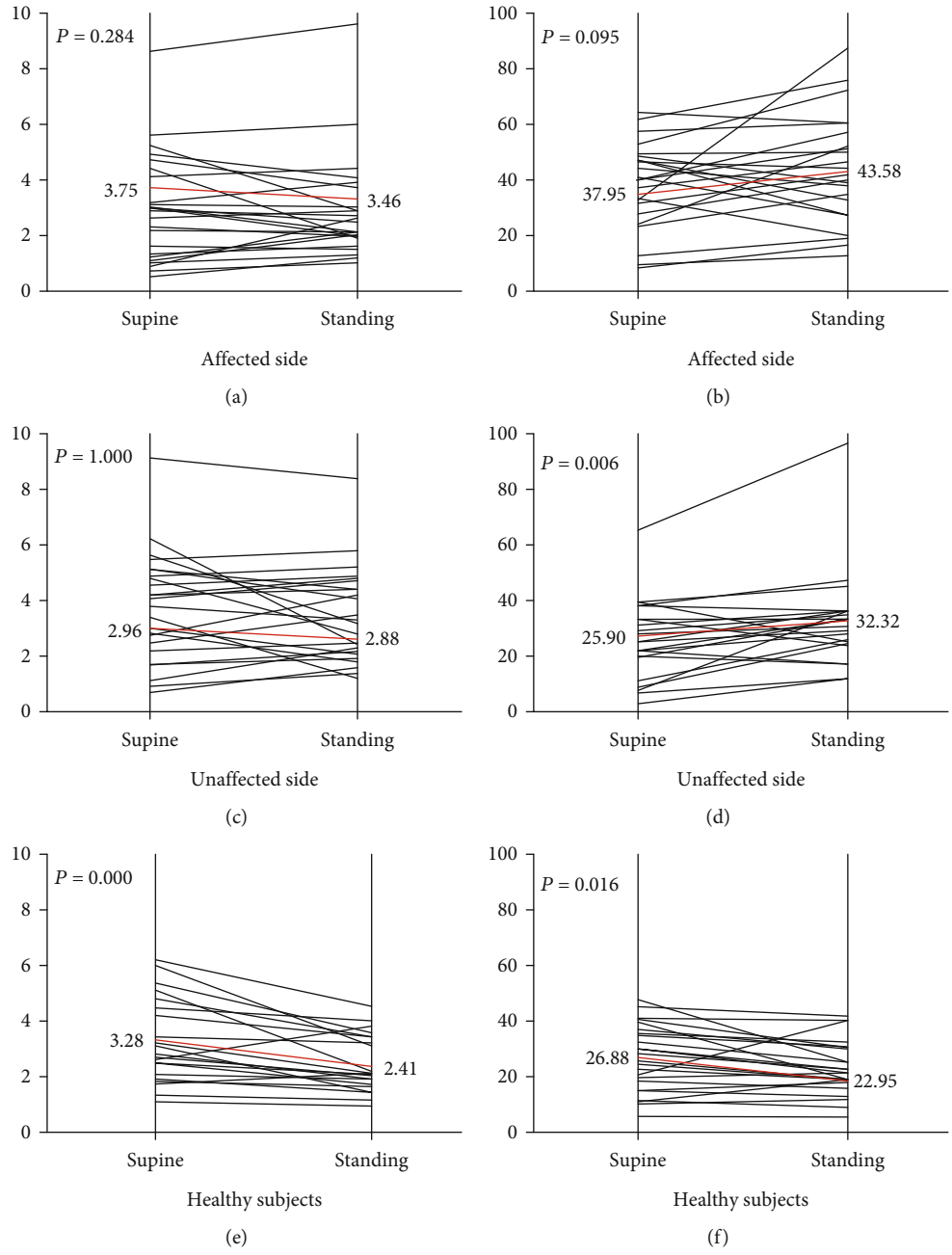

Figure 3: The individual results of H-reflex on the affected side (a, b), the unaffected side (c, d) of stroke patients, and in healthy subjects (e, f) from the prone position (left panels) to the standing position (right panels). (a, c, e) Hmax. (b, d, f) Hmax/Mmax ratio. The individual values (thin line) and mean (thick red line, values indicated beside the vertical line) obtained on the affected and unaffected sides from 24 stroke patients and 12 healthy subjects.

the balance function of the spastic patients, the less the depression modulation of the H-reflex in the standing position. We inferred that the impaired Ia afferent pathway might be the cause of the postural control defects in spastic patients. In the standing position, the abnormal Ia spinal cord afferent pathway participates in the defective spinal cord control, which not only aggravates the severity of the spasticity but might also exacerbate motion control.

This study has some limitations. First, we found a clinical phenomenon which might be explained by RST, but we did not verify this hypothesis. Therefore, our further study will focus on exploring the underlying mechanisms in stretch reflex hyperexcitability involving the role of RST using indirect noninvasive measure such as acoustic startle reflex (ASR) to make a further investigation about the spinal or supraspinal mechanism of H-reflex changes in standing position. Secondly, the current study was based on a small sample of participants. Despite it, we still observed the H-reflex difference between the two postures in the same patient.

5. Conclusions

In standing position, the H-reflex excitability of the tibial nerve is partially upregulated in stroke patients with spasticity on both sides. The findings also suggested that the impaired regulation of Ia afferent pathway may be a potential source of postural control defects in poststroke spasticity.

Data Availability

The data that support the findings of this study are available from the corresponding author upon reasonable request.

Conflicts of Interest

None of the authors have any conflicts of interest with respect to the authorship and/or publication of this article.

Authors' Contributions

Wenting Qin and Anjing Zhang contributed equally to this work.

Acknowledgments

We are particularly grateful to the people who volunteered to take part in this study. This research received grants from the National Key Research and Development Program of China (No. 2018YFC2001604), the Shanghai Medical Key Specialty (Project No. ZK2019B11), and the Shanghai Yangpu District Health and Family Planning System "Good Physician" Construction Engineering subject youth backbone, 2017-2019.

References

[1] J. W. Lance, "The control of muscle tone, reflexes, and movement: Robert Wartenberg lecture," *Neurology*, vol. 30, no. 12, pp. 1303–1313, 1980.

[2] R. D. Zorowitz, P. J. Gillard, and M. Brainin, "Poststroke spasticity: sequelae and burden on stroke survivors and caregivers," *Neurology*, vol. 80, Issue 3, Supplement 2, pp. S45–S52, 2013.

[3] W. T. Qin, M. Z. Yang, F. Li, C. Chen, L. Zhen, and S. Tian, "Influence of positional changes on spasticity of the upper extremity in poststroke hemiplegic patients," *Neuroscience Letters*, vol. 712, article 134479, 2019.

[4] S. Wang, X. Chen, R. Zhuang, Z. Yang, W. Jiang, and T. Wang, "Flexors activity of affected upper extremity in stroke patients during different standing conditions and their relationships with clinical scales: a cross-sectional study," *Neurological Research*, vol. 42, no. 3, pp. 244–252, 2020.

[5] E. R. de Azevedo, R. M. Maria, K. C. Alonso, and A. Cliquet Jr, "Posture influence on the pendulum test of spasticity in patients with spinal cord injury," *Artificial Organs*, vol. 39, no. 12, pp. 1033–1037, 2015.

[6] D. Burke, J. Wissel, and G. A. Donnan, "Pathophysiology of spasticity in stroke," *Neurology*, vol. 80, Issue 3, Supplement 2, pp. S20–S26, 2013.

[7] V. Dietz and T. Sinkjaer, "Spastic movement disorder: impaired reflex function and altered muscle mechanicsSpastic movement disorder: impaired reflex function and altered muscle mechanics," *Lancet Neurology*, vol. 6, no. 8, pp. 725–733, 2007.

[8] C. Y. Huang, C. H. Wang, and I. S. Hwang, "Characterization of the mechanical and neural components of spastic hypertonia with modified H reflex," *Journal of Electromyography and Kinesiology*, vol. 16, no. 4, pp. 384–391, 2006.

[9] T. Cattagni, A. Martin, and G. Scaglioni, "Is spinal excitability of the triceps surae mainly affected by muscle activity or body position?," *Journal of Neurophysiology*, vol. 111, no. 12, pp. 2525–2532, 2014.

[10] K. M. Kim, J. M. Hart, and J. Hertel, "Influence of body position on fibularis longus and soleus Hoffmann reflexes," *Gait & Posture*, vol. 37, no. 1, pp. 138–140, 2013.

[11] R. Katz and E. Pierrot-Deseilligny, "Recurrent inhibition of α-MOTONEURONS in patients with upper motor neuron lesions," *Brain*, vol. 105, no. 1, pp. 103–124, 1982.

[12] A. Thibaut, C. Chatelle, E. Ziegler, M. A. Bruno, S. Laureys, and O. Gosseries, "Spasticity after stroke: physiology, assessment and treatment," *Brain Injury*, vol. 27, no. 10, pp. 1093–1105, 2013.

[13] S. Li, "Spasticity, motor recovery, and neural plasticity after stroke," *Frontiers in Neurology*, vol. 8, p. 120, 2017.

[14] S. Cecen, I. K. Niazi, R. W. Nedergaard et al., "Posture modulates the sensitivity of the H-reflex," *Experimental Brain Research*, vol. 236, no. 3, pp. 829–835, 2018.

[15] W. Taube, M. Gruber, and A. Gollhofer, "Spinal and supraspinal adaptations associated with balance training and their functional relevance," *Acta Physiologica*, vol. 193, no. 2, pp. 101–116, 2008.

[16] M. Knikou, C. A. Angeli, C. K. Ferreira, and S. J. Harkema, "Soleus H-reflex gain, threshold, and amplitude as function of body posture and load in spinal cord intact and injured subjects," *The International Journal of Neuroscience*, vol. 119, no. 11, pp. 2056–2073, 2009.

[17] J. F. Fleuren, M. J. Nederhand, and H. J. Hermens, "Influence of posture and muscle length on stretch reflex activity in poststroke patients with spasticity," *Archives of Physical Medicine and Rehabilitation*, vol. 87, no. 7, pp. 981–988, 2006.

[18] C. P. Phadke, F. J. Thompson, C. G. Kukulka et al., "Soleus H-reflex modulation after motor incomplete spinal cord injury: effects of body position and walking speed," *The Journal of Spinal Cord Medicine*, vol. 33, no. 4, pp. 371–378, 2010.

[19] N. Kawashima, H. Sekiguchi, T. Miyoshi, K. Nakazawa, and M. Akai, "Inhibition of the human soleus Hoffman reflex during standing without descending commands," *Neuroscience Letters*, vol. 345, no. 1, pp. 41–44, 2003.

[20] T. Drew, S. Prentice, and B. Schepens, "Cortical and brainstem control of locomotion," *Progress in Brain Research*, vol. 143, pp. 251–261, 2004.

[21] A. G. Davidson and J. A. Buford, "Bilateral actions of the reticulospinal tract on arm and shoulder muscles in the monkey: stimulus triggered averaging," *Experimental Brain Research*, vol. 173, no. 1, pp. 25–39, 2006.

[22] S. K. Jankelowitz and J. G. Colebatch, "The acoustic startle reflex in ischemic stroke," *Neurology*, vol. 62, no. 1, pp. 114–116, 2004.

[23] S. Li, Y. T. Chen, G. E. Francisco, P. Zhou, and W. Z. Rymer, "A unifying pathophysiological account for post-stroke spasticity and disordered motor control," *Frontiers in Neurology*, vol. 10, p. 468, 2019.

[24] T. Afzal, M. K. Chardon, W. Z. Rymer, and N. L. Suresh, "Stretch reflex excitability in contralateral limbs of stroke survivors is higher than in matched controls," *Journal of Neuroengineering and Rehabilitation*, vol. 16, no. 1, p. 154, 2019.

[25] C. D. Tokuno, M. G. Carpenter, A. Thorstensson, S. J. Garland, and A. G. Cresswell, "Control of the triceps surae during the postural sway of quiet standing," *Acta Physiologica*, vol. 191, no. 3, pp. 229–236, 2007.

[26] Y. S. Chen and S. Zhou, "Soleus H-reflex and its relation to static postural control," *Gait & Posture*, vol. 33, no. 2, pp. 169–178, 2011.

[27] C. H. Pion, M. St-Pierre Bolduc, Z. Miranda, M. MacMahon, and D. Barthélemy, "Alteration of H-reflex amplitude modulation is a marker of impaired postural responses in individuals with incomplete spinal cord injury," *Experimental Brain Research*, vol. 239, no. 6, pp. 1779–1794, 2021.

[28] E. B. Simonsen, "Contributions to the understanding of gait control," *Danish Medical Journal*, vol. 61, no. 4, article B4823, 2014.

Hindawi
Neural Plasticity
Volume 2021, Article ID 8966584, 8 pages
https://doi.org/10.1155/2021/8966584

Research Article

Preconditioning with Cathodal High-Definition Transcranial Direct Current Stimulation Sensitizes the Primary Motor Cortex to Subsequent Intermittent Theta Burst Stimulation

Wenjun Dai,[1] **Yao Geng**,[1] **Hao Liu**,[2] **Chuan Guo**,[1] **Wenxiang Chen**,[3] **Jinhui Ma**,[4] **Jinjin Chen**,[1] **Yanbing Jia**,[2] **Ying Shen**,[1] **and Tong Wang**[1]

[1]*Rehabilitation Medicine Center, The First Affiliated Hospital of Nanjing Medical University, Nanjing, China*
[2]*Neuro-Rehabilitation Center, JORU Rehabilitation Hospital, Yixing, China*
[3]*Department of Rehabilitation, Children's Hospital of Nanjing Medical University, Nanjing, China*
[4]*Department of Health Research Methods, Evidence, and Impact, McMaster University, Hamilton, ON, Canada*

Correspondence should be addressed to Ying Shen; shenying_1981@hotmail.com and Tong Wang; wangtong60621@163.com

Received 22 June 2021; Revised 23 August 2021; Accepted 18 September 2021; Published 21 October 2021

Academic Editor: Rongrong Lu

Noninvasive brain stimulation techniques such as transcranial magnetic stimulation (TMS) and transcranial direct current stimulation (tDCS) can induce long-term potentiation-like facilitation, but whether the combination of TMS and tDCS has additive effects is unclear. To address this issue, in this randomized crossover study, we investigated the effect of preconditioning with cathodal high-definition (HD) tDCS on intermittent theta burst stimulation- (iTBS-) induced plasticity in the left motor cortex. A total of 24 healthy volunteers received preconditioning with cathodal HD-tDCS or sham intervention prior to iTBS in a random order with a washout period of 1 week. The amplitude of motor evoked potentials (MEPs) was measured at baseline and at several time points (5, 10, 15, and 30 min) after iTBS to determine the effects of the intervention on cortical plasticity. Preconditioning with cathodal HD-tDCS followed by iTBS showed a greater increase in MEP amplitude than sham cathodal HD-tDCS preconditioning and iTBS at each time postintervention point, with longer-lasting after-effects on cortical excitability. These results demonstrate that preintervention with cathodal HD-tDCS primes the motor cortex for long-term potentiation induced by iTBS and is a potential strategy for improving the clinical outcome to guide therapeutic decisions.

1. Introduction

Noninvasive brain stimulation (NIBS) techniques such as transcranial magnetic stimulation (TMS) and transcranial direct current stimulation (tDCS) can induce a long-term potentiation- (LTP-) like facilitation or long-term depression- (LTD-) like suppression [1–3]. Depending on the stimulus frequency of repetitive (r)TMS or the polarity of electrodes placed on the scalp in tDCS, these 2 types of stimulation can bidirectionally regulate the excitability of neurons in neural networks [4–6]. Whether a greater effect can be achieved by combining TMS and tDCS is an open question.

Preconditioning with tDCS can alter the functional state of the motor cortex, resulting in TMS-induced changes in cortical plasticity [7–9]. When applied to the primary motor cortex (M1), inhibitory preconditioning with cathodal tDCS and subsequent 5-Hz rTMS significantly increased the excitability of the corticospinal tract, whereas facilitatory preconditioning with anodal tDCS and subsequent 5-Hz rTMS decreased excitability [7, 9]. The preconditioning effects of tDCS may be related to synaptic homeostatic plasticity which is thought to maintain neural activity within a certain physiological range and ensure the stability of neural network activity [10]. As described in the Bienenstock–Cooper–Munro (BCM) theory of bidirectional synaptic

plasticity [11], it states that stable neuronal activity is achieved through dynamic regulation of the threshold of synaptic modification. The threshold is decreased by a reduction in postsynaptic activity, which can induce LTP, whereas increased postsynaptic activity raises the threshold and induces LTD. Thus, the state of synaptic activation before stimulation influences the after-effects of NIBS.

Intermittent theta burst stimulation (iTBS) activates N-methyl-D-aspartate (NMDA) receptor [12], shortens the time for therapy [13], and induces LTP-like when assessed in humans with brain stimulation [14]. Conventional tDCS modulates the excitability in the brain with constant, low-intensity direct current (1–2 mA) [15]. Anodal tDCS was shown to depolarize the membrane potential by activating Na^+ and Ca^{2+} voltage-gated channels and increasing neuronal excitability and cortical activity, while cathodal tDCS caused the opposite effects by inducing membrane hyperpolarization [15, 16]. In clinical applications, conventional tDCS electrodes have the disadvantage of insufficient spatial resolution because of their large size (16–35 cm^2). High-definition (HD) tDCS has improved resolution because it uses electrodes in a 4×1 ring configuration that is based on a high-resolution magnetic resonance imaging-based finite element model [17]. Given its unique advantages in regulating cortical excitability, the combined application of HD-tDCS and iTBS deserves further investigation.

Here, we hypothesized that preconditioning with cathodal HD-tDCS would sensitize the primary motor cortex to subsequent iTBS, and the after-effect would last longer compared to iTBS without the preconditioning in healthy young adults.

2. Materials and Methods

2.1. Participants. A total of 24 healthy volunteers (4 males, 20 females; mean age 21.29 ± 0.73 years) participated in the experiments (Table 1). Inclusion criteria were as follows: (1) no neurologic or psychiatric disorders or serious illnesses and (2) right-handed, as verified using the Edinburgh Handedness Inventory. Exclusion criteria were as follows: (1) a history of epilepsy, idiopathic epilepsy in a first-degree relative, and use of epileptogenic drugs and (2) implants including an artificial metal heart valve, insulin pump, drug treatment pump, or aneurysm clip (nonparamagnetic, except titanium alloy). All subjects participated in the study voluntarily and signed the written informed consent form. The study was approved by the Ethics Committee of JORU Rehabilitation Hospital (approval no. 20201130A02) and was registered with the China Clinical Trial Registration Center (http://www.chictr.org.cn; no. ChiCTR2000041144). All experimental procedures were carried out according to the principles outlined in the Declaration of Helsinki.

2.2. Experimental Design. This study adopted a randomized crossover design (Figure 1). All subjects were randomized to receive preconditioning with cathodal HD-tDCS or sham cathodal HD-tDCS prior to iTBS with a washout period of 1 week. We measured the amplitude of MEPs at baseline and at different time points (5, 10, 15, and 30 min) after the intervention.

Table 1: Characteristics of the study subjects.

Characteristics	Results ($n = 24$)
Age (years), mean (SD)	21.3 (0.7)
Female, *n* (%)	20 (83.3%)
Hand of preference (right hand), *n* (%)	24 (100%)
RMT (%MSO), mean (SD)	46.3 (8.8)

SD: standard deviation; RMT: resting motor threshold; MSO: maximal stimulator output.

2.3. Assessment

2.3.1. Determination of Motor Hotspots. The experiment was conducted in a quiet isolated room. During the experiment, subjects were prohibited from talking, sleeping, and using their mobile phones. The subjects were comfortably seated on a reclining chair with neck, arms, and legs supported in a relaxed position and were asked to wear a positioning scalp cap to reduce sliding between their hair and the stimulus coil. The center of the coil was placed tangentially on the scalp over the motor hotspot for the right abductor pollicis brevis (AFB) that was marked beforehand, with the handle posterior to the midline at an angle of 45°. The surface electromyography (sEMG) recording electrode was placed on the APB of the right hand and MEPs were recorded using the CCY-I TMS system (Yiruide, Wuhan, China) and were analyzed with the accompanying software. The optimal scalp location was the one that produced the maximum response in EMG recordings of the APB. The motor hotspot was marked on the scalp for reference and was continually monitored throughout the experiment.

2.3.2. Measurement of Cortical Plasticity. Cortical plasticity was assessed by investigating changes in the amplitude of MEPs in the left M1 recorded during complete relaxation of the APB of the right hand. Twenty consecutive MEPs (5 s interval) were evoked by single-pulse TMS with an intensity of 130% resting motor threshold (RMT). RMT was defined as the lowest stimulation intensity to evoke an MEP > 50 μV in the relaxed APB for at least 5 of 10 consecutive TMS pulses [18, 19]. MEP amplitudes were extracted and calculated as peak-to-peak amplitudes of trials, without elimination of the maximum and minimum MEP amplitudes. The peak-to-peak value was averaged as the baseline. Two baseline measurements were obtained (separated by 5 min) before any intervention in order to assure the intraindividual reliability of cortical excitability [20], and the plasticity protocol was applied if there was no more than a 10% difference between the 2 baseline values.

2.4. Interventions

2.4.1. Cathodal HD-tDCS. The device used a 4×1 HD-tDCS adaptor (Soterix Medical, New York, NY, USA). Five small circular electrodes (1 cm^2) replaced the traditional large sponge electrode. The central cathodal electrode was placed

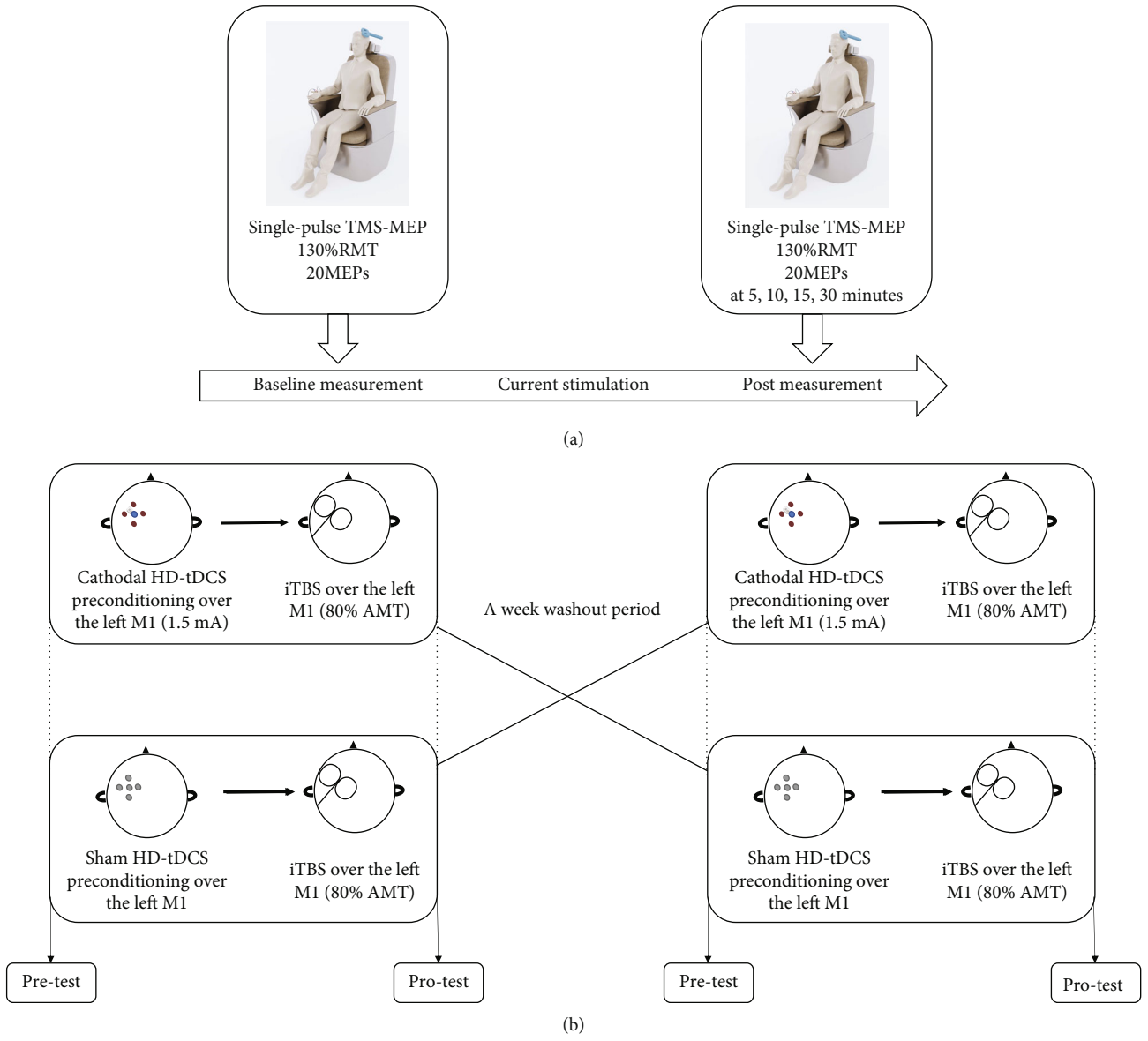

Figure 1: Experimental design. Single-pulse TMS was delivered to the left M1. The coil was first placed on the motor hotspot that produced an optimum response defined by electromyography recordings of abductor pollicis brevis (APB) muscle. Twenty MEPs induced at a TMS intensity of 130% resting motor threshold (RMT) were averaged as the baseline cortical excitability (a). MEPs were recorded in the pretest block. Subjects received twenty consecutive single pulses over the target site of the left M1 with an interval of 5 s. Preconditioning with cathodal HD-tDCS or sham prior to iTBS was applied. One week later, the interventions were switched (b). The after-effects were measured as the amplitude of MEPs at 5, 10, 15, and 30 min after the intervention. AMT: active motor threshold.

on the scalp above the left M1 where the motor hotspot was previously marked, and the 4 return electrodes (separated from the central electrode by a distance of 3.5 cm) were placed so as to form a circular current loop after applying conductive paste. The tDCS was delivered at a current intensity of 1.5 mA for 20 min after checking the connection quality. For the sham protocol, the current was increased slowly to 1.5 mA in the first 15 s and then gradually decreased to 0 in 15 s; the other settings were the same as for the real stimulation.

2.4.2. iTBS. iTBS was performed with a CCY-I TMS stimulator using a figure 8-shaped coil for accurately targeted stimulation. The magnetic stimulus had a biphasic waveform. It can produce a maximum stimulator output (MSO) of 3.0 Tesla [21]. The iTBS pattern, which has been described in a previous study [14], consisted of bursts of 3 pulses at 50 Hz repeated at 5 Hz; a 2 s train of TBS was repeated every 10 s for a total of 192 s (600 pulses). The stimulation intensity of the experiment was 80% of the active motor threshold. iTBS was delivered over the left motor hotspot to modulate cortical plasticity.

2.5. Data Analysis. A total of 24 subjects were required to detect a standardized effect size of 0.8 (cathodal HD-tDCS+iTBS vs. sham cathodal HD-tDCS+iTBS) based on

Table 2: Summary of MEP amplitudes at baseline.

Subjects	Before crossover mean (SD)	After crossover mean (SD)	p value
Sham➔cathodal HD-tDCS+iTBS ($n = 12$)	721 (294)	718 (300)	0.83
Cathodal➔sham HD-tDCS+iTBS ($n = 12$)	817 (408)	862 (437)	0.14
All ($n = 24$)	769 (351)	790 (373)	0.24

MEP: motor evoked potential; SD: standard deviation, ➔: crossover from … to ….

data from our pilot study with a statistical power of 80% at the significance level of 0.01 (2-sided test).

Both raw MEP amplitude and normalized MEP were analyzed. Normalized MEPs were calculated as raw MEP amplitude divided by the mean of MEP at baseline in the same intervention group and presented in percentage. MEP data at each time point were summarized as mean and standard deviation (SD). The MEP data were analyzed using two-way repeated-measures analysis of variance (ANOVA). A p value < 0.05 was considered statistically significant. Since the interaction between time and intervention group was statistically significant, we further estimated the within- and between-group difference and the corresponding 95% confidence interval (CI).

3. Results

All 24 subjects participated in 2 intervention sessions. Table 1 shows the demographic characteristics of the subjects. Twelve subjects (including 3 males) received cathodal HD-tDCS+iTBS in the first session, and the others (including 1 male) were assigned to the sham cathodal HD-tDCS+iTBS group. The experimental procedure was well tolerated and none of the subjects experienced any adverse effects (e.g., headache, giddiness, and fidgeting) during or after the intervention.

The MEP measures at baseline before and after the crossover were compared, and there were no significant differences (Table 2). In addition, the MEP measures at different time points are presented in Table 3. Preconditioning with cathodal HD-tDCS and iTBS had a marked effect on cortical excitability. Subjects showed an increase in MEP amplitude at 5 min postintervention compared to the respective baseline values in both intervention groups (increase = 258 μV, 95%CI = $(100, 417)$, $p < 0.001$ for the sham group; increase = 529 μV, 95%CI = $(371, 687)$, $p < 0.001$ for the cathodal HD-tDCS prior to iTBS group). The MEP amplitude in subjects receiving cathodal HD-tDCS prior to iTBS increased continuously up to 15 min and then decreased slightly thereafter; by 30 min, MEP amplitude was still greater than at baseline (increase = 645 μV, 95%CI = $(487, 803)$; $p < 0.001$). In contrast, in subjects receiving the sham intervention, MEP amplitude dropped slightly between 5 and 15 min and decreased substantially by 30 minutes. The results from the repeated-measures ANOVA on raw MEP showed that cathodal HD-tDCS and iTBS increased MEP amplitude to a greater extent than the sham intervention overall ($F(1, 207) = 75.3$, $p < 0.001$ for intervention; $F(4, 207) = 26.53$, $p < 0.001$ for time; and $F(4, 207) = 7.23$, $p < 0.001$ for intervention and time interaction).

Table 3: Summary of MEP amplitudes at different time points.

Time	Sham cathodal HD-tDCS+iTBS mean (SD)	Cathodal HD-tDCS+iTBS mean (SD)
Raw MEP (μV)		
Baseline	792 (372)	767 (354)
5 minutes	1051 (528)	1296 (567)
10 minutes	1090 (501)	1448 (654)
15 minutes	1068 (522)	1518 (681)
30 minutes	883 (446)	1412 (692)
Normalized MEP (%)		
Baseline	100 (47)	100 (46)
5 minutes	133 (67)	169 (70)
10 minutes	138 (63)	189 (85)
15 minutes	135 (66)	198 (89)
30 minutes	112 (56)	184 (90)

MEP: motor evoked potential; SD: standard deviation.

Results from the same analysis on normalized MEP were similar to those on raw MEP. These results indicate that cathodal HD-tDCS enhances the effects of iTBS as evidenced by increased MEP amplitude compared to iTBS without the preconditioning and that the effect is long-lasting. Detailed results from two-way repeated-measures ANOVA are presented in Table 4 and Figure 2.

4. Discussion

The combination of tDCS and TMS is increasingly being applied in clinical and research settings to induce LTP-like and LTD-like plasticity [7, 8, 10]. There have been few studies to date investigating whether preconditioning with HD-tDCS can enhance the effect of iTBS in healthy subjects and patients.

In this study, we found that the cortical excitability of M1 was increased with iTBS after inhibitory preconditioning by cathodal HD-tDCS compared to sham HD-tDCS; MEP amplitudes at nearly all postintervention time points showed obvious changes, with the effects lasting for 5–30 min. This is in agreement with previous studies demonstrating that a preconditioning protocol with cathodal tDCS potentiated cortical plasticity induced by 5 Hz rTMS [7] and altered the baseline state of motor cortical excitability, thereby reversing or enhancing the after-effects of rTMS [8].

In contrast to previous studies, we used HD-tDCS for preconditioning. The central electrode was placed at the

Table 4: Comparison of MEP at different intervention groups and at different time points.

Time	Within-group change (95% CI)		Between-group difference in change (95% CI)
	Sham cathodal HD-tDCS+iTBS	Cathodal HD-tDCS+iTBS	
Raw MEP (μV)			
From 5 min to baseline	258 (100, 417)**	529 (371, 687)**	270 (47, 494)*
From 10 min to baseline	297 (140, 456)**	680 (522, 839)**	383 (159, 606)**
From 15 min to baseline	276 (118, 434)**	750 (593, 909)**	475 (251, 698)**
From 30 min to baseline	91 (-67, 249)	645 (487, 803)**	554 (330, 777)**
Normalized MEP (%)			
From 5 min to baseline	33 (12, 53)**	69 (48, 89)**	36 (7, 65)*
From 10 min to baseline	38 (17, 58)**	89 (68, 109)**	51 (22, 80)**
From 15 min to baseline	35 (14, 55)**	98 (77, 118)**	63 (34, 92)**
From 30 min to baseline	12 (-9, 32)	84 (63, 105)**	73 (44, 102)**

MEP: motor evoked potential; CI: confidence interval; *$0.01 < p < 0.05$; **$p < 0.001$.

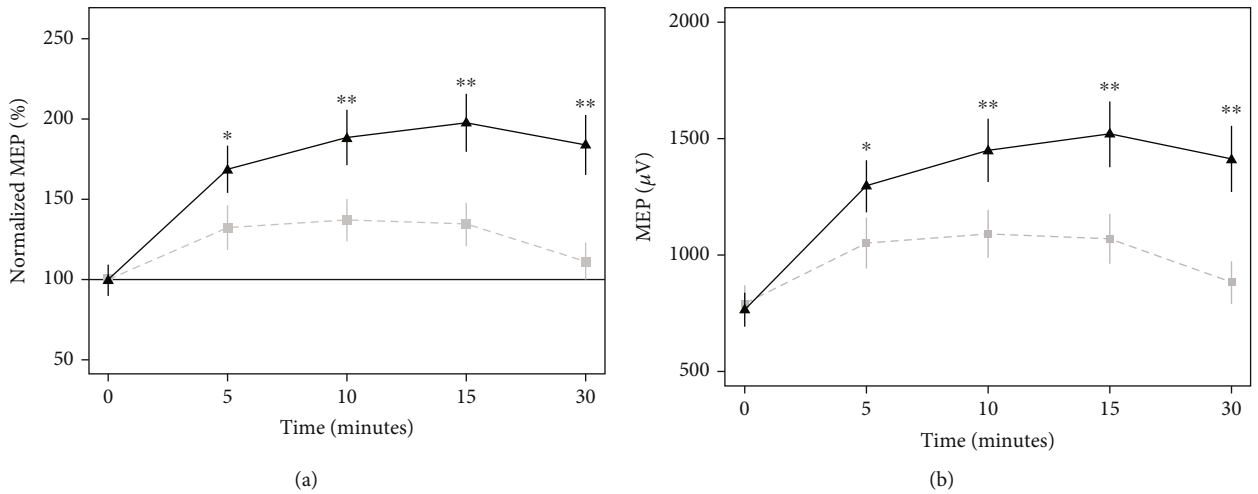

Figure 2: Time course of corticospinal excitability. The grey square represents mean MEP amplitude for subjects receiving sham cathodal HD-tDCS and iTBS. The black triangle represents mean MEP amplitude for subjects receiving cathodal HD-tDCS and iTBS. Vertical lines indicate standard error of the mean of MEP amplitudes. (a) Shows the normalized MEP (%) over time. (b) Shows MEP (μV) over time. $*$ indicates that the between-group difference is significant with $0.001 < p < 0.05$. $**$ indicates the between-group difference is significant with $p < 0.001$.

stimulation target surrounded by 4 return electrodes; the 4 $\times$1 ring configuration of the electrodes was effective in inducing plasticity in M1 [22, 23]. Conventional tDCS delivers diffuse current to the cerebral cortex, making it difficult to establish a causal relationship between cortical stimulation and behavioral changes [24]. In contrast, the electrode placement for HD-tDCS creates a peak induction field under the active electrode, and the distance between the active and return electrodes limits the spatial distribution of the electric field and current delivered to the brain, thereby improving current stimulation focality [17, 25]. Additionally, HD-tDCS achieves a longer-lasting aftereffect than conventional tDCS [23]. We used iTBS for the subsequent test NIBS. Compared with rTMS, iTBS imitates endogenous theta rhythms, which results in better induction of synaptic LTP [26]. iTBS intervention, as an extremely efficient and useful protocol for basic and clinical applications, enables the delivered time shorter than standard rTMS protocols [13]. Also, the most distinguished originality in our research is that the application of iTBS follows with HD-tDCS immediately. Lang et al. found that the combination of cathodal tDCS and 5 Hz rTMS with an interval of 10 minutes increased MEP amplitude [7], while the combination of anodal tDCS and 1 Hz rTMS with an interval of 10 minutes decreased MEP amplitude [8].

All in all, compared with previous studies about combined intervention of rTMS and tDCS, iTBS shortened the duration of intervention. In addition, preconditioning with cathodal HD-tDCS followed by iTBS without time intervals could also induce LTP-like plasticity.

The effect of preconditioning can be explained by the mechanism of synaptic homeostatic plasticity [7, 8]. The

induction and direction of synaptic plasticity depend on the excitability of the postsynaptic neuron at the time of stimulation [27], which is significant for the stability stable neuronal networks [28, 29]. During the learning and development processes of the brain, synaptic excitability is modulated by homeostasis [30], which depends on intracellular Ca^{2+} level; the firing rate remains relatively constant, and neural network activity is stable [29]. With changes in neural activity and intracellular Ca^{2+} level, the firing rate of neurons is stabilized through an increase or decrease in synaptic strength, thus ensuring normal information processing and storage [29, 31].

Studies have indicated that the combined application of various NIBS procedures could induce synaptic homeostatic plasticity [10]. A preconditioning NIBS procedure could enhance the effect of a subsequent NIBS procedure with an opposing effect. In contrast, if the influence of the two procedures was the same, preconditioning with a NIBS procedure could weaken the response to a subsequent NIBS procedure [7–9]. According to the BCM theory of bidirectional synaptic plasticity, a high level of postsynaptic activity favors LTD whereas a low level of that induces LTP [11, 32]. Moreover, the theory proposes that the sliding threshold (i.e., the critical point at which LTD-like plasticity becomes LTP-like) is not fixed but is dependent on postsynaptic activity [10]. Application of LTD-like preconditioning lowers the sliding threshold, contributing to a decrease in postsynaptic activity and thereby facilitating LTP induction. Thus, homeostatic mechanisms compensate for decreased firing owing to a reduction in or loss of activity, leading to compensatory changes in excitatory synapses and improved synaptic efficiency.

Homeostatic plasticity of synapses has also been observed in animal experiments [33, 34]. By monitoring the response of extracellular excitatory postsynaptic potentials in the hippocampal CA1 stratum radiatum to Schaffer collateral stimulation, it was found that preconditioning applied to a specific synaptic pathway altered the effect of a subsequent stimulation protocol; for example, preconditioning with high-frequency stimulation increased neuronal excitability but the excitatory effect was reversed by stimulation at 10 Hz, resulting in LTD induction [34].

Some researches also illustrated that the interval between the two NIBS protocols could influence the direction of cortical excitability affected by the subsequent NIBS intervention [35, 36]. It is important for deciding the direction of subsequent plasticity; however, the direction of response can be variable. Tse et al. found that a shorter interval of 5 minutes could invert cortical excitability, while a longer interval of 15 minutes could enhance the after effects induced by preconditioning, which led to a potentiation compared with a single stimulation [36]. According to the existing researches, the results indicated that there was LTD-like effect in the brain cortex after preconditioning with cathodal HD-tDCS [15, 16]. Based on synaptic homeostatic plasticity, cathodal HD-tDCS reduced the average postsynaptic activity in M1, decreasing the threshold for LTP induction. Subsequent iTBS, which had the opposite effect to HD-tDCS, resulted in prolonged excitability of the corticospinal tract.

Although we demonstrated the effectiveness of the combined NIBS procedure, the safety and tolerability of TMS and tDCS are important considerations. The symptoms of headache, tingling, and itching associated with TMS or tDCS are usually mild and short-lived [37–40], but few studies have systematically investigated the tolerability of these procedures, which has prevented the widespread application of NIBS to the intervention of neurologic or psychiatric disorders. No serious adverse events occurred during the course of the present study, and there was no increase in the risk of intervention-related adverse events following the intervention. In the future, we will review the safety of the protocol in a larger sample.

Preconditioning with cathodal HD-tDCS enhanced iTBS-induced cortical plasticity in the M1 area of the brain, and its duration of after-effect was prolonged. We aimed to search for a novel pattern by which the excitability of cerebral cortex could be better and steadily regulated. This preliminary study provides a basis for investigating the best stimulation parameters of this combined intervention in the future. Additionally, these unclear factors need to be verified in further relevant RCTs, which may be the existence or nonexistence of the synaptic homeostatic plasticity mechanism in people of different ages and diseases, the safety of the combination of tDCS and TMS, and the effect of different intervals between the two NIBS interventions.

5. Conclusions

In conclusion, cathodal HD-tDCS followed by iTBS in M1 increased MEP amplitude and enhanced cortical plasticity with long-lasting effects compared to iTBS without HD-tDCS preconditioning in healthy young adults. These results suggest that preconditioning with cathodal HD-tDCS can be used to improve the therapeutic efficacy of iTBS and have prolonged after-effects, which has a high potential for clinical application and deserves to be explored in further studies.

Data Availability

The data presented in this article can be obtained from the corresponding author on reasonable request.

Conflicts of Interest

The authors declare that the research was conducted in the absence of any commercial or financial relationships that could be construed as a potential conflict of interest.

Authors' Contributions

TW and YS conceived and designed the study; WD, YG, HL, and CG performed the study and collect materials; JM analyzed the results; WD, YG, and WC wrote the manuscript; TW, YS, HL, JC and YJ helped coordinate the study and reviewed the manuscript. All authors contributed to the article and approved the submitted version. Wenjun Dai, Yao

Geng, Hao Liu, Chuan Guo, and Wenxiang Chen contributed equally to this work.

Acknowledgments

We thank all the subjects' voluntary contributions during the completion of this study. This study was funded by the Nanjing Municipal Science and Technology Bureau (grant No. 2019060002), the National Key R&D Program of China (grant Nos. 2018YFC2001600 and 2018YFC2001603), Special Fund Project for Science and Technology Innovation (Social Development) in Yixing (grant No. 2019SF01), and the fund project of JORU Rehabilitation Hospital (grant No. JY-2018001A).

Supplementary Materials

We describe raw MEP amplitudes during the pilot study in Supplementary Table 1. *(Supplementary Materials)*

References

[1] M. Kobayashi and A. Pascual-Leone, "Transcranial magnetic stimulation in neurology," *The Lancet Neurology*, vol. 2, pp. 145–156, 2003.

[2] C. Chisari, C. Fanciullacci, G. Lamola, B. Rossi, and L. G. Cohen, "NIBS-driven brain plasticity," *Archives Italiennes de Biologie*, vol. 152, no. 4, pp. 247–258, 2014.

[3] Y.-Z. Huang, M.-K. Lu, A. Antal et al., "Plasticity induced by non-invasive transcranial brain stimulation: a position paper," *Clinical Neurophysiology*, vol. 128, no. 11, pp. 2318–2329, 2017.

[4] P. Fitzgerald, "Intensity-dependent effects of 1 Hz rTMS on human corticospinal excitability," *Clinical Neurophysiology*, vol. 113, pp. 1136–1141, 2002.

[5] P. Fitzgerald, S. Fountain, and Z. Daskalakis, "A comprehensive review of the effects of rTMS on motor cortical excitability and inhibition," *Clinical Neurophysiology*, vol. 117, pp. 2584–2596, 2006.

[6] Y. H. Kwon, M.-H. Ko, S. H. Ahn et al., "Primary motor cortex activation by transcranial direct current stimulation in the human brain," *Neuroscience Letters*, vol. 435, no. 1, pp. 56–59, 2008.

[7] N. Lang, H. R. Siebner, D. Ernst et al., "Preconditioning with transcranial direct current stimulation sensitizes the motor cortex to rapid-rate transcranial magnetic stimulation and controls the direction of after-effects," *Biological Psychiatry*, vol. 56, no. 9, pp. 634–639, 2004.

[8] H. R. Siebner, "Preconditioning of low-frequency repetitive transcranial magnetic stimulation with transcranial direct current stimulation: evidence for homeostatic plasticity in the human motor cortex," *Journal of Neuroscience*, vol. 24, pp. 3379–3385, 2004.

[9] G. Cosentino, B. Fierro, P. Paladino et al., "Transcranial direct current stimulation preconditioning modulates the effect of high-frequency repetitive transcranial magnetic stimulation in the human motor cortex," *European Journal of Neuroscience*, vol. 35, no. 1, pp. 119–124, 2012.

[10] A. Karabanov, U. Ziemann, M. Hamada et al., "Consensus Paper: Probing Homeostatic Plasticity of Human Cortex With Non- invasive Transcranial Brain Stimulation," *Brain Stimulation*, vol. 8, no. 5, pp. 993–1006, 2015.

[11] L. Bienenstock, N. Cooper, and W. Munro, "Theory for the development of neuron selectivity: orientation specificity and binocular interaction in visual cortex," *The Journal of Neuroscience*, vol. 2, no. 1, pp. 32–48, 1982.

[12] Y.-Z. Huang, R.-S. Chen, J. C. Rothwell, and H. Y. Wen, "The after-effect of human theta burst stimulation is NMDA receptor dependent," *Clinical Neurophysiology*, vol. 118, no. 5, pp. 1028–1032, 2007.

[13] A. M. Hurtado-Puerto, K. Nestor, M. Eldaief, and J. A. Camprodon, "Safety considerations for cerebellar theta burst stimulation," *Clinical Therapeutics*, vol. 42, no. 7, pp. 1169–1190.e1, 2020.

[14] Y.-Z. Huang, M. J. Edwards, E. Rounis, K. P. Bhatia, and J. C. Rothwell, "Theta burst stimulation of the human motor cortex," *Neuron*, vol. 45, no. 2, pp. 201–206, 2005.

[15] M. A. Nitsche and W. Paulus, "Excitability changes induced in the human motor cortex by weak transcranial direct current stimulation," *The Journal of Physiology*, vol. 527, pp. 633–639, 2000.

[16] C. J. Stagg and M. A. Nitsche, "Physiological basis of transcranial direct current stimulation," *The Neuroscientist*, vol. 17, pp. 37–53, 2011.

[17] A. Datta, V. Bansal, J. Diaz, J. Patel, D. Reato, and M. Bikson, "Gyri-precise head model of transcranial direct current stimulation: improved spatial focality using a ring electrode versus conventional rectangular pad," *Brain Stimulation*, vol. 2, no. 4, pp. 201–207.e1, 2009.

[18] P. M. Rossini, D. Burke, R. Chen et al., "Non-invasive electrical and magnetic stimulation of the brain, spinal cord, roots and peripheral nerves: basic principles and procedures for routine clinical and research application. An updated report from an I.F.C.N. Committee," *Clinical Neurophysiology*, vol. 126, no. 6, pp. 1071–1107, 2015.

[19] J. Long, P. Federico, and M. A. Perez, "A novel cortical target to enhance hand motor output in humans with spinal cord injury," *Brain*, vol. 140, pp. 1619–1632, 2017.

[20] F. Yu, X. Tang, R. Hu et al., "The after-effect of accelerated intermittent theta burst stimulation at different session intervals," *Frontiers in Neuroscience*, vol. 14, p. 576, 2020.

[21] T. Lin, L. Jiang, Z. Dou et al., "Effects of theta burst stimulation on suprahyoid motor cortex excitability in healthy subjects," *Brain Stimulation*, vol. 10, no. 1, pp. 91–98, 2017.

[22] P. Minhas, V. Bansal, J. Patel et al., "Electrodes for high-definition transcutaneous DC stimulation for applications in drug delivery and electrotherapy, including tDCS," *Journal of Neuroscience Methods*, vol. 190, no. 2, pp. 188–197, 2010.

[23] H.-I. Kuo, M. Bikson, A. Datta et al., "Comparing cortical plasticity induced by conventional and high-definition 4×1 ring tDCS: a neurophysiological study," *Brain Stimulation*, vol. 6, no. 4, pp. 644–648, 2013.

[24] J. Hogeveen, J. Grafman, M. Aboseria, A. David, M. Bikson, and K. K. Hauner, "Effects of high-definition and conventional tDCS on response inhibition," *Brain Stimulation*, vol. 9, no. 5, pp. 720–729, 2016.

[25] A. Datta, M. Elwassif, F. Battaglia, and M. Bikson, "Transcranial current stimulation focality using disc and ring electrode configurations: FEM analysis," *Journal of Neural Engineering*, vol. 5, no. 2, pp. 163–174, 2008.

[26] A. Suppa, Y.-Z. Huang, K. Funke et al., "Ten years of theta burst stimulation in humans: established knowledge, unknowns and prospects," *Brain Stimulation*, vol. 9, no. 3, pp. 323–335, 2016.

[27] M. C. Ridding and U. Ziemann, "Determinants of the induction of cortical plasticity by non-invasive brain stimulation in healthy subjects: induction of cortical plasticity by non-invasive brain stimulation," *The Journal of Physiology*, vol. 588, pp. 2291–2304, 2010.

[28] W. C. Abraham and M. F. Bear, "Metaplasticity: the plasticity of synaptic plasticity," *Trends in Neurosciences*, vol. 19, no. 4, pp. 126–130, 1996.

[29] G. Turrigiano, "Homeostatic synaptic plasticity: local and global mechanisms for stabilizing neuronal function," *Cold Spring Harbor Perspectives in Biology*, vol. 4, pp. a005736–a005736, 2012.

[30] G. G. Turrigiano and S. B. Nelson, "Homeostatic plasticity in the developing nervous system," *Nature Reviews. Neuroscience*, vol. 5, pp. 97–107, 2004.

[31] G. G. Turrigiano, "The self-tuning neuron: synaptic scaling of excitatory synapses," *Cell*, vol. 135, pp. 422–435, 2008.

[32] L. N. Cooper and M. F. Bear, "The BCM theory of synapse modification at 30: interaction of theory with experiment," *Nature Reviews. Neuroscience*, vol. 13, pp. 798–810, 2012.

[33] Y. Huang, A. Colino, D. Selig, and R. Malenka, "The influence of prior synaptic activity on the induction of long-term potentiation," *Science*, vol. 255, no. 5045, pp. 730–733, 1992.

[34] H. Wang and J. J. Wagner, "Priming-induced shift in synaptic plasticity in the rat hippocampus," *Journal of Neurophysiology*, vol. 82, pp. 2024–2028, 1999.

[35] K. Fricke, A. A. Seeber, N. Thirugnanasambandam, W. Paulus, M. A. Nitsche, and J. C. Rothwell, "Time course of the induction of homeostatic plasticity generated by repeated transcranial direct current stimulation of the human motor cortex," *Journal of Neurophysiology*, vol. 105, no. 3, pp. 1141–1149, 2011.

[36] N. Y. Tse, M. R. Goldsworthy, M. C. Ridding et al., "The effect of stimulation interval on plasticity following repeated blocks of intermittent theta burst stimulation," *Scientific Reports*, vol. 8, no. 1, p. 8526, 2018.

[37] S. Rossi, M. Hallett, P. M. Rossini, A. Pascual-Leone, and Safety of TMS Consensus Group, "Safety, ethical considerations, and application guidelines for the use of transcranial magnetic stimulation in clinical practice and research," *Clinical Neurophysiology*, vol. 120, no. 12, pp. 2008–2039, 2009.

[38] S. Rossi, A. Antal, S. Bestmann et al., "Safety and recommendations for TMS use in healthy subjects and patient populations, with updates on training, ethical and regulatory issues: expert guidelines," *Clinical Neurophysiology*, vol. 132, no. 1, pp. 269–306, 2021.

[39] S. Nikolin, C. Huggins, D. Martin, A. Alonzo, and C. K. Loo, "Safety of repeated sessions of transcranial direct current stimulation: a systematic review," *Brain Stimulation*, vol. 11, no. 2, pp. 278–288, 2018.

[40] P. E. Tarapore, T. Picht, L. Bulubas et al., "Safety and tolerability of navigated TMS in healthy volunteers," *Clinical Neurophysiology*, vol. 127, no. 3, pp. 1916–1918, 2016.

Hindawi
Neural Plasticity
Volume 2021, Article ID 7266263, 9 pages
https://doi.org/10.1155/2021/7266263

Research Article

Associated Mirror Therapy Enhances Motor Recovery of the Upper Extremity and Daily Function after Stroke: A Randomized Control Study

Jin-Yang Zhuang,[1] **Li Ding**,[1] **Bei-Bei Shu**,[2] **Dan Chen**,[2] **and Jie Jia**[1,2,3]

[1]*Department of Rehabilitation Medicine, Huashan Hospital, Fudan University, Shanghai, China*
[2]*Department of Rehabilitation Medicine, Shanghai Jing'an District Central Hospital, Shanghai, China*
[3]*National Clinical Research Center for Aging and Medicine, Huashan Hospital, Fudan University, China*

Correspondence should be addressed to Jie Jia; shannonjj@126.com

Received 13 April 2021; Accepted 31 August 2021; Published 29 September 2021

Academic Editor: Xu-Yun Hua

Bimanual cooperation plays a vital role in functions of the upper extremity and daily activities. Based on the principle of bilateral movement, mirror therapy could provide bimanual cooperation training. However, conventional mirror therapy could not achieve the isolation of the mirror. A novel paradigm mirror therapy called associated mirror therapy (AMT) was proposed to achieve bimanual cooperation task-based mirror visual feedback isolating from the mirror. The study was aimed at exploring the feasibility and effectiveness of AMT on stroke patients. We conducted a single-blind, randomized controlled trial. Thirty-six eligible patients were equally assigned into the experimental group (EG) receiving AMT and the control group (CG) receiving bimanual training without mirroring for five days/week, lasting four weeks. The Fugl-Meyer Assessment Upper Limb subscale (FMA-UL) for upper extremity motor impairment was used as the primary outcome. The secondary outcomes were the Box and Block Test (BBT) and Functional Independence Measure (FIM) for motor and daily function. All patients participated in trials throughout without adverse events or side effects. The scores of FMA-UL and FIM improved significantly in both groups following the intervention. Compared to CG, the scores of FMA-UL and FIM were improved more significantly in EG after the intervention. The BBT scores were improved significantly for EG following the intervention, but no differences were found in the BBT scores of CG after the intervention. However, no differences in BBT scores were observed between the two groups. In summary, our study suggested that AMT was a feasible and practical approach to enhance the motor recovery of paretic arms and daily function in stroke patients. Furthermore, AMT may improve manual dexterity for poststroke rehabilitation.

1. Introduction

Stroke is a leading cause of mortality and long-term disability worldwide [1], which results in a global economic burden for health care [2, 3]. Currently, many advanced technologies have been worked out and used for stroke survivors. Nevertheless, we still face many challenges for poststroke rehabilitation, for instance, the paretic upper extremity. After stroke, about 80% of patients remain having upper extremity motor impairment [4]. Besides, researchers have found that the ipsilesional upper limb also suffered motor dysfunction in 3 months after the onset of stroke [5], which hinders physical function and independent daily activities.

Compared to the healthy population, stroke patients tend to avoid bilateral motor patterns in daily activities [6]. Lots of daily activities are inseparable from bimanual cooperation, such as twisting the towel, driving the car, and getting dressed. For this reason, bilateral task relearning is essential for stroke patients. However, most therapeutic methods for stroke are concentrated on improving the

contralesional arm function, ignoring participation of the less affected side [7–9]. It is remarkable that protocols of bilateral treatment (BT) which involve bilateral training with rhythmic auditory cues, bilateral priming, and device-driven bilateral training have been used as clinical treatments for stroke rehabilitation [10–12]. Based on bilateral, repetitive, and symmetrical motor principles, most bilateral treatments (BTs) are executed through two independent and paralleled actions, which ignore cooperation between the hands; for instance, Sainburg et al. proposed the symmetrical cooperative tasks regarded as a bilateral synergy framework for post-stroke rehabilitation [6].

In addition to conventional physical intervention methods, mirror therapy (MT) which relies on visual illusion is regarded as a bilateral treatment [13, 14]. Under the MT environment, a plane mirror is placed in the median sagittal plane between upper limbs to induce the visual illusion, and patients are asked to move both arms as far as possible. Contrary to viewing directly on both arms, MT can provide normal visual stimulation of bilateral movement, which has been proven to promote better the activation and functional connectivity in the somatosensory system of the brain [15]. In addition, better than most protocols of BT, MT may have a priming effect on motor recovery through mirror illusion [14, 16]. Hence, compared to conventional BTs, MT may be a superior approach for bilateral task relearning for stroke patients. Following the types of action, the protocols of MT contain manipulation of objects, manipulation without objects, and both in combination [17]. However, relying entirely on a plane mirror or "mirror box," the conventional protocol of MT cannot achieve it for isolating two hands from the mirror and only provides unilateral visual feedback. Due to the limitations, manipulation of objects under MT cannot attain bimanual cooperation and may affect the priming activation of mirror visual feedback (MVF) [18–20]. Besides, the poor posture in the conventional MT procedure can easily cause pressure on the spine and impede effective bimanual cooperation relearning [21].

To overcome the limitations of the traditional MT, researchers have proposed novel mirror setups. Camera technique-based MVF, which offered bilateral visual feedback, was one of those, and previous researches have been verified that camera technique-based MVF can promote the functional recovery of stroke [22–24].

We previously put forward a novel camera technique-based MVF with an operable mirror environment [21]. Patients can achieve synchronous movement of both upper extremities isolated from the mirror in such an environment. Previous studies have proven its clinical feasibility and effectiveness for stroke rehabilitation [21, 25]. Based on the setup, we developed a novel MT paradigm, in which both upper extremities were associated with one object, and patients were asked to complete the same tasks to realize the association of both sides. In the paradigm of MT, we named it associated mirror therapy (AMT). We conducted a randomized controlled trial to certificate AMT's feasibility and clinical efficacy, and we hypothesized that AMT could promote the recovery of the paretic upper extremity and daily function for stroke patients.

2. Methods

2.1. Study Design. This study was an assessor-blinded, pretest-posttest, randomized controlled trial. A separate investigator was responsible for the clinical assessments but blinded to the allocation. Meanwhile, two occupation therapists who were responsible for the therapeutic regimens were trained by one researcher. All patients received assessments before the intervention, after 2-week and 4-week intervention. The study was approved by the ethics committee institutions of Huashan Hospital (KY2017-230) and registered at the Chinese Clinical Trial Registry (ChiCTR1800018351).

2.2. Participants. Patients were recruited from the Department of Rehabilitation Medicine, Huashan Hospital Affiliated Jing'an Branch. Patients who had a first-ever ischemic or hemorrhagic stroke, occurring three months to one year, aged between 25 and 75 years without severe cognitive impairment
(Mini-Mental State Examination (MMSE) score > 24), were included. All patients were within the Brunnstrom stage of hand over III and with modified Ashworth scale ≤ 2. Patients who met any of the following conditions were excluded: (i) the condition deteriorated during the intervention; that is, the stroke relapsed or a new infarction occurred; (ii) psychiatric disorder or other serious illness that interfered with the patients' ability to obey the therapists; (iii) and having experienced other central intervention methods, for instance, transcranial direct current stimulation (tDCS). The enrolled patients were given written informed consent before the study.

We speculated that the primary outcome (FMA-UL) had a group × time interaction. Based on the previous camera technique-based MVF studies [21, 25, 26], an effect size of 0.27 to 0.45 was expected to detect the differences in the improvements between groups. Given the reliability and safety margin, an effect size of 0.27 was anticipated for repeated analysis of variance (ANOVA). Then, we estimated a total sample size of 30 which was needed for providing 80% power to detect the differences between groups on FMA-UL with a type I error of 0.05 and a dropout rate of 20%. In addition, we reviewed all published clinical trials on MT, and the sample size of most studies ranged from 10 to 20 patients in each group. Therefore, we planned to recruit 18 patients in each group. The process of recruiting patients is shown in Figure 1.

2.3. Randomization and Allocation. Eligible patients were randomly assigned to the control group (CG) and experimental group (EG). An independent researcher executed the randomization procedure, generated through a random data generator on the computer. A sealed envelope was used to confirm the group of each patient who was satisfied with recruitment criteria. When receiving an envelope, therapists were informed to perform the patient assignment.

2.4. Intervention. All enrolled patients received the conventional stroke rehabilitation program for four weeks, five days/week, and around four hours/day. The conventional stroke

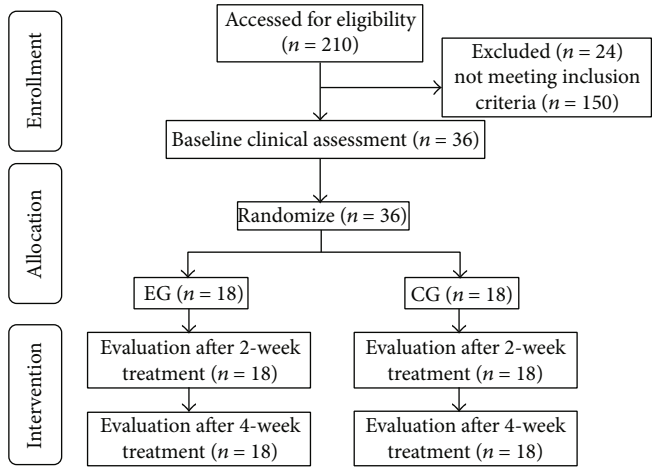

Figure 1: The flowchart of recruiting patients.

program consisted of physiotherapy, occupation therapy, speech therapy, and respiratory management.

2.4.1. Experimental Group

(1) Setup. The setup (1200 mm × 940 mm × 702 mm) was mounted with a 23.8-inch light-emitting diode screen of 30° tilt, fixed on the mirror setup to present the mirror image, and blocked the direct view of both hands [21]. Two cameras were mounted on the top of the mirror setup to capture the movements of the hands. In the mirrored environment, patients were allowed to put both hands on the bottom of the "mirror box", of which one side opening was beneath the screen. The therapist could assist the patients on the other side. Patients could sit in a suitable and comfortable position by adjusting the setup height during the treatment.

(2) Associated Mirror Therapy (AMT). Based on the above setup, we created a novel clinical paradigm of MT, in which patients not only could see the regular bimanual cooperation but also could attain the bilateral cooperative tasks with the assistance of therapists. In the paradigm, both upper extremities were associated with the identical object and completed synchronously the same task, e.g., holding a ball, grabbing and rolling a cylinder, stacking of towels, lifting a stick, and pushing a sanding board (see Figures 2(a) and 2(b)). Patients were required to focus on the screen and imagined doing cooperative tasks with both arms. Meanwhile, patients were asked to perform the same training synchronously by the affected side as much as possible. During the trial, therapists offered essential directions to make patients concentrate on the screen and immerse themselves in mirror illusion. Another role of therapists was to supervise and ensure the completion of actual bilateral cooperative tasks of patients. Conforming to the motion of the less affected arm of the patient, the therapist could provide active, assisted, or passive movement for the affected side alternatively. We named the novel paradigm "associated mirror therapy" (AMT) for achieving a practical bimanual interaction under camera technique-based MVF.

In addition to the conventional rehabilitation, patients in EG received half an hour of AMT firstly. Based on the patient's condition, therapists selected 2 to 3 kinds of bilateral cooperative tasks. Subsequently, another half-hour upper limb training was applied, including stretching, relaxing, and functional activities.

2.4.2. Control Group. Patients in CG received the same dose of training as EG. However, the only difference was that CG received bimanual cooperation training without camera technique-based MVF, where patients had a direct view of both arms. To assure the performance of bilateral cooperative tasks, therapists also provided necessary assistance to help patients (see Figures 2(c) and 2(d)).

2.5. Assessments. The basic information, including age, sex, lesion side of the brain, stroke type, and duration after stroke onset, was recorded. The clinical outcomes were concerned with motor impairment, motor function, and daily function. The outcome measures were evaluated repeatedly before the intervention, after 2-week and 4-week intervention to verify clinical efficacy. The specific evaluation details of outcome measures were as follows.

The primary outcome was the change of motor impairment measured through the Fugl-Meyer Assessment Upper Limb subscale (FMA-UL). The FMA-UL subscale with good psychometric properties indicated high reliability and validity for motor impairment [27]. The FMA-UL subscale included 33-item upper limb activities. Each item was rated on a 0 to 2 ordinal scale. The maximum score of the FMA-UL subscale was 66.

Secondary outcomes were the performances of motor and daily function. The Box and Block Test (BBT) with satisfactory reliability and validity was used to assess motor function for manual dexterity in stroke patients [28]. The BBT contains 150 colored wooden cube blocks (1 inch, 2.5 cm × 2.5 cm × 2.5 cm). The participants were told to move one-by-one blocks as many as possible from a rectangular box container to the other of equal size within 60 seconds. Both hands' scores of the BBT were calculated, respectively, by the number of blocks transferred. The Functional

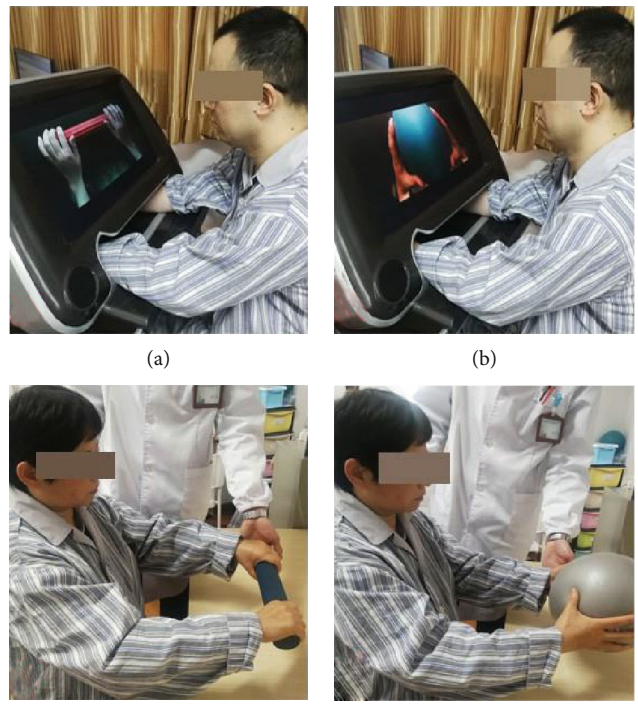

Figure 2: AMT and conventional bimanual training for stroke rehabilitation: (a, b) AMT: grabbing and rolling a cylinder/holding a ball; (c, d) conventional bimanual training: grabbing and rolling a cylinder/holding a ball.

Independent Measurement (FIM) was widely applied to evaluate participation after stroke [29]. FIM involved six aspects of daily function: self-care, sphincter control, transfer, locomotion, communication, and social cognition ability. It was made of 18 items, and each item was graded on a 1 to 7 ordinal scale. The total score ranged from 7 to 126.

2.6. Statistical Analyses. The data were analyzed by using SPSS version 20.0 for Windows (SPSS Inc., Chicago, IL, USA). We used Shapiro-Wilk's test to check the underlying model assumptions for normality of distribution entirely. None of evaluation indicators satisfied the normal distribution. Baseline characteristics of the patients between groups were compared by using chi-square tests or Fisher's exact test (including gender, side of paralysis, stroke types, and Brunnstrom stage) when appropriate. The Mann–Whitney U test was used to examine the baseline data of continuous variables between groups (including age and course of the disease). The generalized estimating equation (GEE) model based on a binary outcome with first-order autoregressive correlation structure (AR (1)) was used to explore multitime repeated measurement analysis [30, 31], including three outcome indicators (FMA-UL, FIM, and BBT). The main effects of group, time, and group-by-time interaction were analyzed in the GEE model. A value of $P < 0.05$ was considered significant.

3. Results

3.1. Baseline Characteristics. From October 2018 to August 2019, 36 stroke patients were recruited, with 18 patients in each group. All patients completed the trial without side effects, and adverse events occurred during the trial.

The clinical characteristics of the two groups of patients were demonstrated in Table 1. The median age (QR) was 54.0 (24.00) and 58.0 (22.75) years for EG and CG, respectively ($P = 0.350$), with no difference in sex between groups. No significant difference was found in the course of stroke ($P = 0.198$). There were no differences in the type and location of stroke between EG and CG ($P = 0.725$, $P = 0.738$). No differences were found between the two groups in the Brunnstrom stages of the proximal and distal areas of the affected upper extremity ($P = 0.464$, $P = 0.876$).

3.2. Treatment Effects on Clinical Outcomes. The improvements of paretic arm impairment and daily function were observed in both groups. Manual dexterity had a significant change in EG after the intervention, whereas the improvement did not occur in CG. Significant group-by-time interaction effects were found in FAM-UL scores ($\text{Wald}_{\chi^2} = 174.434$, $P < 0.001$), BBT scores ($\text{Wald}_{\chi^2} = 18.594$, $P = 0.002$), and FIM scores ($\text{Wald}_{\chi^2} = 100.165$, $P < 0.001$) after the intervention; therefore, the single group or time effect estimate was not applicable during the study (see Table 2). The treatment effects of clinical outcomes are shown in Tables 3–5. The detailed comparisons between the two groups were reported below.

After the 4-week trial, FMA-UL scores in both groups were significantly higher than before ($P < 0.001$ and $P < 0.001$, respectively). Both EG and CG had a continuous improvement in FMA-UL scores over time, including the

Table 1: Characteristics of study participants ($n = 36$).

Variable	EG ($n = 18$)	CG ($n = 18$)	P value
Age (years), M (QR)	54.0 (24.00)	58.0 (22.75)	0.350
Sex, N			
Male/female	12/6	12/6	1.000
Lesion side, N			
Left/right	9/9	10/8	0.738
Stroke type, N			
Hemorrhagic/schemic	13/5	11/7	0.725
Months after stroke onset, M (QR)	4.0 (5.25)	5.0 (7.25)	0.198
Brunnstrom (3/4/5/6), N			
Distal	12/2/2/2	14/1/1/2	0.876
Proximal	12/2/2/2	16/1/0/1	0.464

EG: experimental group; CG: conventional group.

Table 2: Description for group effect, time effect, and group × time effect on motor impairment, motor function, and daily function.

Outcomes	Group		Time		Group × time	
	Wald_{χ^2}	P	Wald_{χ^2}	P	Wald_{χ^2}	P
FAM-UL	4.858	0.028	141.058	<0.001	174.434	<0.001
FIM	3.893	0.048	58.687	<0.001	100.165	<0.001
BBT	0.192	0.662	17.310	<0.001	18.594	0.002

FAM-UL: Fugl-Meyer Assessment Upper Limb subscale; BBT: Box and Block Test; FIM: Functional Independence Measure.

Table 3: Description and comparison between groups for statistical outcomes on motor impairment, motor function, and daily function.

Outcomes	Pretest			After 2 weeks			After 4 weeks		
	EG	CG	P	EG	CG	P	EG	CG	P
FMA-UL	32.5 (25.50)	28.0 (11.00)	0.290	41.5 (13.25)	30.0 (11.75)	0.018	45.0 (22.50)	30.5 (13.50)	0.001
FIM	108.0 (8.00)	104.5 (15.00)	0.287	111.(8.50)	106.0 (15.50)	0.041	113.5 (8.50)	107.0 (14.50)	0.003
BBT	0.5 (12.00)	0.0 (3.00)	0.780	2.0 (21.50)	0.0 (3.25)	0.569	3.0 (24.00)	0.0 (6.25)	0.377

EG: experimental group; CG: conventional group; FAM-UL: Fugl-Meyer Assessment Upper Limb subscale; BBT: Box and Block Test; FIM: Functional Independence Measure.

Table 4: Description for motor impairment, motor function, and daily function in EG.

Outcomes	Pretest	After 2 weeks	After 4 weeks	P
FMA-UL	32.5 (25.50)	41.5 (23.25)[a]	45.0 (22.50)[b]	<0.001
FIM	108.0 (8.00)	111.0 (8.50)	113.5 (8.50)	<0.001
BBT	0.5 (12.00)	2.0 (21.50)	3.0 (24.00)	<0.001

[a]Comparison between pretest and after 2-week intervention. $P_{\text{FMA-UL}} < 0.001$, $P_{\text{FIM}} < 0.001$, and $P_{\text{BBT}} = 0.002$. [b]Comparison between after 2-week intervention and after 4-week intervention. $P_{\text{FMA-UL}} < 0.001$, $P_{\text{FIM}} < 0.001$, and $P_{\text{BBT}} < 0.001$. EG: experimental group; FAM-UL: Fugl-Meyer Assessment Upper Limb subscale; BBT: Box and Block Test; FIM: Functional Independence Measure.

Table 5: Description for motor impairment, motor function, and daily function in CG.

Outcomes	Pretest	After 2 weeks	After 4 weeks	P
FMA-UL	28.0 (11.00)	30.0 (11.75)[c]	30.5 (13.50)[d]	<0.001
FIM	104.5 (15.00)	106.0 (15.50)	107.0 (14.50)	<0.001
BBT	0.0 (3.00)	0.0 (3.25)	0.0 (6.25)	0.107

[c]Comparison between pretest and after 2-week intervention. $P_{\text{FMA-UL}} < 0.001$, $P_{\text{FIM}} < 0.001$, and $P_{\text{BBT}} = 1$. [d]Comparison between after 2-week intervention and after 4-week intervention. $P_{\text{FMA-UL}} < 0.001$, $P_{\text{FIM}} = 0.006$, and $P_{\text{BBT}} = 0.043$. CG: conventional group; FAM-UL: Fugl-Meyer Assessment Upper Limb subscale; BBT: Box and Block Test; FIM: Functional Independence Measure.

first two weeks ($P < 0.001$ and $P < 0.001$, respectively) and the last two weeks of intervention ($P < 0.001$ and $P < 0.001$, respectively). Post hoc analyses indicated no difference in FAM-UL between EG and CG before the trial ($P = 0.290$). Moreover, the scores of FMA-UL in the EG were significantly higher than those in the CG after 2 and 4 weeks ($P = 0.018$ and $P = 0.001$, respectively).

Significant improvements of BBT scores in the first and the last two weeks were observed in EG ($P = 0.002$ and $P < 0.001$). After the intervention, BBT scores in the EG were significantly improved ($P < 0.001$). However, in the CG, only in the last two weeks, the BBT scores were significantly improved ($P = 0.043$). After the 4-week intervention, no difference in BBT scores was observed in the CG than before ($P = 0.107$). By comparing EG with CG, no differences in BBT scores were observed before the trial, after 2-week and 4-week intervention ($P = 0.780$, $P = 0.569$, and $P = 0.377$, respectively). Although the difference in manual dexterity measured by BBT scores was not significant between both groups, a clinical improvement is in favor of AMT.

After the 4-week trial, FIM scores in both groups were significantly higher than before ($P < 0.001$ and $P < 0.001$, respectively). A significant improvement of FIM scores in the first and the last two weeks was observed in the EG ($P < 0.001$ and $P < 0.001$, respectively). FIM scores in the CG were also improved in the first and the last two weeks ($P < 0.001$ and $P = 0.006$, respectively). When compared between groups, no difference in FIM scores was observed before the trial ($P = 0.287$). However, improvement of FIM scores in the EG was better than the CG after 2 and 4 weeks ($P = 0.041$ and $P = 0.003$, respectively).

4. Discussion

In the present study, we proposed a novel paradigm of MT, called AMT, which achieved bimanual cooperation under camera technique-based MVF. Besides, we testified to the feasibility and effectiveness of AMT. All patients participated in trials throughout without adverse events or side effects, proving that the AMT was safe and feasible. The study demonstrated that using AMT as an auxiliary therapy to usual care could decrease the motor impairment of the paretic upper extremity and enhance daily function for stroke patients. In addition, AMT may increase manual dexterity after stroke.

The coordinated control was also regarded as an essential function of the standard upper extremities, especially for instrumental activities of daily living (IADL) [32–34]. After stroke, patients lacked the participation of the paretic upper extremity in daily tasks [35]. Previous studies combined MT with daily functional activities, demonstrating that the MT paradigms could enhance the motor recovery of the paretic upper extremity in stroke patients [36, 37]. Although many protocols of MT were proposed, few of those achieved practical bimanual tasks to associate both upper extremities. Rodrigues et al. developed the bilateral task-based MT, which related both arms to one object under the mirror environment [38]. As far as we know, this was the first study to propose bilateral tasks based on MT. Despite proving the feasibility of combining bilateral symmetrical tasks with MT, patients were asked to concentrate on the reflection side of the mirror and could not ensure the participation of the paretic side. New setups for MT conquered the limitations of the conventional mirror, for instance, the camera technique-based MT proposed by Lee et al., which realized MVF effect delay and bilateral movements [22, 24]. We previously put forward novel camera technique-based MVF [21]. To achieve bimanual coordination control under the mirror, we designed bimanual cooperation tasks in which both arms were associated with one object and completed the same tasks synergistically.

Compared to usual care, camera technique-based MVF was proven to enhance the motor impairment of the upper extremity after stroke [22, 25]. In line with the results of previous studies, the improvements in motor impairment measured by FAM-UL were observed in both groups after the intervention, and patients in the EG were improved more significantly than the CG. Furthermore, compared with bilateral arm training, researchers also found a more significant improvement for the distal arm which was in favor of MT [39]. Our results were similar to the above study. Previous studies revealed that MVF might have the potential to promote motor learning by activating neural areas related to spatial attention, which was beneficial to enhance the perception of the paretic arm [40, 41]. Therefore, compared to conventional BT, the result might be interpreted that MVF activated the related sensorimotor brain area through visual illusion. Previously, Rodrigues et al. put forward adding an object to the plane mirror to realize bilateral symmetrical training under MT [38]. Researchers discovered that no differences were found between bilateral symmetrical tasks with or without MT. Our results were different from it. Noticeably, the MT paradigm in our study was different from the one Rodrigues et al. proposed. The main difference was that we used camera technique-based MVF rather than a plane mirror. In addition, in the present study, patients could accomplish practical bimanual tasks under the therapist's assistance, but the paretic upper extremity's quality could not be guaranteed in the above conventional MT paradigm.

When it came to motor function, one previous study pointed out that MT could promote the manual dexterity of stroke patients evaluated by BBT [42]. Our finding was similar to the study. In the comparison before and after the intervention, there was no difference of manual dexterity in CG. However, a significant effect of gross hand dexterity measured by BBT was found in AMT after the intervention. Although the difference in motor function improvements between both groups was not statistically significant, the performance was better in AMT. Besides, interestingly, a sustained motor function improvement of the upper extremity changed with time in EG, but not in CT. This phenomenon might be caused where AMT had a sustained regular visual input of movement, which may better promote central brain remodelling [15]. Our previous studies revealed that camera technique-based MVF could activate motor preparation and brain network segregation by inducing mirror illusion, which might promote motor execution for stroke patients [21, 25].

In this study, we used bilateral cooperation tasks with or without camera technique-based MVF for stroke patients. All patients had gained significant improvement in daily function after the trial, in line with previous studies of BT or MT [43, 44]. In addition, previous studies showed that MT was more effective than conventional methods in improving the daily function of stroke patients [36, 45]. Our result was similar to the above conclusion. A more significant improvement in daily function was observed in AMT when comparing the differences between both groups. It might be related to the more significant improvement of motor impairment of paretic arms in EG after the intervention. The daily function is related closely to the upper extremity function, for instance, self-care. However, in the present study, we did not compare the improvements between both groups in different aspects of daily function based on FIM. Then, the improvements of specific daily functions in AMT were unknown.

The study has some limitations. Firstly, the novel paradigm relied on camera technique-based MVF which is labour intensive. Secondly, though we have estimated the sample size, the results should be considered cautiously because of the small sample size. Thirdly, we only conduct the 4-week intervention without follow-up, and the long-term and sustained intervention effects for stroke patients are unknown. Hence, we will search for a more convenient and economical method of AMT by equipment upgrade. In addition, a larger RCT should be conducted to certify further the long-term and sustained effects of AMT on stroke patients.

5. Conclusions

In summary, this is the first study to propose a novel and advantageous MT paradigm achieving bimanual cooperation under camera technique-based MVF. The present study demonstrates that AMT is a feasible and effective method to improve motor impairment of the paretic arm, enhance daily function, and may increase the ability of manual dexterity after stroke.

Data Availability

We have utilized an unauthorized translation of the Chinese MMSE in the research, and we have received the permission of Psychological Assessment Resources (PAR). The study data are available from the corresponding author.

Conflicts of Interest

The authors declare no conflicts of interest.

Authors' Contributions

Jie Jia conceived the study design and provided the research theories to support the study. Jin-Yang Zhuang and Li Ding collected the data, wrote the manuscript, and conducted the experiment. Bei-Bei Shu and Dan Chen edited the manuscript. All the authors have reviewed the manuscript and agreed to its submission. Jin-Yang Zhuang and Li Ding contributed equally to this work.

Acknowledgments

We would like to thank all the patients who participated in the study. This study was funded by the National Key R&D Program of China (Grant Nos. 2018YFC2002300 and 2018YFC2002301), National Natural Science Foundation for Innovative Research Group Project of China (Grant No. 82021002), National Natural Science Foundation of China Major Research Program Integration Project (Grant No. 9194830003), National Natural Science Foundation of China (Grant No. 82002385), and Shanghai Sailing Program (Grant No. 20YF1403400).

References

[1] C. O. Johnson, M. Nguyen, and G. A. Roth, "Global, regional, and national burden of stroke, 1990-2016: a systematic analysis for the Global Burden of Disease Study 2016," *The Lancet Neurology*, vol. 18, no. 5, pp. 439–458, 2019.

[2] S. I. Hay, A. A. Abajobir, and K. H. Abate, "Global, regional, and national disability-adjusted life-years (DALYs) for 333 diseases and injuries and healthy life expectancy (HALE) for 195 countries and territories, 1990-2016: a systematic analysis for the Global Burden of Disease Study 2016," *The Lancet*, vol. 390, no. 10100, pp. 1260–1344, 2017.

[3] M. Katan and A. Luft, *Global burden of stroke. Seminars in neurology*, Thieme Medical Publishers, 2018.

[4] P. Langhorne, F. Coupar, and A. Pollock, "Motor recovery after stroke: a systematic review," *The Lancet Neurology*, vol. 8, no. 8, pp. 741–754, 2009.

[5] J. Metrot, J. Froger, I. Hauret, D. Mottet, L. van Dokkum, and I. Laffont, "Motor recovery of the ipsilesional upper limb in subacute stroke," *Archives of Physical Medicine and Rehabilitation*, vol. 94, no. 11, pp. 2283–2290, 2013.

[6] R. Sainburg, D. Good, and A. Przybyla, "Bilateral synergy: a framework for post-stroke rehabilitation," *Journal of neurology & translational neuroscience*, vol. 1, no. 3, 2013.

[7] C. Albert, M. D. Lo, P. D. Guarino, and L. G. Richards, "Robot-assisted therapy for long-term upper-limb impairment after stroke," *Th e new engl and journal o f medicine*, vol. 362, pp. 1772–1783, 2010.

[8] S. L. Wolf, C. J. Winstein, J. P. Miller et al., "Effect of constraint-induced movement therapy on upper extremity function 3 to 9 months after stroke: the EXCITE randomized clinical trial," *Jama*, vol. 296, no. 17, pp. 2095–2104, 2006.

[9] A. Pollock, S. E. Farmer, M. C. Brady et al., "Interventions for improving upper limb function after stroke," *The Cochrane Database of Systematic Reviews*, vol. 11, 2014.

[10] C. M. Stinear, M. A. Petoe, S. Anwar, P. A. Barber, and W. D. Byblow, "Bilateral priming accelerates recovery of upper limb function after stroke: a randomized controlled trial," *Stroke*, vol. 45, no. 1, pp. 205–210, 2014.

[11] A. Wolf, R. Scheiderer, N. Napolitan, C. Belden, L. Shaub, and M. Whitford, "Efficacy and task structure of bimanual training post stroke: a systematic review," *Topics in Stroke Rehabilitation*, vol. 21, no. 3, pp. 181–196, 2014.

[12] A. L. E. Q. van Delden, C. L. E. Peper, G. Kwakkel, and P. J. Beek, "A Systematic Review of Bilateral Upper Limb Training

Devices for Poststroke Rehabilitation," *Stroke Research and Treatment*, vol. 2012, 17 pages, 2012.

[13] M. A. R. Y. E. L. L. E. N. S. T. O. Y. K. O. V. DMC, "A review of bilateral training for upper extremity hemiparesis," *Occupational Therapy International*, vol. 16, no. 3-4, 2009.

[14] Y.-c. Li, C.-y. Wu, Y.-w. Hsieh et al., "The priming effects of mirror visual feedback on bilateral task practice: a randomized controlled study," *Occupational Therapy International*, vol. 2019, 9 pages, 2019.

[15] C. H. Cheng, "Effects of observing normal and abnormal goal-directed hand movements on somatosensory cortical activation," *European Journal of Neuroscience*, vol. 47, no. 1, pp. 48–57, 2018.

[16] M. E. Stoykov and S. Madhavan, "Motor priming in neurorehabilitation," *Journal of Neurologic Physical Therapy*, vol. 39, no. 1, pp. 33–42, 2015.

[17] N. Morkisch, H. Thieme, and C. Dohle, "How to perform mirror therapy after stroke? Evidence from a meta-analysis," *Restorative Neurology and Neuroscience*, vol. 37, no. 5, pp. 421–435, 2019.

[18] K.-B. Lim, H.-J. Lee, J. Yoo, H.-J. Yun, and H.-J. Hwang, "Efficacy of mirror therapy containing functional tasks in post-stroke patients," *Annals of Rehabilitation Medicine*, vol. 40, no. 4, pp. 629–636, 2016.

[19] K. N. Arya, S. Pandian, D. Kumar, and V. Puri, "Task-based mirror therapy augmenting motor recovery in poststroke hemiparesis: a randomized controlled trial," *Journal of Stroke and Cerebrovascular Diseases*, vol. 24, no. 8, pp. 1738–1748, 2015.

[20] R. W. Selles, M. E. Michielsen, J. B. J. Bussmann et al., "Effects of a mirror-induced visual illusion on a reaching task in stroke patients: implications for mirror therapy training," *Neurorehabilitation and Neural Repair*, vol. 28, no. 7, pp. 652–659, 2014.

[21] L. Ding, X. Wang, X. Guo et al., "Camera-based mirror visual feedback: potential to improve motor preparation in stroke patients," *IEEE Transactions on Neural Systems and Rehabilitation Engineering*, vol. 26, no. 9, pp. 1897–1905, 2018.

[22] C.-S. Chang, Y.-Y. Lo, C.-L. Chen, H.-M. Lee, W.-C. Chiang, and P.-C. Li, "Alternative motor task-based pattern training with a digital mirror therapy system enhances sensorimotor signal rhythms post-stroke," *Frontiers in Neurology*, vol. 10, 2019.

[23] S. Hoermann, L. F. dos Santos, N. Morkisch et al., "Computerised mirror therapy with augmented reflection technology for early stroke rehabilitation: clinical feasibility and integration as an adjunct therapy," *Disability and Rehabilitation*, vol. 39, no. 15, pp. 1503–1514, 2017.

[24] H.-M. Lee, P.-C. Li, and S.-C. Fan, "Delayed mirror visual feedback presented using a novel mirror therapy system enhances cortical activation in healthy adults," *Journal of Neuroengineering and Rehabilitation*, vol. 12, no. 1, 2015.

[25] L. Ding, X. Wang, S. Chen et al., "Camera-based mirror visual input for priming promotes motor recovery, daily function, and brain network segregation in subacute stroke patients," *Neurorehabilitation and Neural Repair*, vol. 33, no. 4, pp. 307–318, 2019.

[26] L. Ding, X. Wang, X. Guo et al., "Effects of camera-based mirror visual feedback therapy for patients who had a stroke and the neural mechanisms involved: protocol of a multicentre randomised control study," *BMJ Open*, vol. 9, no. 3, p. e022828, 2019.

[27] J. Sanford, J. Moreland, L. R. Swanson, P. W. Stratford, and C. Gowland, "Reliability of the Fugl-Meyer assessment for testing motor performance in patients following stroke," *Physical Therapy*, vol. 73, no. 7, pp. 447–454, 1993.

[28] V. Mathiowetz, G. Volland, N. Kashman, and K. Weber, "Adult norms for the Box and Block Test of manual dexterity," *American Journal of Occupational Therapy*, vol. 39, no. 6, pp. 386–391, 1985.

[29] D. Chumney, K. Nollinger, K. Shesko, K. Skop, M. Spencer, and R. A. Newton, "Ability of Functional Independence Measure to accurately predict functional outcome of stroke-specific population: systematic review," *Journal of rehabilitation research & development*, vol. 47, no. 1, p. 17, 2010.

[30] S. L. Zeger and K.-Y. Liang, "Longitudinal data analysis for discrete and continuous outcomes," *Biometrics*, vol. 42, no. 1, pp. 121–130, 1986.

[31] Y. Ma, M. Mazumdar, and S. G. Memtsoudis, "Beyond Repeated-Measures analysis of Variance," *Regional Anesthesia and Pain Medicine*, vol. 37, no. 1, pp. 99–105, 2012.

[32] V. Krishnan and S. Jaric, "Effects of task complexity on coordination of inter-limb and within-limb forces in static bimanual manipulation," *Motor Control*, vol. 14, no. 4, pp. 528–544, 2010.

[33] J. H. Cauraugh and S. Kim, "Two coupled motor recovery protocols are better than One," *Stroke*, vol. 33, no. 6, pp. 1589–1594, 2002.

[34] J. Jia, "Implication of left-right coordination and counterbalance for rehabilitation of upper limbs and hand function post stroke (review)," *Chinese Journal of Rehabilitation Theory and Practice*, vol. 24, no. 12, pp. 1365–1369, 2018.

[35] L. E. H. van Dokkum, E. le Bars, D. Mottet, A. Bonafé, N. M. de Champfleur, and I. Laffont, "Modified brain activations of the nondamaged hemisphere during ipsilesional upper-limb movement in persons with initial severe motor deficits post-stroke," *Neurorehabilitation and Neural Repair*, vol. 32, no. 1, pp. 34–45, 2018.

[36] K. Kim, S. Lee, D. Kim, K. Lee, and Y. Kim, "Effects of mirror therapy combined with motor tasks on upper extremity function and activities daily living of stroke patients," *Journal of Physical Therapy Science*, vol. 28, no. 2, pp. 483–487, 2016.

[37] K. N. Arya, S. Pandian, and D. Kumar, "Task-based mirror therapy enhances ipsilesional motor functions in stroke: a pilot study," *Journal of Bodywork and Movement Therapies*, vol. 21, no. 2, pp. 334–341, 2017.

[38] L. C. Rodrigues, N. C. Farias, R. P. Gomes, and S. M. Michaelsen, "Feasibility and effectiveness of adding object-related bilateral symmetrical training to mirror therapy in chronic stroke: a randomized controlled pilot study," *Physiotherapy Theory and Practice*, vol. 32, no. 2, pp. 83–91, 2016.

[39] A. Samaie and K. M. Amoozadeh, "A comparetive study on the effects of mirror therapy and bilateral arm training on hand function of chronichemiparetic patients," *Koomesh*, vol. 17, no. 3, pp. 589–595, 2016.

[40] F. J. A. Deconinck, A. R. P. Smorenburg, A. Benham, A. Ledebt, M. G. Feltham, and G. J. P. Savelsbergh, "Reflections on mirror therapy: a systematic review of the effect of mirror visual feedback on the brain," *Neurorehabilitation and Neural Repair*, vol. 29, no. 4, pp. 349–361, 2015.

[41] C.-H. Cheng, S.-H. Lin, C.-Y. Wu, Y.-H. Liao, K.-C. Chang, and Y.-W. Hsieh, "Mirror illusion modulates M1 activities and functional connectivity patterns of perceptual-attention

circuits during bimanual movements: a magnetoencephalography study," *Frontiers in Neuroscience*, vol. 13, 2020.

[42] S. Samuelkamaleshkumar, S. Reethajanetsureka, P. Pauljebaraj, B. Benshamir, S. M. Padankatti, and J. A. David, "Mirror therapy enhances motor performance in the paretic upper limb after stroke: a pilot randomized controlled trial," *Archives of Physical Medicine and Rehabilitation*, vol. 95, no. 11, pp. 2000–2005, 2014.

[43] J.-H. L. Min-Jae Lee, H.-M. Koo, and S.-M. Lee, "Effectiveness of bilateral arm training for improving extremity function and activities of daily living performance in hemiplegic patients," *Journal of Stroke and Cerebrovascular Diseases*, vol. 26, 2017.

[44] G. Yavuzer, R. Selles, N. Sezer et al., "Mirror therapy improves hand function in subacute stroke: a randomized controlled trial," *Archives of Physical Medicine and Rehabilitation*, vol. 89, no. 3, pp. 393–398, 2008.

[45] Y. Park, M. Chang, K.-M. Kim, and D.-H. An, "The effects of mirror therapy with tasks on upper extremity function and self-care in stroke patients," *Journal of Physical Therapy Science*, vol. 27, no. 5, pp. 1499–1501, 2015.